THE UNIVERSITY OF QUEENSLAND

AUSTRALIA

The function of NFIX during developmental and adult neurogenesis

Lachlan Ian Harris

Bachelor of Science (Biomedical), Honours Class I

A thesis submitted for the degree of Doctor of Philosophy at

The University of Queensland in 2017

Faculty of Medicine

Abstract

Understanding the transcription factor proteins that control the biology of neural stem cells during embryogenesis provides insight into brain development as well as neurodevelopmental disorders. Likewise, studying the function of transcription factors in adult neural stem cells allows us to appreciate the dynamics of these cells and their contribution to normal cognitive function. It also provides a knowledge base so as to one day harness the activity of adult neural stem cells to treat degenerative conditions of the nervous system.

One family of transcription factors key to brain development are the Nuclear Factor Ones (NFIs). Comprised of four members in mammals (NFIA, NFIB, NFIC and NFIX) these proteins promote both neuronal and glial differentiation during mouse forebrain development, and in general, appear to have a highly similar function. This thesis addressed two outstanding questions regarding the function of one these proteins, NFIX, in mouse neural stem cell biology. The first question concerned refining our understanding of NFIX function during forebrain development by determining, which stage of neuron differentiation, from a stem cell to a mature neuron, is controlled by NFIX? I answered this question by studying early changes in progenitor populations in loss-of-function mice, revealing that NFIX promotes the production of intermediate neuronal progenitors by directing stem cells to divide in an asymmetric manner. Mechanistically, this was because NFIX, and NFIA/B activated the expression of the spindle regulator *Inscuteable,* which changes cleavage plane orientations to direct an intermediate neuronal progenitor cell fate. The significance of this finding to neurodevelopmental disorders caused by *de* novo *NFIX* mutations is discussed.

The second question I addressed in this thesis, was that if NFI proteins are so important for regulating neural stem cell biology during brain development, then do they also regulate adult neural stem cell biology? I addressed this question by breeding inducible, conditional mice to allow for deletion of *Nfix* from adult hippocampal neural stem cells and separately, immature neurons. I found that NFIX is essential for adult-borne neuron differentiation, so that in the absence of NFIX, mature neurons are not generated and behavioural deficits ensue. Mechanistically, we found that NFIX is essential for primary dendrite formation, and that without NFIX a proportion of adult hippocampal progenitors switch fate to become oligodendrocytes or aberrantly express increased levels of oligodendrocyte *mRNA*. In addition to demonstrating the absolute requirement of the NFIX protein for the generation of adult-borne neurons, these findings reveal the surprising tri-

potency of adult hippocampal progenitor cells. This information may prove useful when considering strategies to harness the endogenous neural stem cell activity of the adult brain to treat demyelination disorders.

Declaration by author

This thesis is composed of my original work, and contains no material previously published or written by another person except where due reference has been made in the text. I have clearly stated the contribution by others to jointly-authored works that I have included in my thesis.

I have clearly stated the contribution of others to my thesis as a whole, including statistical assistance, survey design, data analysis, significant technical procedures, professional editorial advice, and any other original research work used or reported in my thesis. The content of my thesis is the result of work I have carried out since the commencement of my research higher degree candidature and does not include a substantial part of work that has been submitted to qualify for the award of any other degree or diploma in any university or other tertiary institution. I have clearly stated which parts of my thesis, if any, have been submitted to qualify for another award.

I acknowledge that an electronic copy of my thesis must be lodged with the University Library and, subject to the policy and procedures of The University of Queensland, the thesis be made available for research and study in accordance with the Copyright Act 1968 unless a period of embargo has been approved by the Dean of the Graduate School.

I acknowledge that copyright of all material contained in my thesis resides with the copyright holder(s) of that material. Where appropriate I have obtained copyright permission from the copyright holder to reproduce material in this thesis.

Publications during candidature

Peer reviewed papers:

1. Fane ME, Chhabra Y, Hollingsworth DE, Simmons JL, Spoerri L, Oh TG, Chauhan J, Chin T, Harris L, Harvey TJ, Muscat GE, Goding CR, Sturm RA, Haass NK, Boyle GM, Piper M, Smith AG. 2017b. NFIB Mediates BRN2 Driven Melanoma Cell Migration and Invasion Through Regulation of EZH2 and MITF. EBioMedicine 16:63-75.

2. Harris L, Zalucki O, Gobius I, McDonald H, Osinki J, Harvey TJ, Essebier A, Vidovic D, Gladwyn-Ng I, Burne TH, Heng JI, Richards LJ, Gronostajski RM, Piper M. 2016a. Transcriptional regulation of intermediate progenitor cell generation during hippocampal development. Development 143:4620-4630.

3. Harris L, Zalucki O, Piper M, Heng JI. 2016b. Insights into the Biology and Therapeutic Applications of Neural Stem Cells. Stem Cells Int 2016:9745315.

4. Heng YH, Zhou B, Harris L, Harvey T, Smith A, Horne E, Martynoga B, Andersen J, Achimastou A, Cato K, Richards LJ, Gronostajski RM, Yeo GS, Guillemot F, Bailey TL, Piper M. 2015. NFIX Regulates Proliferation and Migration Within the Murine SVZ Neurogenic Niche. Cereb Cortex 25:3758-3778.

5. Harris L, Genovesi LA, Gronostajski RM, Wainwright BJ, Piper M. 2015. Nuclear factor one transcription factors: Divergent functions in developmental versus adult stem cell populations. Dev Dyn 244:227-238.

6. Piper M, Barry G, Harvey TJ, McLeay R, Smith AG, Harris L, Mason S, Stringer BW, Day BW, Wray NR, Gronostajski RM, Bailey TL, Boyd AW, Richards LJ. 2014. NFIB-mediated repression of the epigenetic factor Ezh2 regulates cortical development. J Neurosci 34:2921-2930.

7. Vidovic D, Harris L, Harvey TJ, Evelyn Heng YH, Smith AG, Osinski J, Hughes J, Thomas P, Gronostajski RM, Bailey TL, Piper M. 2015. Expansion of the lateral ventricles and ependymal deficits underlie the hydrocephalus evident in mice lacking the transcription factor NFIX. Brain Res 1616:71-87.

Publications included in this thesis

Incorporated as Chapter 1.

Harris L, Genovesi LA, Gronostajski RM, Wainwright BJ, Piper M. 2015. Nuclear factor one transcription factors: Divergent functions in developmental versus adult stem cell populations. Dev Dyn 244:227-238.

Contributor	Statement of contribution
Lachlan Harris (Candidate)	Wrote and edited the paper (80%)
Laura A. Genovesi	Wrote and edited paper (9%)
Brandon J. Wainwright	Edited paper (1%)
Michael Piper	Wrote and edited paper (10%)

Incorporated as Chapter 3.

Harris L, Zalucki O, Gobius I, McDonald H, Osinki J, Harvey TJ, Essebier A, Vidovic D, Gladwyn-Ng I, Burne TH, Heng JI, Richards LJ, Gronostajski RM, Piper M. 2016a. Transcriptional regulation of intermediate progenitor cell generation during hippocampal development. Development 143:4620-4630.

http://dev.biologists.org/content/143/24/4620

Contributor	Statement of contribution
Lachlan Harris (Candidate)	Designed experiments (90%) Performed experiment (80%) Analysed data (90%) Wrote the paper (90%)
Oressia Zalucki	Performed experiments (11%)
Ilan Gobius	Performed experiments (5%)
Hannah Mcdonald	Performed experiment (1%) Analysed data (4%)
Jason Osinki	Performed experiment (1%)
Tracey Harvey	Performed experiment (1%)

Alexander Essebier	Analysed data (5%)
Diana Vidovic	Analysed data (1%)
Ivan Gladwyn-Ng	Performed experiment (1%)
Thomas H. Burne	Edited manuscript (10%)
Julian I. Heng	Edited manuscript (10%)
Richard Gronostajski	Edited manuscript (10%) Contributed reagents (10%)
Michael Piper	Designed experiments (10%) Wrote the paper (10%) Edited manuscript (70%) Contributed reagents (90%)

Contributions by others to the thesis

Chapter 4

Dr Oressia Zalucki assisted by performing the immunostaining and imaging in Figure 2D. Dr Dhanisha Jhaveri and Professor Perry Bartlett donated brain tissue of *Hes5*::GFP mice.

Chapter 5

Dr Oressia Zalucki contributed to the cutting and staining of adult brains in Chapter 5, and performed the behavioural experiments. She also researched the protocol outlined in Chapter 5 to isolate adult hippocampal neural stem cells for fluorescent activated cell sorting, and contributed to helpful discussions regarding experimental design, analysis and project direction

Statement of parts of the thesis submitted to qualify for the award of another degree

None.

Acknowledgements

I thank the many people who contributed to this work.

Firstly, I thank my principal supervisor Michael Piper. Thank you for your scientific input, and most of all thank you for your steadfast support, encouragement, advice and trust, which far exceeded what one could or should expect to receive.

Thank you to rest of the Piper group, in particular to Oressia Zalucki, without whom the last few years would have been far less productive and far less enjoyable.

Thank you to Thomas Burne, my co-supervisor, for your advice and support throughout.

Thank you to Richard Gronostajski and his lab at SUNY Buffalo for his input, advice, support and contribution of mouse lines. Thank you to Dhanisha Jhaveri and Perry Bartlett for their contribution of mouse tissue.

I thank my PhD committee of Sean Millard, Brian Key, Aaron Smith and Dominic Ng.

I thank the QBI Microscopy team – particularly, Luke Hammond.

Thank you also to the QBI animal team – particularly, Michael Lutkins, Robyn Rachow and Trish Hitchcock.

Most importantly, I thank my partner and my family. Thank you Sarah for being there for me through all the hills and valleys, and for teaching me that there are more important things in life than to worry about experiments. Thank you also to my parents, siblings and dog for their encouragement, love and support without which, this would not have been possible or a worthwhile endeavour to attempt. This thesis is dedicated to them.

Keywords

Nfix, *Nfib*, transcription factor, neurogenesis, lineage determination, asymmetric, inscuteable.

Australian and New Zealand Standard Research Classifications (ANZSRC)

110902: Cellular Nervous System (100%)

Fields of Research (FoR) Classification

1109: Neurosciences (100%)

Table of Contents

List of Figures

List of Tables

List of Abbreviations

AH-NSC	Adult hippocampal neural stem cell
ASCL1	Achaete-scute like 1
BLBP	Brain lipid-binding protein
BrdU	5-Bromo-2'-deoxyuridine
BSA	Bovine serum albumin
ChIP-Seq	Chromatin immunprecipitation sequencing
CNS	Central nervous sytem
CRISPR	Clustered regularly interspaced short palindromic repeats
DAPI	4',6-Diamidino-2-Phenylindole
DCX	Doublecortin
DPI	Days Post Injection
E	Embryonic day
EdU	5-ethynyl-2'-deoxyuridine
EGFR	Epidermal growth factor receptor
EGL	External granule layer
ES	Embryonic stem
FACS	Fluorescent activated cell sorting
GFAP	Glial fibrillary acidic protein
GNP	Granule neuron progenitors
GO	Gene ontology
GR	Glucocorticoid receptor
Hes1	Hairy-Enhancer-of-Split 1
Hes5	Hairy-Enhancer-of-Split 5
HFSC	Hair follicle stem cell
HSC	Hematopoietic stem cells
IGL	Internal granule layer
IP	Intermediate progenitor
IPC	Intermediate progenitor cell
NFI	Nuclear Factor One

NFIA	Nuclear Factor One A
NFIB	Nuclear Factor One B
NFIC	Nuclear Factor One C
NFIX	Nuclear Factor One X
P	Postnatal day
PBS	Phospho-buffered saline
PFA	Paraformaldehyde
PHH3	Phosop-histone H3
PI	Post-injection
qPCR	quantitative Polycmerase Chain Reaction
RNA-seq	RNA sequencing
TBR2	T-box brain protein 2
Tc	Cell-cycle duration
Ts	S-phase duration

Chapter 1 Nuclear Factor One transcription factors: divergent functions in developmental versus adult stem cell populations?

1.1 Scope of thesis and structure

This thesis examines the transcriptional regulation of neural stem cell biology, both in the developing brain and in the adult hippocampus. It uses mouse as a model and focuses predominantly on the function of one transcription factor called *nuclear factor one x* (*Nfix*). This thesis identifies and compares *Nfix* function across development (Chapter 3) with its function in the adult hippocampus (Chapter 5). This thesis also contributes a new histological method for identifying dividing adult hippocampal stem cells (Chapter 4), which was integral to the analysis in Chapter 5. The structure of thesis is as follows:

Chapter 1: Literature review – "Nuclear Factor One transcription factors: divergent functions in developmental versus adult stem cell populations?"

Chapter 2: Methods chapter – "Production of transgenic mouse strains"

Chapter 3: Data chapter – "Transcriptional regulation of intermediate progenitor cell production by NFIX during cortical development".

Chapter 4: Data chapter – "A morphology independent approach to identifying dividing adult hippocampal neural stem cells".

Chapter 5: Data chapter – "NFIX is essential for neuronal fate in the adult hippocampus"

Chapter 6: General discussion.

1.2 Aims of Chapter 1

The aim of this chapter is to provide an overview of the field's current understanding of NFI transcription factors in developmental stem cells and in adult stem cells. The scope of this chapter is broad, covering the function of NFIs not only in the nervous system but also in the many other organ systems. I make the generalisation in this chapter that NFIs promote differentiation during development, while also acknowledging exceptions to this rule, and gaps in our knowledge. One of the major knowledge gaps I highlight is that while NFIs promote neuronal differentiation during the development of the dorsal telencephalon, the stage of neuronal lineage progression regulated by NFIs is unknown. Addressing this gap forms Chapter 3 of my thesis.

The second generalisation I argue for in this chapter is that NFIs may play a different, and/or additional role within adult stem cell populations. The few studies published on NFI function in adult stem cells suggest that NFIs regulate quiescence, a state of reversible cell-cycle exit unique to adult tissue stem cells. Interestingly, of the few studies published thus far, NFI deletion from adult tissue stem cells had little effect on processes of differentiation. These few studies, suggest that NFIs regulate quiescence and are not integral to differentiation programs in adult stem cells, unlike during development. This discussion backgrounds Chapter 5 of my thesis, wherein, I directly address the function of NFIX in adult stem cells in the hippocampus, assessing both the regulation of quiescence and the differentiation of this population. In doing so, by the end of this thesis I provide an informed discussion (Chapter 6) directly comparing and contrasting the functions of NFIs during brain development (Chapter 3) and in adult neural stem cells (Chapter 5).

The text in the following chapter was published in the journal Developmental Dynamics, on August 20, 2014.

Harris L, Genovesi LA, Gronostajski RM, Wainwright BJ, Piper M. 2015. Nuclear factor one transcription factors: Divergent functions in developmental versus adult stem cell populations. Dev Dyn 244:227-238.

1.3 Introduction

A stem cell is an undifferentiated cell that has the capacity to retain stem cell identity through self-renewal, and to differentiate to generate multiple cell types (Weissman, 2000). Broadly speaking, there are two classes of stem cells, those present in the developing embryo and those resident in adult tissues. In the developing embryo, each organ system has a set of lineage restricted stem cells that proliferate in a continuous manner and which, through their differentiation, produce the post-mitotic cellular components of the particular organ system in a relatively short period of time. In contrast, resident adult tissue stem cells, which function to replace and repair tissue throughout life, comprise a relatively scarce and long-lived cellular population. Because of this, a proportion of these cells exist in a non-proliferative state (*quiescence*) for prolonged periods, thereby preserving the adult stem cell pool by preventing proliferative stress and precocious commitment to differentiation (Valcourt et al., 2012; Cheung and Rando, 2013).

A key determinant of stem cell proliferation and differentiation are the gene regulatory networks governed by transcription factors. One group of transcription factors that is highly expressed by stem cells during development, as well as by adult stem cells across a range of tissue types, is the NFI family. The first NFI factor isolated was described as a host-encoded protein required for the initiation of adenovirus replication (Nagata et al., 1982). Subsequently, four genes encoding *Nfi* family members in mammals have been isolated, namely *Nfia*, *Nfib*, *Nfic* and *Nfix* (Rupp et al., 1990; Kruse et al., 1991). NFIs interact with double-stranded DNA as either hetero- or homodimers by binding to the palindromic sequence TTGGC(N5)GCCAA with high affinity, thereby activating or repressing gene transcription depending on the cellular context and gene promoter [for an in depth review of these topics see (Gronostajski, 2000)].

The expression pattern of NFIs during development was characterized over 15 years ago (Chaudhry et al., 1997); from this study and subsequent analyses it has been demonstrated that NFIs are highly expressed by embryonic stem and progenitor cells within the central nervous system (CNS), lung and skeletomuscular tissue, amongst others. This initial expression analysis, combined with the generation of *Nfia* null mice, provided the first indicators that *Nfi* genes are important regulators of stem cell biology during development (das Neves et al., 1999). Subsequent cellular and molecular characterization of *Nfia, Nfib, Nfic* and *Nfix* null mice (see Table 1.1) demonstrated that NFI factors play multiple roles during development that promote cellular differentiation, including activating cell-type specific programs of gene expression and repressing the transcription of genes encoding

factors mediating stem cell self-renewal (Messina et al., 2010; Piper et al., 2010; Lajoie et al., 2014). Consistent with their role in promoting stem and progenitor cell differentiation during development, NFIs have been implicated in a number of developmental disorders (Lu et al., 2007; Malan et al., 2010; Priolo et al., 2012; Yoneda et al., 2012), and have been reported to act as tumor suppressors in some cancers, including medulloblastoma (Genovesi et al., 2013).

Recently, the development of novel *in vitro* models and the use of conditional knockout technologies have shown that NFIs are also important regulators of stem cell biology in adult tissues, including melanocyte stem cells within the hair follicle niche (Chang et al., 2013) and hematopoietic stem cells in adult bone marrow (Holmfeldt et al., 2013). Intriguingly, in these studies, loss-of-function analyses did not lead to a delay in the differentiation of the adult stem cell populations as would be expected based on the role of NFIs during development. Instead, the loss of NFI function led to the loss of stem cell quiescence, precocious differentiation and the loss, or cellular death, of the stem population. In this review we discuss the role of NFI factors in development, largely as promoters of differentiated states, and reconcile this with the emerging evidence for NFIs as mediators of quiescence and survival within adult stem cell niches.

1.4 NFIs drive stem and progenitor cell differentiation during development

There is strong evidence that the major role of NFIs during development is to promote differentiation at the expense of stem cell self-renewal. NFIs carry out this role by exerting multiple effects on stem cell populations that act cumulatively to promote differentiation. Evidence for this role is found across a range of tissue types, including the CNS (Barry et al., 2008; Piper et al., 2010; Heng et al., 2014), musculoskeletal system (Messina et al., 2010; Pistocchi et al., 2013) and lung (Hsu et al., 2011) as well as in a range of other contexts such as in the development of teeth (Park et al., 2007) and the mammary gland (Murtagh et al., 2003; Nilsson et al., 2006).

Within the developing CNS, neural stem cells give rise to post-mitotic cells in a temporally distinct manner, first generating neurons and subsequently glia. These post-mitotic cells then migrate away from the germinal zones of the developing brain and integrate into the emerging cellular layers where they terminally differentiate (Kriegstein and Alvarez-Buylla, 2009). Results to date have shown that NFIA, NFIB and NFIX all have multifaceted roles in regulating neural stem and progenitor cell differentiation during development, including driving the differentiation of stem cells within the developing cerebral cortex and neuronal progenitors within the nascent cerebellum.

1.4.1 NFIs promote cortical neural stem cell differentiation

Radial glial cells are the principal class of stem cell in the developing cerebral cortex (dorsal telencephalon), generating the majority of the post-mitotic neurons and glia present in the mature cortex (Casper and McCarthy, 2006). During early development, radial glial cells, which are located in the cortical ventricular zone, predominantly divide symmetrically to expand the population of stem cells. As development progresses, radial glial cells switch to dividing asymmetrically, generating a secondary pool of progenitor cells called intermediate progenitor cells (IPCs) (or basal progenitors) that migrate to the subventricular zone region, followed by glia such as astrocytes and oligodendrocytes (Kriegstein and Alvarez-Buylla, 2009).

NFIs were first implicated in regulating the differentiation of radial glial cells by expression analysis, which revealed that NFIA, NFIB (Plachez et al., 2008), and NFIX (Plachez et al., 2008) are all expressed within the ventricular zone of the telencephalon from embryonic day 12 (E12) in mice until the end of corticogenesis at E18. Subsequent examination of the neocortical and

hippocampal phenotype of *Nfia* and *Nfix* null mice revealed that there was an expansion of the pool of radial glia from approximately E16 onwards, as identified through immunohistochemical staining for stem cell markers such as PAX6 and SOX2 (Piper et al., 2010; Heng et al., 2014). Similarly, in a recent study examining the neocortical and hippocampal phenotype of *Nfib* null mice, more PAX6-positive stem cells were identified within the ventricular zone, indicating that in mice lacking *Nfib,* cortical stem cell populations are also expanded (Betancourt et al., 2014). Despite the greater number of cortical radial glia within *Nfia, Nfib* and *Nfix* null mice at E16, these mouse lines do not display a concomitant increase in the expression of the intermediate progenitor cell marker TBR2 at this age (Piper et al., 2010; Betancourt et al., 2014; Heng et al., 2014); nor do they display increased expression of the astrocytic protein GFAP, which is instead dramatically reduced (Shu et al., 2003; Piper et al., 2010; Heng et al., 2014). Therefore, these data argue that in the absence of NFIs radial glial cells fail to differentiate down neuronal and glial lineages according to normal developmental timelines resulting in severe morphological defects such as the dramatically reduced size of the hippocampal dentate gyrus in postnatal *Nfia* and *Nfix* null animals (das Neves et al., 1999; Heng et al., 2014).

Molecular studies and expression analyses suggest that NFIs may promote the differentiation of radial glial cells into neurons and glia through a dual mechanism of directly inducing glial (and potentially neuronal) specific gene expression, while repressing the transcription of genes associated with the maintenance of stem cell populations (Figure 1.1). While earlier studies showed a decrease in glial-specific markers in *Nfia* (das Neves et al., 1999) and *Nfib* null mice (Steele-Perkins et al., 2005), the first evidence that NFIs directly induce glial-specific gene expression came from rat cortical cell cultures, where a pan-NFI antibody was used to demonstrate that NFI occupies the *Gfap* promoter prior to the induction of astrocyte differentiation, and that mutation of the NFI binding site correlates with reduced GFAP expression (Cebolla and Vallejo, 2006). Subsequent to this, using an *in vitro* model of cortical neural stem cells derived from mouse, Namihira et al. (2009) implicated NFIA as an intermediary factor in the canonical Notch/JAK/STAT pathway, which functions instructively during development to drive glial differentiation within the cortex. Specifically, they demonstrated that activation of Notch signaling induced NFIA expression in cortical neural stem cells, and that subsequent NFIA expression was correlated with disassociation of the inhibitory factor DNA methyltransferase 1 from the *Gfap* regulatory region, and with STAT3 binding site to the *Gfap* promoter. These findings illustrate that another pathway through which NFIs may induce expression of the *Gfap* locus is via the inhibition of repressive promoter methylation. Intriguingly, recent studies in human neural progenitor cell cultures have further shown that the NFIX-3 splice variant is also a potent activator of the *Gfap* promoter, in this case

through regulating nucleosome architecture and the recruitment of RNA polymerase to the transcription complex rather than via the modulation of DNA methylation (Singh et al., 2011). Together these findings illustrate the different ways in which NFIs can regulate the molecular pathway driving *Gfap* expression during glial differentiation. The precise mechanisms governing how NFI factors regulate the expression of other astrocyte specific genes currently thought to be downstream of NFIs, such as *B-fabp* (Bisgrove et al., 2000), *Sparcl1* (Wilczynska et al., 2009)*, Apcdd1, Mmd2* and *Zcchc24* (Kang et al., 2012) are yet to be determined.

Repression of stem cell self-renewal pathways represents a second, complementary mechanism that may contribute to the delays in neuronal and glial development seen in *Nfi* null mice. Work from our group has shown that two genes implicated in cortical stem cell self-renewal, the epigenetic factor *Ezh2* (Pereira et al., 2010) and the transcription factor *Sox9* (Scott et al., 2010), are repressed by NFIB (Piper et al., 2014) and NFIX (Heng et al., 2014) respectively *in vitro*, and that the expression of these factors is upregulated in null mice. Similarly, we have also demonstrated that expression of the *Hairy-Enhancer-of-Split (Hes)* genes *Hes1* and *Hes5,* which are key regulators of Notch signaling-induced stem cell self-renewal, are upregulated in *Nfia* and *Nfib* null mice (Piper et al., 2010), suggesting that NFIs may repress elements of the Notch pathway associated with self-renewal, while simultaneously co-operating with the JAK/STAT element of the Notch pathway that promotes glial differentiation (Figure 1.1). Collectively, these findings strongly support the idea that NFIs promote cortical stem cell differentiation through direct activation of cell-type-specific genes, while repressing the expression of loci that maintain stem cell fate. It will be critical for further studies to delineate the specific functions of each individual NFI factor regulating the differentiation of cortical stem cell populations. Such studies will provide insight into whether it is the overall level of NFI factors that is crucial, or whether each individual factor regulates a unique set of genes. Next-generation genomic techniques such as chromatin immunoprecipitation followed by sequencing (ChIP-seq) using antibodies specific to individual NFI factors, combined with RNA sequencing (RNA-seq) of the different *Nfi* null mouse lines, have the capacity to provide these answers.

1.4.2 NFIs promote cerebellar granule neuron development

NFI proteins also play key roles as transcriptional regulators of the development of the most abundant neuron of the brain, the cerebellar granule neuron [reviewed in (Kilpatrick et al., 2012)]. Towards the end of embryonic mouse development (~E18), granule neuron progenitors (GNPs) surround the primordial cerebellum, comprising a cell layer known as the external granular layer

(EGL). This represents the main secondary germinal site for neurogenesis in the postnatal cerebellum. Granule neuron development from the EGL provides an elegant system in which to explore the molecules that mediate the switch from a proliferating neuronal progenitor cell to a terminally differentiated granule neuron [reviewed in (Martinez et al., 2013)]. Specifically, GNPs proliferate in the outer EGL before exiting the cell cycle and commencing their migration inwards towards the internal granule layer (IGL). Within the EGL, GNPs begin to differentiate, extending bipolar axons that form fascicles of parallel fibres, and subsequently migrate tangentially before reaching the pre-migratory zone of the EGL. Here, GNPs extend long radial processes and migrate down through the molecular layer, to form the IGL. Within the IGL, GNPs complete the final stages of maturation and terminally differentiate, extending dendrites that form synapses with mossy fibres and additional neurons. Although a number of studies have contributed to our current understanding of the signaling pathways responsible for driving the proliferation of GNPs in the EGL (Dahmane and Ruiz i Altaba, 1999; Wallace, 1999; Lewis et al., 2004), what drives these cells to exit the cell cycle and ultimately differentiate to granule neurons remains poorly understood.

The NFI transcription factors have now been shown to play key roles in the progressive stages of post-mitotic GNP migration and differentiation. The identification of NFI proteins as directly regulating the transcription of *Gabra6*, a gene expressed in differentiated granule neurons residing in the IGL of the cerebellum (Kato, 1990), provided the first evidence of a role for the NFI family as transcriptional regulators in GNPs (Wang et al., 2004). Following this, expression analyses of cerebellar tissue isolated from post-natal day 7 (P7) mice suggested a role for these factors in the migration of GNPs to the IGL, with NFIA, NFIB and NFIX being expressed by GNPs residing in the deeper pre-migratory zone of the EGL, as well as by cells migrating through the molecular layer to the IGL (Wang et al., 2007). Using a variety of tools to manipulate NFI function in GNP culture *in vitro,* Wang et al. (2007) demonstrated that NFI proteins are critical for axon outgrowth and migration of post-mitotic GNPs. These findings were confirmed in P6 cerebellar slice cultures, in which the inhibition of NFI function induced the defasciculation of previously formed parallel fibres within the pre-migratory zone of the EGL, and subsequently impeded the radial migration of GNPs from the pre-migratory zone of the EGL to the IGL. In addition to these GNP differentiation events within the pre-migratory zone of the EGL, studies in *ex vivo* cerebellar slice cultures also revealed that the length and number of dendrites formed from GNPs once they had migrated to the IGL was disrupted by blocking NFI function. The cerebellar phenotype of *Nfia* null mice is consistent with *in vitro* and *ex vivo* findings, with P17 *Nfia*-deficient mice exhibiting shortened and disorientated parallel fibres and retarded migration of GNP cells within the cerebellum (Wang et al., 2007). Similarly, delayed GNP maturation was also observed in *Nfix*-deficient mice; however this

was not thought to be a consequence of a migratory defect of GNPs *per se*, but rather an overall delay in the development and differentiation of GNPs (Piper et al., 2011). Together these data strongly implicate NFI transcription factors in regulating various aspects of GNP maturation, including the switch from an immature, proliferating GNP to a post-mitotic GNP that has commenced its migration.

More recent studies have begun to elucidate the transcriptional targets of the NFIs that mediate both the early and late stages of GNP maturation. The cell adhesion molecules, *N-cadherin* and *ephrin-B1*, have been identified as NFI gene targets responsible for mediating a range of differentiation defects, consistent with previous studies demonstrating their role in the migration of GNPs (Karam et al., 2000; Taniguchi et al., 2006). Functional inhibition of ephrin B1 or N-cadherin in GNPs *in vitro* and in *ex vivo* cerebellar slice cultures disrupts axon extension, migration and dendrite formation, with both proteins also reduced in migrating GNPs in the molecular layer and IGL of *Nfia* null mice (Wang et al., 2007). One subsequent study has identified an additional cell adhesion molecule, transient axonal glycoprotein 1 (Tag1), as an NFI downstream target implicated in post-mitotic GNP differentiation (Wang et al., 2010). More recently, the NFI family has been demonstrated to play a central role in regulating a developmental switch program in GNPs during late stages of maturation, whereby genes required for mature granule neuron function, including dendrite and synapse formation, are upregulated at the expense of genes expressed in more immature GNPs (Ding et al., 2013). NFIs were shown to mediate this late developmental switch in gene expression in response to temporally regulated changes in membrane potential. Typically in GNPs depolarization maintains immature GNPs via the activation of the calcineurin/nuclear factor of activated T-cells, cytoplasmic (NFATc) pathway. NFATc was found to occupy and block the promoters of the late-expressed NFI genes. However, as GNPs begin to mature and undergo a hyperpolarizing shift in membrane potential, NFATc binding subsides, allowing the NFI family of proteins to bind to promoters of late-expressing genes in GNPs and induce dendrite formation.

Together, these data indicate the importance of NFI family members as critical regulators of a gene network that orchestrates several stages of GNP maturation, including axonogenesis, radial migration, dendritogenesis and synaptogenesis. Further advances are required to identify target genes of NFI family members in GNP development and to delineate the overlapping and non-overlapping roles of each NFI family member.

1.4.3 NFIs are potential drivers of medulloblastoma tumorigenesis

Given the central role of NFI family members in GNP differentiation, it is perhaps not surprising that NFI family members have recently been implicated in medulloblastoma, a disorder of GNP proliferation and differentiation. Medulloblastoma is a common malignant brain tumour of childhood, and certain subtypes of this disease have long been known to arise from GNPs of the EGL (Marino et al., 2000; Oliver et al., 2005; Schuller et al., 2008). Recently, a number of studies identified NFI factors as potential drivers of medulloblastoma tumorigenesis, with transposon-mediated inactivation of *Nfia, Nfib* and/or *Nfix* shown to accelerate medulloblastoma initiation and/or progression in a mouse model of medulloblastoma derived from GNPs (Wu et al., 2012; Genovesi et al., 2013; Lastowska et al., 2013). *Nfia* was subsequently confirmed as a specific driver of medulloblastoma *in vivo*, with combined haploinsufficiency for both *Nfia* and *Ptch1* exacerbating tumour development compared to the *Ptch1* haploinsufficiency alone (Genovesi et al., 2013). Given the role of NFIA in the regulation of GNP differentiation, these findings further emphasize the link between the differentiation status of GNPs and the development of medulloblastoma. A similar role was previously observed for proneural transcription factor Math1, whereby the overexpression of Math1 blocked the trajectory of GNP differentiation, thereby significantly increasing tumour incidence and reducing tumour latency (Ayrault et al., 2010). Collectively, these studies demonstrate that medulloblastoma development is strongly linked to the differentiation status of GNPs. As such, further studies are required to assess the relevance of other NFI family members in medulloblastoma and to define the repertoire of target genes regulated by this family of transcription factors relevant to tumour development.

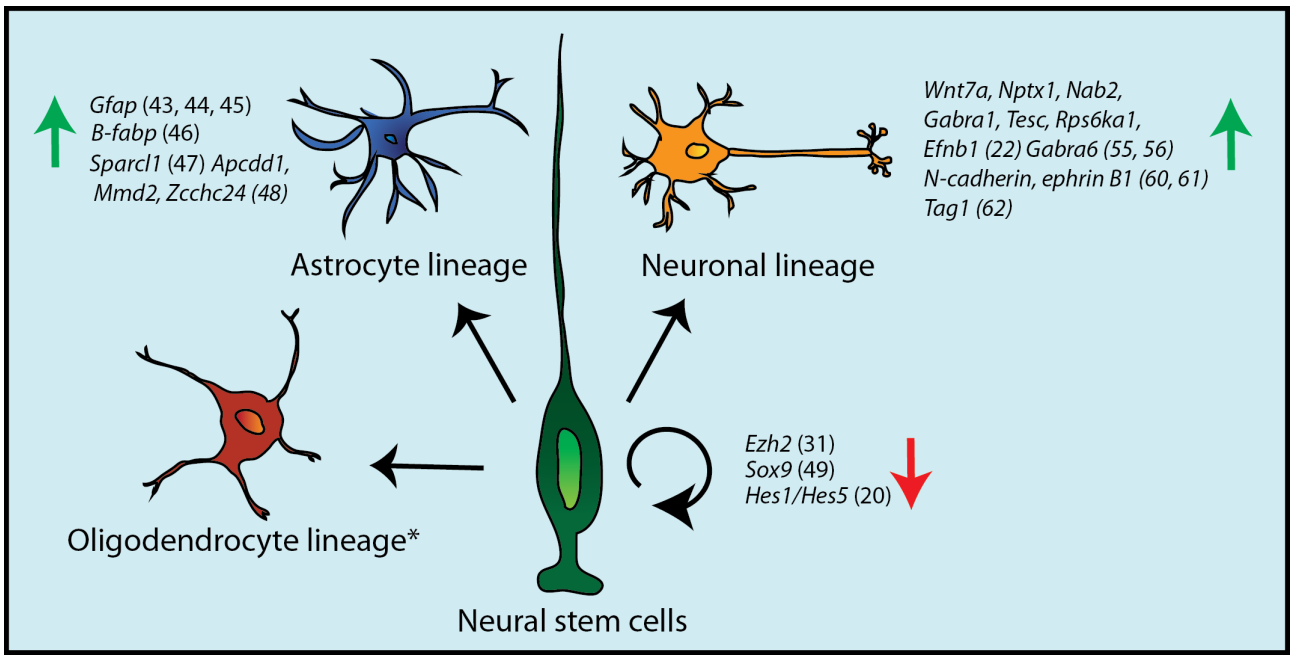

Figure 1.1: NFIs promote neural stem cell differentiation

NFIs repress the expression of genes associated with self-renewal of neural stem cells, and activate the expression of genes associated with neuronal and astrocyte differentiation. In this instance, NFI target genes were defined as misregulated genes identified via loss- or gain-of-function experiments which were further validated as downstream NFI targets via techniques such as ChIP-PCR, luciferase assays and gel-shift assays. *No direct NFI targets associated with the oligodendrocyte lineage have yet been identified. References: [1](Piper et al., 2014), [2](Heng et al., 2014), [3](Piper et al., 2010), [4](Cebolla and Vallejo, 2006), [5](Namihira et al., 2009), [6](Singh et al., 2011), [7](Gopalan et al., 2006), [8](Bisgrove et al., 2000), [9](Wilczynska et al., 2009), [10](Kang et al., 2012), [11](Ding et al., 2013), [12](Wang et al., 2004), [13](Wang et al., 2007), [14](Wang et al., 2010).

1.4.4 NFIX promotes the embryonic to fetal myoblast transition during musculoskeletal development

Another developmental context in which NFIs have been shown to drive the differentiation of stem and progenitor cells by activating cell-type-specific programs, while repressing the undifferentiated states of parental cells, is in the formation of the musculoskeletal system. With respect to muscle development, NFIX has been shown to activate an important transcriptional transition within muscle progenitors (myoblasts). Muscle development occurs in two stages, with each stage requiring distinct myoblast populations (Tajbakhsh, 2005; Biressi et al., 2007a). The first stage of muscle development or 'primary myogenesis' occurs from E10-E12.5 in mice. During this initial phase a small fraction of the myoblast pool, referred to as 'embryonic myoblasts', terminally differentiate, fuse and give rise to the multinucleated muscle fibers. The remaining myoblast population remains committed to the muscle lineage but exists in an undifferentiated state until secondary myogenesis takes place between E14.5 and E17.5 (Relaix et al., 2005). Myoblasts that participate in secondary myogenesis are called fetal myoblasts. Embryonic myoblasts and fetal myoblasts represent two distinct progenitor cell populations that produce muscle fibers that differ in morphology and in the myosin heavy chain (MyHC) isoforms and enzymes that they express (Barbieri et al., 1990; Zappelli et al., 1996; Ferrari et al., 1997; Biressi et al., 2007b).

To determine the molecular players that regulate this embryonic to fetal myoblast transcriptional switch, Biressi et al. (2007b) performed a genome wide-expression analysis on purified embryonic and fetal myoblasts and identified *Nfi* genes as potential candidates for this process. The expression of all four *Nfi* genes was robustly induced in fetal myoblasts, particularly NFIX, which was highly expressed in fetal myoblasts but virtually absent from the embryonic myoblast population. Functional analyses revealed that, similar to the role of NFIs in the development of the CNS, NFIX acted as a binary switch during the embryonic-fetal myoblast transition, inducing fetal-specific gene transcription while repressing the expression of genes associated with embryonic myoblasts. More specifically, conditional deletion of *Nfix* using a muscle-specific *MyoD* promoter prevented the initiation of fetal-specific transcription at E16; whereas in a gain-of-function mouse line overexpressing NFIX, fetal-specific genes were precociously expressed and embryonic myoblast gene expression was downregulated (Messina et al., 2010). Molecular analysis demonstrated that these changes in gene expression were due to direct regulation by NFIX, with NFIX activating the expression of the fetal-specific gene *Mck* by forming a transcriptional complex with MEF2 and the kinase PKC-theta, and blocking the expression of the embryonic myoblast protein, slow MyHC, by suppressing its transcriptional activator NFATc4 (Calabria et al., 2009).

The musculature of *Nfix* loss- or gain-of-function embryos demonstrated the importance of correctly coordinating the embryonic-to-fetal transcriptional switch. Loss-of-function embryos were much smaller and the muscle fibers in hind-limb sections were disorganized, whereas in gain-of-function embryos the reciprocal phenotype was observed. Collectively, the molecular and anatomical experiments showed that NFIX plays a vital role during muscle development by activating the expression of fetal genes and repressing embryonic gene expression, a function that has recently been shown to be mostly conserved across evolutionary phyla (Pistocchi et al., 2013). Future experiments examining the role of NFIX in muscle development should examine whether NFIX regulates the differentiation of a third type of myogenic progenitor, the satellite cell. These cells act as adult stem cells that regenerate muscular tissue in response to injury or exercise (Collins et al., 2005; Biressi et al., 2007a). Due to the emerging role of *Nfi* genes in other adult stem cell niches (see *Nfis in adult stem cell niches*), this avenue of research is of particular interest.

NFIX also appears to have a role in the development of the skeleton. Loss-of-function or dominant-negative mutations in *Nfix* are causative factors of Sotos Syndrome and Marshall-Smith Syndrome respectively (Malan et al., 2010; Yoneda et al., 2012). These disorders, which have a combined incidence of approximately 1:10,000 live births, are characterized by overgrowth and cognitive deficits, as well as skeletal defects such as kyphosis (curvature of the spine), advanced bone age and reduced bone density with increased propensity to fracturing. Although there is not currently a mechanistic understanding of how NFIX confers the skeletal phenotype of these disorders, similar skeletal defects including kyphosis and reduced bone density are observed in *Nfix* null mice; this mouse line may therefore provide a suitable model to probe this aspect of NFIX function (Driller et al., 2007; Harris et al., 2013).

Similarly, in addition to *Nfix*, *Nfic* has recently been shown to play an important role in postnatal bone formation. *Nfix* null mice were shown initially to have severe defects in postnatal tooth development (Steele-Perkins et al., 2003). These postnatal tooth defects appear to be mediated at least in part by antagonistic interactions between NFIC and the TGF-β signaling pathway during tooth development (Lee et al., 2011). In addition, NFIC interacts with TGF-β signaling during postnatal wound healing (Plasari et al., 2010) suggesting that NFIC-TGF-β interactions may represent a recurrent theme in postnatal NFIC function. More recently, NFIC has been shown to play a major role in postnatal osteoblast maturation through the regulation of the key osteoblast transcription factor Osterix (Lee et al., 2014). Of interest, no such effect on osteoblast formation

was seen during fetal bone formation. Thus NFIC appears to have important roles in development primarily during the postnatal period.

1.4.5 Mesenchymal NFIB regulates lung development

NFIs have also been implicated in the development of a range of epithelial appendages, including the formation of teeth, and the development of the mammary glands (Kannius-Janson et al., 2002; Murtagh et al., 2003; Johansson et al., 2005), hair follicles (Plasari et al., 2010) and digestive tract (Driller et al., 2007). However, the best understood function of NFIs during epithelial appendage formation is the role of NFIB during lung development, where it has recently been shown to drive lung epithelial cell differentiation at the expense of stem and progenitor cell proliferation.

NFIB was linked to lung development by the observation that *Nfib* null mice die within 15 minutes postpartum due to respiratory stress, a phenotype not seen in other *Nfi* null mice (Grunder et al., 2002). Prenatal mouse lung development has four distinct stages. In the embryonic state (~E9.5-E10.5) the lung bud extends from the primitive gut endoderm and bifurcates. In the pseudoglandular stage (~E11-E16.5), the paired lung buds invade the mesenchyme to form an undifferentiated primordial bronchiole tree, and in the canalicular stage (E16.5-E17.5), the terminal sacs lined with epithelial cells develop, a process that is accelerated during the saccular stage (~E17.5-P5), during which further differentiation and diversification of epithelial cell sub-types occurs (Costa et al., 2001). Initial analyses of *Nfib* null mice demonstrated that lung development was apparently normal until E15.5, at which point development was arrested, with mutant lungs failing to form lung saccules (Steele-Perkins et al., 2005). Underpinning this gross histological phenotype was an increased proportion of proliferating cells in mutant lungs (Hsu et al., 2011; Holmfeldt et al., 2013) and a dramatic failure of differentiation of lung epithelial cell sub-types, including alveolar epithelial cells and bronchiolar exocrine cells in the distal lung, and ciliated cells in the proximal lung (Hsu et al., 2011). Collectively, these lines of evidence pointed to NFIB having a role in promoting lung epithelial differentiation at the expense of stem and progenitor proliferation during development.

Although the precise mechanism by which NFIB exerts this function is not clear, two recent studies have provided significant insights into this. Firstly, evidence from Hsu et al. (2011) suggests that NFIB may regulate lung epithelial cell differentiation though a non-cell-autonomous means. In this study the authors demonstrated that NFIB was predominantly expressed in the lung mesenchyme

during development, and that conditional deletion of *Nfib* from the mesenchyme almost entirely recapitulated the defects in lung epithelial cell differentiation observed in *Nfib* null mice. Secondly, Lajoie et al. (2014) hypothesized that mesenchymal NFIB might regulate lung development in conjunction with the glucocorticoid receptor (GR). Similar to the phenotype in *Nfib* mutants, disruption of the gene encoding GR, *Nr3c1*, results in an immature lung phenotype in mice, with excess cellular proliferation and reduced expression of markers of epithelial cell differentiation (Cole et al., 1995). Using microarray data from lung tissue derived from both *Nfib* and *Nr3c1* null mice at E18.5 the authors demonstrated that of the mis-regulated genes, 52 were under-expressed in both null lines, an overlap that was approximately 13 times larger than that expected by chance, suggesting that a subset of these genes may be directly activated by the coordinated activity of NFIB and GR proteins. These results are particularly significant as prenatal administration of glucocorticoids can stimulate lung maturation in premature infants (Seckl, 2004), suggesting that further characterization of the regulatory relationship between NFIB and GR may be of clinical value in treating lung immaturity.

1.4.6 Genetic redundancy of *Nfis* during development

Genetic redundancy is where two or more genes perform similar functions so that inactivation of one of these genes has no or little phenotypic effect. There is very limited evidence so far that NFIs have redundant functions. For example, in the developing CNS inactivation of *Nfia, Nfib* or *Nfix* alone, is sufficient to render severe forebrain defects (Shu et al., 2003; Steele-Perkins et al., 2005; Campbell et al., 2008). Likewise in the developing cerebellum, NFIA, NFIB and NFIX are alone functionally required for normal development (Steele-Perkins et al., 2005; Wang et al., 2010; Piper et al., 2011). Interestingly however, these null lines still exhibit broadly similar phenotypes. This suggests that it is the overall level of NFI expression that is more important than the function of individual *Nfi* genes during CNS development. In support of this, haploinsufficiency for *Nfia* or *Nfix* has been implicated as causative factors in neurodevelopmental disorders and mice lacking one functional copy of *Nfix* display cognitive and neuroanatomical defects (Lu et al., 2007; Malan et al., 2010; Harris et al., 2013).

One potential scenario where NFIs may function redundantly is during lung development. *Nfib* null mice die from severe respiratory distress (Grunder et al., 2002), and although *Nfia, Nfic* and *Nfix* are all expressed during lung development none of these mouse lines have obvious lung defects. This indicates that loss of these factors alone is insufficient to adversely affect lung development, which could be due to genetic redundancy. One way to test this hypothesis would be to closely examine

the lung phenotype of *Nfia* and *Nfic* (or *Nfix*) null mice. If neither of these null lines display clear lung phenotypes, the generation of a double *Nfia/Nfic* knockout mouse line with a subsequent lung phenotype would indicate redundancy.

1.5 NFIs in adult stem cell niches: a putative function in cell-cycle regulation and survival

In addition to being important regulators of stem cell biology during development, NFIs are highly expressed by adult tissue stem cells (see Table 1.2). Most mammalian adult tissues contain a resident stem cell population, which function to repair and regenerate tissue in response to stress or injury throughout the life of the organism (Cheung and Rando, 2013). A cardinal feature of adult tissue stem cells, even in high-turnover tissue such as the skin and the intestines, is that a proportion of the stem cell population resides outside the cell-cycle (is *quiescent*) for long periods of time, preventing metabolic and proliferative stress and thereby preserving genomic integrity and stem cell function (Valcourt et al., 2012).

The perinatal lethality of *Nfia* and *Nfib* null mice, and the severe developmental defects of viable *Nfix* null pups had until recently prevented analysis of NFI function in adult stem cell compartments. However, studies employing conditional knockout strategies and/or *in vitro* models have begun to uncover NFI function in these cellular populations. Intriguingly, these studies suggest that, in adult tissue, NFI factors play a contrasting role to that during development, serving to promote quiescence and/or survival of stem cells, rather than their differentiation (Chang et al., 2013; Holmfeldt et al., 2013; Martynoga et al., 2013).

Table 1.1: Summary of major phenotypes identified in *Nfi* null mice.

Phenotype	*Nfia* KO	*Nfib* KO	*Nfic* KO	*Nfix* KO
Survival	Majority die at birth (das Neves et al., 1999).	All die at birth (Grunder et al., 2002).	Survive to adulthood (Steele-Perkins et al., 2003).	Postnatal lethal (3-4 week) (Plachez et al., 2008)
CNS	Delayed glial and neuronal differentiation (Piper et al., 2010). Corpus callosum agenesis. Communicating hydrocephalus (das Neves et al., 1999).	Delayed glial and neuronal differentiation (Barry et al., 2008; Betancourt et al., 2014; Piper et al., 2014). Corpus callosum dysgenesis (Steele-Perkins et al., 2005).	Phenotype not examined. Weak expression detected in developing CNS (Chaudhry et al., 1997).	Delayed glial and neuronal differentiation (Heng et al., 2014). Corpus callosum dysgenesis (Plachez et al., 2008).
Lung	No obvious phenotype. Expressed in developing lung (Steele-Perkins et al., 2005).	Severe lung hyperplasia. Die from respiratory defects (Steele-Perkins et al., 2005).	Phenotype not examined. Expressed in developing lung (Steele-Perkins et al., 2005).	Phenotype not examined. Expressed in developing lung (Steele-Perkins et al., 2005).
Muscle and skeletal tissue	No gross skeletal defects (das Neves et al., 1999). Musculature not examined, expressed by muscle progenitors (Biressi et al., 2007b).	Skeletal and muscular phenotype not examined. Expressed by muscle progenitors (Biressi et al., 2007b).	Skeletal and muscular phenotype not examined. Expressed by muscle progenitors (Biressi et al., 2007b).	Reduced and disorganized musculature (Messina et al., 2010). Kyphosis and reduced bone density (Driller et al., 2007).
Other	Abnormal ureteropelvic and ureterovesical junctions, bifid and megaureter (Lu et al., 2007).	-	Multiple tooth pathologies (Steele-Perkins et al., 2003). Wound healing defects (Plasari et al., 2009).	-

1.5.1 NFIB coordinates quiescence in melanocyte stem cells

The first of these studies (Chang et al., 2013) examined the role of NFIB in stem cells of the hair follicle niche. Previously, NFIB expression had been shown to be elevated in hair follicle stem cells (HFSCs) relative to their differentiated progeny (hair cell), which led the authors to hypothesize that NFIB might be a key regulator of this niche (Tumbar et al., 2004). Normal hair production occurs in three phases: anagen (growth), catagen (cessation) and telogen (quiescence). Upon initiation of a new hair cycle (anagen phase), HFSCs and melanocyte stem cells enter the cell cycle in synchrony, enabling hair growth and pigmentation. Conditional deletion of *Nfib* from HFSCs failed to lead to HFSC stem cell lineage defects; instead, surprisingly, it led to melanocyte lineage abnormalities at the niche base. Specifically, differentiated melanocytes were ectopically found in the stem niche during the quiescent telogen phase. The authors demonstrated that these ectopic cells were caused by the precocious proliferation and differentiation of melanocyte stem cells, demonstrating that NFIB expression in HFSCs inductively coordinates quiescence in the melanocyte stem cell population during hair cycling, significantly increasing our understanding of how synchronous stem cell proliferation and differentiation within this adult hair follicle niche is regulated. Interestingly the authors found that upregulation of a single NFIB target, *endothelin 2* (*Edn2*), identified through RNA-seq and ChIP-seq analyses was sufficient to phenocopy the effect of conditional *Nfib* deletion. As some endothelins such as *Edn3* are crucial molecules for melanocyte specification during embryogenesis (Baynash et al., 1994), it will be important to examine whether NFIs also function in melanocyte development. Moreover, defining the role of NFIs within cancers of the skin remains an open question, with an initial study having found *Nfib* to be amplified and/or present at oncogenic chromosomal breakpoints in the epithelial based small cell lung cancer (Dooley et al., 2011).

1.5.2 NFIX is a mediator of quiescence in neural stem cells

As with NFIB within the hair follicle niche, *in vitro* studies have recently implicated NFIX in mediating quiescence in neural stem cells (Martynoga et al., 2013). Due to the relative low turnover of stem cells in the adult brain, the majority of stem cells in the adult brain are quiescent (Suh et al., 2007). In an attempt to identify the transcription factors that regulate quiescence in adult neural stem cells, Martynoga and colleagues (2013), employed an *in vitro* model of neural stem cell quiescence. Specifically, they artificially induced a state of cellular quiescence by exposing highly proliferative neural stem cells derived from pluripotent embryonic stem cells to BMP4, a known cell-extrinsic mediator of adult neural stem cell quiescence (Mira et al., 2010; Sun et al., 2011). Epigenomic profiling was then used to identify active enhancer regions in both proliferating and

quiescent neural stem cells. Subsequent motif analysis demonstrated that the binding domain of NFI transcription factors was highly enriched in active enhancer regions of the quiescent neural stem cell population. Next, using ChIP-seq with a pan-NFI antibody, the authors demonstrated that NFI proteins bound to 73% of the quiescent specific-enhancers, and that one member of the NFI family, NFIX, was robustly induced in quiescent neural stem cells, whereas NFIA and NFIB were downregulated. These findings provided tantalizing evidence that NFIX actively regulates cellular quiescence within this paradigm, a hypothesis that was further supported by both gain-of-function experiments and by knockdown of *Nfix* expression through the use of RNAi molecules.

While this study strongly implicates NFIX as a central regulator of quiescence in neural stem cells, there are caveats to these findings. Firstly, modeling neural stem cell quiescence *in vitro* removes the influence of the cellular environment, which can dramatically alter stem cell behavior. Indeed, signals within the stem cell niches of the adult brain have been shown to greatly influence proliferation and differentiation of neural progenitor cells (Ming and Song, 2011). Moreover, as neural stem cell quiescence was modeled using a neural stem cell line originally derived from pluripotent embryonic stem cells, it is difficult to reconcile how closely the findings of this study resemble the epigenomic landscape of adult neural stem cells *in vivo*. The authors did attempt to address this limitation by examining the phenotype of the *Nfix* null mutants, and found a significantly reduced proportion of quiescent stem cells within the hippocampal dentate gyrus at P15. However, due to the significant developmental defects of this mutant line (see Table 1), it is difficult to definitively determine if the phenotype observed was due to a reduction in stem cell quiescence in the mutant, or was a reflection of the delayed maturation of the mutant dentate gyrus (Heng et al., 2014). Using conditional knockout models to specifically delete *Nfix* from quiescent adult neural stem cell populations *in vivo* (Chapter 5) will provide the data needed to determine if the findings in this *in vitro* model are recapitulated in the adult brain.

1.5.3 NFIX promotes survival of hematopoietic stem and progenitor cells

NFIX has also been shown to have a critical role in the survival of hematopoietic stem cells (HSCs) in adult bone (Holmfeldt et al., 2013). HSCs maintain hematopoiesis throughout life, self-renewing and also differentiating to give rise to all major lineages of the peripheral blood. Furthermore, after chemotherapy or irradiation, infused HSCs have the remarkable capacity to target the bone marrow stem cell niche and to repopulate the entire hematopoetic cellular cohort. Holmfeldt and colleagues (2013) found that NFIX was highly expressed in HSCs and that silencing of NFIX expression in

HSCs greatly reduced repopulation capacity in lethally irradiated mice. Molecular analyses demonstrated that this phenotype was not due to the inability of NFIX-depleted HSCs to target the niche, but rather was a result of increased levels of apoptotic cell death after establishment within the niche. Consistent with this, *Nfix* knockdown led to significant downregulation of genes associated with HSPC survival demonstrating that NFIX maintains the adult HSPC population post-transplantation by preventing apoptotic death through a cell-autonomous means. While these data clearly indicate a role for NFIX in survival of HSCs post-transplantation it is unclear whether *Nfix* is functionally important in steady-state (homeostatic) blood production. Indeed, because *Nfix* null mice survive up to 3 weeks after birth (see Table 1) this suggests that *Nfix* may be dispensable for homeostatic blood production. Conditional deletion of *Nfix* from HSCs *in vivo,* which will circumvent the premature lethality and skeletal defects of the *Nfix* null line would provide a suitable model to address this question.

Table 1.2: Summary of known expression and/or function of NFIs in adult stem cell populations.

	Nfia	*Nfib*	*Nfic*	*Nfix*
Adult neural stem cells	Expressed in stem cell niches of adult CNS. (Plachez et al., 2008; Plachez et al., 2012)	Expressed in stem cell niches of adult CNS. (Plachez et al., 2008; Plachez et al., 2012)	Expression not examined.	Expressed in stem cell niches of adult CNS. Implicated in neural stem cell quiescence. (Campbell et al., 2008; Martynoga et al., 2013)
Adult haematopoietic stem cells	Moderate-high expression in adult whole bone marrow. Loss of repopulating potential after knockdown (Holmfeldt et al., 2013).	Low expression. (Holmfeldt et al., 2013).	Moderate-high expression in adult whole bone marrow. (Holmfeldt et al., 2013).	Highly expressed in adult bone marrow. Promotes survival of HSCs and thereby repopulating potential. (Holmfeldt et al., 2013).
Hair follicle	No increase in transcript levels within HFSCs relative to progeny (Tumbar et al., 2004).	Transcript levels are elevated in HFSCs relative to progeny. (Tumbar et al., 2004). (Tumbar et al). Coordinates quiescence in melanocyte stem cells (Chang et al., 2013).	No increase in transcript levels within HFSCs relative to progeny (Tumbar et al., 2004).	No increase in transcript levels within HFSCs relative to progeny (Tumbar et al., 2004).
Adult muscle progenitors (satellite cells)	Expression unknown.	Expression unknown.	Expression unknown.	Expression unknown.

1.6 Conclusions

1.6.1 NFI function during development versus NFI function in adult stem cells

While further testing of the different NFI factors across a broader range of adult stem cell niches is required, initial loss- or gain-of-function experiments suggest that NFIs serve to mediate quiescence and/or survival of adult stem cell populations (Chang et al., 2013; Holmfeldt et al., 2013; Martynoga et al., 2013). These findings appear inconsistent with one of the major functions of NFI factors during development, which is to promote stem and progenitor cell differentiation. What could account for the unexpected findings from these studies? The simplest explanation is that NFI factors or a subset of NFI factors regulate different sets of genes in adult stem cells compared with stem and progenitor populations during development. For example, instead of regulating sets of genes that promote differentiation during development, NFI factors may repress gene expression associated with cell cycle progression and activate genes associated with cellular survival in adult stem cell populations. A powerful way to test this hypothesis could use next-generation sequencing techniques such as ChIP-seq on embryonically derived stem and progenitor cell populations, and comparing these datasets with those ChIP-seq experiments performed on stem and progenitor populations isolated from adult tissue. A second potential way to test the hypothesis that NFI factors function differently in developmental versus adult contexts would be to examine pathologies in cancers of differential origin. For example, if NFIs drive differentiation during development, then it is a strong possibility that inactivating mutations in *Nfi* genes will be identified in developmental based cancers. Indeed, as discussed in this review, there are a number of recent studies that have shown a potential role for inactivating mutations in NFIs in driving tumorigenesis in medulloblastoma, the most common childhood brain cancer (Wu et al., 2012; Genovesi et al., 2013; Lastowska et al., 2013). It might therefore be interesting to determine whether NFIs act as oncogenes in adult-derived cancers, particularly as these cancers are thought to be caused by deregulated or chronic repair mechanisms, whereby stem cells are recruited to repopulate tissues. Currently, however, there are only a limited number of examples in which NFIs have been identified as putative oncogenes such as small cell lung cancer (Dooley et al., 2011) and glioblastoma (Glasgow et al., 2013). Furthermore, this approach is limited in that the mutant state of most cancers may obfuscate the function of NFIs in healthy tissue, thus a more fruitful approach to understand the differences in NFI function across developmental and adult contexts might be to

introduce targeted mutations in a temporally controlled manner using conditional and inducible technologies.

Are there any phenotypic similarities in the NFI loss-of-function experiments performed during development *versus* those in adult stem cell niches? A common phenotype observed in *Nfi* null mice during development and in loss-of-function experiments performed in adult tissue is an initial increase in the number of proliferating cells. Considering the stem cell differentiation defects of *Nfi* null mice, this increase in proliferating cells during development is at least in part due to increased self-renewal, and delayed differentiation; however, no experiments have directly tested whether the cell cycle is also deregulated amongst these stem cell populations, which could also contribute to the overall developmental phenotype of the null mice. Future research aimed at establishing to what extent (if any) NFIs directly regulate aspects of cell-cycle dynamics during development, akin to what is observed in the adult, may therefore provide further insight into the various differences and similarities in NFI function across developmental and adult contexts, thereby informing our understanding of the role of NFIs in stem cell biology more broadly, and the involvement of these transcription factors in developmental disorders and cancer.

Chapter 2 Production of transgenic mouse strains

2.1 Aims of Chapter 2

The aim of this chapter is to describe the various mouse strains bred and used in this thesis. Included within, is a description of how I removed a contaminating neomycin cassette from the *Nfix*$^{f/f}$ mouse strain that was interfering with normal *Nfix* expression. A description of other experimental methods, for example antibody staining, imaging and analysis are found in each data chapter so that chapter-specific protocols can be described.

2.2 Transgenic animals

There were several genetically modified mouse lines used in this thesis, these were all maintained on a C57BL/6J background. Genotyping primers are found in Table 2.1 of this chapter. All experimental protocols were performed with the approval of The University of Queensland Animal Ethics Committee in accordance with the Australian Code of Practice for the Care and Use of Animals for Scientific Purposes.

2.2.1 *Nfix* knockout line

Mice from this strain contain a null *Nfix* allele (Campbell et al., 2008). Homozygous null ($Nfix^{-/-}$) and wild-type animals were generated from crossing heterozygous studs and dams. $Nfix^{-/-}$ mice are not viable past P20. This strain of mice was a kind gift from our collaborator Richard M. Gronostajski at the University of New York, Buffalo, USA. PCR genotyping resulted in a 309 base-pair band for the knockout allele, and a 213 base-pair band for wild-type allele.

2.2.2 $Nfix^{f/f}$ line

Animals from this strain contain *loxp* sites flanking exon 2 of the *Nfix* gene (*floxed* allele), enabling conditional deletion of this exon through *cre*-recombinase activity to render a null allele (Messina et al., 2010). These animals also contain a neomycin cassette 5' to the 3' *loxp* site, a by-product of the cloning procedure. Unfortunately, I found the presence of the neomycin cassette resulted in a global reduction in NFIX expression independent of *cre* activity (Figure 2.1). Removal of this neomycin cassette returned NFIX expression to wild-type levels and is described in Section 2.3 '*Removal of the neomycin cassette from* $Nfix^{f/f}$ *mice*'. These mice were a kind gift from our collaborator Richard M. Gronostajski at the University of New York, Buffalo, USA. PCR genotyping resulted in a 421 band for the *floxed* allele (neomycin removed), and a 203 band for wild-type allele.

The FlpeR mouse line expresses the FLPe variant of the *Flp1*-recombinase gene driven by the ubiquitous human *Rosa26* promoter, enabling efficient, germline transmitted deletion of FRT-flanked DNA sequences (Raymond and Soriano, 2007). These mice were purchased from The Jackson Laboratory. PCR genotyping resulted in a 725 base-pair band for the *Flp* allele, and a 500 base-pair band for wild-type allele.

The construct used to generate the *Nfix*$^{f/f}$ mouse strain contained a neomycin cassette. This neomycin cassette was not removed at the embryonic stem cell stage, and as a result the transgenic *Nfix*$^{f/f}$ mouse line retained this cassette. Despite being in reverse transcriptional orientation to the *Nfix* gene, immunostaining with a NFIX antibody revealed that these mice had a dramatic reduction in NFIX expression compared to controls (Figure 2.1). This reduction in NFIX expression was concerning, as we had previously described that low NFIX expression during development (in a mouse line heterozygous for a null *Nfix* allele) results in morphological brain defects and behavioural abnormalities in adult mice (Harris et al., 2013). We hypothesised that the reduced NFIX expression was likely due to the presence of the neomycin cassette causing transcriptional interference, based on similar reports in the literature where the neomycin cassette was also shown to affect the expression of other transgenes (Bader et al., 2011). To remove the neomycin cassette, which is flanked by *frt* sequences, I crossed *Nfix*$^{f/f}$ mice to the *Flp-frt* driver mouse line (2.2.3). In this mouse line, *flp-recombinase* is ubiquitously expressed, allowing for the germline deletion of *frt* flanked genomic sequences. After crossing the *Nfix*$^{f/f}$ line to the *Flp-frt strain*, and then in-crossing the F1 generation, I selected mice that were homozygous for the *Nfix* conditional allele (*Nfix*$^{f/f}$) but negative for *Flp.* These F2 mice had normal levels of NFIX expression (Figure 2.2), and were subsequently used throughout this thesis to cross to different *cre*-recombinase drivers, and reporter mouse lines.

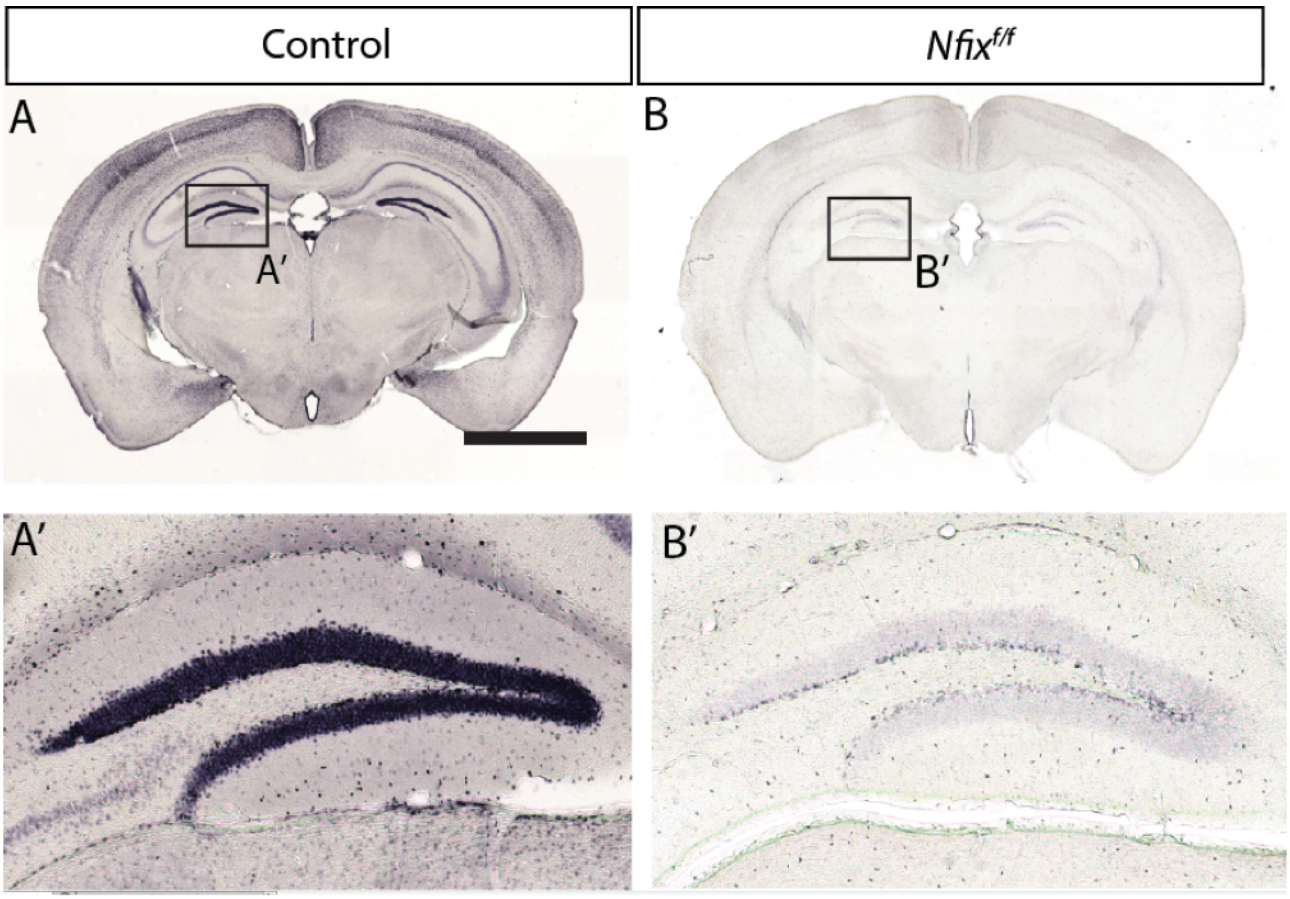

Figure 2.1: *Nfix*$^{f/f}$ mice retaining a neomycin cassette have reduced expression of NFIX compared to control animals

(**A**, **B**) NFIX DAB immunohistochemistry performed on the brains of 10-week old C57Bl/6 control (**A**) and *Nfix*$^{f/f}$ mice retaining a neomycin cassette (**B**). Boxed regions in **A** and **B** are shown in **A'** and **B'** respectively, and show the levels of NFIX expression within the hippocampal dentate gyrus. Scale bar (in **A**): **A**, **B** 5mm; **A'**, **B'** 300μm,

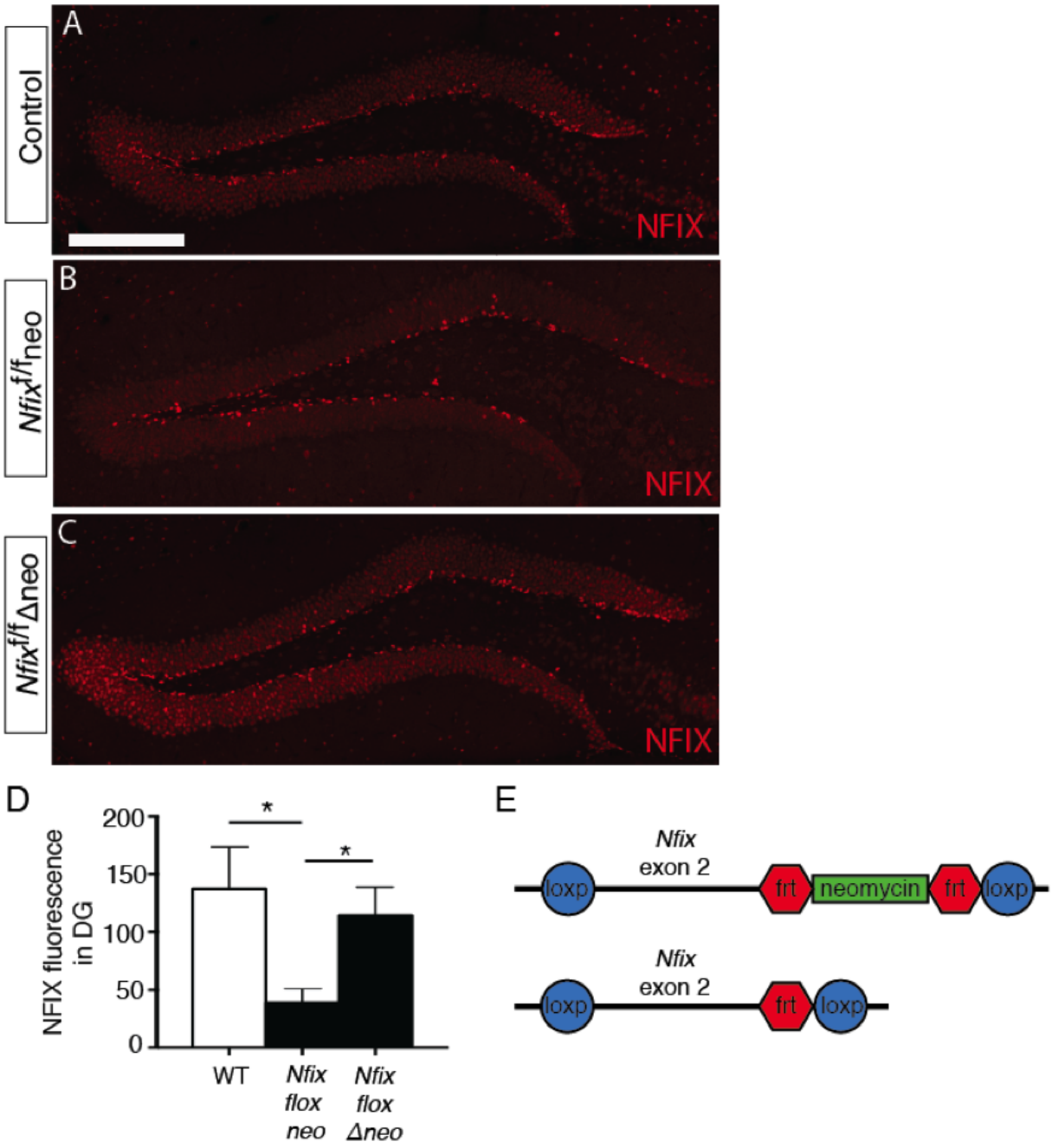

Figure 2.2: Removal of the neomycin cassette from *Nfix*$^{f/f}$ mice restores NFIX expression to control levels.

(**A-C**) The dentate gyrus of 10-week old (**A**) control, (**B**) *Nfix*$^{f/f}$ neo, (**C**) *Nfix*$^{f/f}$ Δneo stained for NFIX (red). *Nfix*$^{f/f}$ neo mice contain the conditional *Nfix* allele with the neomycin cassete, and *Nfix*$^{f/f}$ Δneo mice have this cassette removed (**D**) Quantification of NFIX fluorescence intensity in the dentate gyrus (DG) of control, *Nfix*$^{f/f}$ neo and *Nfix*$^{f/f}$ Δneo animals. (**E**) Schematic of *Nfix*$^{f/f}$ allele before and after FLP-mediated deletion of neomycin. Scale bar (in **A**): A-C 300µm.

2.2.3 *Nestin-creER^{T2}*

The *nestin*-creER^{T2} mouse strain expresses a *cre*-recombinase protein fused to an estrogen receptor domain, under the control the rat *nestin* gene promoter. The modified *cre*-recombinase gene is expressed in nestin-positive cells but is restricted to the cytoplasm. Upon administration of the estrogen receptor agonist tamoxifen, the *cre*-recombinase relocates to the nucleus where it acts as a site-specific nuclease. There are several independently generated *nestin*-creER^{T2} mouse strains that exist (Sun et al., 2014). This strain was generated by Imayoshi and colleagues (2006) and uses 5.8 kb of the rat nestin promoter and 1.8 kb spanning the second intron. Compared with the two other most commonly used *nestin*-creER^{T2} mouse strains (Lagace et al., 2007; Dranovsky et al., 2011; Sahay et al., 2011), this strains shows intermediate specificity and intermediate efficiency (Sun et al., 2014). PCR genotyping resulted in a 340 bp band if the *nestin*-creER^{T2} allele was present, and no band appears in wild-type mice negative for the transgene.

2.2.4 *Dcx-creER^{T2}*

The *dcx-creER^{T2}* mouse strain expresses a *cre*-recombinase protein fused to an estrogen receptor domain, under the control the mouse *dcx* gene promoter. The modified *cre*-recombinase gene is expressed in dcx-positive cells but is restricted to the cytoplasm. Upon administration of the estrogen receptor agonist tamoxifen, the *cre*-recombinase relocates to the nucleus where it acts a site-specific nuclease. The line was generated using a bacterial artificial chromosome clone (RP23-462G16, Rosewall Park Cancer Institute) that contained the *dcx* gene (90 kb), comprised of 30 kb upstream and 60 kb downstream of the *dcx* gene locus (Cheng et al., 2011). PCR genotyping amplified a 500 bp band if the *dcx-creER^{T2}* allele was present. No band was amplified from the DNA of wild-type mice.

2.2.5 *tdtomato cre*-lox reporter

The *tdtomato cre*-lox reporter strain (*Gt*(ROSA)26Sor$^{tm9(CAG\text{-}tdTomato)Hze}$) harbors a loxP-flanked STOP codon that prevents the transcription of a CAG-promotor driven fluorescent protein called tdtomato (Madisen et al., 2010) Upon *cre*-recombinase mediated deletion of the stop codon, the tdtomato protein is expressed. This mouse strain was used in this study to enable the permanent marking of cells and their progeny after activation of *cre*-recombinase. PCR genotyping resulted in a 196 base-pair band for the *tdtomato* allele, and a 297 base-pair band for the wild-type allele.

2.3 Breeding of transgenic animals for experimental analyses

Of the transgenic lines described above in 1.2, many were bred together to generate double or triple transgenic lines. A brief description of how these lines were bred and the precautions taken are described below.

2.3.1 *Nfix*^{iNestin}

The *Nfix*^{iNestin} double transgenic strain was generated by crossing *Nfix*$^{f/f}$ mice with the *nestin-creER*^{T2} line. To generate experimental animals the following cross was used:

$$Nfix^{f/f} \; x \; Nfix^{f/f}; \text{nestin-creER}^{T2}$$

By ensuring that only one parent was positive for the *nestin-creER*^{T2} transgene all progeny could be used for experimental analyses, with 50% of animals being *cre*-positive (treatment animals) and the other 50% of animals being *cre*-negative (control animals). This also meant that mice had at maximum one copy (heterozygous) of the *nestin-creER*^{T2} transgene. Maintaining heterozygosity for this transgene was an important way of minimising any potential impact that the *nestin-creER*^{T2} transgene has on the transcription of endogenous genetic elements.

2.3.2 *Nfix*$^{iNestin\text{-}TD}$

The *Nfix*$^{iNestin\text{-}TD}$ triple transgenic strain was generated by crossing the *Nfix*$^{f/f}$ mouse line, with the *nestin*-creER^{T2} and *tdtomato cre*-lox reporter strain. The final cross that was used to generate experimental animals is as follows:

$$Nfix^{f/WT}; \text{tdtom}^{f/f} \; x \; Nfix^{f/WT}; \text{tdtom}^{f/WT}; \textit{nestin-creER}^{T2}$$

Treatment animals were homozygous for the floxed *Nfix* allele, *cre*-positive, and heterozygous or homozygous for the *tdtomato* reporter. Because of the brightness of the tdtomato protein, the ability to detect reporter-positive cells was not affected by whether a mouse was heterozygous or homozygous for the *tdtomato* allele. Approximately 1 in 8 live births were this genotype. The control animals were wild-type for the *Nfix* allele, *cre*-positive, and heterozygous or homozygous for the *tdtomato* reporter. Again, approximately 1 in 8 live births were this genotype.

2.3.3 *Nfix*^{iDcx}

The *Nfix*^{iDcx} double transgenic strain was generated by crossing *Nfix*$^{f/f}$ mice with the *dcx-creER*^{T2} line. To generate experimental animals the following cross was used:

$$Nfix^{f/f} \; x \; Nfix^{f/f}; dcx\text{-}creER^{T2}$$

By ensuring that only one parent was positive for the *dcx-creER*^{T2} transgene all progeny could be used for experimental analyses, with 50% of animals being *cre*-positive (treatment) and the other 50% *cre*-negative (control animals). This also meant that mice had at maximum one copy (heterozygous) of the *dcx-creER*^{T2} transgene. Maintaining heterozygosity for this transgene was an important way of minimising any potential impact that the *dcx-creER*^{T2} transgene has on the transcription of endogenous genetic elements.

2.3.4 *Nfix*$^{iDcx\text{-}TD}$

The *Nfix*$^{iDcx\text{-}TD}$ triple transgenic strain was generated by crossing the *Nfix*$^{f/f}$ mouse line, with the *dcx-creER*^{T2} and *tdtomato cre*-lox reporter strain. The final cross that was used to generate experimental animals is as follows:

$$Nfix^{f/WT}; tdtom^{f/f} \; x \; Nfix^{f/WT}; tdtom^{f/WT}; dcx\text{-}creER^{T2}$$

Treatment animals were homozygous for the floxed *Nfix* allele, *cre*-positive, and heterozygous or homozygous for the *tdtomato* reporter. Because of the brightness of the tdtomato protein, the ability to detect reporter-positive cells was not affected by whether a mouse was heterozygous or homozygous for the *tdtomato* allele. Approximately 1 in 8 live births were this genotype. The control animals were wild-type for the *Nfix* allele, *cre*-positive, and heterozygous or homozygous for the *tdtomato* reporter. Again, approximately 1 in 8 live births were this genotype.

2.4 Transgenic strains donated by collaborators

Collaborating scientists donated fixed brain tissue for two transgenic strains used in this thesis. Professor Richard Gronostajski donated the *Nfib*$^{f/f}$; *Nfix*$^{f/f}$; *Rosa26creER*^{T2} brains used in Chapter 3 (Messina et al., 2010; Hsu et al., 2011), and Dr Dhanisha Jhaveri the *Hes5*::GFP (Basak and Taylor, 2007) brains used in Chapter 4.

Table 2.1: Genotyping primers used in thesis.
PCR protocol parameters were determined according to standard procedures of determining annealing temperature and predicted amplicon size (see section 2.2).

Primer set	**Sequence**
***Nfix* KO strain**	
Nfix IF5	ATGGACATGTCATGGGTGCGA
Nfix IR1	AACCAGAGGCACGAGAGCTT
Nfix I2R2 KO	AAGCCCCTCAGCTCTAGCACAGAG
***Nfix*$^{f/f}$ strain (neomycin removed)**	
Nfix I2F1	TAGTTGGGATCTGGCATATGAGG
Nfix 12R2 KO	AAGCCCCTCAGCTCTAGCACAGAG
***Nestin-creER*^{T2} strain**	
Nestin-creER^{T2} forward	TAATCGCGAACATCTTCAGGTTCTGC
Nestin-creER^{T2} reverse	TTCCGCTGGGTCACTGTCGCCGCTAC
***Dcx-creER*^{T2} strain**	
Dcx-creER^{T2} forward	GGGTATTCCCTGGAGGCTG
Dcx-creER^{T2} reverse	TTCTTGCGAACCTCATCACT
***tdtomato cre-lox* reporter strain**	
Wild-type forward	AAG GGA GCT GCA GTG GAG TA
Wild-type reverse	CCG AAA ATC TGT GGG AAG TC
Mutant forward	GGC ATT AAA GCA GCG TAT CC
Mutant reverse	CTG TTC CTG TAC GGC ATG G
***Flp-Frt* strain**	
Wild-type forward	TGT TTT GGA GGC AGG AAG CAC TTG
Wild-type reverse	AAA TAC TCC GAG GCG GAT CAC AAG
Mutant forward	CAC TGA TAT TGT AAG TAG TTT GC
Mutant reverse	CTA GTG CGA AGT AGT GAT CAG G

Chapter 3 Transcriptional regulation of intermediate neuronal progenitor production by NFIX during hippocampal development

3.1 Aims of Chapter 3

The aim of this chapter is to refine our understanding of how NFI transcription factors function in regulating neurogenesis in the developing dorsal telencephalon of mice. Previous studies had demonstrated that *Nfia*$^{-/-}$, *Nfib*$^{-/-}$ and *Nfix*$^{-/-}$ mice all have delayed neuronal differentiation in this brain region. However, it was unclear at what point from the transition of radial glial stem cell to a mature neuron is affected in these mice. Based on published data, in this chapter I pursue the hypothesis that NFIs may function to promote the production of intermediate neuronal progenitor cells (IPCs) from radial glia during development. This hypothesis aligns with published histological data of *Nfi*$^{-/-}$ mice where elevated numbers of radial glia but fewer IPCs were seen during early development. This hypothesis also predicts that long-term, the increased stem cell numbers would results in more neurons; thus, I was attracted to this hypothesis as it had the potential to explain the postnatal macrocephaly exhibited by *Nfix*$^{-/-}$ mice and humans with *NFIX* mutations. Finally, this chapter also seeks to find a transcriptional target common to NFIA, NFIB and NFIX that could account (at least partially) for the role of NFIs in promoting IPC production.

The text in the following chapter was published in the journal *Development*, on December 16, 2016.

Harris L, Zalucki O, Gobius I, McDonald H, Osinki J, Harvey TJ, Essebier A, Vidovic D, Gladwyn-Ng I, Burne TH, Heng JI, Richards LJ, Gronostajski RM, Piper M. 2016a. Transcriptional regulation of intermediate progenitor cell generation during hippocampal development. Development 143:4620-4630.

3.2 Abstract

During forebrain development radial glia generate neurons through the production of intermediate progenitor cells (IPCs). The production of IPCs is a central tenet underlying the generation of the appropriate number of cortical neurons, but the transcriptional logic underpinning this process remains poorly defined. Here, we examined IPC production using mice lacking the transcription factor *nuclear factor one x* (*Nfix*). We show that *Nfix* deficiency delays IPC production and prolongs the neurogenic window, resulting in an increased number of neurons in the postnatal forebrain. Loss of additional *Nfi* alleles (*Nfib*) resulted in a severe delay in IPC generation, and conversely overexpression of NFIX led to precocious IPC generation. Mechanistically, analyses of microarray and ChIP-seq datasets, coupled with the investigation of spindle orientation during radial glial cell division, revealed that NFIX promotes the generation of IPCs via the transcriptional upregulation of *inscuteable* (*Insc*). These data thereby provide novel insights into the mechanisms controlling the timely transition of radial glia into IPCs during forebrain development.

3.3 Introduction

The coordinated proliferation and lineage-specific differentiation of neural progenitor cells plays an integral role in the formation of the mammalian cerebral cortex. The primary neural progenitor cells that generate the neurons of this structure are the radial glia, which develop from neuroepithelial cells around embryonic day (E) 10.5 in rodents (Anthony et al., 2004; Mori et al., 2005). Since the large number of neurons generated during development comes from a relatively small initial population of progenitor cells, the radial glial cell pool is first amplified by undergoing symmetric proliferative divisions, also known as self-expanding divisions. Subsequently, radial glial cells undergo asymmetric divisions to give rise to either a neuron that migrates directly to the cortical plate (direct neurogenesis), or, more frequently, an IPC (indirect neurogenesis) (Gotz and Huttner, 2005; Huttner and Kosodo, 2005). IPCs are morphologically different from radial glia in that they are delaminated from the adherens junctional belt at the ventricular surface of the brain (Noctor et al., 2004). The majority of cortical neurons arise through the production, expansion and differentiation of IPCs (Haubensak et al., 2004; Sessa et al., 2008).

The timely generation of IPCs is required for normal neuron number in the postnatal brain. Despite the importance of IPCs, our understanding of the mechanism by which asymmetric division of radial glia is coordinated to ensure timely IPC production is limited. In the classical model of neural stem cell division, inferred largely from work in *Drosophila melanogaster* (*D. melanogaster*), large changes in spindle orientation result in the asymmetric inheritance of the apical membrane into one daughter cell and an asymmetric cell fate (Knoblich, 2008). However, the vast majority of radial glial cell cleavage planes in the mammalian telencephalon are perpendicular to the ventricular surface, and deviate only slightly from this angle. As a result, the apical membrane typically segregates into both daughter cells (Konno et al., 2008; Asami et al., 2011; Shitamukai et al., 2011). Therefore, it is unlikely that unequal segregation of the apical membrane accounts for IPC and neuron generating divisions in the mammalian cortex. Rather, one proposed model is that small fluctuations in cleavage plane orientation [reviewed in (Matsuzaki and Shitamukai, 2015)] leads to changes in cell volume and intracellular organelle inheritance to promote IPC production (Wang et al., 2009).

The argument that small fluctuations in spindle orientation promote IPC production largely comes from loss and gain-of-function studies of the mammalian homolog of the *D. melanogaster* adaptor protein, Inscuteable (INSC) (Konno et al., 2008; Postiglione et al., 2011; Petros et al., 2015). INSC

regulates the spindle orientation of radial glia and IPC production in a gene dose-dependent manner, whereby loss of *Insc* reduces oblique divisions and IPC number, and a high level of *Insc* increases oblique divisions and IPC number (Postiglione et al., 2011; Petros et al., 2015). Currently, it remains unclear whether INSC-dependent spindle orientation directly regulates IPC production or whether another INSC-dependent mechanism might regulate the development of IPCs. However, a pivotal question that arises from these data, is how is *Insc* expression itself regulated during cortical development to facilitate IPC development?

Transcription factors of the Nuclear factor one (*Nfi*) family (*Nfia, Nfib, Nfix*) play a crucial role in astrogliogenesis. Mice lacking *Nfix* exhibit markedly reduced numbers of astrocytes throughout the embryonic cerebral cortex and cerebellum (Piper et al., 2011; Heng et al., 2014). In addition to promoting astrocyte lineage progression, individual *Nfi* knockout mice also exhibit elevated numbers of progenitor cells and delayed expression of neuronal markers within the ammonic neuroepithelium of the presumptive hippocampus during embryonic development (Piper et al., 2010; Heng et al., 2014; Piper et al., 2014). From these findings we posited that NFIs could play a previously unrecognised role in the production of IPCs. Here, we use the ammonic neuroepithelium of mice lacking *Nfix* and *Nfib* as a model to investigate this hypothesis. We demonstrate that NFIs are autonomously required by radial glia for timely IPC production, and that NFIs directly activate the expression of *Insc,* providing a novel insight into the cellular processes governing the transition of radial glial cells to IPCs during hippocampal development.

3.4 Methods

3.4.1 Animal ethics

The work performed in this study conformed to The University of Queensland's Animal Welfare Unit guidelines for animal use in research (AEC approval numbers: QBI/353/13/NHMRC and QBI/355/13/NHMRC/BREED) and those of the Institutional Animal Care and Use Committee (IACUC) at the University of Buffalo, New York, USA. All experiments were performed in accordance with the Australian Code of Practice for the Care and Use of Animals for Scientific Purposes, and were carried out with approval from The University of Queensland Institutional Biosafety committee.

3.4.2 Animals

Nfix$^{-/-}$ and *Nfix*$^{+/+}$ littermates used in this study have been described previously (Campbell et al., 2008). Conditional *Nfix* and *Nfib* alleles, each of which contain *loxp* sites flanking the respective exon 2 of the gene were generated as described previously (Messina et al., 2010; Hsu et al., 2011). The conditional lines were then bred together to produce the double conditional strain (*Nfix*$^{fl/fl}$; *Nfib*$^{fl/fl}$), which was subsequently crossed to *Rosa26-creER*^{T2} mice (#008463, The Jackson Laboratory). Animals of either sex were used.

3.4.3 Immunofluorescence and immunohistochemistry

Embryos were immersion-fixed at E14.5 or younger in 4% PFA or perfused transcardially (E15.5 and older) with phosphate-buffered saline (PBS), followed by 4% PFA, then post-fixed for 48-72 h before long term storage in PBS at 4°C. Brains were embedded in noble agar and sectioned in a coronal plane at 50 µm using a vibratome (Leica, Deerfield, IL). Sections were mounted on slides before heat-mediated antigen retrieval was performed in 10 mM sodium-citrate solution at 60°C for 20 min (for GFP and TBR2 immunostaining) or 95°C for 15 min (for all other co-immunostaining). A standard fluorescence immunohistochemistry protocol was then performed. Briefly, sections were covered in a blocking solution for 2 h containing 2% normal serum and 0.2% Triton-X-100 made in PBS. The primary antibodies were diluted in this blocking solution and incubated with the sections overnight at 4°C. The following day the primary antibodies were detected with fluorescently conjugated secondary antibodies diluted in block for 2 h. When dual or triple labelling was being performed the secondary antibodies used were derived from the same species to prevent

cross-species reactivity. Sections were then counterstained with DAPI (Invitrogen, Carlsbad, CA) and coverslipped using DAKO fluorescent mounting media. Chromogenic immunohistochemistry using 3,3'-diaminobenzidine was performed as above but with a goat anti-rabbit biotin-conjugated secondary antibody. The reaction was visualised by incubating the sections in avidin-biotin complex (ABC elite kit; Vector Laboratories, Burlingame, CA) for 1 h, followed by a nickel-DAB solution, and was terminated by washing multiple times in PBS when a purple precipitate had formed.

The primary rabbit species antibodies used were anti-PAX6 (AB2237 1/400, Millipore, Billerica, MA), anti-NFIX (AB101341 1/500, Abcam Cambridge, UK), anti-NFIB (HPA003956 1/200 Sigma-Aldrich, St Louis, MO) anti-PHH3 (#06-570 1/200, Millipore), anti-NeuN (EPR12763 1/800, Abcam), anti-TBR2 (ab23345, 1/800, Abcam) and anti-INSC (gift from Juergen Knoblich) (Zigman et al., 2005). The primary mouse species antibodies used were anti-BrdU (G3G4 1/100, DHSB, Iowa city, IA), anti-NFIX clone 3D2 (SAB1401263 1/400, Sigma-Aldrich), anti-NeuN (MAB377 1/150, Millipore) and anti-alpha-tubulin (ab7291 1/400 Sigma-Aldrich). The primary rat species antibodies used were anti-Ki67 FITC clone SolA15 (11-5698-80 1/400, San Diego, CA), anti-EOMES (TBR2) Alexa Fluor® 488 (53-4875-82 1/400, Ebioscience). The primary chicken species antibody used was anti-GFP (A10262, 1/500, Thermo Fisher Scientific).

3.4.4 *Nfix*$^{-/-}$ mouse hippocampal cell counts

For counts of PAX6^{+ve}; TBR2^{-ve} nuclei and TBR2^{+ve} nuclei the number of immunopositive cells from two 100 µm sampling fields, spanning the width of the hippocampal primordium, positioned along the medial to lateral extent of the hippocampal ammonic neuroepithelium (E13.5-E18.5) or neocortex (E18.5) were counted. This analysis was completed at two different levels along the rostrocaudal axis for each brain examined. Fluorescent images were captured using a 20X objective on a Zeiss inverted Axio-Observer fitted with a W1 Yokogawa spinning disk module and Hamamatsu Flash4.0 sCMOS camera using 3i Slidebook software (Denver, CO).

3.4.5 *Nfix*$^{-/-}$ mouse birth-dating experiments

Two birth-dating experiments were performed with 5-bromo-2'deoxyuridine (BrdU, Sigma-Aldrich) in this study. In the first experiment, pregnant dams were injected with low-dose (50 mg/kg) or high-dose (200 mg/kg) BrdU at E13.5 and embryos were perfused 24 h or 48 h later, respectively. The 200 mg/kg dose, while high, has been used in previous studies (Kempermann et

al., 1997; Cameron and McKay, 2001; Seib et al., 2013) and was demonstrated to be within the upper range of acceptable doses for such experiments (Wojtowicz and Kee, 2006). This dose of BrdU ensured the continued labelling of radial glia despite multiple rounds of cellular division during this period. The number of $BrdU^{+ve}$ cells that labeled as $PAX6^{+ve}$; $TBR2^{-ve}$ or $Ki67^{-ve}$ at E15.5 was calculated as a proportion of the total number of $BrdU^{+ve}$ cells. Cell counts were performed from two 100 μm sampling fields spanning the width of the hippocampal primordium at two different levels along the rostrocaudal axis of the ammonic neuroepithelium. Fluorescent sections for this experiment were imaged using a 40X objective on a spinning disk confocal microscope. In the second birth-dating experiment, pregnant dams were injected with a standard dose (50 mg/kg) of BrdU at E18.5 and the resulting litter was collected at P20. This dose of BrdU was sufficient to label neurons generated at E18.5. The total number of $BrdU^{+ve}$; $NeuN^{+ve}$ cells in CA neuronal layers, and layer II/III of the neocortex was then calculated from a 100 μm sampling field. For the CA counts this was performed on three different levels along the rostrocaudal axis of the brain, in both the CA1 and CA3 neuronal layer and averaged. The neocortical counts were performed on single section at the level of the corpus callosum. Fluorescent sections for this experiment were imaged using a 20X objective on a spinning disk confocal microscope. For both birth-dating experiments the pattern of BrdU staining depended on the chromatin structure at time of fixation, and was pan-nuclear during S-phase or in post-mitotic cells, and punctate during G2/M phase, thus $BrdU^{+ve}$ cells were scored as any nuclei showing nuclear immunoreactivity regardless of the staining pattern.

3.4.6 Measurement of cell cycle kinetics in *Nfix*$^{-/-}$ radial glia

The mean total cell cycle (T_C) and synthesis (S) phase duration (T_S) of radial glia in the ammonic neuroepithelium at E14.5 was determined using a dual-pulse labeling protocol modified from the methodology presented by Martynoga and colleagues (2005). Briefly, pregnant dams were injected with 50 mg/kg of 5-ethynyl-2'-deoxyuridine (EdU), followed 1 h later with 50 mg/kg BrdU. At 1.5 h post-EdU injection the dam was sacrificed and embryos immersion-fixed in 4% PFA. Sections were stained for BrdU, EdU, TBR2 and DAPI. Fluorescent sections were imaged using a 40X objective on a spinning disk confocal microscope, and cell counts were performed from two 100 μm sampling fields at each of two different levels along the rostrocaudal axis per brain (Supp Fig. 3.6). Radial glia were then identified as $TBR2^{-}$ nuclei located in the ventricular zone. The pattern of BrdU and EdU staining depends on the chromatin structure at time of fixation, and is pan-nuclear during S-phase, and punctate during G2/M phase. $BrdU^{+ve}$ and EdU^{+ve} radial glia were therefore scored as any nuclei showing immunoreactivity for these markers regardless of the staining pattern.

The T_S of radial glia is equal to the injection interval of 1 h multiplied by the ratio of radial glia that remain in S-phase to the number of radial glia that leave S-phase prior to BrdU injection, given by the equation $T_S = 1*(EdU^{+ve}; BrdU^{+ve}/EdU^{+ve}; BrdU^{-ve})$. The T_C of radial glia is equal to T_S divided by the proportion of radial glia that are in S-phase, given by the equation $T_c = T_S/(BrdU^{+ve}/BrdU^{-ve})$.

3.4.7 Measurement of cleavage plane orientation in *Nfix*$^{-/-}$ radial glia

To analyse cleavage plane orientation within radial glia, we stained sections with phospho-histone H3 (PHH3), alpha-tubulin and with DAPI. Sections were imaged using a 63X objective on a spinning disk confocal microscope through a depth of 10 µm (consecutive 1 µm z-steps). Hippocampal radial glia undergoing mitosis were identified as PHH3^{+ve} cells located at the ventricular surface of the ammonic neuroepithelium. For each cell 3 angle measurements were taken from adjacent z stacks and averaged. Because the metaphase plate of radial glia rocks extensively until anaphase (Haydar et al., 2003; Sanada and Tsai, 2005), only cells that were in anaphase or telophase were analysed, as revealed by chromosomal (DAPI and PHH3 staining) and mitotic spindle arrangement (alpha-tubulin staining). We measured cleavage plane orientation by the angle created by the vector that runs parallel to the ventricular surface and the vector that runs through the cleavage plane of the dividing cell.

3.4.8 *In utero* electroporation

In utero electroporation was performed as previously described (Suarez et al., 2014), with minor modifications whereby 0.5-1 µl of plasmid DNA was injected into one lateral ventricle and electroporated caudomedially into the presumptive hippocampus using 35 V. Plasmid expression constructs were pCAG IRES GFP (pCAGIG) or NFIX pCAG IRES GFP (NFIX pCAGIG). For the rescue experiment, g*Nfix*-CAS9, *glacZ*-CAS9, INSC pCAGIG and pCAGIG constructs were used. For details of plasmid construction, see plasmid construction in methods.

3.4.9 *Nfix*$^{fl/fl}$*; Nfib*$^{fl/fl}$; *Rosa26-creER*^{T2} tamoxifen treatment and cell analysis

Nfix$^{fl/fl}$; *Nfib*$^{fl/fl}$ dams time-mated to *Nfix*$^{fl/fl}$; *Nfib*$^{fl/fl}$; *cre* sires were injected with 2 mg of tamoxifen dissolved in corn oil (10 mg/ml) at E10.5 and E11.5, and the embryos were collected at E15.5 and immersion-fixed in 4% PFA. Quantification and imaging of total hippocampal PAX6^{+ve}; TBR2^{-ve} nuclei and TBR2^{+ve} nuclei was performed from two 100 µm sampling fields spanning the width of

the hippocampus from two different levels along the rostrocaudal axis of the ammonic neuroepithelium. Fluorescent sections were imaged for this experiment using a 20X objective on a spinning disk confocal microscope. For analysis of NFIX^{-ve}; NFIB^{+ve} clones in the hippocampus of *Nfix*$^{fl/fl}$; *Nfib*$^{fl/fl}$; *cre* mice, sections were imaged using a 40X objective, on a spinning disk confocal microscope, through a depth of 10 μm (consecutive 1 μm z-steps). The z-stack was then flattened and the analysis was performed so that the proportion of NFIB^{+ve} nuclei expressing TBR2 in the VZ/SVZ was compared to an adjacent region where VZ/SVZ nuclei were NFIX^{-} NFIB^{-}. A minimum of two NFIX$^{-ve;}$ NFIB^{+ve} clones were analyzed per animal.

3.4.10 Quantitative real-time PCR (qPCR)

The E13.5 medial cortex (hippocampal primordium and medial neocortex) or entire E16.5 hippocampal primordium of *Nfix*$^{-/-}$ and *Nfix*$^{+/+}$ littermates were microdissected and snap frozen. RNA was extracted (RNeasy Micro Kit, Qiagen, Valencia, CA) and reverse transcription was performed using Superscript III (Invitrogen) with 1 μg of total RNA using random hexamers according to manufactures protocol. qPCR was performed using SYBR green (Qiagen) and 500 nM of the *Insc* forward primer (5' CACTTTGCTCCTAGCTTCTGGA 3') and reverse primers (5'CCCAATCTGCAGCAATGCCT 3'). Expression of *Insc* in *Nfix*$^{-/-}$ and *Nfix*$^{+/+}$ littermates is expressed relative to the housekeeping gene *Glyceraldehyde-3-phosphate dehydrogenase* (*Gapdh*), which is presented as proportion of *Gapdh* transcript levels. Each sample at E13.5 (n = 5) and E16.5 (n = 3) was also performed in technical triplicate.

3.4.11 Reporter gene assays

The constructs used in the luciferase assays were NFIX pCAGIG, NFIB pCAGIG and NFIA pCAGIG expression constructs, an empty vector control pCAGIG and a luciferase construct (1358 base pairs) spanning –1078 base pairs to +279 base pairs from the transcriptional start site (TSS) of the mouse *Insc* promoter (UCSC genome browser track *uc009jii.2*, GRCM38/mm10). DNA was transfected into Neuro2A cells ($1*10^4$ cells) in a 96 well plate using Lipofectamine 2000 (Invitrogen), and Cypridina luciferase was added to each transfection as an internal control. After 24 h luciferase activity was measured using a dual luciferase system (Switchgear Genomics, Menlo Park, CA). Each condition, for each experiment, was performed in technical triplicate, and the experiment itself was replicated 5 times.

3.4.12 ChIP-qPCR

Whole E14.5 mouse forebrains were dissociated and fixed in 1% formaldehyde for 8 minutes. Nuclei were lysed and chromatin sonicated using 8 cycles (30s ON/30s OFF) of the Bioruptor Pico (Diagenode, Belgium) so that the majority of chromatin was between 100-500 base pairs in length. Immunoprecipitation was performed with 8 µg of goat anti-NFI (sc-30918, Santa Cruz) or 8 µg of goat IgG (AB-108-C, R&D Systems) control antibody coupled to 40 ul of Protein G Dynabeads (10003D, Thermo Fisher Scientific). DNA purification was performed using Qiagen PCR purification kit. ChiP-DNA was quantified using SYBR Green qPCR. A primer set for the *Insc* promoter was used (Forward: 5'TTAGCATCAAGAGCTCAGGACATT, Reverse: 5' TGCCAAGAAAAGACAGTTCACCA) as well as a negative control primer set in a gene desert region devoid of histone modification marks and transcription factor binding (Active Motif, #71011). Enrichment of NFI in the INSC promoter was calculated relative to IgG control using the delta CT method, and was further normalised to the negative control primer set to negate non-specific enrichment caused by residual, undersonicated chromatin. All primers for ChIP-PCR were used at a final concentration of 300 nM.

The peaks from the ChIP-seq experiment using a pan-NFI antibody that was performed on embryonic stem cell-derived neural stem cells (Mateo et al., 2015; Supplementary Table 3, NFI tab) were annotated to the nearest gene using ChIPSeeker (Yu et al., 2015). Specifically, the following command was used: annotatePeak(chipPeaks, tssRegion = c(-3000, 1000), TxDb = txdb) where 'chipPeaks' is the bed file containing the locations of all peaks and 'txdb' is TxDb.Mmusculus.UCSC.mm9.knownGene (Carlson and Maintainer, R package version 3.2.2). The 'distance to TSS' value in the resulting annotation file was used to refine the search to identify NFI proteins bound 5000 base pairs downstream (a minimum distance of -5000 base pairs) or 1000 base pairs upstream (a maximum distance of 1000 base pairs) of a TSS. The resulting genes associated with the NFI bound TSSs were then cross-referenced with the genes identified as misregulated in all three microarray datasets to identify key NFI target genes.

3.4.13 Plasmid construction

Two CRISPR constructs encoding a single gRNA against the bacterial *LacZ* gene or mouse *Nfix* gene were used in this study. For the *LacZ* construct a previously published gRNA sequence targeting *LacZ* (5'TGCGAATACGCCCACGCGATCGG; underlined nucleotides, PAM motif) was used (Platt et al., 2014; Kalebic et al., 2016). To design a gRNA against the mouse *Nfix* gene, we used

software from DNA 2.0 to generate a gRNA sequence that recognises within exon 2 of *Nfix* (5'TGAGTTCCACCCGTTTATCGAGG). DNA oligonucleotides encoding the *LacZ* and *Nfix* gRNA sequences (as above but excluding the PAM motif) were then ligated into the pD1321-AP plasmid (DNA2.0). In this plasmid the hU6 promoter controls expression of the gRNA, and a CAG promoter controls the expression of the CAS9-2A-PaprikaRFP cassette. For the rescue experiment a construct expressing full-length mouse INSC was generated by PCR amplifying the INSC open reading frame from IMAGE clone 4211657 into pCAGIG as described elsewhere (Petros et al., 2015). Other constructs used in this study were full-length NFIX pCAGIG, NFIB pCAGIG and NFIA pCAGIG constructs (Piper et al., 2010; Piper et al., 2011; Piper et al., 2014).

3.4.14 Statistical analyses

Two-tailed unpaired Students *t* tests were performed when comparing two groups. For experiments with comparisons between more than two groups ANOVAs were first performed, followed by multiple comparisons analysis, where a pooled estimate of variance was used if appropriate, and statistical significance was corrected for using the Holm-Sidak method in Prism 6.0 (Graphpad). All data that was analysed using Students *t* tests was performed with a minimum sample size of 4 and assumed to be normally distributed. For analysis of the *Insc* qPCR data at E16.5, and ChIP-qPCR data, a sample size of 3 was analysed. In this case we did not assume a normal distribution of the data and, as such, we performed a one-sided Mann-Whitney U test in Prism 6.0. Because the test was based on a directional hypothesis (validating existing microarray or sequencing data), the one-sided test was justified. When the sample size is 3, the minimum *p*-value achievable from this nonparametric test is 0.05. All data analysis was performed blind to the genotype.

3.5 Results

3.5.1 NFIX is expressed by radial glia and IPCs during hippocampal development

To investigate whether NFIX promotes indirect neurogenesis and IPC production during the development of the cerebral cortex, we focused predominantly on the ammonic neuroepithelium of the hippocampus. This region was chosen for two reasons; firstly, NFIX expression within the ventricular zone (VZ) and subventricular zone (SVZ) of the cerebral cortex exhibits a gradient such that expression is highest in the caudo-medial cortex, particularly within the presumptive hippocampal primordium (Figure 3.1A, B). Secondly, newly generated neurons from the ammonic neuroepithelium (predominantly pyramidal neurons) migrate only a short distance radially before settling in the *cornu ammonis* (CA) region (Altman and Bayer, 1990) rendering it a simpler model of development than the six-layered neocortex. Previous studies have demonstrated that neural progenitor cells in the hippocampal neuroepithelium express NFIX during development from at least E13.5 onwards (Heng et al., 2014); however, the cell-type specific identity of these cells has not been established. The transition of radial glia to IPCs during development is demarcated by the sequential expression of PAX6, then TBR2 (EOMES) (Englund et al., 2005). We classified radial glia as $PAX6^{+ve}$; $TBR2^{-ve}$ rather than using PAX6 expression alone as a marker for these cells, thereby excluding newborn radial glia-derived IPCs that also express low to moderate levels of PAX6 (Arai et al., 2011). Co-immunofluorescence at E14.5 (Figure 3.1C) revealed that radial glia express NFIX (209/209 cells), as did the vast majority of IPCs ($TBR2^{+ve}$ nuclei; 208/209 cells). Moreover, the expression of NFIX was maintained in radial glia and IPCs throughout the stages of the cell cycle including mitosis (Supp. Figure 3.1). This same expression pattern was also observed at E13.5 and E15.5 (Supp. Figure 3.1).

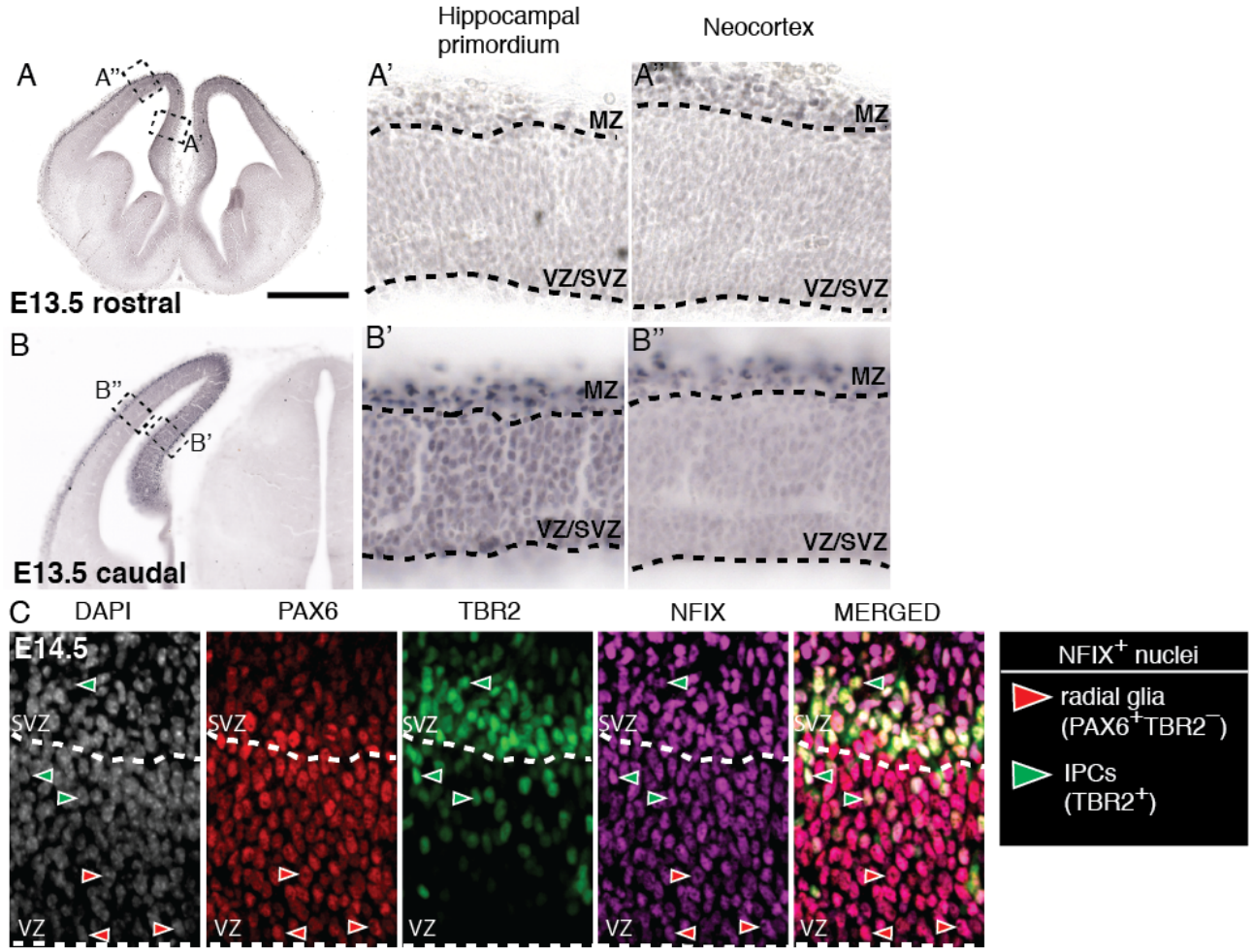

Figure 3.1: NFIX is expressed in hippocampal radial glia and IPCs.

(**A**, **B**) NFIX immunohistochemistry at E13.5 in the mouse telencephalon. Panel (**A'**, **B'**) and (**A''**, **B"**) are higher magnification images taken from boxed regions in (**A**) and (**B**) respectively, with dashed lines demarcating the ventricular zone (VZ)/subventricular zone (SVZ) and marginal zone (MZ). (**C**) NFIX immunofluorescence within the presumptive hippocampus at E14.5. Dashed lines indicate the boundary between the VZ and SVZ. NFIX (magenta) colocalizes with both PAX6 (red) and TBR2 (green). $NFIX^{+ve}$ radial glia and IPCs were identified as per the legend to the right of the panel. Scale bar (in **A**): **A**, **B** 800 µm; **A'-A''**, **B'-B"** 80 µm; C, 50 µm.

3.5.2 Delayed IPC development in *Nfix*$^{-/-}$ mice

We have previously reported elevated numbers of PAX6^{+ve} cells (indicative of increased numbers of radial glial cells) and delayed neuronal differentiation in the hippocampus of *Nfix*$^{-/-}$ mice at E16.5 (Heng et al., 2014). It remained unclear however, when these developmental defects first became apparent and at which stage of the lineage transition from a stem cell to a mature neuron was affected in these mice. Using PAX6 and TBR2 co-labeling, we investigated how the numbers of radial glial cells in the ammonic neuroepithelium of *Nfix*$^{-/-}$ mice changed from the onset of hippocampal neurogenesis at E13.5 to the peak of neurogenesis at E15.5. Relative to controls, we found significantly more radial glia (PAX6^{+ve}; TBR2^{-ve}) in *Nfix*$^{-/-}$ mice at E13.5, E14.5 and E15.5 (Figures 3.2A-E). Moreover, the magnitude of the change was smallest at E13.5 (P = 0.022) and became progressively larger at E14.5 (P = 0.0096) and E15.5 (P = 0.014), from which we infer that the lack of *Nfix* culminates in an ongoing (rather than a temporally restricted) delay in the transition of radial glia into IPCs. In support of this, we found fewer IPC cells at E13.5 in *Nfix*$^{-/-}$ mice compared to controls (P = 0.00013) (Figure 3.2F) demonstrating that radial glia generate IPCs less efficiently in these mice. By E14.5 and E15.5, the total number of IPCs in *Nfix*$^{-/-}$ mice was comparable to that in wild-types (Figure 3.2F), likely because the increased size of the radial glial pool resulted in an increase in the absolute number of IPC-generating divisions. However, measured as a proportion of all cell types in the VZ-SVZ, the number of IPCs remained reduced at E15.5 in *Nfix*$^{-/-}$ mice (data not shown).

Collectively, these data suggest that *Nfix*-deficient radial glial cells undergo increased self-expanding divisions and reduced IPC-generating divisions during early hippocampal development. To examine this further, we performed birth-dating experiments by injecting time-mated dams with the DNA analog BrdU at E13.5 before sacrificing embryos 24 h later, thereby labeling all proliferating cells (predominantly radial glia) that were in S-phase at the time of injection, as well as their progeny. We found that 24 h later (at E14.5) there were substantially fewer IPCs generated by BrdU-labelled radial glia in *Nfix*$^{-/-}$ mice than in controls (P = 0.0001) (Figure 3.2G). The impaired IPC development observed in *Nfix*$^{-/-}$ mice could potentially occur as a result of increased direct neurogenesis from radial glia, similar to that observed in *Elp3* conditional knockout mice (Laguesse et al., 2015). To determine whether this was the case we performed a 48 h BrdU chase experiment (labelling with BrdU from E13.5). We found that there were significantly fewer BrdU^{+ve} cells that had exited the cell cycle (BrdU^{+ve}; Ki67^{-ve}) in mutant mice relative to controls at E15.5 (P = 0.00016) (Figure 3.2H-J). This argues that the impaired IPC development in *Nfix*$^{-/-}$ mice is not offset by an increase in direct neurogenesis. Indeed, a significantly greater number of BrdU^{+ve} cells

remained as PAX6^{+ve}; TBR2^{-ve} radial glia at E15.5 (P = 2.2*10^{-5}). These data, coupled with the expansion of the radial glial population from E13.5-E15.5, support the hypothesis that *Nfix*-deficient radial glia undergo more self-expanding divisions at the expense of IPC development during this stage of hippocampal development.

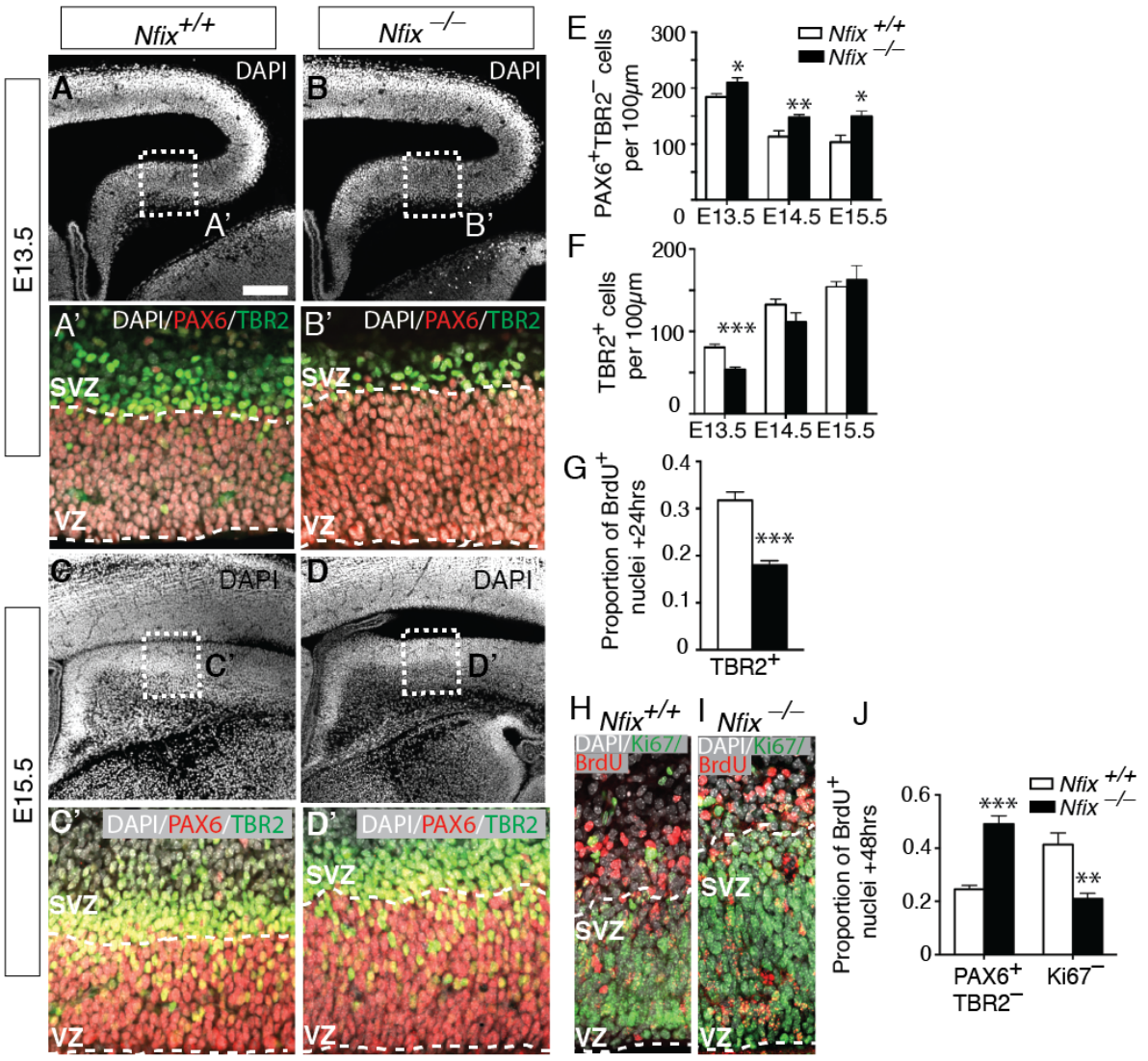

Figure 3.2: Increased numbers of radial glia and delayed IPC generation in the hippocampus of *Nfix*$^{-/-}$ mice from E13.5-E15.5

(**A**) to (**D**) DAPI staining (white) in wild-type and *Nfix*$^{-/-}$ mice at E13.5 and E15.5. Boxed regions in (**A**) to (**D**) are shown in higher magnification in (**A'**) to (**D'**) respectively and show DAPI (white), PAX6 (red) and TBR2 (green) staining, with dashed lines demarcating the ventricular zone (VZ)/subventricular zone (SVZ). (**E**) Cell counts of radial glia and (**F**) IPCs from E13.5-E15.5 in wild-type and *Nfix*$^{-/-}$ mice. Graphs depict mean ± SEM of 7, 8 and 5 embryos at E13.5, E14.5 and E15.5 respectively *$p < 0.05$, **$p < 0.01$, ***$p < 0.001$ (**G**) Cell counts of the proportion of total BrdU^{+ve} cells expressing TBR2 in wild-type and *Nfix*$^{-/-}$ mice at E14.5 following a BrdU chase at E13.5. Graphs depict mean ± SEM of 5 embryos ***$p < 0.001$ (**H**) and (**I**) show DAPI (white), BrdU (red) and Ki67 (green) staining in wild-type and *Nfix*$^{-/-}$ mice at E15.5 following a BrdU chase at E13.5. (**J**) Cell counts reveal the proportion of BrdU^{+ve} cells that were PAX6^{+ve}; TBR2^{-ve} or Ki67^{-ve} in wild-type and *Nfix*$^{-/-}$ mice. Graphs depict mean ± SEM of 5 embryos **$p < 0.05$, ***$p <$ 0.001. Scale bar (in **A**): **A-D** 220 μm; **A'-D'** 50 μm, **G**, **H** 40 μm.

3.5.3 *Nfix*-deficient radial glia have a longer S-phase duration

We next posited that *Nfix*-deficient radial glial cells should also display cellular characteristics associated with fewer IPC-generating divisions. Interestingly, a recent study revealed that radial glia committed to neurogenic divisions have a shorter S-phase duration (1.8 h) than radial glia during self-expanding divisions (8 h) (Arai et al., 2011). To further assess if NFIX promotes IPC production, we measured S-phase duration as a proxy for the frequency of neurogenic divisions. We hypothesized that the population of *Nfix*-deficient radial glial cells would exhibit a longer average S-phase duration due to the reduction in neurogenic divisions. To test this, we performed consecutive injections of the S-phase markers EdU and BrdU at E14.5 to determine the relative rate of progression through S-phase, as well as cell cycle duration (see materials and methods, Figure 3.3A-C) (Martynoga et al., 2005). We identified radial glia as $TBR2^{-ve}$ nuclei in the VZ, defined as the region apical to the thick band of $TBR2^{+ve}$ cells (Figure 3.3C). Consistent with our hypothesis we found that $Nfix^{-/-}$ radial glia had a significantly longer S-phase duration than wild-type radial glia ($P = 0.025$) (Figure 3.3D). Total cell cycle duration in $Nfix^{-/-}$ radial glia was not significantly different ($P = 0.051$) (Figure 3.3E), nor was G1/G2/M phase length ($P = 0.11$) (Figure 3.3F). Thus the increased S-phase duration in mutant mice further indicates that $Nfix^{-/-}$ radial glia undergo proportionally fewer IPC generating divisions during the period of peak neurogenesis.

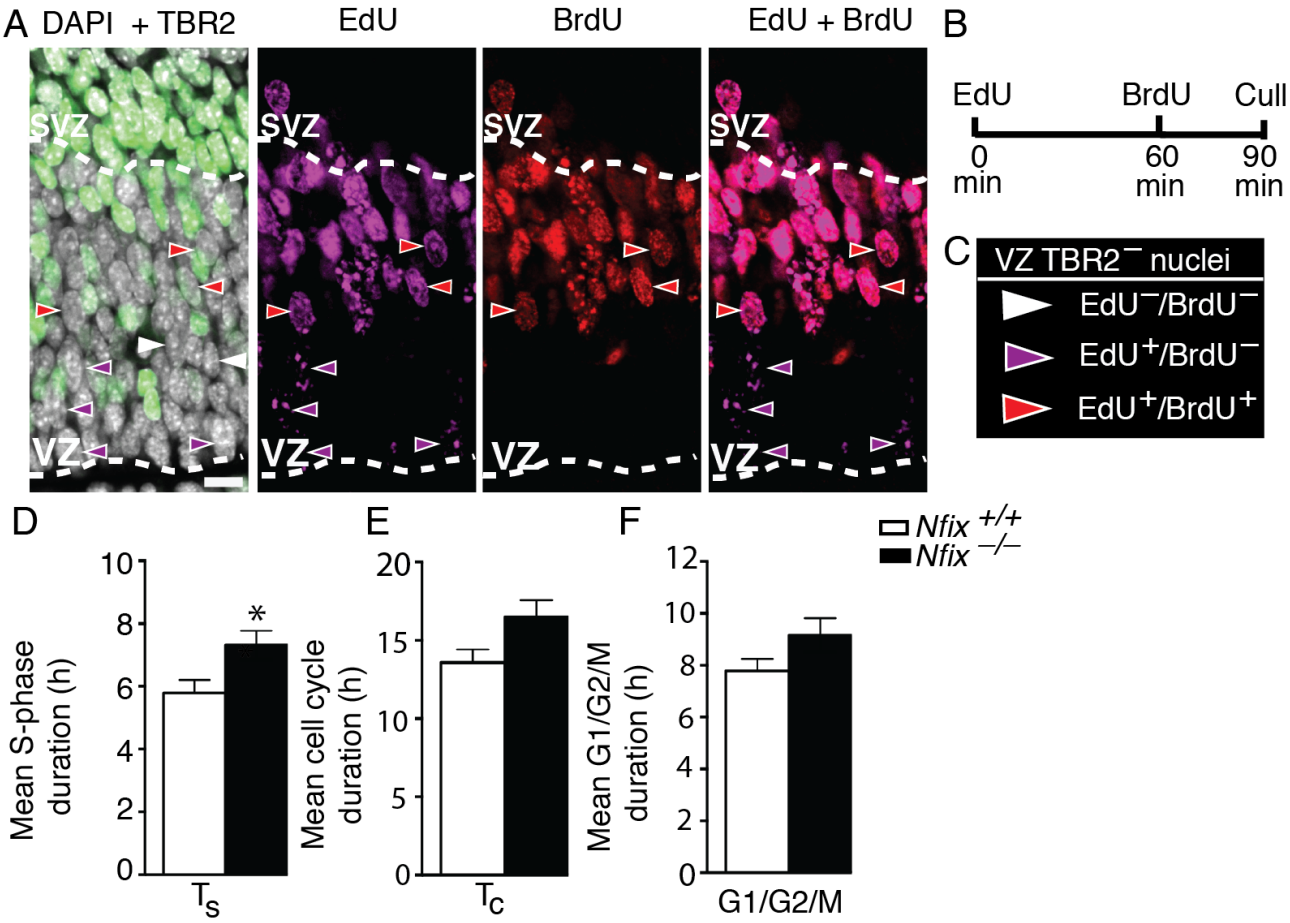

Figure 3.3: *Nfix*$^{-/-}$ radial glia undergo proportionally fewer neurogenic divisions.

(**A**) Wild-type hippocampus showing DAPI (white), TBR2 (green), EdU (magenta), BrdU (red) staining at E14.5, with dashed lines demarcating the ventricular zone (VZ)/subventricular zone (SVZ). (**B**) Pregnant dams were injected with EdU, followed by BrdU 60 min later, and sacrificed at 90 min. (**C**) Radial glia were identified as cells with TBR2^{-} nuclei in the VZ. (**D**) Quantification of cell cycle kinetics for mean S-phase duration (Ts), (**E**) mean total cell cycle duration (Tc) and (**F**) mean G1/G2/M phase length in radial glia of wild-type and *Nfix*$^{-/-}$ mice. Graphs depict mean ± SEM of 8 embryos *$p < 0.05$. Scale bar (in **A**)**: A** 22.5 µm.

3.5.4 Overexpression of NFIX *in vivo* promotes IPC and neuron generation

If loss of NFIX impairs IPC generation, then NFIX overexpression should result in an increased rate of IPC and neuronal differentiation. To investigate this, we used *in utero* electroporation to overexpress a HA-tagged mouse NFIX construct containing a bicistronic GFP reporter (NFIX pCAGIG) (Heng et al., 2014) or vector only control (pCAGIG) in the presumptive hippocampus of wild-type CD1 mice at E12.5 (Figure 3.4A, B). At E14.5 we found that NFIX overexpression led to a significantly higher percentage of electroporated cells becoming IPCs ($P = 0.037$) and neurons ($p = 0.016$), while fewer cells remained as radial glia ($P = 1.8*10^{-5}$) compared to electroporated cells in the control condition (Figure 3.4C-E). Importantly, co-staining for the neuronal marker TBR1 revealed that all neurons were located basal to the band of $TBR2^{+ve}$ cells, demonstrating that NFIX overexpression did not induce gross neuronal migration errors (data not shown). Together, these data are supportive of a role for NFIX in promoting the commitment of radial glia into IPCs.

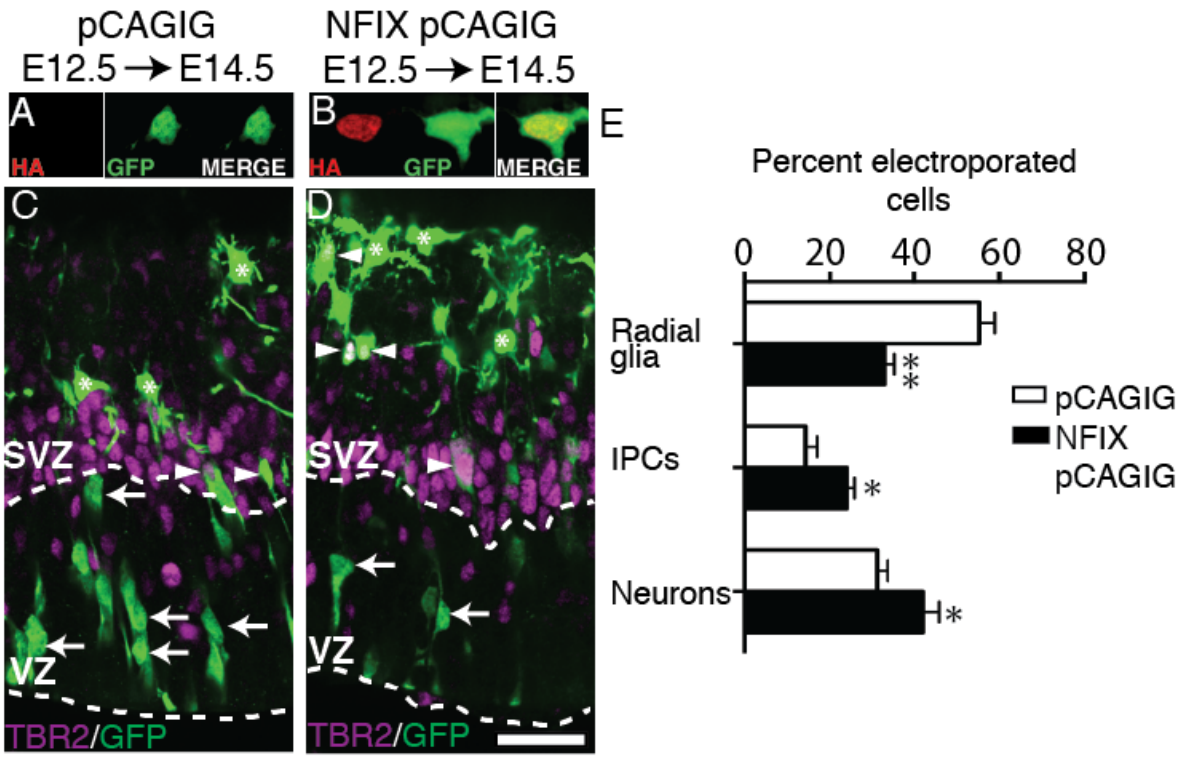

Figure 3.4: Overexpression of NFIX promotes IPC and neuron generation *in vivo*

(**A**, **B**) Images showings cortical neurons from E14.5 hippocampi expressing (**A**) the empty vector control pCAGIG or (**B**) NFIX pCAGIG with HA in red, and GFP in green. pCAGIG (**C**) and NFIX pCAGIG (**D**) were targeted to the hippocampal primordium of wild-type CD1 mice at E12.5 using *in utero* electroporation. Electroporated brains were collected and analysed at E14.5. Image shows GFP in green, and TBR2 in magenta, with dashed lines demarcating the ventricular zone (VZ)/subventricular zone (SVZ). (**E**) Quantification of the percent of electroporated (GFP^{+ve}) cells that are radial glia, IPCs or neurons in pCAGIG and NFIX pCAGIG hippocampi. Radial glia were identified in this experiment as $TBR2^{-}$ nuclei in the VZ (arrows), IPCs were identified as any cell expressing TBR2 (arrowheads) and neurons were identified as $TBR2^{-}$ nuclei basal to the SVZ (asterisks). Graph depicts mean ± SEM of 5 embryos (pCAGIG) and 7 embryos (NFIX pCAGIG), $*p < 0.05$, $**p < 0.01$. Scale bar (in **D**): **A**, **B** 24 µm; **C**, **D** 40 µm.

3.5.5 Loss of four *Nfi* alleles results in a more severe IPC phenotype

We have thus far demonstrated that *Nfix*-deficient radial glia generate IPCs with reduced efficiency. Despite this, $Nfix^{-/-}$ mice lack the gross morphological abnormalities often associated with mouse models in which radial glial populations are expanded and there is decreased neurogenesis (Chenn and Walsh, 2002; Farkas et al., 2008). For example, these phenotypes are usually associated with increased tangential length of the cortex and reduced radial thickness. We therefore questioned whether the loss of additional *Nfi* alleles would result in a more severe phenotype. To investigate this, we removed four *Nfi* alleles by intercrossing conditional floxed *Nfix* and *Nfib* mice, which were then crossed to a mouse line expressing a tamoxifen-activated form of *cre*-recombinase under the control of the ubiquitous *Rosa26* promoter. Time-mated dams were then injected with tamoxifen (two sequential injections at E10.5 and the other at E11.5) to delete *Nfix* and *Nfib,* and embryos were analysed at E15.5. We found that *cre*-expressing $Nfix^{fl/fl}$; $Nfib^{fl/fl}$ (hereafter referred to as $Nfix^{fl/fl}$; $Nfib^{fl/fl}$; *cre*) embryos were almost entirely devoid of NFIX and NFIB immunoreactivity (Figure 3.5H, I), whereas *cre*-negative animals retained NFIX and NFIB expression (Figure 3.5E, F). In $Nfix^{fl/fl}$; $Nfib^{fl/fl}$; *cre* animals, the tangential length to radial width (length/width) ratio of the presumptive hippocampus was markedly (251%) increased compared to control animals ($p < 0.0001$), as was that of the neocortex ($P = 0.025$) (Figure 3.5A-C). The length/width ratio of the $Nfix^{fl/fl}$; $Nfib^{fl/fl}$; *cre* hippocampus was also significantly larger than in $Nfix^{-/-}$ mice ($P = 0.0008$), suggestive of a more severe phenotype than in $Nfix^{-/-}$ animals (Figure 3.5C). Furthermore, cellular analysis revealed that, compared to controls, $Nfix^{fl/fl}$; $Nfib^{fl/fl}$; *cre* animals had a greater increase in radial glial cell number ($PAX6^{+ve}$; $TBR2^{-ve}$) ($P = 0.0006$) (Figure 3.5D) than in $Nfix^{-/-}$ mice at E15.5 (Figure 3.2E). Moreover, $Nfix^{fl/fl}$; $Nfib^{fl/fl}$; *cre* animals had a two-fold reduction in IPC number at E15.5 ($P = 0.0002$) (Figure 3.5D), whereas in $Nfix^{-/-}$ mice, the IPC number was not significantly different from that of wild-types at this age (Figure 3.2F). Together, these data demonstrate that the loss of additional *Nfi* alleles results in morphological and cellular phenotypes associated with reduced IPC production.

During development, the cell-cell interactions between different progenitor populations is important for regulating the balance between the self-expansion of radial glia or the commitment of radial glia to IPC and neuronal differentiation (Namihira et al., 2009). Due to the ubiquitous expression of NFIs by radial glia during cortical development, it is possible that NFIs promote the generation of IPCs by regulating the expression of extrinsic signaling molecules that affect the fate of neighboring radial glial cells (non-cell autonomous effect), rather than the host cell itself (cell-autonomous effect). Distinguishing between these different scenarios could provide an important

insight into the mechanisms through which NFIs drive the generation of IPCs from radial glia. To analyse these possibilities, we took advantage of the different DNA recombination efficiencies of the floxed *Nfix* and *Nfib* alleles (Supp. Figure 3.2). Due to the reduced recombination efficiency of the *Nfib* floxed allele, this resulted in a stochastic effect whereby in random areas of the cortex both *Nfix* alleles had recombined after administration of tamoxifen, but both *Nfib* alleles had not. The result was that at E15.5, *Nfix*$^{fl/fl}$; *Nfib*$^{fl/fl}$; *cre* cortices were sparsely patterned with NFIX^{-ve}; NFIB^{+ve} clones (Figure 3.5E-K). We took advantage of this serendipitous occurrence to determine whether NFIs were cell-autonomously required by radial glia for IPC development. Were this the case, NFIX^{-ve}; NFIB^{+ve} clones should show increased numbers of IPCs compared to the cells surrounding the clone. Conversely, a non-cell autonomous requirement for NFI would predict that the number of IPCs within NFIX^{-ve}; NFIB^{+ve} clones would be similar to that in the surrounding cells. To distinguish between these possibilities, we stained *Nfix*$^{fl/fl}$; *Nfib*$^{fl/fl}$; *cre* hippocampi for NFIB, NFIX and TBR2, and analysed the proportion of cells within NFIX^{-ve}; NFIB^{+ve} clones that were IPCs (TBR2^{+ve}). We found that within these NFIX^{-ve}; NFIB^{+ve} clones there was a greater proportion of cells that were IPCs compared to immediately adjacent NFIX^{-}NFIB^{-} regions (P = 0.0029) (Figure 3.5J-L). These data, together with our results from overexpressing NFIX through *in utero* electroporation (Figure 3.4), support a model in which NFIs are autonomously required by radial glia for normal IPC development.

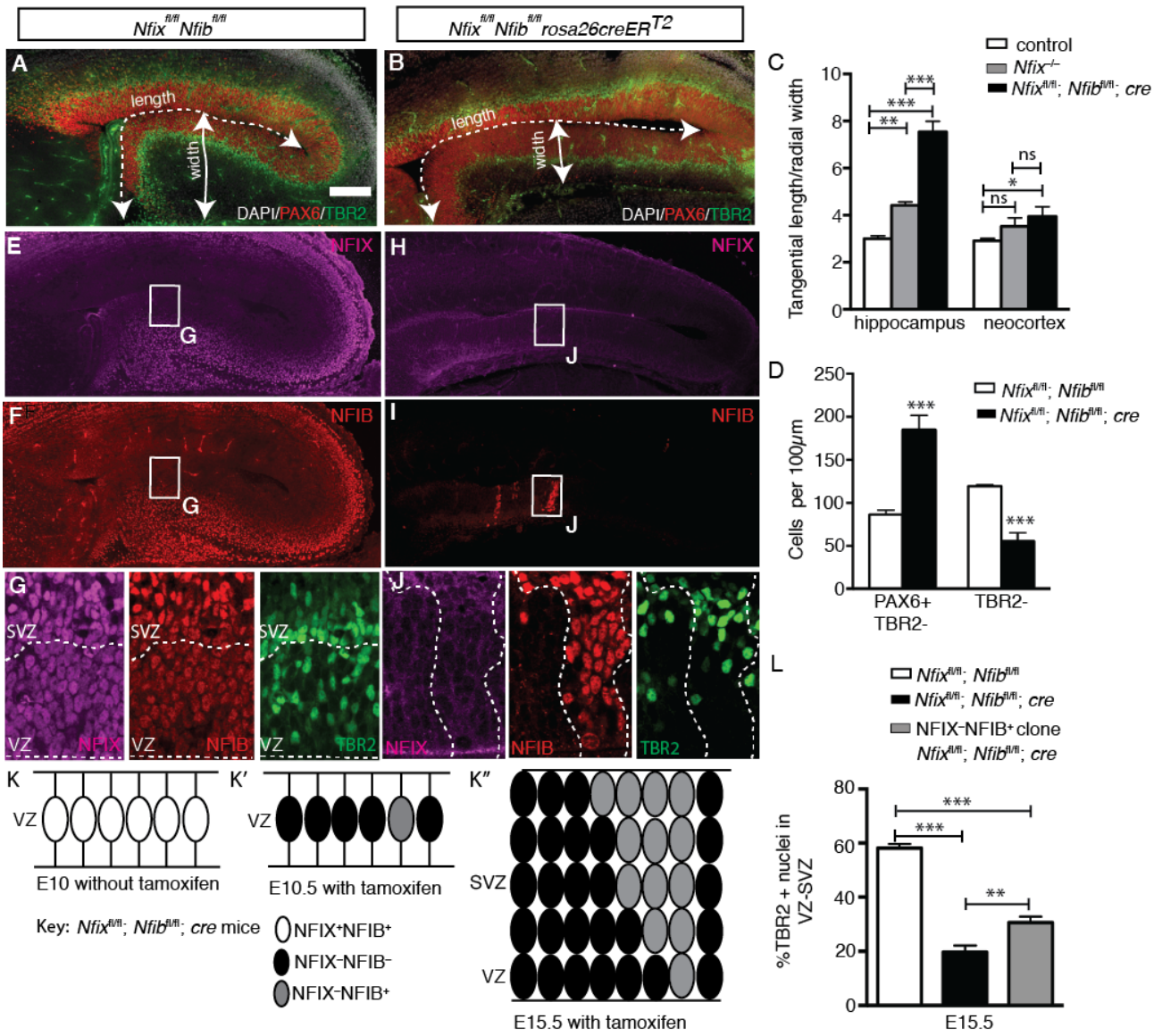
Nfix fl/fl Nfib fl/fl
Nfix fl/fl Nfib fl/fl rosa26creER T2
A
length
width
DAPI/PAX6/TBR2
B
length
width
DAPI/PAX6/TBR2
C
control
Nfix −/−
Nfix fl/fl; Nfib fl/fl; cre
Tangential length/radial width
hippocampus
neocortex
ns
D
Nfix fl/fl; Nfib fl/fl
Nfix fl/fl; Nfib fl/fl; cre
Cells per 100μm
PAX6+ TBR2-
TBR2-
E
NFIX
G
H
NFIX
J
F
NFIB
G
I
NFIB
J
G
SVZ
VZ
NFIX
SVZ
VZ
NFIB
SVZ
VZ
TBR2
J
NFIX
NFIB
TBR2
K
VZ
E10 without tamoxifen
K′
VZ
E10.5 with tamoxifen
K″
SVZ
VZ
E15.5 with tamoxifen
Key: Nfix fl/fl; Nfib fl/fl; cre mice
NFIX+NFIB+
NFIX-NFIB-
NFIX-NFIB+
L
Nfix fl/fl; Nfib fl/fl
Nfix fl/fl; Nfib fl/fl; cre
NFIX-NFIB+ clone
Nfix fl/fl; Nfib fl/fl; cre
%TBR2 + nuclei in VZ-SVZ
E15.5

Figure 3.5: Loss of four *Nfi* alleles results in a more severe IPC phenotype.

(**A**) and (**B**) show DAPI (white), PAX6 (red) and TBR2 (green) expression in *Nfix*$^{fl/fl}$; *Nfib*$^{fl/fl}$ and *Nfix*$^{fl/fl}$; *Nfib*$^{fl/fl}$; *cre* mice at E15.5. (**C**) Quantification of tangential length/radial width of the hippocampus and neocortex in control, *Nfix*$^{-/-}$ and *Nfix*$^{fl/fl}$; *Nfib*$^{fl/fl}$; *cre* mice. Graphs depict mean ± SEM from 10 control, 5 *Nfix*$^{-/-}$ and 5 *Nfix*$^{fl/fl}$; *Nfib*$^{fl/fl}$; *cre* embryos, *$p < 0.05$, **$p < 0.01$, ***$p < 0.001$. (**D**) Cell counts of radial glia and IPCs in E15.5 *Nfix*$^{fl/fl}$; *Nfib*$^{fl/fl}$ and *Nfix*$^{fl/fl}$; *Nfib*$^{fl/fl}$; *cre* mice. Graphs depict mean ± SEM from 5 embryos ***$p < 0.001$. (**E**) and (**H**) show NFIX (magenta) and (**F**) and (**I**) NFIB (red) expression in *Nfix*$^{fl/fl}$; *Nfib*$^{fl/fl}$ and *Nfix*$^{fl/fl}$; *Nfib*$^{fl/fl}$; *cre* mice at E15.5. Boxed regions in (**E** and **F**) and (**H** and **I**) are shown at higher magnification in (**G**) and (**J**) respectively. Dashed lines in (**J**) demarcate the border of the NFIB^{+ve} clone. (**K**) Schematic representing stochastic deletion of the *Nfib*$^{fl/fl}$ allele in *Nfix*$^{fl/fl}$; *Nfib*$^{fl/fl}$; *cre* mice. Radial glia express NFIX and NFIB (open ovals). (**K'**) Upon administration of tamoxifen, *Nfib* and *Nfix* are deleted in most radial glia (black ovals) but some cells do not delete *Nfib* fully (grey ovals). (**K''**) Incomplete recombination at the *Nfib* locus results in *Nfix*$^{fl/fl}$; *Nfib*$^{fl/fl}$; *cre* hippocampi being sparsely patterned with NFIX^{-ve}; NFIB^{+ve} clones. (**L**) Quantification of total ventricular zone (VZ)/subventricular zone (SVZ) nuclei that were TBR2^{+ve} in *Nfix*$^{fl/fl}$; *Nfib*$^{fl/fl}$ mice (white bar) and *Nfix*$^{fl/fl}$; *Nfib*$^{fl/fl}$ *cre* mice (black bar), including NFIX^{-ve}; NFIB^{+ve} cells in *Nfix*$^{fl/fl}$; *Nfib*$^{fl/fl}$; *cre* mice (grey bar). Graphs depict mean ± SEM from 5 embryos **$p < 0.01$, ***$p < 0.001$. Scale bar (in **A**)**:** **A**, **B**, **E**, **H**, **F**, **I** 100 μm, **G**, **J** 25 μm.

3.5.6 *Insc* is a target for transcriptional activation by NFIs during hippocampal development

What are the transcriptional mechanisms through which NFIs promote IPC production? To address this question, we analysed existing microarray datasets that examined alterations in gene expression within the entire hippocampal primordium of E16.5 *Nfix*$^{-/-}$ (Heng et al., 2014), *Nfib*$^{-/-}$ (Piper et al., 2014) and *Nfia*$^{-/-}$ mice (Piper et al., 2010). In these datasets there were 668, 1893 and 1099 misregulated genes relative to wild-type controls, respectively (±1.5 fold change, $p<0.05$). To focus our search, we further filtered these data using a number of stringent parameters. Firstly, we refined our analysis so that we only included genes that were misregulated in all three of the microarray datasets. We took this approach because it is likely that NFIs promote IPC production through a common transcriptional mechanism; this is supported by previous data highlighting the functional similarity of NFIs in the development of other cortical phenotypes (Vidovic et al., 2015), the additive effects of deleting NFIX and NFIB on IPC development (Figure 3.5), and our analysis of the microarray datasets, which revealed that a highly significant proportion of genes are commonly misregulated across each of the three datasets (Supp. Table 3.1). Next, we only included genes with a greater than ±2.5 fold change (Figure 3.6A and Supp. Table 3.2). Finally, we used a recently derived ChIP-seq dataset (performed using a pan-NFI antibody on embryonic stem cell-derived neural stem cell cultures) to identify which of these remaining genes had a promoter region bound by an NFI protein (Figure 3.6B) (Mateo et al., 2015). After this final filter only 6 candidate genes remained in the analysis pipeline (Figure 3.6C). Crucially, one of these 6 genes was *Gfap,* an established target of NFI transcriptional activation *in vitro* (Namihira et al., 2009) and *in vivo* (Heng et al., 2014), highlighting the effectiveness of our filters. *Ncam1,* which regulates neural cell adhesion and migration, was also misregulated, as were three genes with unknown functions in central nervous system development (*Rasd2*, *Entpd2*, *Il16*). Significantly, the final gene in the analysis pipeline was the mammalian homolog of *Drosophila insc.* Because *Insc* promotes IPC production during mouse cortical development (Postiglione et al., 2011) we inferred that NFIs might activate *Insc* expression, and that the downregulation of *Insc* in *Nfi* null mice (Figure 3.6C) contributes to the IPC phenotype observed within these lines.

3.5.7 NFIs activate *Insc*-promoter driven transcriptional activity

To investigate whether NFIs activate transcription of *Insc*, we first validated the microarray results from *Nfix*$^{-/-}$ E16.5 hippocampi (Heng et al., 2014). Using qPCR we determined that there was a ~50% reduction of hippocampal *Insc* mRNA compared to that in wild-type littermates at E16.5 (P =

0.05) (Figure 3.6D). Importantly, *Insc* was also downregulated in the medial cortex (hippocampal primordium and medial neocortex) of *Nfix*$^{-/-}$ mice at E13.5 when the IPC phenotype of these mice first becomes apparent (P = 0.044). Next, we verified the capacity of NFI proteins to physically bind to the *Insc* promoter by performing an *in vivo* ChIP assay on tissue isolated from E14.5 forebrains using a pan-NFI antibody. The ChIP-assay revealed enrichment of NFI protein binding at a region in the *Insc* promoter that corresponds to both the NFI dyad consensus site (P = 0.05) (Figure 3.6E) and the NFI ChIP-peak detected by Mateo and colleagues (2015) *in vitro*. Finally, we asked whether NFIs could active *Insc*-promoter driven transcriptional activity. A region of the *Insc* promoter, which included the dyad consensus site, was cloned upstream of the *luciferase* gene (Figure 3.6F, G). Co-transfection of the *Insc luciferase* construct with an NFIX expression plasmid in Neuro2a cells revealed that NFIX strongly activated *Insc* promoter-driven transcriptional activity ($P = 1.8*10^{-6}$) (Figure 3.6H). Likewise, NFIA (P = 0.0001) and NFIB (P = 0.0026) also enhanced *Insc* promoter-driven transcriptional activity (Figure 3.6H).

3.5.8 NFI-deficient radial glia phenocopy the cleavage plane defects of *Insc* knockout mice

If the downregulation of *Insc* contributes to the impaired generation of IPCs in *Nfix*$^{-/-}$ mice, then we would anticipate that the spindle orientation and cleavage plane deficits seen within *Insc* conditional knockout-mice (Postiglione et al., 2011) would be recapitulated within the radial glia of *Nfix*$^{-/-}$ mice. We assessed cleavage plane orientation of the dividing progenitor cell relative to the ventricular surface (Figure 3.6I-L). At E14.5 in wild-type mice, 71% of radial glia divided with a vertical cleavage plane (the angle between the cleavage plane and the ventricular surface was between 90° and 60°), whereas 23.5% of radial glia divided with an oblique division plane (between 60° and 30°; Figure 3.6M). Consistent with previous reports (Postiglione et al., 2011; Insolera et al., 2014), mitotic radial glia with a horizontal cleavage plane (between 30° and 0°) were rare, occurring in only 4.7% of cells (Figure 3.6M). In *Nfix*$^{-/-}$ mice, however, the vast majority of radial glia divided with a vertical cleavage plane (89.9%), and the proportion of oblique divisions was greatly reduced (10.1%) (Figure 3.6N). Moreover, no radial glial cell was observed to divide with a horizontal cleavage plane in *Nfix*$^{-/-}$ mice. Similarly, in *Nfix*$^{fl/fl}$; *Nfib*$^{fl/fl}$; *cre* radial glia at E15.5, 98.4% of radial glia divided with vertical cleavage plane, 1.6% with an oblique cleavage plane and no cells were observed dividing horizontally (Figure 3.6O). This phenotype is reminiscent of the cleavage plane phenotype of *Insc* conditional knockout mice, where there are substantially fewer oblique divisions and horizontal cleavage planes are not seen (Insolera et al.,

2014). Thus, the data support a model whereby downregulation of *Insc* in *Nfi*-deficient mice results in fewer oblique divisions in radial glia.

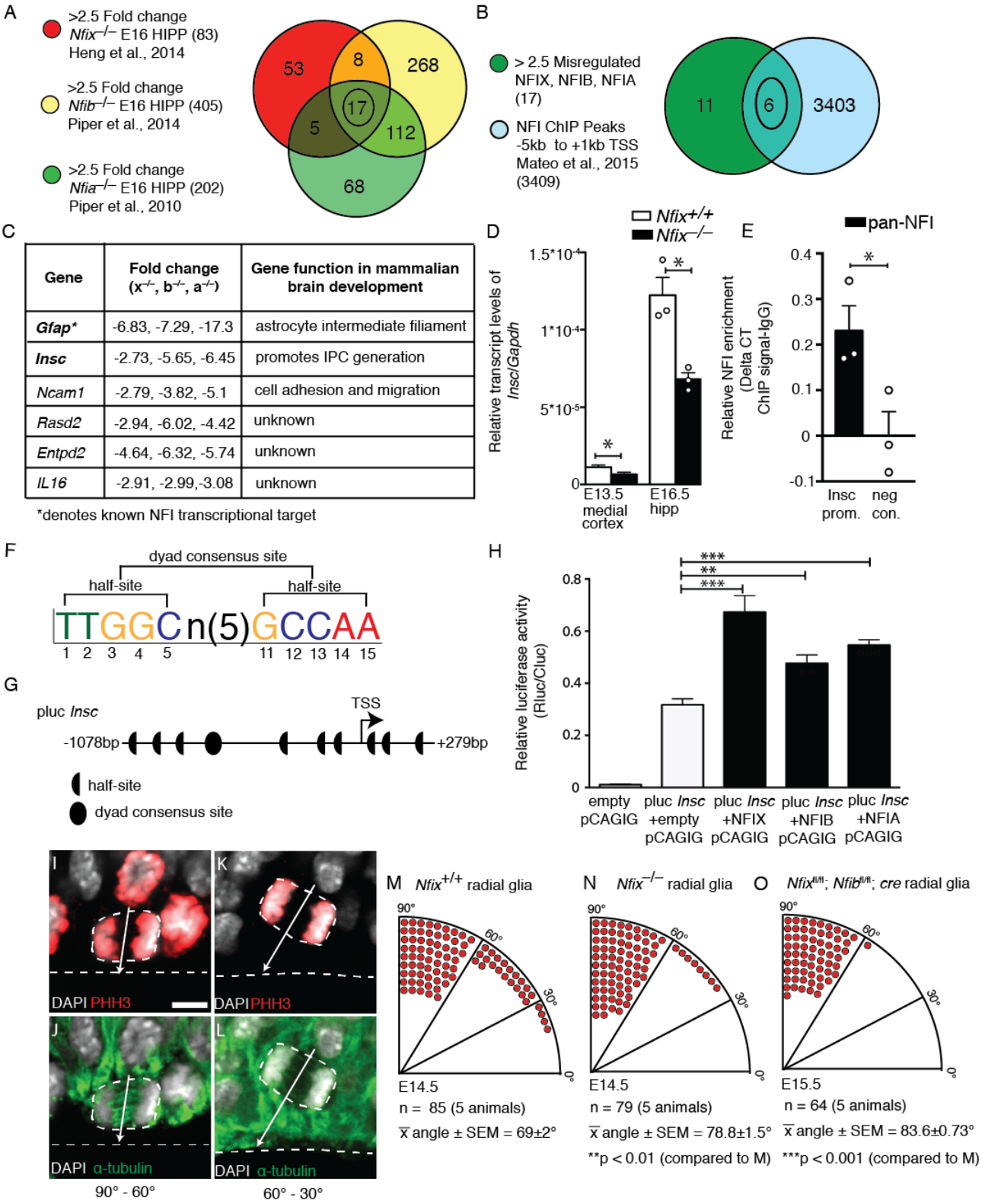
A
>2.5 Fold change
Nfix−/− E16 HIPP (83)
Heng et al., 2014
>2.5 Fold change
Nfib−/− E16 HIPP (405)
Piper et al., 2014
>2.5 Fold change
Nfia−/− E16 HIPP (202)
Piper et al., 2010
53
8
268
17
5
112
68
B
> 2.5 Misregulated
NFIX, NFIB, NFIA
(17)
NFI ChIP Peaks
-5kb to +1kb TSS
Mateo et al., 2015
(3409)
11
6
3403
C
Gene
Fold change (x−/−, b−/−, a−/−)
Gene function in mammalian brain development
Gfap*
-6.83, -7.29, -17.3
astrocyte intermediate filiament
Insc
-2.73, -5.65, -6.45
promotes IPC generation
Ncam1
-2.79, -3.82, -5.1
cell adhesion and migration
Rasd2
-2.94, -6.02, -4.42
unknown
Entpd2
-4.64, -6.32, -5.74
unknown
IL16
-2.91, -2.99,-3.08
unknown
*denotes known NFI transcriptional target
D
Nfix+/+
Nfix−/−
Relative transcript levels of Insc/Gapdh
1.5*10-4
1*10-4
5*10-5
0
E13.5 medial cortex
E16.5 hipp
E
pan-NFI
Relative NFI enrichment (Delta CT ChIP signal-IgG)
0.4
0.3
0.2
0.1
0
-0.1
Insc prom.
neg con.
F
dyad consensus site
half-site
half-site
TTGGCn(5)GCCAA
1 2 3 4 5
11 12 13 14 15
G
pluc Insc
TSS
-1078bp
+279bp
half-site
dyad consensus site
H
Relative luciferase activity (Rluc/Cluc)
0.8
0.6
0.4
0.2
0
***
**
***
empty pCAGIG
pluc Insc +empty pCAGIG
pluc Insc +NFIX pCAGIG
pluc Insc +NFIB pCAGIG
pluc Insc +NFIA pCAGIG
I
K
DAPI PHH3
DAPI PHH3
J
L
DAPI α-tubulin
DAPI α-tubulin
90° - 60°
60° - 30°
M Nfix+/+ radial glia
N Nfix−/− radial glia
O Nfixfl/fl; Nfibfl/fl; cre radial glia
90°
60°
30°
0°
E14.5
n = 85 (5 animals)
x̄ angle ± SEM = 69±2°
E14.5
n = 79 (5 animals)
x̄ angle ± SEM = 78.8±1.5°
**p < 0.01 (compared to M)
E15.5
n = 64 (5 animals)
x̄ angle ± SEM = 83.6±0.73°
***p < 0.001 (compared to M)

Figure 3.6: *Insc* is a target for transcriptional activation by NFIs during cortical development. **(A)** Venn diagram of >2.5 fold misregulated genes in *Nfix*$^{-/-}$ (red), *Nfib*$^{-/-}$ (yellow), *Nfia*$^{-/-}$ (green) E16 hippocampal microarrays. (**B**) Venn diagram of common misregulated genes (green) from (**A**) overlapped with NFI ChIP peaks from within -5kb to +1kb of the gene transcriptional start site (TSS) (blue). (**C**) 6 genes were identified in (**B**). (**D**) qPCR of *Insc* expression in the E13.5 medial cortex (hippocampal primoridum and medial neocortex) and E16.5 hippocampus from wild-type and *Nfix*$^{-/-}$ mice. Graphs depict mean ± SEM from 5 (E13.5) and 3 (E16.5) embryos respectively $*p \leq 0.05$. (**E**) ChIP-PCR showing enrichment of pan-NFI antibody (relative to IgG) within the *Insc* promoter, and no enrichment (relative to IgG) in a negative control primer located within a gene dessert. (**F**) NFI half-site and dyad consensus site sequence. (**G**) Schematic of cloned region of the *Insc* promoter showing NFI half-sites and the dyad consensus site. (**H**) Relative luciferase activity (Rluc/Cluc) after cotransfection of NFIX, NFIB, or NFIA with the *Insc* luciferase construct. Graphs depict mean ± SEM from 5 experiments $**p < 0.01$, $***p < 0.001$. (**I-L**) Representative images of wild-type radial glia stained with DAPI (white), alpha-tubulin (green) and PHH3 (red) revealing vertical (90°-60°; **I** and **J**) or oblique (60°-30°; **K** and **L**) cleavage planes. (**M-O**) Graphical representation of the number of radial glia undergoing vertical (90°-60°), oblique (60°-30°), or horizontal (30°-0°) cleavage in wild-type (**M**), *Nfix*$^{-/-}$ (**N**) and *Nfix*$^{fl/fl}$; *Nfib*$^{fl/fl}$; *cre* (**O**) radial glia. Mean ± SEM from 5 embryos $**p < 0.01$, $***p < 0.001$. Scale bar (in I)**: I-L** 5.5 μm

3.5.9 *In vivo* rescue of IPC number in *Nfix*$^{-/-}$ radial glia through INSC overexpression

If NFIX promotes IPC development, in part or wholly through activating *Insc* expression, then overexpressing INSC in *Nfix*$^{-/-}$ radial glia should help restore IPC generation to wild-type levels. To test this hypothesis, we used the CRISPR/Cas system to delete *Nfix* from radial glia within the ammonic neuroepithelium of embryonic CD1 wild-type mice. After electroporation at E12.5 with plasmids encoding *Nfix*-CAS9 and pCAGIG (knockout condition) or *lacZ*-CAS9 and pCAGIG (control condition), embryos were assessed for NFIX expression. In the knockout condition, only 8% of electroporated (GFP^{+ve}) cells retained NFIX immunoreactivity compared to 96% in the control (Supp. Figure 3.3). We then assessed TBR2 expression, and found proportionally fewer TBR2^{+ve}; GFP^{+ve} cells in the knockout compared to the control condition ($P = 0.03$), reminiscent of our findings using *Nfix*$^{-/-}$ mice (Figure 3.7A-D). Finally, for the rescue condition we co-electroporated the *Nfix*-CAS9 plasmid with INSC pCAGIG (Supp. Figure 3.3). In this rescue condition there was an increased proportion of TBR2^{+ve}; GFP^{+ve} cells compared to the knockout condition ($P = 0.023$). Moreover, the number of TBR2^{+ve}; GFP^{+ve} cells in the rescue condition was not significantly different from the control condition ($P = 0.62$) (Figure 3.7A-D). Thus *Insc* overexpression in *Nfix*$^{-/-}$ radial glia was sufficient to restore IPC number to wild-type levels, confirming that NFIX regulation of INSC contributes to IPC production during hippocampal development.

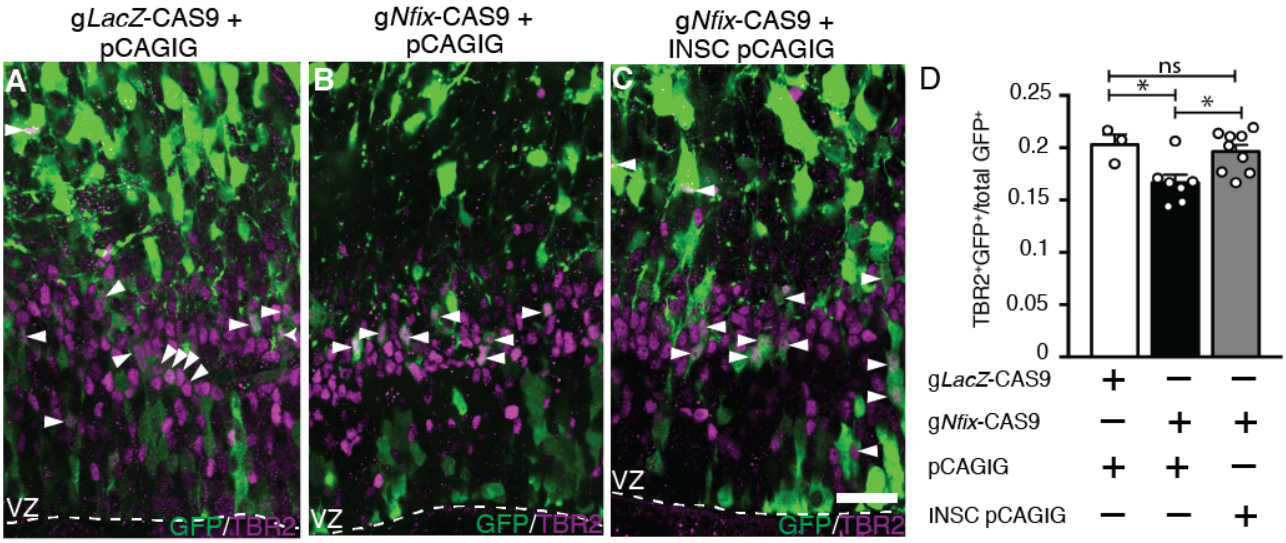

Figure 3.7: Rescue of IPC number in *Nfix*$^{-/-}$ radial glia through INSC overexpression

(**A-C**) show GFP (green) and TBR2 (magenta) in hippocampal sections of E15.5 CD1 mice electroporated at E12.5. The dashed line depicts the VZ. (**A**) Depicts the control condition (*gLacZ*-CAS9 + pCAGIG), (**B**) the knockout condition (g*Nfix*-CAS9 + pCAGIG) and (**C**) the rescue condition (g*Nfix*-CAS9 + INSC pCAGIG). Arrowheads indicate TBR2^{+ve}; GFP^{+ve} cells. IPCs were identified as any cell expressing TBR2 (**D**) Quantification of the proportion of total GFP^{+ve} cells that express TBR2. Graph depicts mean ± SEM of 3 (control), 7 (knockout) and 9 (rescue) embryos *$p < 0.05$. Scale bar (in **C**): **A-C** 30µm.

3.5.10 A prolonged neurogenic window results in increased neuron number in the hippocampus and neocortex of P20 *Nfix*$^{-/-}$ mice

What effects do the increased self-expanding divisions of radial glia and delayed IPC generation have on the late embryonic phenotype of *Nfix*$^{-/-}$ mice? We had previously observed that the reduction in TBR2^{+ve} cells in the *Nfix*$^{-/-}$ hippocampus was not permanent, so that at E18.5 there were greater numbers of these cells than in wild-type mice (Heng et al., 2014). This suggested that the expansion of the radial glial population in the presumptive hippocampus of *Nfix*$^{-/-}$ mice during early development would sustain the pool of radial glia and prolong the period of neurogenesis. In turn, resulting in an overall greater production of neurons. We investigated this by immunostaining wild-type mouse hippocampal sections for PAX6 and TBR2 at E18.5. This revealed very few radial glia or IPCs in the ammonic neuroepithelium, signaling the end of hippocampal neurogenesis. By contrast, in *Nfix*$^{-/-}$ mice at E18.5 the radial glial ($P = 2.9*10^{-5}$) and IPC ($P = 1*10^{-5}$) populations were approximately 2.5 and 3.5 fold larger than in the control, respectively (Figure 3.8A-C). We then asked whether this increase in radial glia and IPC number culminated in the increased production of CA pyramidal neurons in the postnatal hippocampus. Counts of the mature neuronal marker NeuN (RbFox3) at P20 revealed significantly more neurons within both the CA1 and CA3 regions of the mutant in comparison to those in controls ($P = 0.0011$) (Figure 3.8D-F). Moreover, we tracked the fate of E18.5 progenitor cells by injecting pregnant dams with BrdU and immunostaining for BrdU and NeuN in *Nfix*$^{-/-}$ and wild-type mice at P20. In wild-type mice there were very few neurons in the P20 CA regions that were born at E18.5 (BrdU^{+ve}; NeuN^{+ve}). Remarkably, however, the number of late-born neurons in *Nfix*$^{-/-}$ mice was approximately 10-fold higher ($P = 0.0002$) (Figure 3.8D-F), which likely contributed to the overall greater number of CA neurons. Additionally, we found a significantly greater number of S100ß$^{+ve}$ astrocytes in the stratum oriens of postnatal *Nfix*$^{-/-}$ mice ($P = 0.0107$) (Supp. Figure 3.4). Despite the increases in neuron and glial number in these regions, the overall size of the hippocampus was not significantly different in *Nfix*$^{-/-}$ mice compared to controls, probably because the dentate gyrus, as previously described (Heng et al., 2014) is much smaller in these mutant mice.

Given that postnatal *Nfix*$^{-/-}$ mice have a dorso-ventral expansion of the cingulate cortex and neocortex (Campbell et al., 2008), we asked whether the increased neuronal generation observed in the postnatal hippocampus was evident within the broader dorsal telencephalon, and so may contribute towards this phenotype. At E18.5 we saw similar phenotypes within the neocortex as in the hippocampal ammonic neuroepithelium, with increased radial glial ($P = 0.031$) and IPC numbers ($P = 0.0002$) compared to controls, although the phenotype was substantially less severe

than that we observed in the hippocampus (Supp. Figure 3.5A-C). BrdU labeling at E18.5 also revealed significantly more late-born neurons ($BrdU^{+ve}$; $NeuN^{+ve}$) in the upper layers of the neocortex (P = 0.0167) (Supp. Figure 3.5D-F). Thus, the prolonged neurogenic period of *Nfix*$^{-/-}$ mice likely contributes to the increased dorsal-ventral size of these regions. Collectively, these findings highlight the crucial role that NFIX plays in promoting indirect neurogenesis within the developing dorsal telencephalon, thereby significantly enhancing our understanding of the transcriptional mechanism underpinning the development of this brain region.

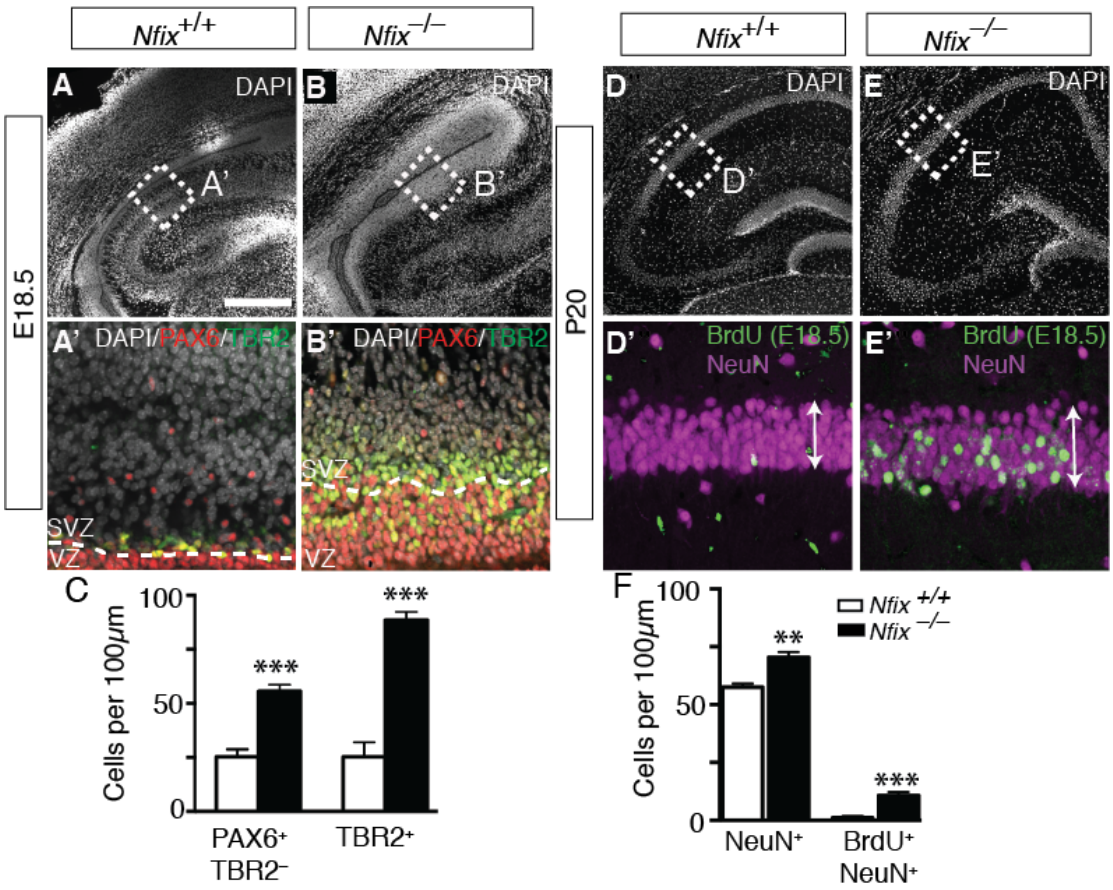

Figure 3.8: Prolonged neurogenic window increases neuron number in hippocampus of *Nfix*$^{-/-}$ mice.

(**A**) and (**B**) show DAPI staining in wild-type and *Nfix*$^{-/-}$ hippocampi at E18.5. Boxed regions in (**A**) and (**B**) are shown at higher magnification in (**A'**) and (**B'**) respectively, revealing DAPI (white) PAX6 (red) TBR2 (green) staining. Dashed lines in (**A'** and **B'**) demarcate ventricular zone (VZ)/subventricular zone (SVZ). (C) Cell counts of radial glia and IPCs in the E18.5 wild-type and *Nfix*$^{-/-}$ hippocampi. Graphs depict mean ± SEM of 5 embryos ***$p < 0.001$. (**D**) and (**E**) show DAPI (white) staining in wild-type and *Nfix*$^{-/-}$ hippocampi at P20, with arrows spanning the width of the CA neuronal layer. Boxed regions in (**D**) and (**E**) are shown at higher magnification in (**D'**) and (**E'**) respectively, revealing BrdU (green) cells labeled from a BrdU injection at E18.5 and NeuN (magenta). (**F**) Cell counts within the *cornu ammonis* (CA) neuronal layer of wild-type and *Nfix*$^{-/-}$ mice of the number of NeuN^{+ve} cells and BrdU^{+ve}; NeuN^{+ve} cells following a BrdU chase at E18.5. Graphs depict mean ± SEM of 5 pups **$p < 0.01$, ***$p < 0.001$. Scale bar (in **A**): **A**, **B**, **D, E** 350 μm; **A'**, **B'** 50 μm; **D'**, **E'** 40 μm.

3.6 Discussion

Studies have begun to reveal the factors that drive the progression of radial glia into IPCs during development (Farkas et al., 2008; Sessa et al., 2008; Saffary and Xie, 2011). For example, loss of the transcription factor PAX6 from radial glia downregulates the expression of the microtubule-associated protein SPAG5, and, in turn, radial glia undergo more divisions with oblique cleavage planes and generate more basal mitoses (Gotz et al., 1998; Asami et al., 2011). However, these basal mitoses retain the hallmarks of radial glial cells, indicating that PAX6 regulates the delamination of radial glia progenitors from adherens junction complexes, but does not regulate other key features of IPC differentiation. Likewise, HES transcription factors inhibit the neurogenic divisions of radial glia by repressing proneural genes (Mizutani et al., 2007; Pierfelice et al., 2011), but it is unclear how this repression directly affects the maintenance of apical-basal polarity, cell cycle progression or other aspects of radial glial cell biology. In this study, we have uncovered a novel role for members of the NFI transcription factor family in orchestrating the transition of radial glia to IPCs. Although NFIs have previously been shown to be important for astrogliogenesis and stem cell maintenance in the neocortex and hippocampus, here we reveal that NFIX-mediated activation of *Insc* expression promotes the timely generation of IPCs.

The function of INSC has been extensively studied during *D. melanogaster* neurogenesis. INSC acts in *D. melanogaster* neuroblasts as an adaptor protein, linking two protein complexes that assemble at the apical cell cortex to control spindle orientation (Wodarz et al., 1999; Schaefer et al., 2000). The control of mitotic spindle orientation by INSC during neuroblast division leads to unequal inheritance of the cell fate determinants Prospero, Numb and Brat to the basal daughter cell and results in neuronal differentiation (Knoblich, 2008). There is a single *insc* homolog in mice (Katoh and Katoh, 2003). INSC is expressed at very low levels within the developing cerebral cortex, which is perhaps why changes in INSC expression results in only modest fluctuations in spindle orientation in mice compared to flies. These modest fluctuations in spindle orientation are however correlated to large increases in IPC number with increased INSC expression, and *vice versa* (Postiglione et al., 2011). Despite the clear relationship between the level of *Insc* expression and the rate of IPC production in the mouse cortex, the mechanism through which *Insc* expression is regulated within the cortex has, until now, remained unclear.

Although we found that the impaired IPC development and spindle defects of *Nfix*-deficient radial glia closely mirror those of *Insc* conditional knockout mice during early development (Postiglione

et al., 2011), there are some important differences between these mutants. One of these differences is that the number of radial glial cells in *Nfix*-deficient mice is substantially increased during early development compared to controls. In contrast, although the radial glia in *Insc* conditional knockout mice were quantified using only PAX6 as a marker (thereby including newborn IPCs that retain PAX6 expression), there were no gross changes in the number of radial glia in these mice. As a corollary to this, we found that the expansion of radial glia in *Nfix*$^{-/-}$ mice sustained the pool of radial glia progenitors into late development, thereby ensuring an overall increase in the number of neurons in the hippocampal CA1/CA3 neuronal layers and neocortex, whereas, the neocortical neuron number in *Insc* conditional knockout mice was reduced (Postiglione et al., 2011). These differences are likely to be explained by the diverse cohort of genes that are likely to be under NFI transcriptional control, in addition to *Insc*. For example, we have previously shown that NFIs can repress genes involved in stem cell maintenance during cortical development such as *Sox9, Ezh2* and *Hes1* (Piper et al., 2010; Heng et al., 2014; Piper et al., 2014). Therefore, although the downregulation of *Insc* contributes to the impaired IPC generation in *Nfix* null mice, the misregulation of these additional factors likely explains the expansion of the radial glial pool beyond that observed following loss of *Insc* alone. NFIX may have functions in cell types other than radial glia that could also account for differences between these mouse lines. For example, NFIX is expressed by IPCs. Does NFIX regulate the differentiation of IPCs to mature neurons, and if so, does this contribute to the accumulation of IPCs at E18.5? Future studies using a *Tbr2* or *Dcx* driven *cre-recombinase* would address this question.

Our data further highlight the pleiotropic roles of NFIs during forebrain development. How NFI proteins promote the generation of IPCs by activating *Insc*-promoter driven transcription, while repressing genes involved in stem cell maintenance, and also being crucial factors in astrocytic lineage progression is a fascinating and open question. Future studies aimed at identifying the genome-wide chromatin binding profile of NFIs in purified populations of neural stem cells, neurons and glia, across developmental time, will lead to a broader understanding of how these transcription factors fulfil these functions during development.

3.7 Supplementary data

Microarray pairwise comparison	Number of unique misregulated genes (>1.5 Fold change)	Number of shared misregulated genes (>1.5 Fold Change)	*p* value
Nfix$^{-/-}$ and *Nfib*$^{-/-}$ E16 hippocampus	*Nfix* (430), *Nfib* (1645)	248	$p < 1*10^{-320}$
Nfix$^{-/-}$ and *Nfia*$^{-/-}$ E16 hippocampus	*Nfix* (466), *Nfia* (887)	212	$p < 1*10^{-320}$
Nfib$^{-/-}$ and *Nfia*$^{-/-}$ E16 hippocampus	*Nfib* (1162), *Nfia* (431)	731	$p < 1*10^{-320}$

Supplementary Table 3.1: Pairwise comparisons of *Nfi*$^{-/-}$ hippocampal microarrays using hypergeometric tests

List of unique genes and shared genes (>1.5 fold change) upon comparing *Nfix*$^{-/-}$ and *Nfib*$^{-/-}$ microarrays, *Nfix*$^{-/-}$ and *Nfia*$^{-/-}$ microarrays, *Nfib*$^{-/-}$ and *Nfia*$^{-/-}$ microarrays. The *P* value for each comparison was determined using a hypergeometric test.

Gene name	Fold change E16 *Nfix*$^{-/-}$ Hipp	Fold change E16 *Nfib*$^{-/-}$ Hipp	Fold change E16 *Nfia*$^{-/-}$ Hipp
Adra2a	-4.054	-3.464	-3.770
Ca3	-3.028	-6.553	-4.450
Caln1	-3.833	-2.530	-2.518
Cpne9	-8.373	-8.293	-7.267
Entpd2	-4.641	-6.316	-5.740
Fn1	2.618	3.401	2.833
Gal	-4.976	-4.996	-5.430
Gfap	-6.838	-7.294	-17.330
Grp	-9.031	-8.705	-11.420
Hey2	2.647	2.933	2.571
Il16	-2.919	-2.986	-3.087
Il31ra	2.769	2.646	2.710
Insc	-2.739	-5.659	-6.452
Kcnk1	-4.154	-3.053	-3.723
Ncam1	-2.799	-3.817	-5.102
Rasd2	-2.940	-6.018	-4.421
Sphk1	-2.875	-2.552	-2.700

Supplemental Table 3.2: Common misregulated genes in *Nfi*$^{-/-}$ hippocampal microarrays, related to Figure 3.6.

List of genes misregulated >2.5 fold change (p <0.05) in all three E16 hippocampal datasets: *Nfix*$^{-/-}$ (Heng et al., 2014), *Nfib*$^{-/-}$ (Piper et al., 2014) and *Nfia*$^{-/-}$ (Piper et al., 2010).

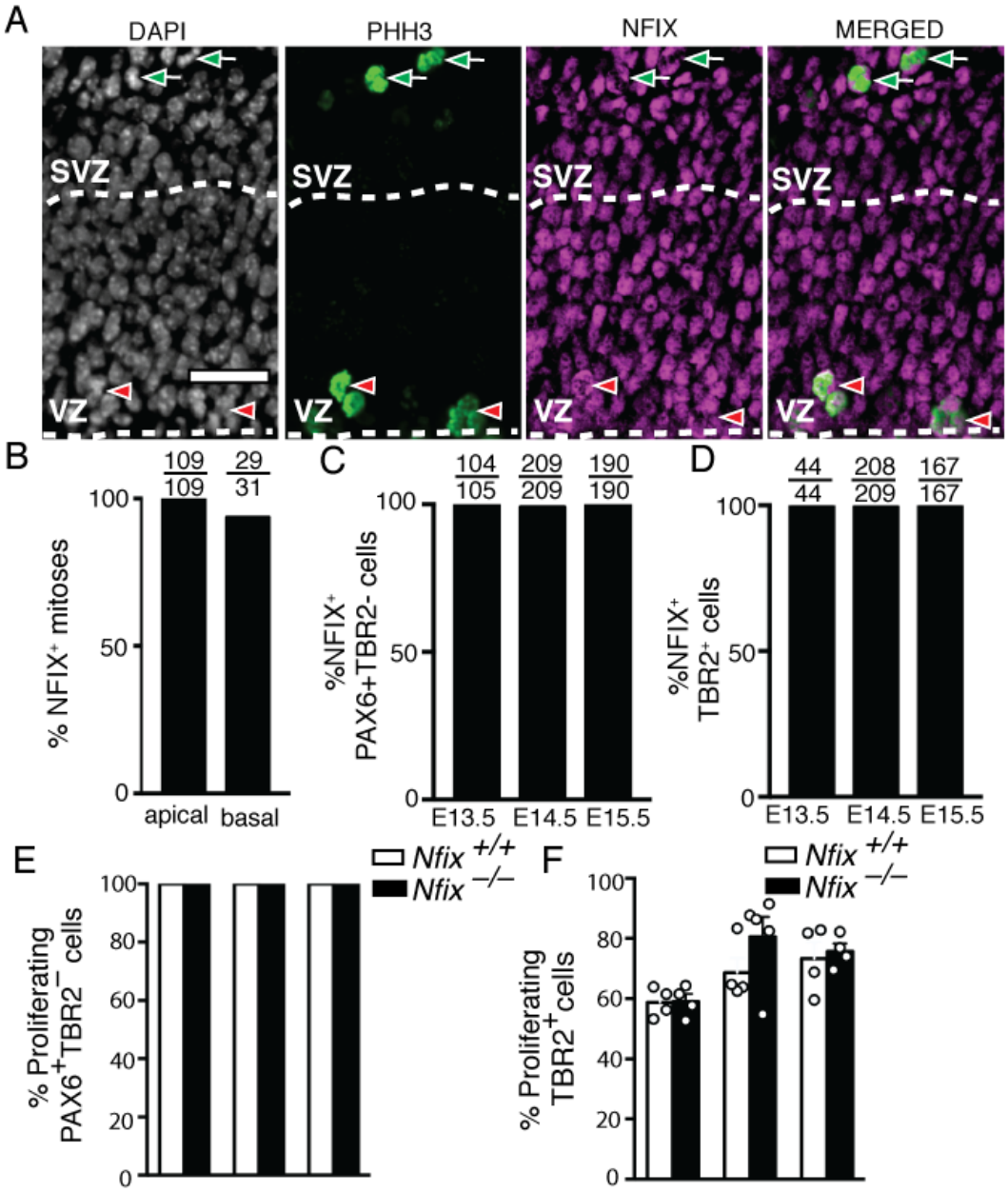

Supplementary Figure 3.1: NFIX is expressed during mitosis, related to Figure 3.1.

(**A**) NFIX immunofluorescence at the level of the hippocampus at E14.5. Dashed lines demarcate the ventricular zone (VZ)/subventricular zone (SVZ). NFIX (magenta) colocalizes with the mitotic marker PHH3 (green). Red arrowheads indicate radial glia undergoing mitosis and green arrows indicate IPCs undergoing mitosis. Scale bar (in **A**)**:** A, 50 µm. Quantification of the percentage of $NFIX^{+ve}$ (**B**) apical and basal mitoses, (**C**) radial glia and (**D**) IPCs at E14.5. (**E**) The percentage of radial glia and (**F**) the percentage of IPCs that are proliferating in wild-type and *Nfix*$^{-/-}$ mice from E13.5-E15.5. Graphs depict mean ± SEM of at least 4 embryos

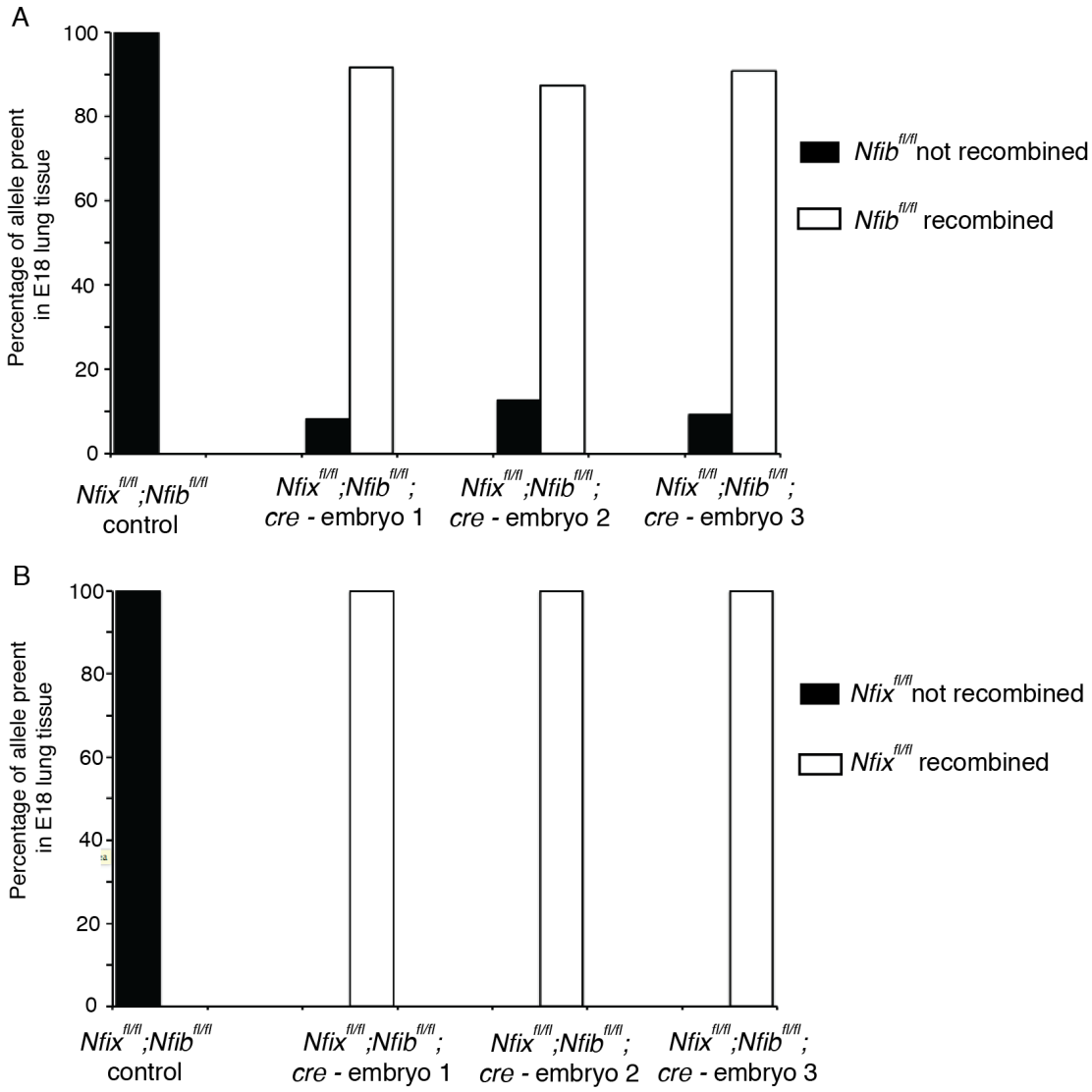

Supplementary Figure 3.2: Incomplete recombination of *Nfib*$^{fl/fl}$ allele in *Nfix*$^{fl/fl}$; *Nfib*$^{fl/fl}$; *Rosa26creER*^{T2} mice upon tamoxifen administration, related to Figure 3.5.

(**A**) qPCR DNA analysis of *Nfib*$^{fl/fl}$ recombination efficiency in *Nfix*$^{fl/fl}$; *Nfib*$^{fl/fl}$; cre mice and *Nfix*$^{fl/fl}$; *Nfib*$^{fl/fl}$ controls from lung tissue. Black bars depict percent of allele that is not recombined, and white bars depict percentage of allele that is recombined.

(**B**) qPCR DNA analysis of *Nfix*$^{fl/fl}$ recombination efficiency as performed in (**A**).

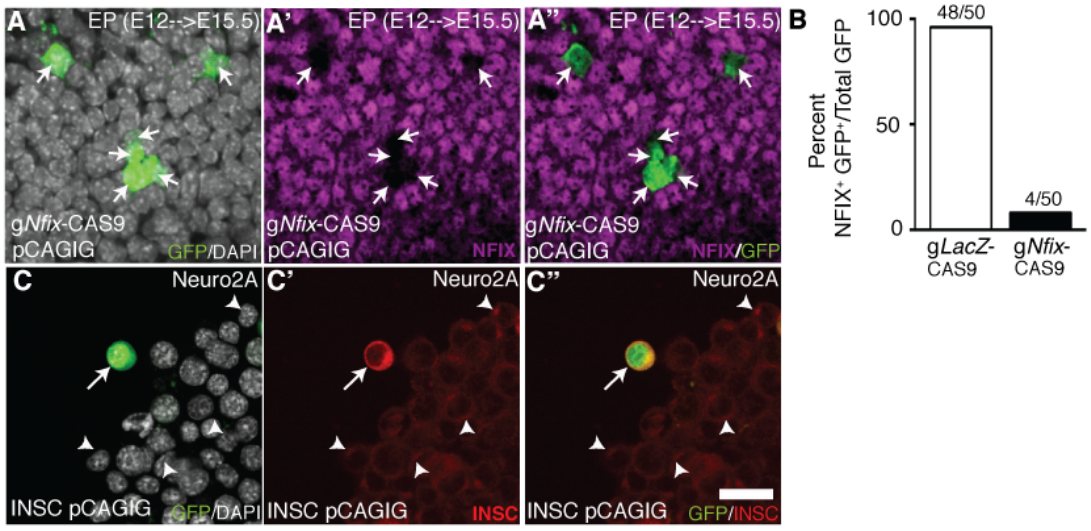

Supplementary Figure 3.3: Validation of CRISPR and overexpression constructs for in utero electroporation, related to Figure 3.7.

(**A-A"**) DAPI (white), GFP (green) and NFIX (magenta) in E15.5 CD1 wild-type mice electroporated at E12.5 with *gNfix*-CAS9 and pCAGIG constructs. Arrows indicate electroporated cells that are negative for NFIX. (**B**) Cell counts of the proportion of electroporated cells expressing NFIX in the control condition (g*LacZ*-CAS9 and pCAGIG) and knockout condition (*gNfix*-CAS9 and pCAGIG). (**C**) DAPI (white), GFP (green) and INSC (red) in Neuro2A cells transfected with INSC pCAGIG and analysed 48h later. Arrow indicates transfected cell expressing high levels of INSC, arrowheads indicate low endogenous levels of INSC in non-transfected cells (arrowheads). Scale bar (in **C"**): A 18.5µm, B 22µm.

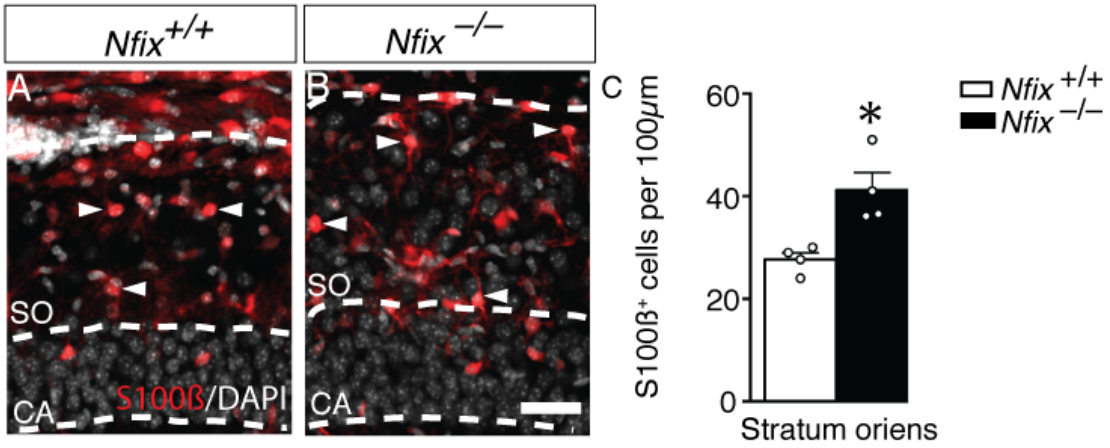

Supplementary Figure 3.4: Increased astrocyte number in the stratum oriens of P15 *Nfix*$^{-/-}$ mice, related to Figure 3.8.

(**A**) and (**B**) show DAPI (white) and S100ß (red) in wild-type and *Nfix*$^{-/-}$ hippocampi at P15, with the dashed lines demarcating the boundary of ammons horn (CA) neuronal layer and the stratum oriens (SO) neuropil. (**C**) Cell counts of the number of S100ß$^{+ve}$ astrocytes in the SO layer. Graphs depict mean ± SEM from 4 embryos *$p < 0.05$. Scale bar (in **B**): **A**, **B** 40 µm.

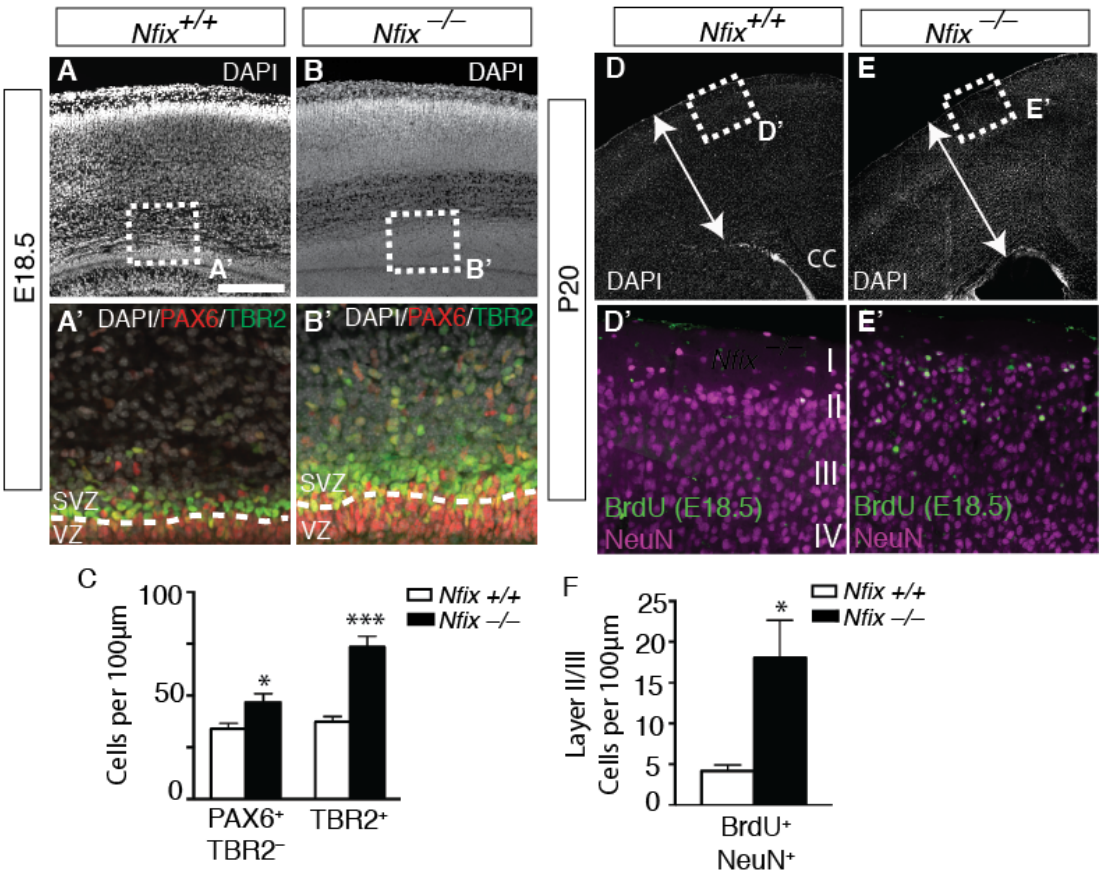

Supplementary Figure 3.5: Prolonged neurogenic window increases neuron number in the neocortex of *Nfix*$^{-/-}$ mice, related to Figure 3.8.

(**A**) and (**B**) show DAPI (white) staining in wild-type and *Nfix*$^{-/-}$ neocortices at E18.5. The boxed regions in (**A**) and (**B**) are shown at a higher magnification in (**A'**) and (**B'**) respectively, showing DAPI (white), PAX6 (red) and TBR2 (green) expression, with the dashed lines demarcating the ventricular zone (VZ)/subventricular zone (SVZ) boundary. (**C**) Radial glia and IPC counts in the E18.5 cortex of wild-type and *Nfix*$^{-/-}$ mice. Graphs depict mean ± SEM of 5 embryos ** $p < 0.01$, *** $p < 0.001$. (**D**) and (**E**) show DAPI (white) staining in wild-type and *Nfix*$^{-/-}$ neocortices at P20, with arrows spanning the neocortex from pial surface to the ventricular surface. The boxed regions in (**D**) and (**E**) are shown at a higher magnification in (**D'**) and (**E'**) respectively, showing BrdU^{+ve} cells (green), which were birthdated at E18, and NeuN staining (magenta), in the upper layers of the cortical plate. (**F**) Quantification of the number of BrdU^{+ve}; NeuN^{+ve} layer II/III cells in wild-type and *Nfix*$^{-/-}$ mice. Graphs depict mean ± SEM of 5 embryos * $p < 0.05$. Scale bar (in **A**) **A**, **B** 200 µm; **A'**, **B'** 50 µm; **C**, **D** 375 µm; **C'**, **D'** 62.5 µm.

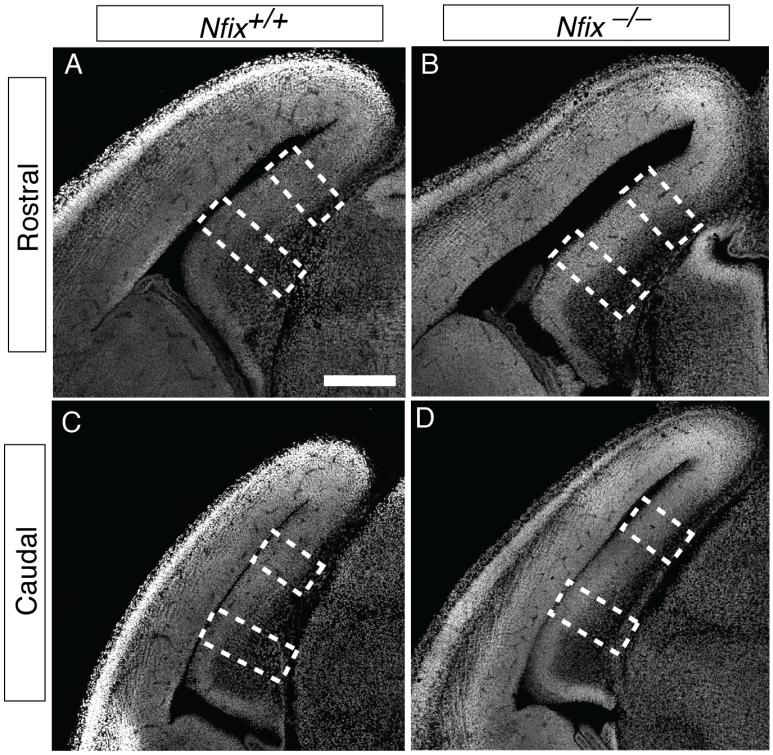

Supplementary Figure 3.6: Sampling areas for hippocampal cell counts, related to Figures 3.2-3.4.

(**A-D)** Representative rostral and caudal E14.5 coronal sections of *Nfix*$^{+/+}$ (**A**, **C**) and *Nfix*$^{-/-}$ (**B**, **D**) mouse brains stained with DAPI (white). To perform the cell counts described in this manuscript, we analysed a rostral and a caudal section for each animal at each age investigated. For each section the number of immunopositive cells in two equally spaced 100 μm sampling columns spanning the dorsal-ventral width of the ammonic neuroepithelium (boxed areas in **A**-**D**) were quantified.

Scale bar (in **A**)**: A**, **B** 250 μm, **C**, **D** 300 μm.

Chapter 4 A morphology independent approach for identifying dividing neural stem cells in the adult mouse hippocampus

4.1 Aims of Chapter 4

Thus far in this thesis I have examined the role of NFIX during the development of the dorsal telencephalon (Chapter 3). The second aim of this thesis, detailed in Chapter 5, is to examine what function NFIX plays in regulating adult neural stem cell biology, specifically within the adult hippocampus.

Before addressing this second aim however, I set out to solve a major problem extant in the field of adult neural stem cells: adult neural stem cells, unlike their embryonic counterparts, are difficult to identify. For example, current methodologies of identifying adult neural stem cells do not account for the morphological heterogeneity of these cells. The existing methods are also inaccurate and time-consuming. The reason I sought solve this problem is two-fold. Firstly, if I were to develop an improved method for identifying adult neural stem cells, it would increase the reproducibility of results across the adult neurogenesis field. Secondly, and pertinently to this thesis, an improved method would best allow me to study the function of NFIX within adult neural stem cells in Chapter 5 of my thesis.

Chapter 4 of my thesis therefore describes the novel methodology I developed to identify adult neural stem cells within the mouse hippocampus. Current methods of identifying adult hippocampal neural stem cells (AH-NSCs) rely on identifying cells that have a radial morphology. Recent evidence suggests however, that the majority of dividing AH-NSCs have a horizontal (non-radial) morphology. These cells would be ignored by current identification approaches. In response to this, I developed a morphology independent approach to identify dividing AH-NSCs. This inclusive approach provides a far more holistic account of AH-NSC division.

4.2 Abstract

AH-NSCs continue to generate neurons throughout life, albeit at a very low rate. The relative quiescence of this population of cells has led to many studies investigating factors that may increase their division. Current methods of identifying dividing AH-NSCs in vivo require the identification and tracing of a radial process back to a nucleus within the subgranular zone. However, caveats to this approach include the time-intensive nature of identifying AH-NSCs with such a process, as well as the fact that this approach ignores the relatively more active population of horizontally oriented AH-NSCs that also reside in the subgranular zone. Here, we describe, and then verify using *Hes5*::GFP mice, that labelling for the cell-cycle marker Ki67, and selection against the intermediate progenitor cell marker TBR2 ($Ki67^{+ve}$; $TBR2^{-ve}$ nuclei) is sufficient to identify dividing horizontally- and radially-orientated AH-NSCs in the adult mouse hippocampus. These findings provide a simple and accurate way to quantify dividing AH-NSCs *in vivo* using a morphology independent approach that will facilitate studies into neurogenesis within the hippocampal stem cell niche of the adult brain.

4.3 Introduction

The continued generation of dentate granule neurons from AH-NSCs is important for multiple cognitive processes, including learning (Akers et al., 2014; Goncalves et al., 2016) and mood regulation in mice (Yun et al., 2016). The level of adult hippocampal neurogenesis in humans is comparable to that in mice, suggesting that ongoing neurogenesis is functionally important for both species (Spalding et al., 2013; Bergmann et al., 2015; Ernst and Frisen, 2015). As a consequence of this, therapies are being developed that aim to specifically increase the levels of hippocampal neurogenesis to circumvent disorders such as depression, where neurogenesis is reduced (Harris et al., 2016b; Yun et al., 2016).

There are three major cell types within the neurogenic lineage of the adult mouse hippocampus [reviewed in (Goncalves et al., 2016)]. These are the AH-NSCs (Type 1 cells), most of which are quiescent, the transient but highly proliferative intermediate progenitors (IPs or Type 2 cells), and finally neuroblasts (Type 3 cells). These cell types are defined by their relative division capacity, lineage potential, and expression of certain markers (von Bohlen und Halbach, 2011). Despite the intense interest in neurogenesis in the adult brain, one of the major challenges in the field is to clearly define these populations, and unequivocally identifying dividing AH-NSCs *in vivo*. The ability to accurately identify dividing AH-NSCs is crucial to determine the relative rates of quiescence or division among this population. A recent study using a novel cell sorting protocol identified and purified to homogeneity almost the entire population of neurosphere-forming precursors comprising both dividing and quiescent AH-NSCs (Jhaveri et al., 2015), however this approach is not easily applied to the histological identification of these cells. In most studies, the histological criteria used to identify dividing AH-NSCs *in vivo* involve linking a radial process, stained for Glial Fibrillary Acidic Protein (GFAP), Nestin, Brain Lipid-binding Protein (BLBP) or Epidermal Growth Factor Receptor (EGFR) expression, back to a nucleus within the subgranular zone (SGZ) and determining whether the nucleus is positive for a cell-cycle marker, such as Ki67 (von Bohlen und Halbach, 2011; Hussaini et al., 2013). Despite the large number of studies to have utilised this approach, there are a number of inherent difficulties evident with this paradigm for identifying dividing AH-NSCs.

Foremost among the problems associated with tracing a radial process is that it ignores a population of horizontally oriented NSCs (Lugert et al., 2010). These horizontal NSCs (not to be confused with IPs, which are also horizontal dividing precursors) have different characteristics from their radial

NSC counterparts. For example, horizontal AH-NSCs divide more frequently, and their numbers change more acutely in response to age or exercise (Lugert et al., 2010). This shortcoming implies that the many studies that have not analysed this cellular population may have underrepresented the number of dividing AH-NSCs present. Therefore, an inclusive approach that accounts for the potential morphological heterogeneity of AH-NSCs needs to be developed. The second problem with the existing radial identification approach is that it is potentially inaccurate and extremely time-consuming. Dividing AH-NSCs and intermediate progenitors (IPs) are frequently found together in clusters (Hodge et al., 2008), and therefore it becomes difficult to determine to which cell a radial AH-NSC process is linked. Finally, there is a lack of standardisation as to which radial markers are appropriate to use when identifying active AH-NSCs, demonstrated by the variety employed in the following studies (Gulbins et al., 2013; Li et al., 2013; Martynoga et al., 2013; Andersen et al., 2014; Kandasamy et al., 2014; Andreu et al., 2015; Nicola et al., 2015; Yousef et al., 2015). Together, these issues pose great challenges to the interpretation and comparison of the many studies in this field.

To address these issues we developed a morphology independent approach for identifying dividing AH-NSCs. Our method is based solely on the exclusion of the IP marker TBR2 (Hodge et al., 2008; Hodge et al., 2012). We found that Ki67^{+ve}; TBR2^{-ve} cells have large nuclei, express higher levels of SOX2 and are Hes5-GFP^{+ve}. Most importantly, we verified in the notch reporter *Hes5*::GFP mouse strain (Jhaveri et al., 2010; Lugert et al., 2010) that a subset of these cells also have a horizontal GFP^{+ve} morphology, consistent with the description of horizontal NSCs by Lugert and colleagues (2010). The approach outlined here is accurate, fast and accounts for the heterogeneous morphology of AH-NSCs, representing a significant advance on previous approaches used to identify and quantify this population in vivo.

4.4 Methods

4.4.1 Animal ethics

The work performed in this study conformed to The University of Queensland's Animal Welfare Unit Guidelines for Animal Use in Research (AEC approval numbers QBI/353/13/NHMRC and QBI/355/13/NHMRC/BREED). All experiments were performed in accordance with the Australian Code of Practice for the Care and Use of Animals for Scientific Purposes, and were carried out in accordance with The University of Queensland Institutional Biosafety Committee.

4.4.2 Animals

Two mouse lines were used in this study, wild-type C57BL/6J mice, and *Hes5::*GFP mice (CD1 background) (Basak and Taylor, 2007; Lugert et al., 2010). These mice contain a 3 kilobase (kb) portion of *Hes5* gene regulatory elements (1.6 kb upstream of the transcriptional start site, 1.4 kb downstream) controlling the expression of GFP. All mice in this study were analysed between 12-16 weeks of age. Both male and female mice were used.

4.4.3 Primary antibodies

The rabbit primary antibodies used in this study were anti-GFAP (Z033429-2, 1/1000, Dako), anti-TBR2 (ab23345, 1/800, Abcam) or monoclonal anti-TBR2 (EPR19012, 1/200, Abcam); the mouse primary antibodies were anti-Ki67 (550609, 1/200, BD Pharmingen) and mouse GFAP (MAB 360, 1/500, Millipore, MA); the rat primary was anti-Ki67 FITC clone SolA15 (11-5698-80 1/400, San Diego, CA); the goat primary was anti-DCX (sc-8066, 1/200, Santa Cruz), and chicken primary was anti-GFP (ab13970, 1/500, Abcam).

4.4.4 Tissue processing and immunofluorescence

Animals were perfused transcardially with PBS followed by 4% PFA in PBS. The dorsal skull of animals was removed and brains were post-fixed for 1-2 weeks. Coronal brain sections were cut with a Vibratome (Leica, Deerfield, IL) at a thickness of 50 μm.

Prior to immunostaining, sections were mounted on Superfrost slides. Heat-mediated antigen retrieval was then performed in 10 mM sodium-citrate solution in PBS (pH 6.0) at 95°C for 15 min.

so as to expose antigens that were hidden by the tissue-processing and fixation process. Exceptions to this protocol were *Hes5*::GFP sections, in which heat-mediated antigen retrieval was performed for only 2 min at 95°C. This shorter retrieval was required so as to not irreversibly damage the GFP epitope (Nakamura et al., 2008). A standard immunofluorescence protocol was then performed as described previously (Chapter 3).

4.4.5 Microscopy and image processing

Confocal images were acquired as 1 μm optical sections spanning a 10 μm thick z-stack on a Zeiss inverted Axio-Observer fitted with a W1 Yokogawa spinning disk module and Hamamatsu Flash4.0 sCMOS camera and Slidebook software (3i). Image channels were pseudocolored to allow for overlay, cropped, and minimum and maximum grey values were adjusted in ImageJ (freeware). Individual images were resized in Photoshop (Adobe), and image tiles were constructed as display items in Illustrator (Adobe).

4.4.6 Fluorescence intensity quantification

A single in focus plane was used to quantify SOX2 fluorescence. An outline was drawn around each cell nuclei using the DAPI channel and the area, mean grey value and integrated density were measured (ImageJ). The total corrected cellular fluorescence (TCCF) = integrated density – (area of selected cell * mean fluorescence of background readings) was then calculated (McCloy et al., 2014).

4.4.7 Statistics

Student's *t*-tests were performed in Graphpad Prism (7.0) to compare the relative SOX2 fluorescence intensity (TCCF) and nuclei area of $Ki67^{+ve}$ $TBR2^{-ve}$ and $Ki67^{+ve}$ $TBR2^{+ve}$ cells. Data was obtained from at least 5 cells from each individual mouse (n = 3). Because we were interested in variability between cells within the SGZ niche, each individual cell was considered a biological replicate. This approach allows for a better measure of the biological variability per cell, rather than when averaging the values from multiple cells per mouse.

4.5 Results

4.5.1 Selecting a nuclear marker for dividing AH-NSCs

To develop a morphology independent approach for identifying dividing AH-NSCs we first needed to identify a suitable nuclear protein to use as a marker. As no protein has been identified that alone specifically labels this population, we sought to identify an approximate marker, which could then used in conjunction with other proteins to identify AH-NSCs. Two criteria were assessed; the percentage of dividing AH-NSCs that are labelled by the nuclear protein (penetrance), and, secondly, the cell types that express the protein (specificity).

Two proteins satisfied these criteria and appeared to be reasonable candidates, namely Achaete-scute like 1 (ASCL1) and Ki67. The basic helix-loop-helix protein ASCL1 is a proneural factor required for AH-NSCs to enter the cell-cycle (Andersen et al., 2014; Urban et al., 2016). Because ASCL1 protein is not expressed by quiescent AH-NSCs and labels only a fraction of IPs (Kim et al., 2011), it displays good specificity. However, ASCL1 is not a completely penetrant marker, as it expressed by only one-third of dividing AH-NSCs (Andersen et al., 2014). Moreover, ASCL1 also has functions in fate specification and differentiation in the embryonic nervous system (Castro et al., 2011; Guillemot and Hassan, 2016), and when ectopically expressed in the adult hippocampus, it leads to the aberrant formation of oligodendrocytes (Braun et al., 2015). Therefore, in mouse models where fate specification is altered it may no longer serve as a reliable readout of AH-NSC division.

In contrast, Ki67 appeared to be a more suitable choice for an approximate marker of AH-NSC division. For example, Ki67 is expressed throughout the cell cycle (Lopez et al., 1991) and therefore should label all dividing AH-NSCs (high penetrance). In the SGZ, it is expressed only by dividing AH-NSCs, dividing IPs and dividing neuroblasts and thereby also displays reasonable specificity (Scholzen and Gerdes, 2000). Moreover, because the function of Ki67 is restricted to chromatin organisation during cell division (Cuylen et al., 2016) it serves as a direct readout of division, which is unlikely to be altered in mouse models where fate specification is altered. Consequently, we chose to investigate whether Ki67, in combination with other markers, could be used to specifically identify dividing AH-NSCs in the hippocampus.

4.5.2 Negative selection against TBR2 is sufficient to exclude dividing IPCs and neuroblasts

To distinguish between dividing nuclei ($Ki67^{+ve}$) that are AH-NSCs, and those that are dividing IPs or neuroblasts, we co-stained 12-16 week-old C57BL/6J mice with Ki67, the IP marker TBR2 and the neuroblast marker DCX (Figure 4.1A, B). We hypothesised that the exclusion of $TBR2^{+ve}$ and DCX^{+ve} cells would leave a population of $Ki67^{+ve}$; $TBR2^{-ve}$; DCX^{-ve} cells that would comprise the dividing AH-NSC pool. To assess the plausibility of this experimental design, we first examined the percentage of IPs and neuroblasts that expressed Ki67. Consistent with previous reports we found that the majority of $TBR2^{+ve}$ cells were labelled with Ki67 (83.1%, Figure 4.1C, D) (Hodge et al., 2008), while only 13.9% of DCX^{+ve} cells were labelled with Ki67 (Figure 4.1E, F). At this stage we also made an important observation. All dividing neuroblasts had an immature IP-like morphology and expressed TBR2 (Figure 4.1F). Because all dividing neuroblasts also expressed TBR2, this led us to posit that selection against TBR2 alone should be sufficient to identify dividing AH-NSCs.

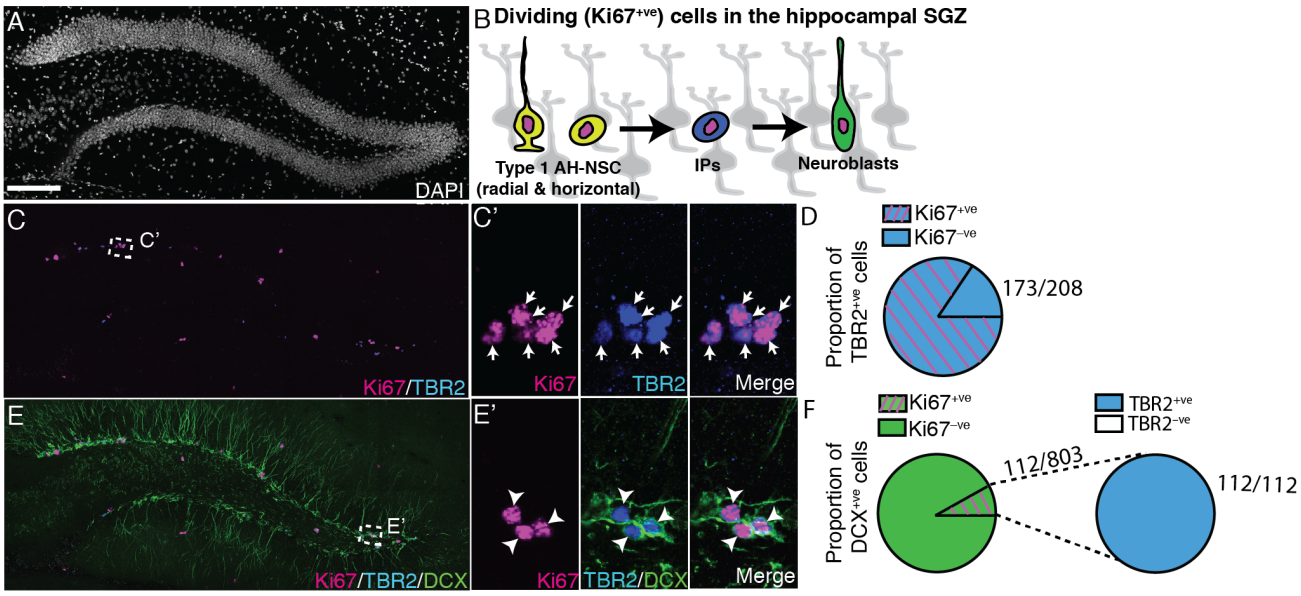

Figure 4.1: Negative selection against TBR2 is sufficient to exclude dividing IPs and dividing neuroblasts

(**A**) Coronal section of an adult mouse brain at the level of the hippocampus stained for DAPI (white). (**B**) A schematic showing the dividing ($Ki67^{+ve}$) cell types in the adult hippocampus. (**C, E**) The same coronal section as in (**A**) showing channels for (**in C**) TBR2 (blue), Ki67 (magenta) or (**in E**) TBR2, Ki67 and DCX (**green**). Boxed regions in **C** and **E** are presented in **C'** and **E'** respectively. (**D**) The majority of $TBR2^{+ve}$ cells (arrows in **C'**) co-label with Ki67. Surprisingly, all dividing DCX^{+ve} neuroblasts also express TBR2 (arrowheads in **E'**), as quantified in (**F**). Scale bar (in **A**): **A**, **C**, **E** 168 µm; **C'**, **E'** 22.5 µm.

4.5.3 Ki67^{+ve}; TBR2^{-ve} cells are dividing AH-NSCs

To assess whether the dividing TBR2^{-ve} cells were AH-NSCs we examined three parameters. First, we measured the relative expression of SOX2. In AH-NSCs the SOX2 transcription factor and its mRNA are downregulated as these cells differentiate, so that AH-NSCs express relatively higher levels of SOX2 than IPs (Hodge et al., 2012; Shin et al., 2015). We stained adult mouse hippocampal sections for Ki67, TBR2 and SOX2. Supporting their identity as AH-NSCs, dividing TBR2^{-ve} cells had a much higher expression of SOX2 than dividing TBR2^{+ve} cells (Figure 4.2A, B) ($P < 0.001$). Next, we measured nuclear size. Consistent with previous observations that NSCs are comparatively large (Rietze et al., 2001), the average area of the nucleus of dividing TBR2^{-ve} cells was approximately two-fold larger than dividing TBR2^{+ve} cells (Figure 4.2A, C) ($P < 0.001$). Finally, if dividing TBR2^{-ve} cells are AH-NSCs then we would expect that some of these cells, except for those that were horizontally orientated or out of focal plane (Lugert et al., 2010), to have a radial GFAP^{+ve} process. We investigated this by staining for Ki67, TBR2 and GFAP and observed that indeed many of the dividing TBR2^{-ve} cells were clearly linked to a radial GFAP^{+ve} process (Figure 4.2D, D'). Together these data suggest that a significant proportion of dividing TBR2^{-ve} cells are AH-NSCs.

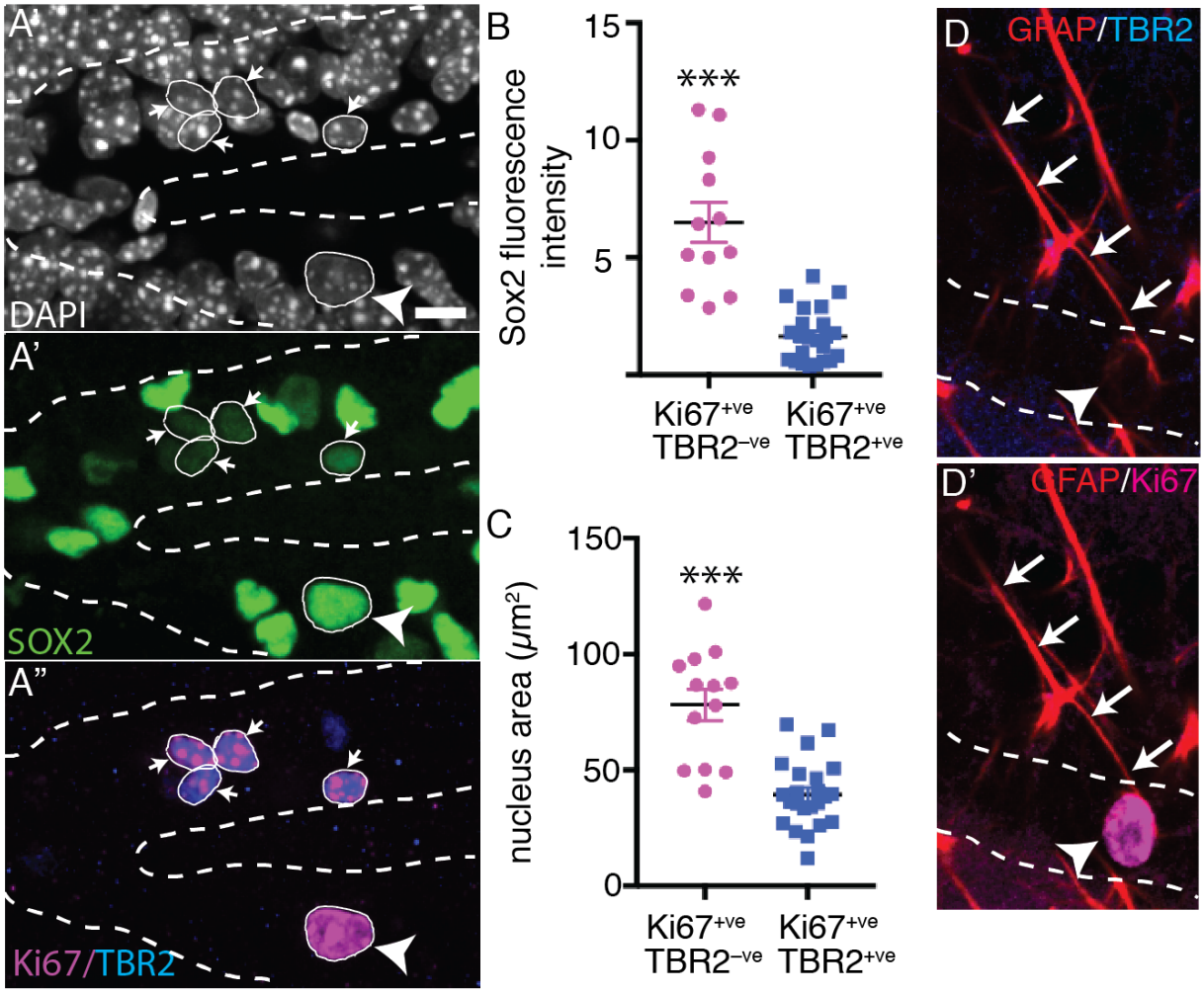

Figure 4.2: Ki67^{+ve}; TBR2^{-ve} nuclei have AH-NSC characteristics

(A-A") Coronal section of an adult mouse brain at the level of the hippocampus, showing DAPI (white, **A**), SOX2 (green, **A'**) TBR2 (blue, **A''**) and Ki67 (magenta, **A''**) staining. The dashed lines demarcate the SGZ of the dentate gyrus. Ki67^{+ve}; TBR2^{-ve} cells (e.g. arrowhead in **A**) have higher SOX2 fluorescence (**A', B**) and relatively larger nuclei (**A-A", C**) than Ki67^{+ve}; TBR2^{+ve} cells (arrows in **A-A"**). (**D, D'**) Coronal section of an adult mouse hippocampus showing TBR2 (blue, **D**), GFAP (red, **D** and **D'**) and Ki67 (magenta, **D'**) staining. Many Ki67^{+ve}; TBR2^{-ve} cells (arrowhead) were linked to a radial GFAP^{+ve} process (arrows). ***$P < 0.001$, *t*-test. Scale bar (in **A)**: **A**, **D** 9 μm.

4.5.4 Ki67^{+ve}; TBR2^{-ve} cells include horizontal AH-NSCs

Are all dividing TBR2^{-ve} cells in the SGZ AH-NSCs? Or does some fraction of these cells have another identity? For example, could some dividing, TBR2^{-ve} cells be IPs that do not express TBR2? To address this, we stained *Hes5*::GFP mice with Ki67 and TBR2, predicting that if dividing TBR2^{-ve} cells were AH-NSCs they should report high notch activity, which is indicated by GFP fluorescence in this line (Basak and Taylor, 2007; Lugert et al., 2010). Significantly, we found that all of the dividing, TBR2^{-ve} cells analysed expressed GFP (24/24 cells) (Figure 4.3A-C). The co-localisation of GFP with all dividing, TBR2^{-ve} cells suggests this population consists entirely of AH-NSCs.

The advantage of the nuclear-only stain described here is that it should enable the identification of dividing AH-NSCs regardless of their orientation. The findings of Lugert and colleagues (2010), revealed that up to two-thirds of dividing AH-NSCs, as defined by *Hes5::*GFP expression, are in a horizontal orientation, while only the remaining third were the classic radially-orientated AH-NSCs. To test whether the dividing TBR2^{-ve} population included both horizontal and radial cells we stained for Ki67 and TBR2 in *Hes5*::GFP mice, and used the cytoplasmic GFP label to examine cellular morphology. We found that approximately half the dividing TBR2^{-ve} cells exhibited a classical radial process (54%, 13/24 cells) (Figure 4.3A, D), while the remaining GFP^{+ve}; TBR2^{-ve} cells exhibited only a short horizontal process, fitting the description of horizontal AH-NSCs by Lugert and colleagues (2010) (46%, 11/24 cells) (Figure 4.3B, D). Together these data demonstrate that dividing TBR2^{-ve} cells, represent a population of AH-NSCs that includes cells with both radial and horizontal morphology.

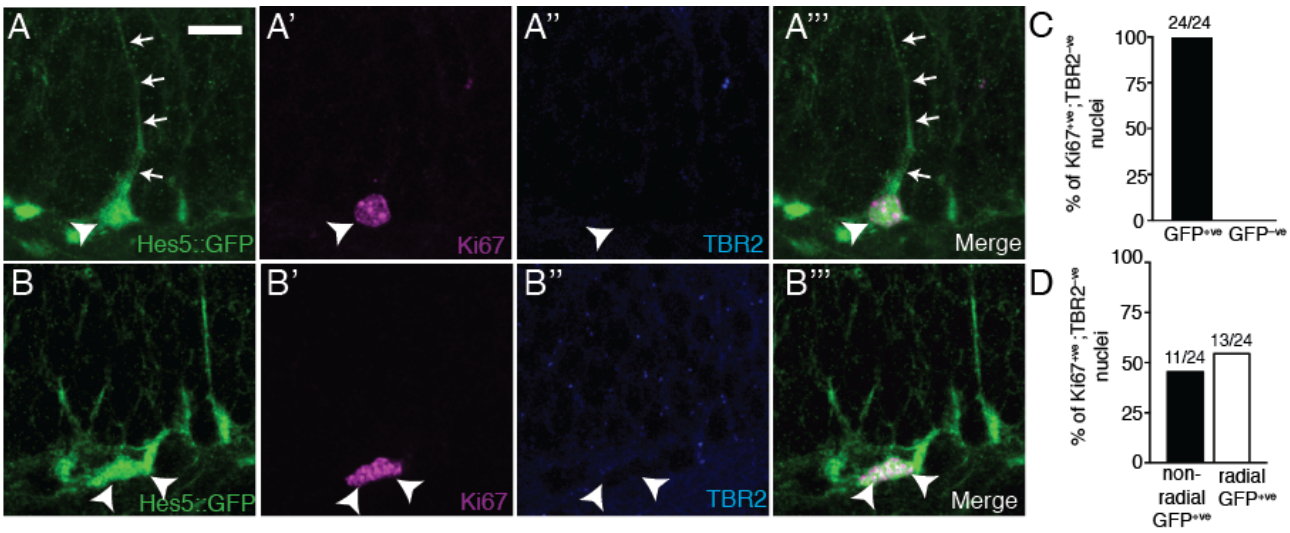

Figure 4.3: Ki67^{+ve}; TBR2^{-ve} nuclei include horizontally orientated *Hes5::*GFP AH-NSCs

(A-A"', B-B"') Coronal section of a mouse hippocampus, showing the dentate gyrus, with *Hes5::*GFP in (green), Ki67 (magenta) and TBR2 (red). (**A-A"'**) Some Ki67^{+ve}; TBR2^{-ve} nuclei (arrowhead) had a radial morphology (arrows), while others (**B-B"'**) had a horizontal morphology (arrowheads). **(C)** All Ki67^{+ve}; TBR2^{-ve} nuclei expressed GFP. (**D**) Radial and horizontal Ki67^{+ve}; TBR2^{-ve} nuclei were present in approximately equal numbers. Scale bar (in **A**): **A** 17 μm.

4.6 Discussion

This study provides a morphology independent approach to identify dividing AH-NSCs. The significance of this study, apart from it's accuracy and simplicity, lies in the fact that the majority of studies into AH-NSCs do not include horizontal AH-NSCs, as they do not possess a radially orientated fibre. Given that at least half (this study) or two-thirds (Lugert et al., 2010) of the dividing AH-NSC pool are horizontal cells, this potentially leads to an underestimation of stem cell numbers, or the misrepresentation of these dividing cells as IPs. Indeed, scenarios potentially exist where the enhancement or inhibition of certain signalling pathways may have no effect on the relative activation of radial AH-NSCs but does have an affect on the activation of horizontal cells. In this vein, there is evidence that subpopulations of AH-NSCs respond differently to signalling cues. For example, reporter strains such as the *Hes5*::GFP and *nestin*::GFP lines have previously been used in conjunction with the expression of EGFR to isolate homogeneous populations of neurosphere forming precursors *in vitro* which contain distinct subpopulations that are responsive to norepinephrine exposure or KCl-depolarisation (Jhaveri et al., 2015). Moreover, this study revealed that approximately one third of GFP^{+ve} cells in the dentate gyrus of adult *nestin*::GFP possessed a radial morphology, whereas the remainder exhibited a non-radial morphology (Jhaveri et al., 2015). Whether or not these morphologically different pools of *nestin*::GFP-expressing precursor cells respond differently to depolarisation or norepinephrine exposure *in vivo* remains a tantalising question.

While the main advantage of our morphology independent approach is that it allows for the quantification of both radially and horizontally orientated AH-NSCs, there are also other advantages. For example, because the stain only uses nuclear-localised antigens, it can be used to quickly quantify dividing AH-NSCs either manually or in an automated manner using image analysis software. This is in stark contrast to the current method that requires users to trace a radial process back to the correct nucleus in the SGZ, which is both time-consuming and difficult to automate. Our approach is also likely to be more accurate. Dividing neural progenitors are often found in cellular clusters (Hodge et al., 2008), and it becomes difficult to trace a radial process back to the correct nucleus. Moreover, because our method relies only on the co-localisation of two nuclear antigens, a relatively low-resolution confocal image is sufficient for the correct identification of these cells. Lastly, our method requires only a dual antibody stain (Ki67 and TBR2). Combining this stain with other markers can provide additional information if required. For example, a triple-stain with GFAP would provide an estimate of the proportion of dividing AH-NSCs that are radial ($GFAP^{+ve}$ radial process) or horizontally orientated. Alternately, a triple stain

with SOX2 could be used to also estimate the number of quiescent AH-NSCs (Ki67^{-ve}; SOX2^{+ve}; TBR2^{-ve}).

This work also serves to provide further evidence for the existence of horizontal AH-NSCs. While the original study describing this cellular population has been highly cited (Lugert et al., 2010), there are very few works that have subsequently investigated these cells (Lugert et al., 2012). This is perhaps surprising given that these cells are suggested to comprise a large proportion of dividing AH-NSCs within the adult brain. As described above, Jhaveri and colleagues reported recently that approximately one-third of *nestin*::GFP^{+ve}; EGFR^{+ve} cells exhibited a radial morphology, while two-thirds had a horizontal morphology (Jhaveri et al., 2015). Another study that supports the existence of horizontal AH-NSCs was published prior to Lugert and colleague's 2010 work. In this paper, similar horizontal precursors were reported within the hippocampus of adult *Sox2*::GFP mice (Suh et al., 2007); however, given that an IP-specific marker such as TBR2 was not used, these cells could have potentially represented IPs, which are known to express detectable levels of SOX2 protein. By using the same *Hes5*::GFP line used by Lugert and colleagues (2010) we have been able to identify *Hes5*::GFP^{+ve}; Ki67^{+ve}; TBR2^{-ve} cells without a radial process, thereby providing additional evidence for the existence of dividing AH-NSCs with a horizontal morphology.

This simple morphology independent approach to identify dividing AH-NSCs described in this study is an improvement over existing methods because it is more inclusive (radial and horizontal AH-NSCs), less time consuming and more accurate. The implementation of this approach will be pivotal to the interpretation of results from studies investigating the molecular control of neurogenesis.

Chapter 5 NFIX is essential for neuronal fate in the adult hippocampus

5.1 Aims of chapter 5

Thus far in this thesis I have examined the function of NFIX in promoting IPC production during the development of the dorsal (Chapter 3). I then proceeded to describe a new method for identifying dividing AH-NSCs (Chapter 4) to allow me to study NFIX function more accurately within this population in Chapter 5.

The aim of Chapter 5 is to define the role of NFIX during adult hippocampal neurogenesis. No previous work has examined the role of NFIX during adult hippocampal neurogenesis. There are a number of reasons why NFIX may play an important role in adult hippocampal neurogenesis. Firstly, as I have shown in this thesis thus far (Chapter 3), NFIX is a key regulator of embryonic neurogenesis during development. This is significant because developmentally important proteins tend to play important roles in adult hippocampal neural stem cells (AH-NSCs) too. Secondly, previous work (Harris et al., 2013) examining the expression pattern of NFIX in the adult brain detected a subset of cells expressing high levels of NFIX within the adult hippocampal stem cell niche. Finally, an *in vitro* study modelling quiescence, a feature unique to adult stem cells, implicated NFIX as a key regulator of this process (Martynoga et al., 2013). In addressing the role of NFIX during adult hippocampal neurogenesis I used strains of mice that allow for inducible deletion of NFIX from AH-NSCs, and secondly, from immature neurons. The fate of these cells was then examined histologically, and transcriptionally using RNA-seq. Behavioural studies were also used to examine the functional consequences of *Nfix*-deletion from hippocampal precursor cells.

5.2 Abstract

The transcriptional program underpinning adult hippocampal neurogenesis is incompletely understood. In mice, under normal physiological conditions adult hippocampal neural stem cells (AH-NSCs) generate neurons and astrocytes, but not oligodendrocytes. The factors limiting the tri-potentiality of AH-NSCs remain unclear. Here, we reveal that the transcription factor NFIX plays a key role within this process. NFIX is expressed by AH-NSCs, and its expression is sharply up regulated within neuroblasts in the adult hippocampus. Conditional ablation of *Nfix* from AH-NSCs, coupled with lineage tracing, transcriptomic sequencing and behavioural studies collectively reveal that NFIX is autonomously required for neuroblast maturation, survival and subsequent function. Moreover, a small number of AH-NSCs also develop into oligodendrocytes following *Nfix* deletion. Remarkably, when *Nfix* is deleted specifically from intermediate progenitor (IP) cells and neuroblasts using a *dcx-creER*^{T2} driver, these cells also display signatures of elevated oligodendrocyte *mRNA* expression. Together, these results demonstrate that NFIX promotes neuronal differentiation while suppressing the capacity of AH-NSCs, and their progeny, to develop into oligodendrocytes.

5.3 Introduction

NFIX is a transcription factor expressed during mouse nervous system development that governs neural stem/progenitor fate (Harris et al., 2015). In the developing dorsal telencephalon (Chapter 3) (Campbell et al., 2008; Heng et al., 2014; Harris et al., 2016a) and cerebellum of mice (Piper et al., 2011; Fraser et al., 2016), NFIX is essential for the timely differentiation of both neurons and astrocytes. The importance of NFIX for mouse brain development appears conserved during human brain development, as patients with *NFIX* mutations present with one of two developmental disorders characterised by a substantial brain phenotype. These disorders are either a Sotos Syndrome caused by loss-of-function *NFIX* mutations or the relatively more severe Marshall-Smith Syndrome caused by dominant-negative *NFIX* mutations (Malan et al., 2010; Sotos, 2014; Deciphering Developmental Disorders, 2017).

In the adult mouse (Goncalves et al., 2016) and human brain (Spalding et al., 2013), neural progenitors persist within the dentate gyrus of the hippocampus, where they generate dentate granule neurons that are thought to be important for learning/memory and mood regulation (Miller and Hen, 2015). We have previously shown that mice that are heterozygous for *Nfix* exhibit abnormal neurogenesis and deficiencies in hippocampal-dependent learning and memory tasks (Harris et al., 2013). However, as NFIX has been shown to modulate the embryonic and postnatal development of the hippocampus, in part via the regulation of intermediate progenitor cell development, it is not possible to definitively determine the role of NFIX in adult neurogenesis using heterozygous mice (Chapter 3) (Heng et al., 2014). As NFIX is highly expressed in adult hippocampal progenitor cells (Harris et al., 2013; Shin et al., 2015; Gao et al., 2016; Chen et al., 2017), and because the use of developmentally important proteins is often reiterated within adult hippocampal progenitor cells to execute similar programs of differentiation as during development (Urban and Guillemot, 2014), we therefore sought an alternative way to determine the role of NFIX within the adult hippocampus.

Using inducible *cre*-recombinase drivers and lineage tracing we reveal that NFIX expression is cell-autonomously required for the maturation and survival immature neurons (neuroblasts) within the mouse hippocampus. The removal of *Nfix* from AH-NSCs (*nestin-creER*^{T2}) culminated in neuroblasts failing to extend a dendritic branch and to mature into dentate granule neurons. Moreover, whereas wild-type AH-NSCs mostly generated neurons and occasionally astrocytes, we found that an increased proportion of *Nfix*-deficient AH-NSCs also generated oligodendrocytes.

Remarkably, these phenotypes were also recapitulated when *Nfix* was conditionally ablated from neuroblasts (*dcx-creER*^{T2}), with *Nfix*-deficient neuroblasts, which are committed to neuronal differentiation, displaying increased *mRNA* expression of oligodendrocyte precursor genes. These results demonstrate that NFIX is required for neuronal differentiation in the adult hippocampus through executing a program of neuronal maturation, and by suppressing the latent tri-potency of hippocampal precursor cells to generate oligodendrocytes. These findings also reveal that NFIX suppresses oligodendrocyte differentiation within neuroblasts themselves, highlighting a previously unknown plasticity in the potential of these cells. Collectively, these data enhance our understanding of the gene regulatory networks governing neural stem and progenitor cell fate within the adult hippocampus.

5.4 Methods

5.4.1 Animal ethics

The work performed in this study conformed to The University of Queensland Animal Welfare Unit guidelines for animal use in research (AEC approval number QBI/353/13/NHMRC). Experiments were performed in accordance with the Australian Code of Practice for the Care and Use of Animals for Scientific Purposes, and were carried out in accordance with The University of Queensland Institutional Biosafety committee.

5.4.2 Animals

The conditional *Nfix* (*Nfix*$^{f/f}$) mouse strain that contains *loxP* sites flanking exon 2 was generated (Messina et al., 2010) and modified through deletion of the PGK promoter-neo cassette as described in Chapter 2. We then crossed *Nfix*$^{f/f}$ mice to the *nestin-creER*^{T2} strain (Imayoshi et al., 2006) to generate *Nfix*^{iNestin} mice, and separately to the *dcx-creER*^{T2} strain (Cheng et al., 2011) to generate *Nfix*^{iDcx} mice. Genotypes for the treatment condition were *Nfix*^{iNestin} or *Nfix*^{iDcx} mice that were given tamoxifen dissolved in corn-oil. Genotypes for the control condition were *cre*-negative *Nfix*^{control} mice treated with tamoxifen or *Nfix*^{iNestin} or *Nfix*^{iDcx} that were given corn-oil only. Finally, the *Nfix*^{iNestin} and *Nfix*^{iDcx} strains were also crossed to a tdtomato reporter line containing a *loxP*-flanked STOP cassette (Madisen et al., 2010) (JAX, strain #007914). The genotypes for the treatment mice in these experiments were *Nfix*$^{iNestin\text{-}TD}$ and *Nfix*$^{iDcx\text{-}TD}$ mice, while the respective controls were Wt$^{iNestin\text{-}TD}$ mice and Wt$^{iDcx\text{-}TD}$ mice. All reporter mice received tamoxifen. Both male and female mice were used throughout this study.

5.4.3 Tamoxifen treatment and BrdU injections

Tamoxifen solution (30mg/ml) was prepared for intraperitoneal injections by dissolving the tamoxifen powder (T5648, Sigma, St Louis, MO) in a mix of 10% ethanol and cornflower oil (C8267, Sigma). Eight to ten week old *Nfix*^{iNestin} mice were injected with tamoxifen (180 mg/kg) daily for four days, and collected 5, 14, 45, 120 or 365 days (1-year) post the final injection (dpi). Likewise, *Nfix*^{iDcx} mice, except where stated (Figure 5.10G) where injected daily for four days, for two consecutive weeks and were collected 7 dpi.

5.4.4 Preparation of fixed brain tissue

Adult mice were perfused transcardially first with PBS (10 ml), followed by 4% PFA (30 ml) then post-fixed for 48-72 h before long term storage in PBS at 4°C. Brains were embedded in noble agar and sectioned in a coronal plane at 50 μm using a vibratome (Leica, Deerfield, IL). Sections were mounted on slides before heat-mediated antigen retrieval was performed in 10 mM sodium-citrate solution at 95°C for 15 min.

5.4.5 Antibodies and immunofluorescence

Immunofluorescence was performed as described in Chapter 3. Primary rabbit species antibodies used were anti-NFIX (AB101341, 1/500, Abcam Cambridge, UK), anti-NeuN (EPR12763, 1/800, Abcam), anti-DCX (AB18723, 1/1000, Abcam), anti-TBR2 (AB23345, 1/800, Abcam), anti-Olig2 (AB9610, 1/300, Millipore**)** and anti-GFAP (Z033429-2, 1/1000, Dako). The primary mouse species antibodies used were anti-BrdU (G3G4, 1/100, DHSB, Iowa city, IA), anti-NFIX clone 3D2 (SAB1401263, 1/400, Sigma-Aldrich), anti-Ki67 (550609, 1/200, BD Pharmingen). The primary rat species antibodies used were anti-SOX2 (53-9811-80, 1/400, Ebioscience). Goat primaries used were anti-tdtomato (AB8181-200, 1/1000, Sicgen) and anti-DCX (sc-8066, 1/200, Santa Cruz).

5.4.6 Imaging and cell counts

Brains were sectioned in a coronal plane at 50μm. Every 6th section, spaced 300μm apart (6 sections per brain) was then immunostained using fluorescent secondary antibodies. Exceptions to these were analyses using tdtomato^{+ve} mice where 3 sections per brain were analysed. Imaging of these stains were performed using a 40X water objective on a Zeiss Axio Observer Z1 spinning disk confocal through a depth of 10μm, with a Z-step size of 1μm (X and Y pixel dimension = 0.3125μm). The area of the dentate gyrus, multiplied by the z-stack depth was used to generate a volumetric measurement against which the number of cells per mm^3 was calculated. All cell counts were performed blind to the genotype and treatment condition.

5.4.7 FACS and extraction of RNA for sequencing

The dentate gyri of reporter mice were dissected in ice-cold PBS according to Hagihara and colleagues (2009) protocol. Tissue was then minced using a scalpel blade for 2 min, before being enzymatically disassociated in 1ml of trypsin (Sigma-Aldrich) for 15 min, with gentle trituration at

the mid-way point using a 1 ml plastic pipette tip. The enzymatic reaction was stopped by addition of 1 volume of trypsin inhibitor (Sigma-Aldrich). The cell suspension was then spun at 300 relative centrifugal force for 5 min, before being resuspended in 4 ml of 1% bovine-serum-albumin (BSA)/PBS solution and passed through a 45 µm filter. The filtered solution was then pelleted, and resuspended in 250 µl of PBS. Zombie violet dye (1:500) (#423113, Biolegend) was incubated with the cell suspension for 5min to label dead cells, and the dye reaction stopped by the addition of 2.5 µl of BSA. Cells were sorted on a BD Influx^{TM} fluorescence activated cell sorter using Sortware 1.2.0141 software. Instrument settings were as follows: 100 µm nozzle, 26.50 KHz drop drive frequency with a 1.0 drop pure sort mode. The tdtomato^{+ve} gate and zombie-violet^{-ve} gate were set relative to the background fluorescence of C57Bl/6 control mice. The number of tdtomato^{+ve} cells sorted per animal varied for each of the two fluorescent activated cell sorting (FACS) experiments. There were approximately 500 sorted cells for each *Nfix*$^{iNestin\text{-}TD}$ mouse, and approximately 250 cells per *Nfix*$^{iDcx\text{-}TD}$ mouse. Cells were sorted directly into 500 µl of buffer RLT, and stored on ice until RNA was extracted using an RNeasy Micro Kit (Qiagen). RNA was amplified according to the Smart-seq2 protocol (Picelli et al., 2013) using 12 cycles for *Nfix*$^{iNestin\text{-}TD}$ animals and 13 cycles for *Nfix*$^{iDcx\text{-}TD}$ animals.

5.4.8 Processing and analysis of RNA-seq data

Data was analysed on the public Galaxy server, Galaxy version 16.07 (Goecks et al., 2010). Raw reads were aligned to the mouse genome (mm10) using Tophat (Trapnell et al., 2009). Transcript levels were quantified in HTSeq-count (Anders et al., 2015) by mapping to known mouse (mm10) RefSeq (NCBI) protein coding sequences, which were downloaded in a GTF format from the UCSC table browser. In HTSeq-count the overlap mode used was "union", and the strandedness set to "no". Differential gene expression analysis was then performed using the DeSeq2 package (Love et al., 2014). Gene ontology (GO) was performed in DAVID (Huang da et al., 2009b; Huang da et al., 2009a). For DAVID analysis the background gene set comprised of any gene with a non-zero count in the DeSeq2 output (Timmons et al., 2015). To summarise redundant GO terms from DAVID, the program REVIGO and the semantic similarity measure Simrel was employed (Supek et al., 2011).

5.4.9 Behavioural analysis

The active place avoidance task assesses hippocampal-dependent spatial learning (Cimadevilla et al., 2001; Stuchlik et al., 2013) and has been described previously (Vukovic et al., 2013; Leinenga

and Gotz, 2015). The apparatus consists of a clockwise-rotating elevated arena (diameter 77cm, Bio-Signal group) rotating at 1 rpm, which had a grid floor and a 32 cm high clear plastic circular fence. Four contrasting visual cues were placed on the walls of the testing room. The position of the mouse in the arena was monitored with an overhead camera linked to tracker software (Bio-Signal group). To commence a trial, the mouse was placed in the arena facing the wall directly opposite the shock zone. A 500 ms, 60 Hz, 0.5 mA mild shock was delivered through the grid floor when the mouse entered the 60 degree shock zone, and every 1,500 ms until the mouse left the shock zone. The shock zone position did not change throughout the experiment. Each session lasted 10 min for 5 consecutive days. Mice were habituated to the arena 24 hrs prior to testing, in which mice were placed in the rotating arena to explore for 5 min but the shock zone was not active during this time. All movies were analyzed offline using Track Analysis software (Bio-Signal Group). Mice were handled for three days prior to habituation. Experiments were perfomed by a female experimenter. All mice that underwent behavioural testing received tamoxifen to control for effect of the drug on performance (Vogt et al., 2008).

5.4.10 Statistical analyses

The parameters of our statistical testing approach were specified prior to data collection. Two-tailed unpaired Students *t* tests were performed when comparing two groups. For experiments involving two independent variables two-way ANOVA was performed, with repeated-measures if applicable*;* *P* values from two-way ANOVA are reported in the text. Any significant main effect of genotype detected by two-way ANOVA was followed by multiple t-tests using a pooled estimate of variance where appropriate.

5.5 Results

5.5.1 NFIX is selectively upregulated during neuronal differentiation in the adult hippocampus

The expression pattern of NFIX in the adult hippocampus may provide clues as to the function of this protein during neurogenesis. There are the four main cell types that comprise the neurogenic lineage in the adult hippocampus. In order of lineage progression these are the mostly quiescent AH-NSCs (type 1), the highly proliferative intermediate progenitors (IPs, type 2), neuroblasts (immature neurons, type 3) and dentate granule neurons (Goncalves et al., 2016). We have previously shown that NFIX is expressed by virtually all cells in the dentate gyrus and that its expression was particularly high in DCX^{+ve} neuroblasts (Harris et al., 2013; Chen et al., 2017). However, a recent single-cell RNA-seq study found that there was a strong positive correlation between *Nfix* expression levels and the transition from an AH-NSC identity to an IP cell identity (Shin et al., 2015), suggesting that NFIX levels may increase prior to the neuroblast stage. To accurately map the expression levels of NFIX during adult hippocampal neurogenesis we examined its expression alongside cell type specific markers of lineage progression. We defined AH-NSCs as $SOX2^{+ve}$ cells positioned within the subgranular zone that were negative for TBR2 (see Chatper 4) (Hodge et al., 2008), IPs as $TBR2^{+ve}$ cells and neuroblasts as DCX^{+ve} cells. Consistent with the single-cell sequencing data (Shin et al., 2015) we found that NFIX expression was relatively low in AH-NSCs but was sharply upregulated in IPs ($P = 0.0042$) (Figure 5.1A-D). This high level of NFIX expression was maintained in neuroblasts including those with a relatively mature morphology, as indicated by the presence of substantial dendritic tree. Finally, we examined the expression of NFIX by dentate granule neurons. Dentate granule neurons were defined as cells positioned in the granule cell layer of the dentate gyrus and exhibited reduced expression of NFIX levels compared to IPs and neuroblasts ($P = 0.011$) (Figure 5.1E-H). These data show that NFIX expression levels peak as hippocampal neural progenitors undergo neuronal differentiation (Figure 5.1I).

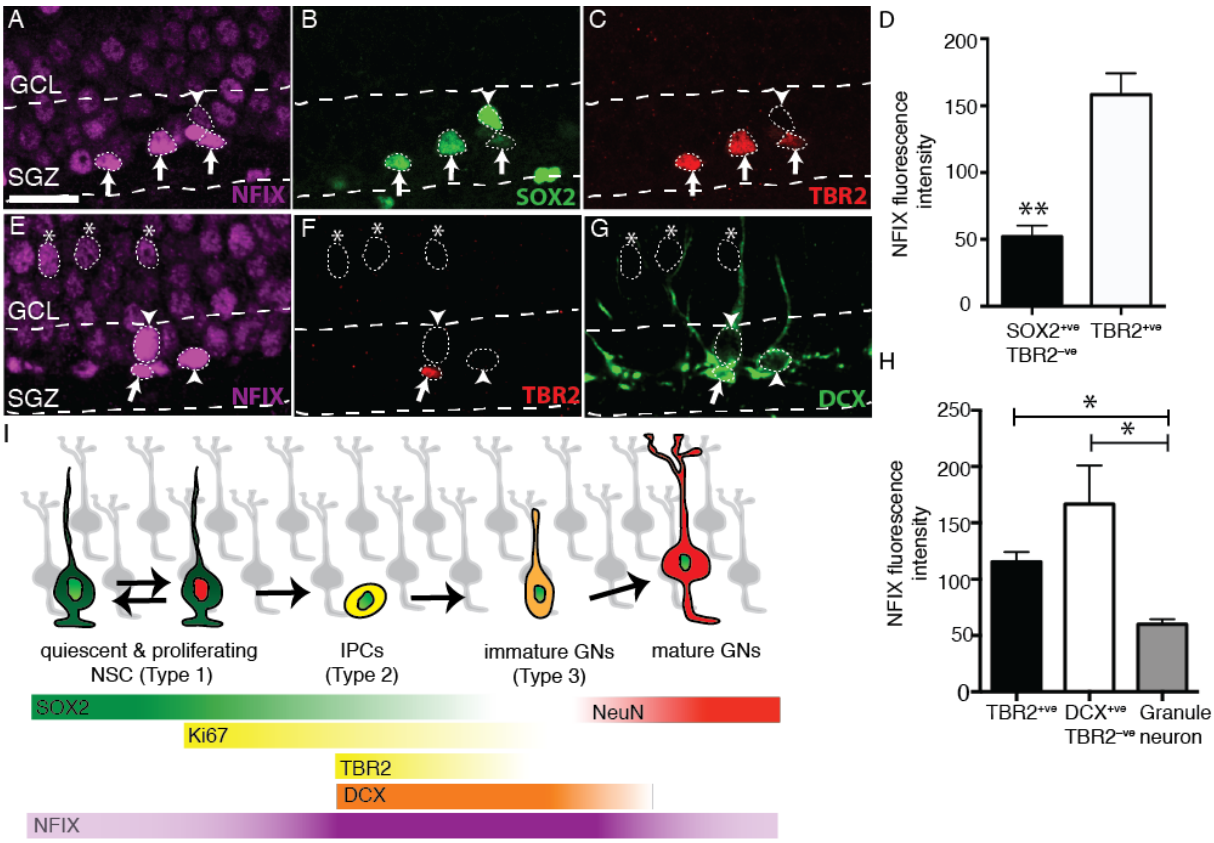

Figure 5.1: NFIX is expressed throughout the hippocampal neurogenic lineage but selectively upregulated during neuronal differentiation

(**A-C**) NFIX (magenta), SOX2 (green) and TBR2 (red) staining in the dentate gyrus of a 10-week old mouse. Dashed lines demarcate the SGZ. The arrowhead indicates an AH-NSC ($SOX2^{+ve}$; $TBR2^{-ve}$), whereas the arrows indicate IPs ($TBR2^{+ve}$). (**D**) The relative NFIX fluorescence intensity is higher in IPs than AH-NSCs. (**E-G**) NFIX (magenta), TBR2 (red) and DCX (green) staining in the dentate gyrus of a 10-week old mouse. The arrow indicates an IP ($TBR2^{+ve}$), the arrowheads indicate mature neuroblasts (DCX^{+ve}; $TBR2^{-ve}$ cells) and the asterisks indicate dentate granule neurons in the GCL. (**H**) NFIX expression is highest in both IPs and neuroblasts and then decreases in mature granule neurons. (**I**) A schematic of the NFIX expression levels during hippocampal neurogenic lineage progression. *$P < 0.05$, **$P < 0.01$. Scale bar (in **A**): **A-C**, **E-G** 24µm. Graphs depict mean ± s.e.m from 3 mice. Abbreviations: subgranular zone (SGZ), granule cell layer (GCL).

5.5.2 Inducible deletion of *Nfix* from AH-NSCs

Nfix null mice are perinatal lethal and have severe developmental defects, which prevents their use to address the role of NFIX during adult hippocampal neurogenesis (Campbell et al., 2008). To circumvent this problem we generated an inducible, loss-of-function mouse line by crossing mice containing a floxed *Nfix* allele to an inducible *nestin-creER*^{T2} deletion strain (Imayoshi et al., 2006), generating *Nfix*^{iNestin} or *Nfix*^{control} mice. Tamoxifen administration to adult *Nfix*^{iNestin} mice activated cre-recombinase in *nestin*-expressing progenitor cells (AH-NSCs and IPs). Five days after tamoxifen administration (5 dpi) to adult (8-10 week old) *Nfix*^{iNestin} mice NFIX was detected in only 39.3% of AH-NSCs and 12.9% of IPCs, compared to 91.7% and 100% respectively in *Nfix*^{control} animals (Figure 5.2A-E). Importantly, we found no evidence that NFIX was deleted from other cell types within the dentate gyrus niche, including from dentate granule neurons and astrocytes (data not shown). Therefore, the *Nfix*^{iNestin} mouse is an efficient and specific deletion strain for interrogating the function of NFIX in AH-NSCs.

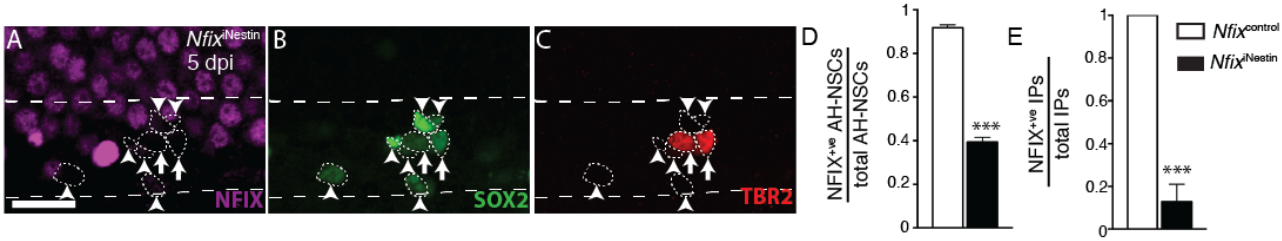

Figure 5.2: *Nfix* deletion in *Nfix*^{iNestin} mice

(**A-C**) NFIX (magenta), SOX2 (green) and TBR2 (red) staining in the dentate gyrus of adult *Nfix*^{iNestin} mice at 5 dpi. Dashed lines demarcate the SGZ. Arrowheads indicate AH-NSCs (SOX2^{+ve}; TBR2^{-ve}), while arrows indicate IPs (TBR2^{+ve}). Both AH-NSCs and IPs lack NFIX expression. Quantification of the proportion of AH-NSCs (**D**) and IPs (**E**) that express NFIX in *Nfix*^{iNestin} and *Nfix*^{control} animals at 5 dpi. Scale bar (in **A**): **A-C** 24µm. ***$P < 0.001$. Graph depicts mean ± s.e.m from 3 *Nfix*^{iNestin} mice and 4 *Nfix*^{control} mice.

5.5.3 NFIX is not required for the long-term maintenance of AH-NSCs

AH-NSCs are mostly quiescent, an adaptive feature of adult stem cells that ensures their long-term survival by protecting against metabolic stress caused by excessive cellular division (Valcourt et al., 2012; Rando et al., 2014). In a recent study using an *in vitro* model of neural stem cell quiescence, NFIX was strongly enriched in active enhancer regions specific to the neural stem cell quiescent state (Martynoga et al., 2013). Furthermore, NFIX overexpression was shown to be sufficient to induce quiescence in normally proliferating neural stem cells. These data led us to hypothesise that *Nfix* deletion in *Nfix*^{iNestin} mice might lead to the premature depletion of AH-NSC pool due to a loss of quiescence. Surprisingly, we found that *Nfix* deletion had no effect on total AH-NSC number (SOX2^{+ve}; TBR2^{-ve}) at 14 dpi, 120 dpi or even 1 year post-injection (Figure 5.3B-D). We verified this observation using an alternative definition of AH-NSCs as SOX2^{+ve} cells that extend a GFAP^{+ve} process into the granule cell layer (Seri et al., 2001; Steiner et al., 2006). Using this definition, we again saw no effect of *Nfix* deletion on the number of AH-NSCs in *Nfix*^{iNestin} mice relative to controls (Figure 5.4A-D). These data demonstrate that NFIX deletion has no effect on the maintenance of AH-NSCs over the long-term.

As the total number of AH-NSCs was not altered following depletion of *Nfix* from AH-NSCs, these data suggest that NFIX may not play as prominent a role in modulating quiescence compared to its role *in vitro* (Martynoga et al., 2013). We addressed this by examining the relative proliferation/quiescence of AH-NSCs in *Nfix*^{iNestin} and control animals using the morphology independent staining method outlined in Chapter 4. At 14 dpi there was an increase in the number of AH-NSCs in *Nfix*^{iNestin} mice that were proliferating (Ki67^{+ve}; SOX2^{+ve}; TBR2^{-ve}) (Figure 5.3E), supporting the *in vitro* observations that NFIX mediates quiescence (Martynoga et al., 2013). However, the effect size was small, and it did not lead to a detectable increase in the number of IPs at 14 dpi (Figure 5.3F). Critically, the effect was also transient, as there was no difference in the relative proliferation of AH-NSCs between groups at 120 dpi or 1 year post-injection (Figure 5.3E). Therefore, NFIX is not essential to maintain AH-NSC quiescence *in vivo*. Interestingly, at 120 dpi there was a small increase in the number of IPs, this together with the increased expression of NFIX in IPs and neuroblasts (Figure 5.1) implies that NFIX may be important for later aspects of lineage progression.

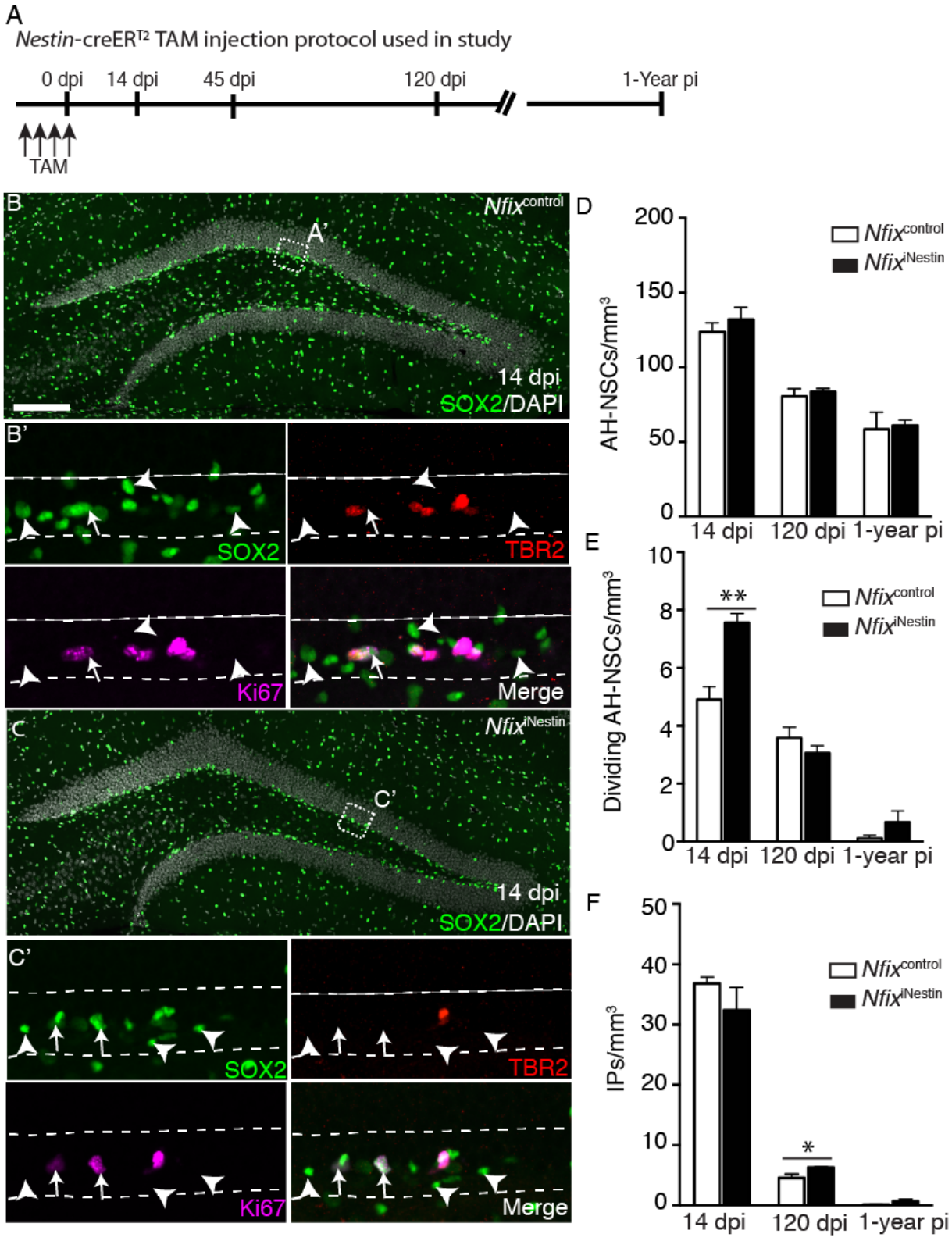
A
Nestin-creER^{T2} TAM injection protocol used in study
0 dpi
14 dpi
45 dpi
120 dpi
1-Year pi
TAM
B
Nfix^{control}
A'
14 dpi
SOX2/DAPI
B'
SOX2
TBR2
Ki67
Merge
C
Nfix^{iNestin}
C'
14 dpi
SOX2/DAPI
C'
SOX2
TBR2
Ki67
Merge
D
AH-NSCs/mm^3
200
150
100
50
0
Nfix^{control}
Nfix^{iNestin}
14 dpi
120 dpi
1-year pi
E
Dividing AH-NSCs/mm^3
10
8
6
4
2
0
**
Nfix^{control}
Nfix^{iNestin}
14 dpi
120 dpi
1-year pi
F
IPs/mm^3
50
40
30
20
10
0
*
Nfix^{control}
Nfix^{iNestin}
14 dpi
120 dpi
1-year pi

Figure 5.3: NFIX is not required for the long-term survival of AH-NSCs

(**A**) Schematic of tamoxifen regime used in *nestin-creER*^{T2} mice. (B) *Nfix*^{control} and (**C**) *Nfix*^{iNestin} mice at 14 dpi showing staining for DAPI (white) and SOX2 (green). Boxed regions in **B** and **C** are shown in panels **B'** and **C'** respectively. **B'** and **C'** show SOX2 (green), TBR2 (red) and Ki67 (magenta), with the dashed lines outlining the SGZ of the dentate gyrus. Marked cells in **B'** and **C'** indicate AH-NSCs (SOX2^{+ve}; TBR2^{-ve}). Arrows indicate dividing AH-NSCs (Ki67^{+ve}), arrowheads indicate quiescent AH-NSCs (Ki67^{-ve}). (**D**) There is no effect of NFIX deletion on AH-NSC number at 14 dpi, 120 dpi or 1 year post-injection (pi). (**E**) At 14 dpi there are more dividing AH-NSCs in *Nfix*^{iNestin} mice than in controls, but this effect was not observed at 120 dpi or 1-year pi. (**F**) IP number was unchanged at 14 dpi and was slightly increased at 120 dpi in *Nfix*^{iNestin} mice. **P* < 0.05, ***P* < 0.01. Scale bar (in **A**): **A**, **B** 159 μm, **A'**, **B'** 44 μm. Graphs depict mean ± s.e.m from 6 control and 4 *Nfix*^{iNestin} mice at 14 dpi, 4 mice per genotype at 120 dpi and 3 mice per genotype at 1 year post-injection.

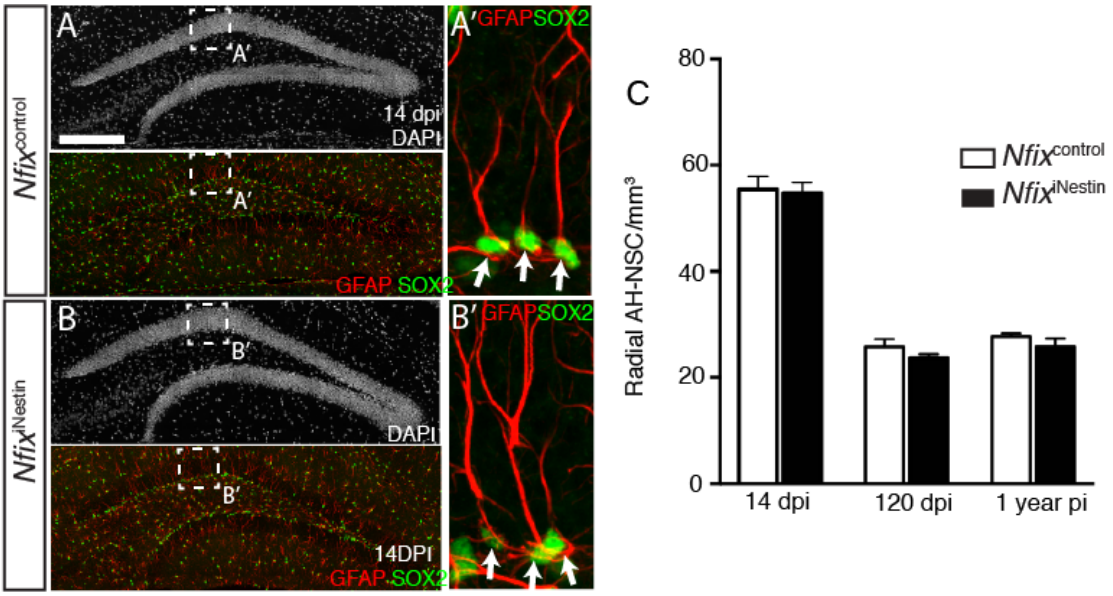

Figure 5.4: No effect of NFIX deletion on the survival of radial AH-NSCs.

Nfix^{control} (**A**) and *Nfix*^{iNestin} mice (**B**) stained for DAPI (white), GFAP (red) and SOX2 (green). Boxed regions in **A** and **B** are shown at higher magnification in **A'** and **B'** respectively and show GFAP and SOX2 staining. Arrows indicate radially oriented AH-NSCs with a GFAP^{+ve} process linked to a SOX2^{+ve} nucleus. (**C**) No differences in the number of radial AH-NSCs were detected at 14 dpi, 120 dpi or 1-year pi. Scale bar (in **A**): **A**, **B** 271 µm; **A'**, **B'** 18 µm. Graph depicts mean ± s.e.m from 6 control and 4 *Nfix*^{iNestin} mice at 14 dpi, 4 mice per genotype at 120 dpi and 3 mice per genotype at 1-year post-injection.

5.5.4 Neuroblasts fail to mature in *Nfix*^{iNestin} mice.

During brain development NFIX promotes neuronal differentiation, with abnormal expression associated with multiple neurodevelopmental disorders (Malan et al., 2010; Yoneda et al., 2012; Heng et al., 2014; Harris et al., 2016a; Deciphering Developmental Disorders, 2017). The increased expression of NFIX in IPs and neuroblasts (Figure 5.1I) suggests that NFIX may play a central role in regulating neuronal differentiation in the adult hippocampus. To investigate whether NFIX regulates neuronal differentiation during adult hippocampal neurogenesis we examined the expression of the neuroblast marker DCX. At 45 dpi (P = 0.0007) and 120 dpi (P = 0.0002) there were 2-3 fold fewer DCX^{+ve} cells in *Nfix*^{iNestin} mice compared with *Nfix*^{control} mice (Figure 5.5A-C). A higher proportion of DCX^{+ve} cells in *Nfix*^{iNestin} mice co-labelled with cleaved-caspase-3 (P = 0.11) (Figure 5.5E) suggesting this decrease in neuroblast number was in part due to increased cell death. Of the remaining neuroblasts in *Nfix*^{iNestin} mice, many had an aberrant morphology. Specifically, only 16.6% of neuroblasts in *Nfix*^{iNestin} mice extended a primary dendrite into the granule cell layer of the dentate gyrus compared to 77.5% of control neuroblasts at 45 dpi (P < 0.0001) with a similar effect at 120 dpi (P = 0.029) (Figure 5.5D). Furthermore, a greater proportion of *Nfix*-deficient neuroblasts retained expression of the IP marker TBR2 at both 45 dpi (P = 0.008) and 120 dpi (P = 0.0011) (Figure 5.5F). These data demonstrate that in the absence of *Nfix*, early-stage neuroblasts fail to mature and an increased proportion of them undergo programmed cell death.

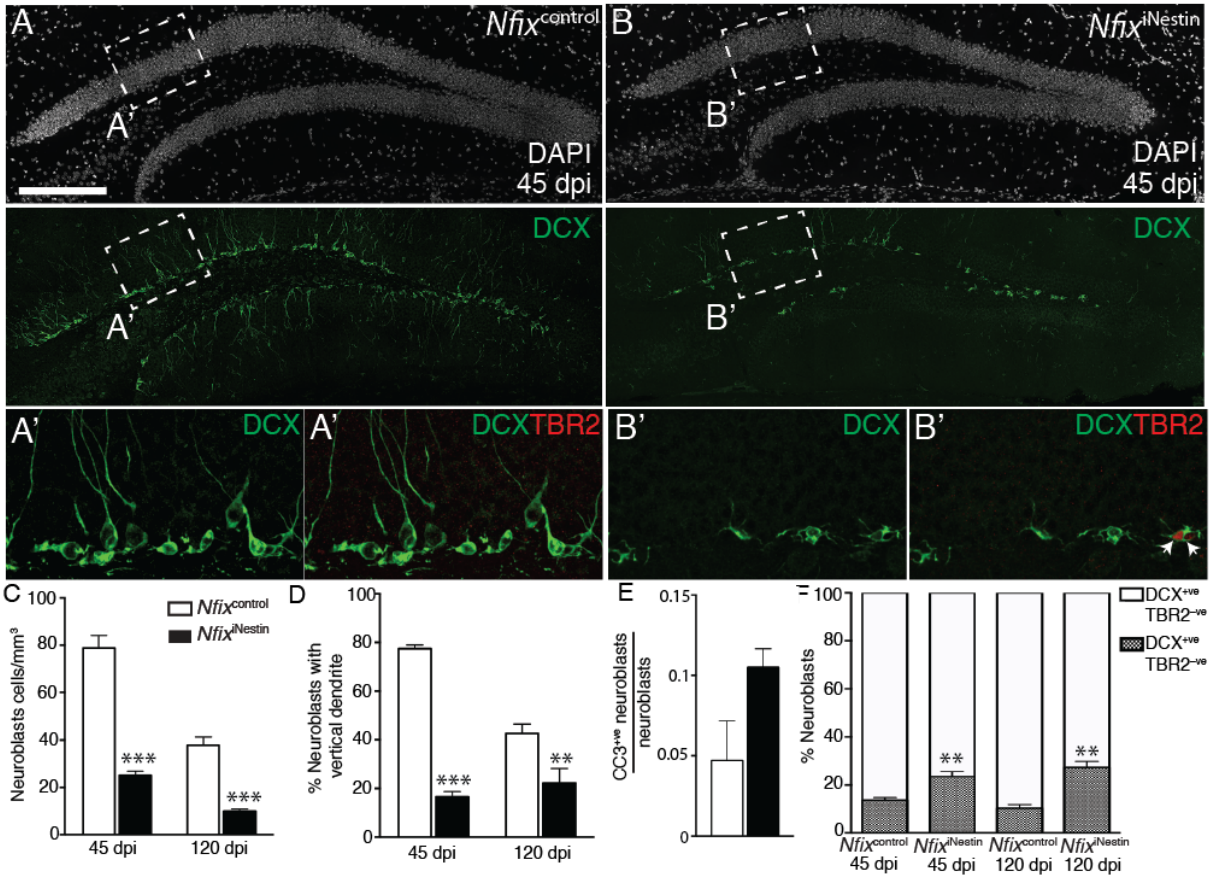

Figure 5.5: Neuroblasts fail to mature in *Nfix*^{iNestin} mice.

Nfix^{control} (**A**) and *Nfix*^{iNestin} mice (**B**) at 45 dpi stained for DAPI (white) and DCX (green). Boxed regions in **A** and **B** are shown at higher magnification in **A'** and **B'** respectively, and show DCX (green) and TBR2 (red). Compared to controls (**A'**), *Nfix*^{iNestin} mice (**B'**) have fewer neuroblasts (DCX^{+ve} cells) at 45 and 120 dpi with tamoxifen (**C**). As a proportion, at both 45 and 120 dpi there are fewer neuroblasts in *Nfix*^{iNestin} mice that have a vertical dendritic process (**D**), while more co-express the apoptotic marker CC3 (**E**), and TBR2 (**F**). $^{**}P < 0.01$, $^{***}P < 0.001$. Scale bar (in **A**): **A**, **B** 243µm; **A'**, **B'** 50 µm. Graphs depict mean ± s.e.m from 4 mice per genotype at 45 and 120 dpi.

5.5.5 *Nfix*^{iNestin} mice generate fewer mature granule neurons and have reduced performance in a hippocampal-dependent memory task

Over a period of 3-4 weeks, neuroblasts integrate into the existing hippocampal circuitry where they facilitate the formation of new memories (Goncalves et al., 2016). Since surviving *Nfix*-deficient neuroblasts exhibit an aberrant and immature morphology (Figure 5.5), we asked whether these cells were capable of differentiating into mature dentate granule neurons. We injected BrdU daily (for 5 days) beginning 2 weeks after tamoxifen administration to label proliferating IPs, and sacrificed these animals 4 weeks after the final BrdU injection (Figure 5.6A). In control animals very few BrdU labelled cells identified as DCX^{-ve}; NeuN^{-ve} progenitors or DCX^{+ve} neuroblasts. Instead, the majority of BrdU labelled cells were negative for DCX and positive for the mature neuron marker NeuN (DCX^{-ve}; NeuN^{+ve}) (Figure 5.6B, D). In *Nfix*^{iNestin} mice however, there were 3 fold fewer DCX^{-ve}; NeuN^{+ve} cells (P = 0.0009) (Figure 5.6D) indicating that NFIX deficient neuroblasts fail to efficiently generate dentate granule neurons.

The generation of adult-borne dentate granule neurons is required for aspects of hippocampal-dependent learning in mice. For example, suppressing neurogenesis is typically associated with impaired encoding of new memories (Deng et al., 2010) and *vice versa* (Sahay et al., 2011; Stone et al., 2011). We next asked whether the reduced production of dentate granule neurons in *Nfix*^{iNestin} mice results in impaired performance in the active place avoidance (APA) task (Cimadevilla et al., 2001; Stuchlik et al., 2013). In this task, mice are placed in a rotating circular enclosure for 10 min, using external cues to learn to avoid a 60° segment of the arena that confers an electric shock upon entry. The ability of mice to learn to avoid the shock zone has previously been shown to rely on the generation of adult-borne neurons (Vukovic et al., 2013), just as with other tasks such as the Morris Water Maze. As expected, on the first day of testing when the mice are naïve to the task, there was no difference between the number of shocks received by *Nfix*^{iNestin} and *Nfix*^{control} animals (Figure 5.6G). However, by day 5 (P = 0.031), control mice had improved their performance, such that they received significantly less shocks than on the first day of testing. In contrast, the number of shocks received by *Nfix*^{iNestin} mice did not improve during testing, and these animals performed significantly worse than controls on day 4 (P = 0.0133) and day 5 (P = 0.0251) of testing (Figure 5.6E-G). On all other parameters tested such as distance travelled and speed of movement *Nfix*^{iNestin} mice performed comparably to controls (Figure 5.7A, B). Furthermore, mutant animals performed comparable to controls during a primary SHIRPA screen (Figure 5.7C, D). These findings

demonstrate that the impaired differentiation of neuroblasts in *Nfix*^{iNestin} mice leads to a specific deficit in a hippocampal-dependent learning task.

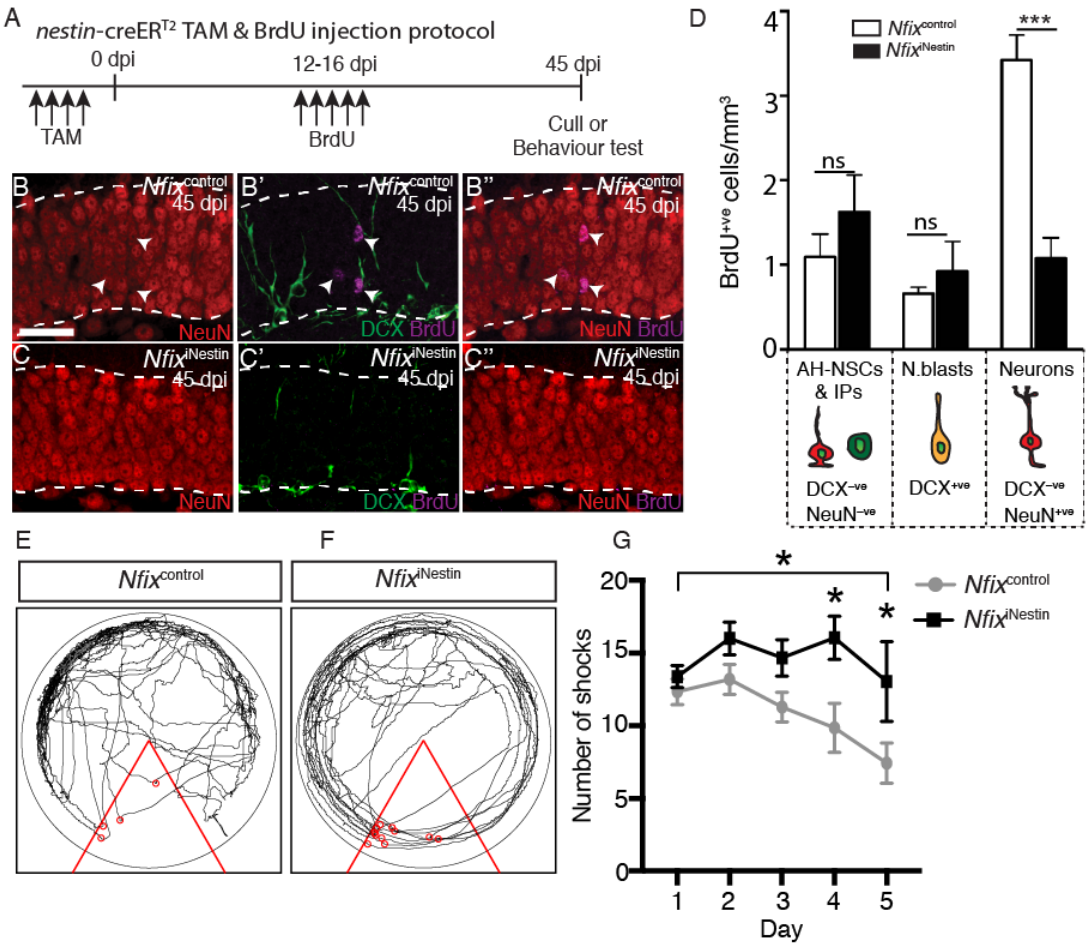

Figure 5.6: *Nfix*^{iNestin} mice generate fewer mature granule neurons and have reduced performance in an APA task

(**A**) The tamoxifen-BrdU injection regime used for *Nfix*^{iNestin} and *Nfix*^{control} mice. (**B-B”**) *Nfix*^{control} and (**C-C**”) *Nfix*^{iNestin} mice at 45 dpi showing DCX (green), NeuN (red) or BrdU (magenta) staining, with dashed lines outlining the granule cell layer of the dentate gyrus. BrdU^{+ve} dentate granule neurons, defined as NeuN^{+ve}; DCX^{-ve} cells, are indicated by the arrows in **B-B”**. (**D**) There were far fewer BrdU^{+ve} dentate granule neurons generated in *Nfix*^{iNestin} mice relative to controls, as quantified in **D**. Representative movement traces of (**E**) *Nfix*^{control} and (**F**) *Nfix*^{iNestin} mice during a 10 min trial of the APA task on the final day of testing (day 5). (**G**) During APA testing, *Nfix*^{iNestin} mice received more shocks on day 4 and day 5 of the task than controls. *$P < 0.05$, ***$P < 0.001$. Scale bar (in **B**): **B-B”**, **C-C”** 30 µm. Graph in **D** depicts mean ± s.e.m from 4 mice per genotype, graph in **G** depicts mean ± s.e.m from 21 mice per genotype.

A

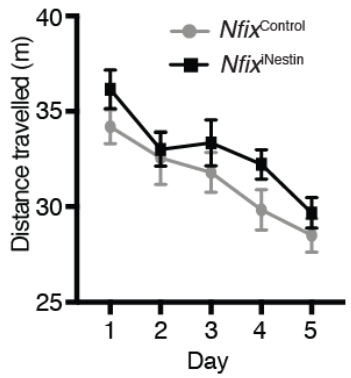

B

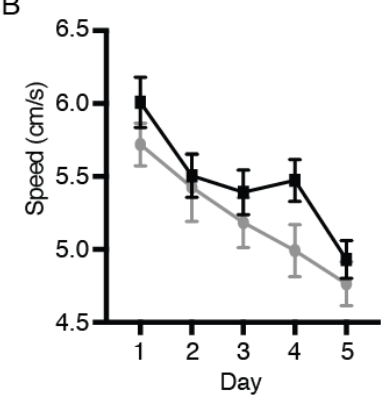

C

Behaviour/Physical Trait		*Nfix*^{Control}	*Nfix*^{iNestin}
Body position	Inactive	25%	20%
	Active	50%	60%
	Very active	25%	20%
Tremor	Present	0%	0%
Palpebral closure	Present	100%	100%
Coat appearance	Normal	100%	100%
Whiskers	Present	100%	100%
Lacrimation	Present	100%	100%
Defecation	Present	50%	60%

D

Behaviour/Physical Trait	Criteria	*Nfix*^{Control}	*Nfix*^{iNestin}
Positional passivity	Struggled when held by tail	100%	100%
Trunk curl	Present	100%	100%
Visual placing	Present	100%	100%
Righting reflex	Present	100%	100%
Vocalisation	Present	50%	40%
Morphology	Normal	100%	100%
Tail pinch	Response	100%	100%
Provoked biting	Present	100%	100%
Limb grasping	Present	75%	60%

Figure 5.7: *Nfix*^{iNestin} mice perform comparably to *Nfix*^{control} mice in other tested behavioural domains

No difference between *Nfix*^{control} and *Nfix*^{iNestin} mice in (**A**) distance travelled per day, and (**B**) mean speed (cm/s) in the APA task. (**C**) and (**D**) show comparable results for *Nfix*^{control} and *Nfix*^{iNestin} mice during a primary SHIRPA screen. The SHIRPA screen was performed on 4 control and 5 *Nfix*^{iNestin} mice.

5.5.6 Reporter *Nfix*^{iNestin} mice generate fewer neurons in the adult hippocampus

We next used a lineage tracing approach, followed by histological and transcriptomic analyses to further examine the failure of neuroblasts to mature in *Nfix*^{iNestin} mice. We crossed *Nfix*^{iNestin} mice to a *flox-stop-flox* tdtomato reporter line, where nestin^{+ve} progenitors and all the progeny from these cells are permanently marked with red fluorescence (Madisen et al., 2010). In this experiment, treatment mice were those in which *Nfix* was deleted (*Nfix*$^{iNestin-TD}$) from tdtomato^{+ve} cells, whereas in the control mice (Wt$^{iNestin-TD}$) tdtomato^{+ve} cells retained NFIX expression. We performed our histological analyses by injecting tamoxifen and analysing animals at 60 dpi, staining for the mature neuron marker NeuN and the neural progenitor marker SOX2. We made the following three observations from this experiment. Firstly, there were fewer total tdtomato^{+ve} cells in the dentate gyrus of *Nfix*$^{iNestin-TD}$ mice than in controls ($P = 0.0099$) (Figure 5.8A-C). Secondly, the reduction in total tdtomato^{+ve} cells was largely because there were far fewer tdtomato^{+ve} dentate granule neurons, both in total numbers ($P = 0.007$) (Figure 5.8E), and as a proportion of the tdtomato^{+ve} pool ($P = 0.0023$) (Figure 5.8G). Finally, while there was no effect on the total number of tdtomato^{+ve}; SOX2^{+ve} progenitors in *Nfix*$^{iNestin-TD}$ mice ($P = 0.47$) (Figure 5.8D), as a proportion, these cells were overrepresented because of the overall smaller tdtomato^{+ve} population in *Nfix*$^{iNestin-TD}$ mice ($P = 0.018$) (Figure 5.8F). Collectively, these findings support our previous data implicating NFIX as a central factor promoting neuronal differentiation in the adult mouse hippocampus.

We next isolated tdtomato^{+ve} cells from treatment and control animals using FACs, and performed RNA-seq. Our data so far had revealed that NFIX is essential for the maturation of neuroblasts into dentate granule neurons, but that earlier precursors were mostly unaffected. We posited that the expression of mature neuronal markers would be reduced, and that conversely an overrepresentation of stem cell and early neuronal differentiation genes would be observed. In total, we identified 153 differentially expressed genes (Figure 5.8H-J) Consistent with our hypothesis, many of the upregulated genes in the *Nfix*-deficient tdtomato^{+ve} cellular cohort were members of the Notch pathway (*Hes5, Hes6*) or other progenitor cell markers and regulators (*Neurdo2* and *Sox9*). Likewise, there were many cell adhesion molecules that were upregulated (*Dscam, Fezf2*, *Nrp1*, *Ptprz1*), genes typically associated with neuron recognition or neuron projection development. Interestingly, many genes associated with the inflammatory response were also upregulated in *Nfix*$^{iNestin-TD}$ animals, consistent with recent data suggesting that many of these molecules are highly expressed in nestin^{+ve} hippocampal progenitors (Walker et al., 2016b). Crucially, the mature neuron marker *Camk1* and the highly specific marker of dentate granule neurons, *Prox1* (Karalay et al.,

2011), were downregulated in this dataset. These histological and transcriptomic data further demonstrate that *Nfix* deletion from nestin^{+ve} progenitors inhibits neuroblast differentiation and thereby neuron generation in the adult mouse hippocampus.

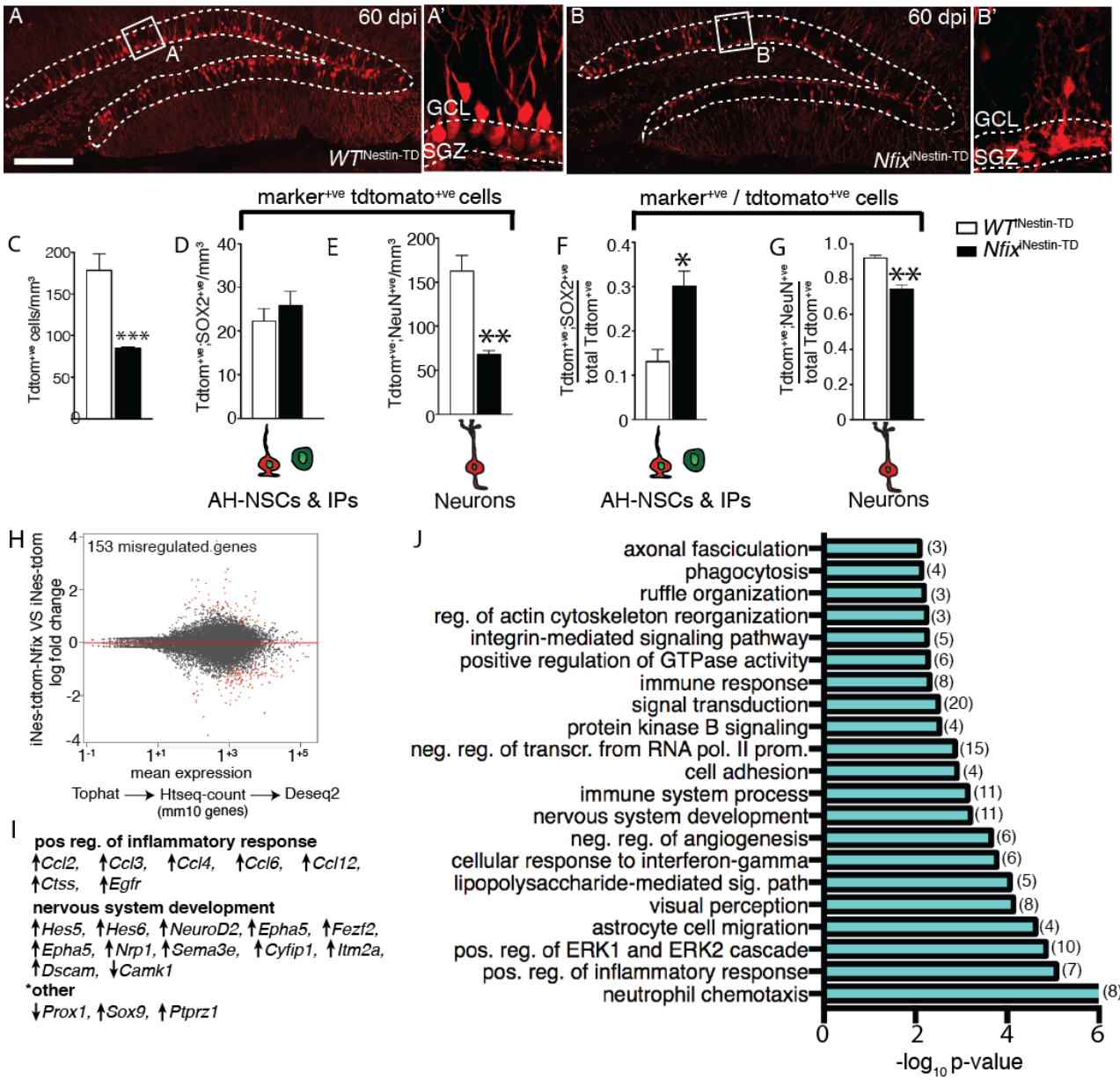
A
60 dpi
A'
GCL
SGZ
WT iNestin-TD
B
60 dpi
B'
GCL
SGZ
Nfix iNestin-TD
marker+ve tdtomato+ve cells
marker+ve / tdtomato+ve cells
WT iNestin-TD
Nfix iNestin-TD
C
Tdtom+ve cells/mm3
***
D
Tdtom+ve;SOX2+ve/mm3
E
Tdtom+ve;NeuN+ve/mm3
**
F
Tdtom+ve;SOX2+ve / total Tdtom+ve
*
G
Tdtom+ve;NeuN+ve / total Tdtom+ve
**
AH-NSCs & IPs
Neurons
AH-NSCs & IPs
Neurons
H
153 misregulated genes
iNes-tdtom-Nfix VS iNes-tdom log fold change
mean expression
Tophat → Htseq-count → Deseq2
(mm10 genes)
I
pos reg. of inflammatory response
↑Ccl2, ↑Ccl3, ↑Ccl4, ↑Ccl6, ↑Ccl12, ↑Ctss, ↑Egfr
nervous system development
↑Hes5, ↑Hes6, ↑NeuroD2, ↑Epha5, ↑Fezf2, ↑Epha5, ↑Nrp1, ↑Sema3e, ↑Cyfip1, ↑Itm2a, ↑Dscam, ↓Camk1
*other
↓Prox1, ↑Sox9, ↑Ptprz1
J
axonal fasciculation (3)
phagocytosis (4)
ruffle organization (3)
reg. of actin cytoskeleton reorganization (3)
integrin-mediated signaling pathway (5)
positive regulation of GTPase activity (6)
immune response (8)
signal transduction (20)
protein kinase B signaling (4)
neg. reg. of transcr. from RNA pol. II prom. (15)
cell adhesion (4)
immune system process (11)
nervous system development (11)
neg. reg. of angiogenesis (6)
cellular response to interferon-gamma (6)
lipopolysaccharide-mediated sig. path (5)
visual perception (8)
astrocyte cell migration (4)
pos. reg. of ERK1 and ERK2 cascade (10)
pos. reg. of inflammatory response (7)
neutrophil chemotaxis (8)
-log10 p-value

Figure 5.8: *Nfix*$^{\text{iNestin-TD}}$ mice generate fewer neurons

Wt$^{\text{iNestin-TD}}$ (**A**) and *Nfix*$^{\text{iNestin-TD}}$ mice (**B**) at 60 dpi stained for tdtomato (red), with the dashed lines outlining the dentate gyrus. The square boxes in **A** and **B** are shown in **A'** and **B'** respectively, where the dashed lines demarcate the SGZ. (**C**) There were fewer tdtomato^{+ve} cells in *Nfix*$^{\text{iNestin-TD}}$ mice relative to controls. (**D-E**) The number of tdtomato^{+ve} cells that were SOX2^{+ve} or NeuN^{+ve} was quantified. There was no difference in the total number SOX2^{+ve} reporter cells (**D**) between genotypes. However, there were fewer NeuN^{+ve} reporter cells (**E**) in *Nfix*$^{\text{iNestin-TD}}$ mice compared to controls. (**F-G**) As a proportion of the tdtomato^{+ve} population, SOX2^{+ve} cells (**F**) were overrepresented, while NeuN^{+ve} cells (**G**) were underrepresented relative to control mice. (**H**) MA plot of RNA-seq data of tdtomato^{+ve} cells from Wt$^{\text{iNestin-TD}}$ and *Nfix*$^{\text{iNestin-TD}}$ mice at 45 dpi. (**I**) Genes and GO terms associated with early progenitor development were up regulated, while the late neuronal genes *Prox1* and *Camk1* were downregulated. (**J**) GO terms ranked according to $-\log_{10}$ p-value. $*P < 0.05$, $**P < 0.01$. Scale bar (in **A**): **A**, **B** = 208 μm; **A'**, **B'** = 14.1μm. Graphs depict mean ± s.e.m from 3 mice per genotype, RNA-seq data generated from 3 mice per genotype.

5.5.7 Deletion of NFIX from hippocampal progenitors leads to the aberrant production of a small number of oligodendrocytes

In the course of the *nestin-creER*^{T2} lineage tracing experiment, we occasionally detected tdtomato^{+ve} cells located on the hilar side of the SGZ within *Nfix*$^{iNestin\text{-}TD}$ mice. NFIX, and other NFIs are well-established regulators of astrocyte (Barry et al., 2008; Kang et al., 2012; Heng et al., 2014) and oligodendrocyte differentiation (Wong et al., 2007; Zhou et al., 2015; Rolando et al., 2016). Under physiological conditions, AH-NSCs generate astrocytes in addition to neurons (Bonaguidi et al., 2011). However, AH-NSCs also have a latent tri-potency (Braun et al., 2015; Sun et al., 2015). Upon the forced *in vivo* expression of transcription factors such as *Olig2* (Braun et al., 2015) or after the deletion of *neurofibromin 1* they robustly generate oligodendrocytes (Sun et al., 2015). While we did not detect a gene expression signature within our RNA-seq experiment that would indicate a shift towards astrocyte or oligodendrocyte production in *Nfix*$^{iNestin\text{-}TD}$ mice, the scarcity of these cells as a proportion of the tdtomato^{+ve} population, would likely render this gene signature undetectable. To investigate the production of astrocytes and oligodendrocytes we co-stained for the astrocyte marker S100ß or the pan-oligo marker OLIG2. We found no difference in the total number of tdtomato^{+ve}; S100ß$^{+ve}$ cells between *Nfix*$^{iNestin\text{-}TD}$ and *WT*$^{iNestin\text{-}TD}$ mice ($P = 0.13$) (Figure 5.9A-C). Surprisingly however, we found a substantial increase in the number of tdtomato^{+ve}; Olig2^{+ve} cells in *Nfix*$^{iNestin\text{-}TD}$ compared to control *WT*$^{iNestin\text{-}TD}$ mice, which were largely devoid of these cells ($P = 0.0099$) (Figure 5.9D-F). Therefore, the deletion of *Nfix* from AH-NSCs leads to the aberrant production of a small number of oligodendrocytes, in addition to the substantial defects seen in neuroblast maturation and survival.

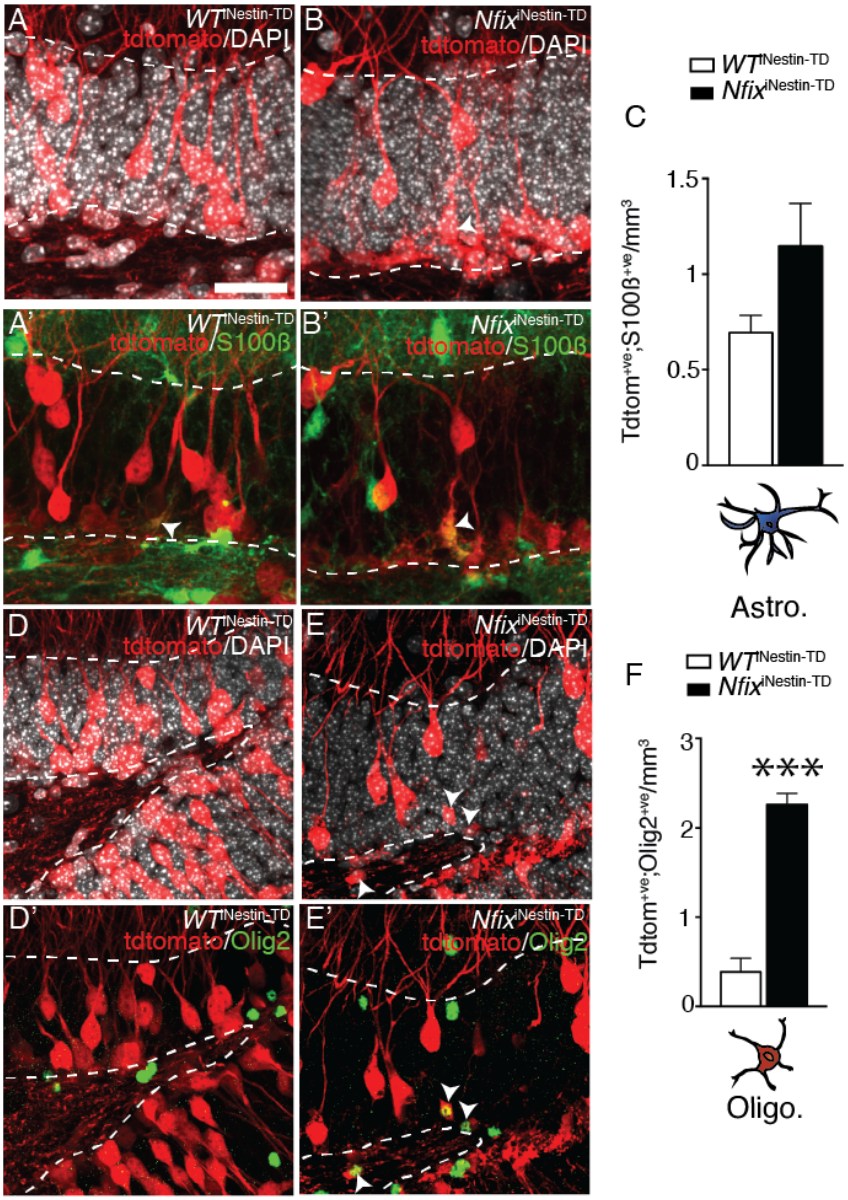

Figure 5.9: *Nfix*$^{iNestin\text{-}TD}$ mice generate oligodendrocytes

Wt$^{iNestin\text{-}TD}$ (**A, A'**) and *Nfix*$^{iNestin\text{-}TD}$ mice (**B, B'**) 60 dpi stained for tdtomato (red), S100ß (green) and DAPI (white) with the dashed lines outlining the dentate gyrus. The arrowhead in **A**' and **B'** points to a tdtomato^{+ve}; S100ß$^{+ve}$ astrocyte. (**C**) There was no difference in the number of tdtomato^{+ve} astrocytes generated in Wt$^{iNestin\text{-}TD}$ and *Nfix*$^{iNestin\text{-}TD}$ mice. Wt$^{iNestin\text{-}TD}$ (**D, D'**) and *Nfix*$^{iNestin\text{-}TD}$ mice (**E, E'**) at 60 dpi stained for tdtomato (red), Olig2 (green) and with DAPI (white). The arrowheads in **E'** point to tdtomato^{+ve}; Olig2^{+ve} oligodendrocytes. (**F**) There were substantially more tdtomato^{+ve} oligodendrocytes labelled in *Nfix*$^{iNestin\text{-}TD}$ mice than in controls. ***$P < 0.001$. Scale bar (in **A**) **A**, **B** 30 µm, **C**, **D** 40 µm. Graphs depict mean ± s.e.m from 3 mice per genotype.

5.5.8 NFIX expression is autonomously required for neuroblast maturation and survival

Is NFIX expression autonomously required for neuroblast maturation and survival, or are the neuroblast maturation defects observed in *Nfix*^{iNestin} mice due to the altered developmental trajectory of AH-NSCs upon *Nfix*-deletion? To address this question we crossed *Nfix*$^{f/f}$ mice to a line expressing a tamoxifen inducible *cre*-recombinase under the control of the *Dcx* promoter (*Nfix*^{iDcx}) (Cheng et al., 2011). Because tamoxifen injections administered to these mice delete NFIX from DCX^{+ve} neuroblasts but not from the AH-NSCs that generate these cells, weekly tamoxifen injections were required to continually deplete NFIX (Figure 5.10A). Seven days after the final tamoxifen injection we analysed the number of neuroblasts in *Nfix*^{iDcx} and *Nfix*^{control} mice. We found a reduced numbers of neuroblasts in the mutant strain (P = 0.028) (Figure 5.10B-D). Moreover, similar to *Nfix*^{iNestin} mice, fewer of the remaining neuroblasts had a vertical dendritic branch (P = 0.002) (Figure 5.10F) and more co-expressed TBR2 (P = 0.047) (Figure 10E). Furthermore, BrdU labelling, followed by a 4 week chase (Figure 5.10G) revealed that *Nfix*^{iDcx} mice generated fewer mature dentate granule neurons than in controls (P = 0.035) (Figure 5.10H), and more neuroblasts co-expressed cleaved-caspase-3 (P = 0.015) (Figure 5.10I). Therefore, the effects seen on neuroblast maturation in *Nfix*^{iNestin} animals are phenocopied upon deletion of *Nfix* from neuroblasts alone. These data demonstrate that *Nfix* expression is autonomously required by neuroblasts for the extension of a primary dendritic process, and subsequently, the survival and maturation of these cells into dentate granule neurons.

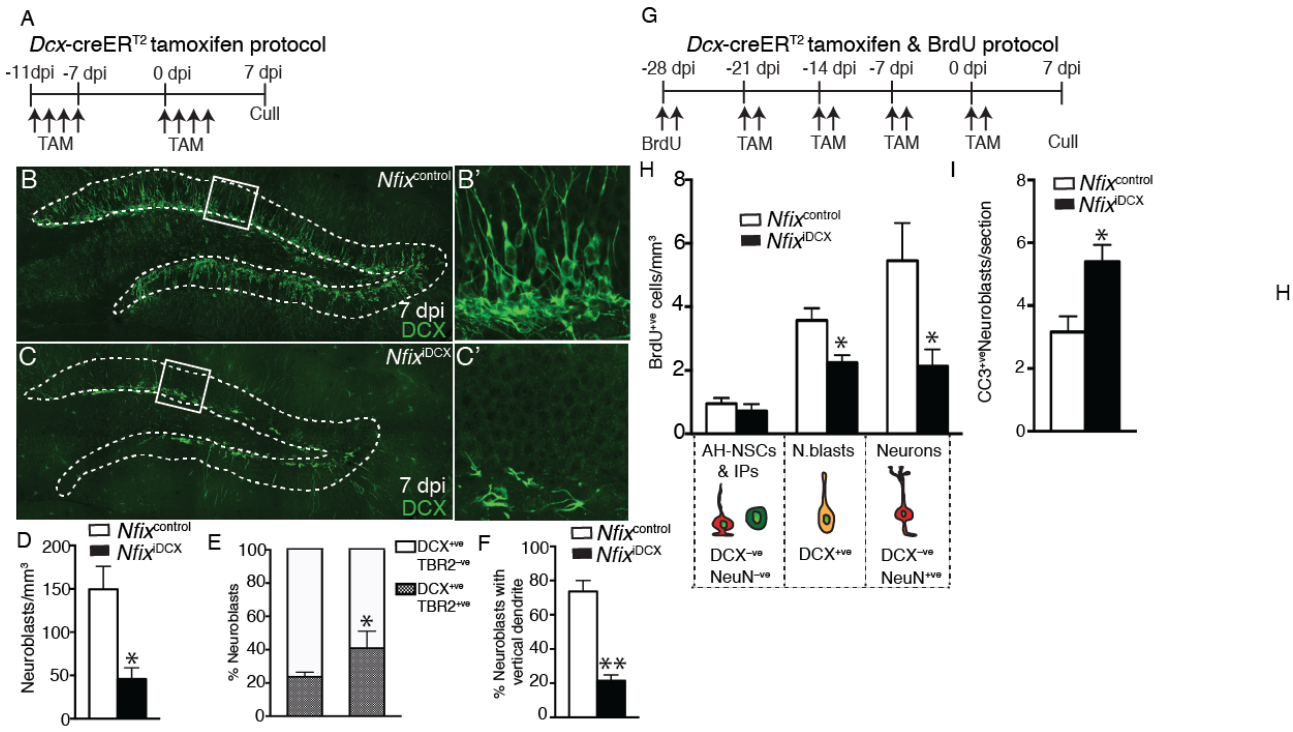

Figure 5.10: Neuroblast specific deletion of NFIX phenocopies deletion from AH-NSCs

(**A**) Tamoxifen injection scheme for *Nfix*^{iDcx} and *Nfix*^{control} mice. *Nfix*^{control} (**B**) and *Nfix*^{iDcx} mice (**C**) at 7 dpi showing DCX (green), with dashed lines outlining the dentate gyrus. Boxed regions in **B** and **C** are shown in **B'** and **C'** respectively. (**D**) Compared to controls there were far fewer DCX^{+ve} cells in *Nfix*^{iDcx} mice. (**E**) As a proportion, more neuroblasts in *Nfix*^{iDcx} mice co-expressed TBR2, (**F**) while fewer had a vertical dendritic process. (**G**) BrdU-Tamoxifen injection scheme for *Nfix*^{iDcx} and *Nfix*^{control} mice. (**H**) 4-weeks after BrdU administration there were fewer BrdU^{+ve} neuroblasts (DCX^{+ve}; NeuN^{-ve}) and fewer BrdU^{+ve} mature neurons (DCX^{+ve}; NeuN^{+ve}) in *Nfix*^{iDcx} mice compared to controls. (**I**) More neuroblasts in *Nfix*^{iDcx} mice co-expressed CC3. *$P < 0.05$, **$P < 0.01$. Scale bar (in **B**): **B**, **C** 235 µm; **B'**, **C'** 47 µm. Graphs in **D-F** depict mean ± s.e.m from 3 mice per genotype, graphs in **H, I** depict mean ± s.e.m from 4 mice per genotype.

We next analysed the cellular and transcriptional changes that occur upon neuroblast-specific deletion of *Nfix* to determine the causative factors underlying the loss of this population. We crossed *Nfix*^{iDcx} to the *flox-stop-flox* tdtomato reporter line to generate *Nfix*$^{iDcx\text{-}TD}$ mice and control *WT*$^{iDcx\text{-}TD}$ mice. Seven days after the final tamoxifen injection (7 dpi), we analysed these reporter mice through immunohistochemistry and via FACS followed by RNA-seq. In *Nfix*$^{iDcx\text{-}TD}$ mice, there were fewer tdtomato^{+ve} cells in *Nfix*$^{iDcx\text{-}TD}$ compared to controls at 7 dpi, highlighting that the deletion of *Nfix* from neuroblasts results in the rapid loss of this population ($P = 0.0163$) (Figure 5.11A-C). Given this finding, we hypothesised that the transcriptomic analysis of tdtomato^{+ve} wild-type and mutant cells would reveal mis-regulation of key genes involved in neuronal maturation. Indeed, the enriched GO terms included neuron projection development, glutamate secretion, long-term synaptic potentiation and neuronal apoptosis (Figure 5.11D-F). The enrichment of these GO terms correlates strongly with the histological evidence of impaired dendrite formation and increased cell death of neuroblasts upon *Nfix*-deletion (Figure 5.10). Therefore, NFIX expression is autonomously required by adult hippocampal neuroblasts to execute a program of gene expression integral to dendrite formation and subsequently survival.

The majority of neuroblasts in wild-type mice do not colocalise with protein markers of the oligodendrocyte lineage. However, at an *mRNA* level, a recent single-cell RNA-seq study of adult hippocampal neuroblasts revealed that a substantial proportion of neuroblasts express putative oligodendrocyte-specific *mRNA* alongside neuronal markers (Gao et al., 2016). With this in mind, the most enriched GO term in our comparison of *Nfix*$^{iDcx\text{-}TD}$ and control mice, remarkably, were for genes involved in oligodendrocyte differentiation (Figure 5.11E). Oligodendrocyte precursor/differentiation markers such as *Cspg4* (*Ng2*) and *Ptprz1* were approximately 3 fold upregulated in *Nfix*$^{iDcx\text{-}TD}$ mice compared to controls, as were the pan-oligo markers *Olig1* and *Olig2*. The expression of mature oligdodendrocyte markers *Cnp*, *Mbp* and *Mog* were unaffected suggesting that NFIX deletion from neuroblasts leads to a specific upregulation of genes associated with early oligodendrocyte development (Figure 5.11G).

To rule out the possibility that the increased oligodendrocyte precursor *mRNA* expression in *Nfix*$^{iDcx\text{-}TD}$ mice could be due to non-specificity of the *cre-recombinase*, where perhaps oligodendrocyte precursor cells were being labelled and amplified upon NFIX deletion, we examined the identity of tdtomato^{+ve} cells in *WT*$^{iDcx\text{-}TD}$ at 7 dpi. The vast majority of tdtomato^{+ve} cells either expressed DCX or were DCX^{-ve} with a neuronal morphology, indicating they were dentate granule neurons that had recently lost DCX expression. In contrast, very few tdtomato^{+ve}

cells expressed Olig2 (48/3113 cells, 1.54%), demonstrating the specificity of the *cre*-recombinase. We next examined whether the upregulation of oligodendrocyte *mRNA* in *Nfix*$^{iDcx\text{-}TD}$ mice was due to the presence of greater numbers of tdtomato^{+ve}; Olig2^{+ve} cells in these mice. There was no gross difference in the total number of tdtomato^{+ve}; Olig2^{+ve} cells in *Nfix*$^{iDcx\text{-}TD}$ compared to controls (P = 0.297) (Figure 5.11H). Nor did tdtomato^{+ve}; Olig2^{+ve} cells account for a more significant proportion of the reporter^{+ve} pool in *Nfix*$^{iDcx\text{-}TD}$ mice than in controls (P = 0.257) (Figure 5.11I). Therefore, NFIX deletion from neuroblasts leads to a de-repression of oligodendrocyte gene expression but not an increase in oligodendrocyte cell number, either because neuroblasts do not have the capacity to convert towards an oligodendrocyte fate, or this fate change is not detectable because of the high rates of neuroblast cell death upon *Nfix*-deletion (Figure 5.10I).

Together, our results demonstrate that NFIX expression is absolutely required for the survival and timely generation of adult borne neurons within the mouse hippocampus. NFIX serves this function by driving the program of neuronal differentiation within neuroblasts. Remarkably, NFIX suppresses oligodendrocyte differentiation in AH-NSCs and the expression of oligodendrocyte *mRNA* within neuroblasts, demonstrating that NFIX also functions as part of the gene regulatory network that suppresses the latent tripotentiality of precusors cells in the adult hippocampus.

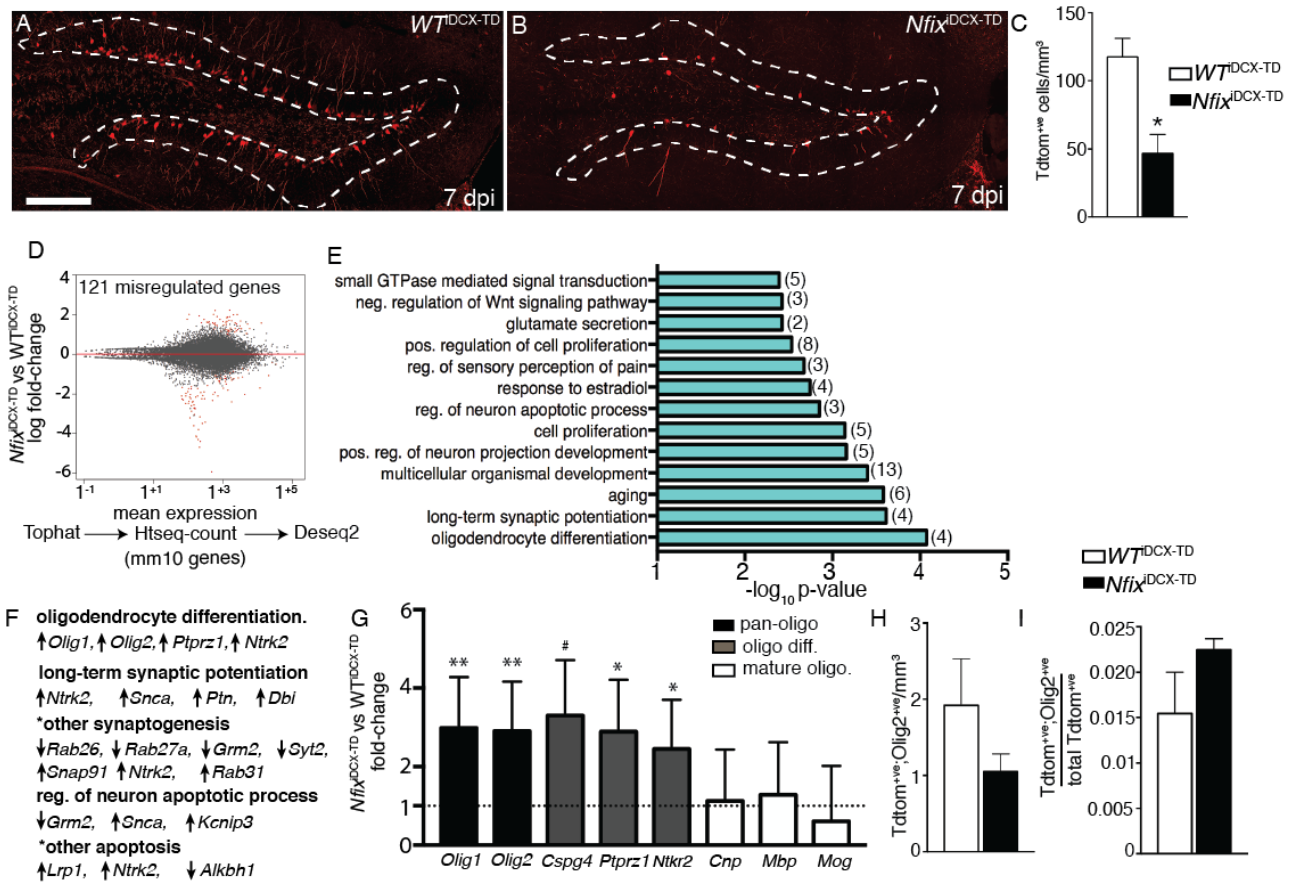

Figure 5.11: Neuroblast specific deletion of NFIX leads to expression changes in neuronal maturation and in oligodendrocyte precursor genes

Wt$^{iDCX\text{-}TD}$ (**A**) and *Nfix*$^{iDCX\text{-}TD}$ mice (**B**) at 7 dpi stained for tdtomato (red), with the dashed lines outlining the dentate gyrus. (**C**) There were fewer tdtomato^{+ve} cells in *Nfix*$^{iDCX\text{-}TD}$ mice relative to controls. (**D**) MA plot of RNA-seq data of tdtomato^{+ve} cells from Wt$^{iDCX\text{-}TD}$ and *Nfix*$^{iDCX\text{-}TD}$ mice at 7 dpi. (**E**) GO terms ranked according to $-\log_{10}$ p-value. GO terms associated with neuronal maturation and oligodendrocyte differentiation were enriched. (**F**) Curated list of genes associated with enriched GO terms. (**G**) Fold change of oligodendrocyte lineage genes, categorised according to whether they are expressed throughout the entire lineage (pan-oligo), during differentiation (oligo. diff.) or by mature oligodendrocytes (mature oligo.). *FDR* adjusted *P*-value $^{\#}P< 0.1$; $*P < 0.05$, $**P < 0.01$. (**H**) No difference was observed between genotypes in the total number of Olig2^{+ve}; tdtomato^{+ve} cells or (**I**) in the proportion Olig2^{+ve} cells comprising the tdtomato^{+ve} pool. Scale bar (in **B**): **A, B** 200µm. Graph in **G** depicts mean ± s.e.m of RNA-seq data generated from 3 mice per genotype. Graphs in **H** and **I** depict mean ± s.e.m of 3 *Nfix*$^{iDCX\text{-}TD}$ and 4 Wt$^{iDCX\text{-}TD}$ mice.

5.6 Discussion

Studies in rodents have begun to reveal the key transcription factor proteins required for the different stages of adult hippocampal neurogenesis. Transcription factor proteins integral to regulating cell-cycle entry such as FOXO and ASCL1 (Paik et al., 2009; Renault et al., 2009; Andersen et al., 2014), stem cell maintenance such as PAX6 and REST (Maekawa et al., 2005; Gao et al., 2011), and the production of IPs such as TBR2 (Hodge et al., 2012) have been identified. The NFI family has been extensively described in the developing brain, and have been implicated in multiple neurodevelopmental disorders (Malan et al., 2010), but how these factors function in the adult hippocampus is unclear. A recent study revealed a role for NFIB in promoting oligodendrogenesis within the adult SGZ (Rolando et al., 2016). Here, we present a contrasting role for NFIX within the adult hippocampus, revealing that NFIX drives a program of neuroblast differentiation and suppresses the latent potency of hippocampal precursor cells to generate oligodendrocytes**.**

There are a number of differences between how NFIX regulates neuronal differentiation during development compared to its function in the adult hippocampus. Two pivotal differences are the relative stages of neuronal lineage progression controlled by NFIX and the effect that *Nfix* deletion has on neuronal survival. In the developing dorsal forebrain, NFIX promotes the asymmetric division of radial glial stem cells and the subsequent production of IPs (Harris et al., 2016a), which is the earliest fate choice that occurs during neuronal differentiation. As a result, in *Nfix*$^{-/-}$ mice, radial glial stem cells undergo more self-expanding divisions, thereby extending the neurogenic period. This results in the production of more neurons and postnatal macrocephaly in this line without any observed negative affects on neuronal survival (Chapter 3) (Campbell et al., 2008; Heng et al., 2014; Harris et al., 2016a). In contrast, in AH-NSCs we found that the deletion of *Nfix* does not affect the production of IPs (Figure 5.3, 5.5). Rather, NFIX expression increases within IPs and neuroblasts (Figure 5.1) to regulate the formation of the primary dendritic process, and to regulate other aspects of neuronal maturation, such as the downregulation of the IP marker TBR2 (Figure 5.5, 5.6). The failure of *Nfix*-deficient neuroblasts to mature culminates in the death of newly generated neuroblasts, which is reflected in the hippocampal-dependent behavioural deficits evident in the *nestin-creER*^{T2} knockout line (Figure 5.6). Therefore, while NFIX functions to promote neuronal differentiation both during development and in adult hippocampal precursor cells, the consequences of NFIX deletion on neuronal survival and neuronal number vary between the two contexts. Whether these differences in NFIX function reflect interactions with different co-

factors or intrinsic differences in chromatin architecture of neural progenitors across these different contexts remain to be seen.

NFIX has been hypothesised to be a central factor in maintaining AH-NSC quiescence. Using an *in vitro* model of NSC quiescence, Martynoga and colleagues (2013) demonstrated that NFIX was a major factor that bound to quiescence-specific enhancer regions, and that loss of NFIX from this culture system led to increased NSC proliferation. Consistent with a role for NFIX in mediating stem cell quiescence, the authors reported an increased number of proliferating AH-NSCs cells in the hippocampus of postnatal day 15 *Nfix*$^{-/-}$ mice. However, an alternative explanation for this phenotype may reside in the fact that these mice display developmental deficits within the dorsal telencephalon (Chapter 3) (Martynoga et al., 2013; Heng et al., 2014). Given the role of NFIX *in vitro*, we posited that the conditional, inducible deletion of *Nfix* from AH-NSCs would lead to a major increase in AH-NSC proliferation and subsequent depletion of this population. Intriguingly, the phenotype we observed was in contrast to our hypothesis. *Nfix* deletion from AH-NSCs led to a small, transient increase in proliferation, but total AH-NSC number remained unchanged even as long as 1 year following *Nfix* deletion. There are a number of factors that may explain the limited effect that *Nfix* deletion had on AH-NSC quiescence/proliferation. Firstly, while NFIX bound to the majority of quiescent specific enhancers *in vitro*, these experiments utilised neural stem cells derived from ES cells that may have a substantially different epigenetic landscape than in a primary culture of AH-NSCs (Martynoga et al., 2013). Secondly, the *in vitro* experimental set-up removes stem cells from their niche, comprising of a dense network of blood vessels, immune cells, neurotransmitters and chemical signals [reviewed in (Goncalves et al., 2016)]. The complexity of the niche signals may have buffered against the effect that NFIX deletion had on the relative quiescence of AH-NSCs. Finally, given the functional overlap between NFIX and other NFIs proteins during brain development (Barry et al., 2008; Piper et al., 2010; Heng et al., 2014), another interesting avenue of future research would be to determine whether the deletion of *Nfib or Nfia* alleles in addition to *Nfix*, would result in a more substantial loss of AH-NSC quiescence.

In this study, we also found that NFIX suppresses the capacity of AH-NSCs to generate oligodendrocytes. AH-NSCs do not extensively generate oligodendrocytes under basal physiological conditions. For example, Bonaguidi and colleagues (2011) demonstrated that there were no cells within 300 clones (generated by a low-dose tamoxifen injection regime in *nestin-creER*^{T2} animals crossed to a reporter line) that co-labelled with oligodendrocyte markers. Similar findings have been made using a *glast-creER*^{T2} line (Sun et al., 2015). Although there is some evidence to argue that the failure of these studies to identify newly generated oligodendrocytes may

reflect the inefficiencies of these *cre* drivers to label the full diversity of hippocampal precursors, as, for example, retroviral label of dividing cells within the hippocampus indicates a low-level of oligodendrocyte production (Braun et al., 2015), this is clearly a restricted process.

A number of recent studies have highlighted that under certain circumstances, AH-NSCs can generate substantial numbers of oligodendrocytes, and have begun to elucidate the pathways that normally act to suppress the production of oligodendrocytes from AH-NSCs *in vivo*. For example, it was recently reported that AH-NSCs possess a substantial tri-lineage potential, as overexpression of *Olig2*, *Sox10* or *Ascl1* using a retrovirus was sufficient to convert a significant proportion of AH-NSCs to generate oligodendrocytes (Braun et al., 2015). A more dramatic effect was seen upon deletion of *neurofibromin 1*, whereupon large numbers of AH-NSCs generated oligodendrocytes (Sun et al., 2015). Our results suggest that NFIX also functions to suppress the tri-potentiality of AH-NSCs. However, unlike earlier studies, which solely used *cre*-recombinase lines and viruses that predominantly labelled AH-NSCs, we also detected a de-repression oligodendrocyte *mRNA* upon *Nfix*-deletion from IPs and neuroblasts using a *dcx-creER*^{T2} line. This de-repression could possibly link to the widespread cell death of tdtomato+ve cells observed in this line. Furthermore, our data suggest that targeting barriers of latent lineage potential, even within cells that ostensibly considered to be committed to neuron production, may be an avenue to generate additional plasticity. It would be of interest to examine the effect that deleting *neurofibromin 1* using a *dcx-creER*^{T2} line has on oligodendrocyte production. *Neurofibromin 1* is a far more potent inhibitor of oligodendrocyte formation than *Nfix* (Sun et al., 2015). Its deletion might be sufficient to convert a substantial number of adult hippocampal neuroblasts to become oligodendrocytes without the concurrent cell death that occurs upon *Nfix* deletion. There is precedent for similar cell-type conversions between disparate cell types, for example it was recently shown that adult striatal astrocytes exhibit a latent neurogenic program that is actively suppressed via Notch signalling (Magnusson et al., 2014) and elicited by injury (Nato et al., 2015).

In summary, this study has uncovered the dual roles of NFIX during adult hippocampal neurogenesis. Firstly, we found that NFIX drives a program of neuroblast differentiation, and secondly, suppresses the latent potency of hippocampal precursor cells to generate oligodendrocytes. These results thereby significantly enhance our understanding of the transcriptional control of adult hippocampal neurogenesis and the latent lineage potential of hippocampal precursor cells.

Chapter 6 General Discussion

6.1 Aims of chapter 6

The aim of this chapter is to place the findings from chapters 3 and chapter 5 into a broader context. I will discuss how the findings from chapters 3 of my thesis relate to human health and disease. For example, I will address how my work provides insight into human neurodevelopmental disorders caused by *NFIX* mutations, namely Sotos Syndrome and Marshall-Smith Syndrome. I will then use the findings from chapters 3 and 5 to compare and contrast the functions of NFIX in developmental neural stem cells to its role in AH-NSCs. I will use this comparison to argue that NFIX/NFIs function as regulators of neural stem cell fate, possibly through regulating chromatin architecture. Finally, I will discuss how through the study of NFIX function in adult hippocampal neural stem cells and their progeny, I have revealed the surprising plasticity of these cells to generate oligodendrocytes. I close by contending that this thesis has significantly enhanced our understanding of the transcriptional control of neural stem cells in the developing and adult brain.

6.2 *Nfix*$^{-/-}$ mouse may provide insight into brain structure of humans with *NFIX* mutations

The findings described in Chapter 3 of this thesis may provide insights into human disorders caused by *NFIX* mutations. Specifically, my finding that the macrocephaly of *Nfix*$^{-/-}$ mice is at least in part, due to increased production of neurons may help to explain the macrocephaly seen in patients with *NFIX* mutations. Currently, the cause of the macrocephaly in these patients is unclear, and our work suggests the overproduction of neurons, due to the delayed differentiation of radial glial stem cells, is one probable contributing factor. In the following text, I discuss this in more detail, as well as future research directions.

6.2.1 *NFIX* mutations cause Sotos syndrome or Marshall-Smith Syndrome

Human *NFIX* mutations can cause one of two neurodevelopmental disorders: Sotos Syndrome or Marshall-Smith syndrome (Malan et al., 2010; Martinez et al., 2015). As to which of these two disorders arises from an *NFIX* mutation, genotype-phenotype correlations have shown that this depends upon the location of the mutation within the *NFIX* gene body and subsequently, whether the mutation leads to a loss-of- or dominant-negative function. For example, heterozygous *NFIX* deletions or nonsense/missense mutations in the DNA-binding/dimerisation domain (exon 2/3) of *NFIX* result in a loss of protein activity and Sotos Syndrome (Malan et al., 2010; Yoneda et al., 2012; Gurrieri et al., 2015; Klaassens et al., 2015) and thus is sometimes referred to as a *NFIX* haploinsufficiency. In contrast, heterozygous frameshift or splice-site variants in exons 6-10 of *NFIX*, positioned close to the C-terminus transactivation domain, escape nonsense-mediated decay (Malan et al., 2010; Klaassens et al., 2015; Martinez et al., 2015) and engender a Marshall-Smith Syndrome. It is thought that the mutated allele in Marshall-Smith Syndrome forms a dominant-negative protein that competes with the wild-type version of the NFIX protein (Malan et al., 2010).

6.2.2 Clinical features of Sotos Syndrome and Marshall-Smith Syndrome

Sotos Syndrome and Marshall-Smith Syndrome are relatively distinct disorders. Sotos Syndrome, first described in 1964, is predominantly caused by mutations in a different transcription factor protein, called the Nuclear Receptor Binding SET domain (*NSD1*) (Kurotaki et al., 2002). Only

recently were *NFIX* mutations found to account for a subset of *NSD1*-negative Sotos Syndrome cases (Malan et al., 2010). While some features of Sotos Syndrome vary depending on whether it is the *NSD1* or *NFIX* gene that is mutated (hence, why *NFIX* haploinsufficiency is sometimes referred to as "Sotos Syndrome 2", "Sotos-like Syndrome" or even "Malan Syndrome") the disorders are highly similar so that differential diagnosis requires patient genotyping. Clinically, Sotos Syndrome is characterised by prenatal overgrowth through childhood, macrocephaly, developmental delay and low IQ in adulthood. Other features include unusual but stereotypic facial features (which may possibly be due to neural crest cell defects) such as a pointed chin, hypotonia (muscle weakness) and kyphosis (curvature of the spine). Behaviourally, individuals score highly on measures of autistic-like traits (Lane et al., 2017). The brain features of Sotos patients are less well characterised, but include communicating hydrocephalus, prominence of trigon and occipital horns and hypoplasia of the corpus callosum (Sotos, 2014).

The characteristics of Marshall-Smith Syndrome are relatively more severe than Sotos syndrome. First described in 1971 (Marshall et al., 1971), the syndrome manifests with severe developmental delay, absent or limited speech, unusual (but not autistic-like) behaviour, short stature and kyphosis and respiratory impairment that sometimes leads to neonatal death, (Shaw et al., 2010). The brain structure of patients with Marshall-Smith Syndrome has not been extensively catalogued.

From the gross description of these disorders it is clear that there is significant overlap between the phenotype of *Nfix*$^{-/-}$ mice and the clinical features caused by *NFIX* mutations. For example, *Nfix*$^{-/-}$ mice have severe kyphosis (Driller et al., 2007; Campbell et al., 2008), hypotonia/impaired muscle development (Messina et al., 2010; Pistocchi et al., 2013; Rossi et al., 2016; Taglietti et al., 2016), and struggle to thrive postnatally, typically dying 3 weeks after birth (Campbell et al., 2008). Both *Nfix*$^{-/-}$ mice and human patients with *NFIX* mutations also have similarities in terms of brain development. For example, both develop communicating hydrocephalus (Vidovic et al., 2015), have a thinner corpus callosum (Campbell et al., 2008), and at least in mice heterozygous for *Nfix* (which survive into adulthood, allowing for behavioural tests to be performed), they show cognitive deficits (Harris et al., 2013). The cognitive tests performed thus far in mice were restricted to memory, however it will be informative to examine whether these animals also display autistic like traits such as those displayed in Sotos Syndrome. This could be achieved using tests that have been developed to examine social interaction behaviours in mice (Kaidanovich-Beilin et al., 2011).

6.2.3 Localised increases in neuron number may contribute to the macrocephaly seen in Sotos Syndrome patients

Pertinent to this thesis, both *Nfix*$^{-/-}$ mice and persons with *NFIX* mutations exhibit macrocephaly (enlarged head size). I described in Chapter 3 that at least one cause of the macrocephaly in *Nfix*$^{-/-}$ mice was because radial glial stem cells exhibited increased symmetric division. This led to an expansion of the radial glial cell pool and delayed IPC production. The increased number of radial glial stem cells culminated in a prolonged period of neurogenesis, ultimately generating more cortical neurons than in comparison to controls. This in turn resulted in *Nfix*$^{-/-}$ mice having increased brain size (megacephaly), which presumably then contributed to the overall increase in head size (macrocephaly).

The cause of macrocephaly in human patients with *NFIX* mutations is unclear. Indeed, the MRI evidence reported in the literature to date does not detail any gross, global increase in brain size (megacephaly), although the reported data is scant. One possibility is that the macrocephaly of human patients is due to changes in cranium structure, rather than brain size. Indeed unusual bone structure underlies the distinctive facial features of this disorder. Equally likely however, is that there are also localised brain regions that are enlarged in persons with *NFIX* mutations that are not readily detected by standard MRI scans, or are not noticed by physicians. These local abnormalities may then contribute to the increased head size of patients. This is supported by the brain structure of *Nfix*$^{-/-}$ mice, which shows increases in brain size in only certain regions. For example, while *Nfix*$^{-/-}$ mice display increased thickness of the dorsal forebrain, the phenotype is most severe in the hippocampus. Other areas of *Nfix*$^{-/-}$ mouse brain are unaffected or indeed are reduced in size. For example, the ventral forebrain is unaffected in *Nfix*$^{-/-}$ mice, probably because the developing ventral telencephalon does not express high levels of NFIX (Plachez et al., 2008), while the postnatal cerebellum of *Nfix*$^{-/-}$ mice is smaller due to defects in terminal cerebellar granule neuron maturation (Piper et al., 2011; Fraser et al., 2016).

This information concerning the areas of brain most affected in *Nfix*$^{-/-}$ mice could be used by paediatricians to phenotype patients more accurately. For example, assessing MRIs with a focus on hippocampal morphology may prove useful. If a standard patient MRI lacks the resolution to examine smaller structures such as the hippocampus, future research studies should be performed at higher scanning resolutions to detect what changes are present in persons with Sotos Syndrome.

6.2.4 Modelling human *NFIX* mutations using cerebral organoids

My hypothesis that defects in radial glial maturation may underpin the human brain phenotype of persons with *NFIX* mutations is dependent upon the assumption that the function of NFIX is conserved between mouse and human. While the phenotypic overlay between *Nfix*$^{-/-}$ mice and human patients support this assumption, direct experimental evidence is lacking. Recent technological advances however, have made testing this hypothesis possible. Specifically, the recent combining of induced pluripotent stem cell technology with the 3-dimensional brain (cerebral organoid) culture systems allow for patient-specific neural tissue to be grown in a manner that mimics the early stages of human brain development. Using this technology, pioneering studies have taken fibroblasts from patients with a neurodevelopmental disorder, reprogrammed these cells to an iPSC state, and differentiated these cells into a 3d mini-brain culture (Lancaster et al., 2013; Pasca et al., 2015). These early works have already provided insight into disorders such as primary microcephaly caused by genetic mutations (Lancaster et al., 2013) or by Zika virus infection (Cugola et al., 2016; Dang et al., 2016), as well as in idiopathic autism spectrum disorder (Mariani et al., 2015). Recapitulating this culture process using fibroblasts from persons with *NFIX* mutations will definitively determine whether NFIX also functions to promote radial glial cell differentiation within the human brain. Moreover, reprogramming of cells from patients with different *NFIX* mutations (for example, loss-of-function *NFIX* mutations *versus* dominant-negative *NFIX* mutations) would permit interpretation of the effect that specific *NFIX* mutations have on human brain development. This may help to parse apart any differences in early brain development that occur between Sotos Syndrome and Marshall-Smith Syndrome patients.

6.2.5 Genetic interaction between *NFIX* and *NSD1*

Another avenue of future research that is fascinating to consider is the possible genetic interactions between *NFIX* and genes that when mutated, cause the same or similar neurodevelopmental disorders. The most interesting example of this may be the transcription factor *NSD1*. Haploinsufficiency for *NSD1* (Kurotaki et al., 2002), like haploinsufficiency for *NFIX,* causes Sotos syndrome. This suggests that these two proteins may be interacting either directly, as binding partners or regulating the expression of similar sets of genes. To test these hypotheses, co-immunoprecipitation could be performed so as to determine whether NFIX and NSD1 physically bind each other. Moreover, transcriptomic profiling of brain regions in mice heterozygous for *Nfix* (Harris et al., 2013) with mice heterozygous for *Nsd1* (which are yet to be generated), would allow determination of whether these proteins regulate similar sets of genes during brain development.

Interrogating this hypothesis would provide substantial insight into *NFIX* and *NSD1* function during brain development, as well as to the pathology of Sotos Syndrome more generally.

6.3 Comparing the function of NFIX in embryonic versus adult neural progenitors

Prior to this thesis, the function of NFIX in adult neural stem cells had not been explored. The analysis of NFIX function during development (Chapter 3) and in AH-NSCs (Chapter 5) places this thesis in the unique position to directly compare the function of NFIX in these two contexts. This comparison is useful as it allows generalisations to be made about how NFIX operates as a transcription factor within the nervous system.

In my thesis, contrary to initial expectations, I failed to find evidence that NFIX has an essential role in maintaining the long-term quiescence of AH-NSCs (see Chapter 1 for discussion, and section 6.4.1, below). Rather, I found that NFIX functions similarly in the adult brain as it does in the developing brain. In both contexts, NFIX promoted neuronal differentiation (Chapter 3 & Chapter 5). Likewise, NFIX also inhibited oligodendrocyte fate in the adult hippocampus (Chapter 5), which matches the function of NFIX during early postnatal development (Zhou et al., 2015). While I did not extensively examine whether NFIX promotes astrocyte production from AH-NSCs (Chapter 5), as it does during development (Heng et al., 2014), these results suggest that NFIX/NFIs govern major transitions in neural stem cell fate in a manner that is at least somewhat consistent across these different biological contexts.

In the following section, the similarities and differences in NFIX/NFI function during development and in AH-NSCs are outlined. I also draw on the literature relating to NFI function in other contexts to postulate that NFIX/NFIs may act by regulating chromatin structure, in addition to directly regulating gene expression through promoter interactions. I postulate that NFIX/NFIs directly, or indirectly through the recruitment of chromatin modifying-proteins, increase the accessibility of genome regions associated with cellular fate changes. This hypothesis may explain how NFIs can regulate all three major facets of neural stem cell differentiation: the production of neuronal, astrocyte and oligodendroglia lineages.

6.3.1 NFIX is not essential for maintaining the long-term quiescent state of AH-NSCs

The starting point of this thesis was the proposal that NFIs may have a different or accessory function within adult neural stem cells, namely in the maintenance of quiescence (Chapter 1). This

proposal was based primarily on two studies, one performed in the skin stem cell niche (Chang et al., 2013), and the other in the haematopoietic system (Holmfeldt et al., 2013). In both these studies, deletion of *Nfix* (haematopoietic system) or *Nfib* (skin stem cell niche) from adult stem cells led to increased proliferation and subsequently the depletion of the stem cell pool, suggesting that NFIs were mediating quiescence in these populations. The logical extension of these studies was that NFIX/NFIs might also regulate quiescence within adult stem cells of the CNS. This idea was strengthened shortly thereafter, by the publication of an *in vitro* study of neural stem cell quiescence (Martynoga et al., 2013). In this study, the authors used neural stem cells derived from an embryonic stem cell line. The exogenous application of BMP4 to these cells induced a state of quiescence. Analysis of chromatin accessibility during periods of proliferation and during periods of quiescence revealed that the NFI binding motif was strongly enriched in the quiescent state. Because only NFIX (and not NFIA, NFIB or NFIC) showed high expression in quiescent cells in this *in vitro* model, it was concluded that NFIX might be a central component of the gene regulatory network underpinning neural stem cell quiescence (Martynoga et al., 2013).

It was thus surprising in this thesis (Chapter 5) that when I tested the hypothesis that NFIX would be essential in regulating quiescence in AH-NSCs, *Nfix* deletion had little effect. *Nfix* deletion led to a small increase in AH-NSC proliferation (and the concomitant loss of quiescence) after 14 dpi, however, the effect size was both small and transient. Instead, *Nfix* deletion from AH-NSCs caused major defects in neuronal differentiation and increased oligodendrocyte generation. This data demonstrated that NFIX functions primarily to regulate differentiation but not the quiescence of AH-NSCs. There are a few explanations that may account for the discrepancy between the *in vitro* data (Martynoga et al., 2013) and our *in vivo* work (Chapter 5). For one, the *in vitro* system lacked the complexity of the *in vivo* niche, which is comprised of a dense network of blood vessels, excitatory and inhibitory inputs and immune cells (Moss et al., 2016). Other explanations may be that Martynoga and colleagues used neural stem cells derived from an embryonic stem cell line, which may have a vastly different epigenetic landscape than AH-NSCs. It would therefore prove interesting to repeat their experiment using a primary culture of AH-NSCs to determine if this accounted for the differences between their work and our *in vivo* findings.

6.3.2 NFIX promotes neuronal differentiation during development and in the adult hippocampus

During development of the mouse CNS, previous work had identified that NFIX was absolutely crucial for promoting the differentiation of neural stem cells. In the developing cerebellum for

example, NFIX has been shown to be required for the timely migration of GNPs towards the internal granule layer and for the axonal extension of these progenitors. Molecular studies identified that NFIs were able to bind to and regulate the expression of many genes involved in the maturation of GNPs, such as *Gabra6* (Wang et al., 2004), *Gabra1*, *Wnt7a* (Ding et al., 2013), *N-cadherin* and *ephrin B1* (Wang et al., 2007). Likewise, previous work cataloguing the dorsal forebrain phenotype of *Nfix*$^{-/-}$ mice had determined there was delayed production of TBR1^{+ve} neurons in the neocortex and hippocampus (Heng et al., 2014). However, it was unclear at what point from the transition of radial glial stem cell to a mature neuron was affected in these mice. In Chapter 3 of this thesis, I clarified this by demonstrating that NFIX regulates neuronal differentiation in the dorsal forebrain by driving the production of IPCs from radial glia, in part, through regulating *Insc* expression.

In this thesis, I also examined the function of NFIX in regulating neuronal differentiation in the adult hippocampus. I found that by deleting NFIX from AH-NSCs using a *nestin-creER*^{T2} transgene, or from neuronally committed cells using a *dcx-creER*^{T2} transgene, this resulted in severely impaired neuronal differentiation (Chapter 5). In the absence of NFIX, adult hippocampal neuroblasts failed to extend a primary dendritic branch, and retained expression of an immature neuronal marker (TBR2) longer than in control neuroblasts. These neuroblasts failed to mature into dentate granule neurons and an elevated proportion of these cells underwent programmed cell death. Therefore, like during development, NFIX expression is required for normal neuronal differentiation.

There are some differences as to how NFIX regulates neuronal differentiation across these different contexts. For example, in the developing dorsal forebrain, NFIX promotes the generation of IPCs from radial glia, which is a very early fate choice during neuronal development, while late aspects of neuronal differentiation appear unaffected (Chapter 3). In contrast, in the developing cerebellum and in the adult hippocampus, NFIX regulates later stages of neuronal differentiation so that primarily, axonal extension or dendritic branching and migration of immature neurons are affected (Piper et al., 2011) (Chapter 5). Another difference is that in the adult hippocampus, NFIX is absolutely required for neuronal differentiation so that the deletion of NFIX from these cells results in cell death. Conversely, during the development of the dorsal telencephalon in *Nfix*$^{-/-}$ mice, the delayed IPC production and expansion of the radial glial cell pool actually results in greater neuron number postnatally. Likewise, the developing cerebellum of *Nfix*$^{-/-}$ mice is initially smaller but largely catches up so that it is of comparable size and neuron number by P20 (Piper et al., 2011). These differences in the effect that NFIX deletion has on neuronal development and survival may

be accounted by different co-factor expression. Currently, little is known as to the different protein co-factors that NFIs may bind to regulate neural stem cell biology. NFI proteins can heterodimerise with other NFI proteins, and have been shown to form a complex with SOX9 to regulate glial differentiation in the spinal cord (Kang et al., 2012). Heterodimerisation of NFIX with dorsal telencephalon specific co-factors could affect neuronal gene expression differently than heterodimerisation of NFIX with co-factors that are specifically expressed in adult neuroblasts. Alternately, the chromatin state of the neural progenitors may account for the phenotypic differences seen upon *Nfix* deletion. ChIP-seq experiments determining the chromatin binding profile of NFIX across radial glial progenitors of the dorsal telencephalon, granule neuron progenitors of the cerebellum, and neuroblasts of the adult hippocampus would address this hypothesis. For example, one might expect to see NFIX binding to regions of the genome that are associated with early neuronal specification in the dorsal telencephalon, whereas in adult neuroblasts, NFIX may bind promoter regions upstream of genes involved in dendritic projection and neuronal survival.

In summary, NFIX is a key transcription factor that regulates neuronal differentiation during brain development and in the adult hippocampus. While the effect that NFIX deletion has on neuronal differentiation may vary per cell population, these differences only serve to highlight that NFIX promotes neuronal differentiation across a wide range of contexts.

6.3.3 NFIX inhibits oligodendrocyte differentiation during postnatal development and in the adult hippocampus

In contrast to their role in neuron differentiation, the relationship between NFIX/NFIs and generation of oligodendrocytes is less understood. This has primarily been because most *Nfi*$^{-/-}$ mice fail to survive after birth, while the majority of oligodendrocytes in the mouse brain are generated postnatally, with peak production at approximately P14 (Sauvageot and Stiles, 2002; Kriegstein and Alvarez-Buylla, 2009; Zuccaro and Arlotta, 2013). Two studies indicate that NFIs may have a complex relationship to oligodendrocyte lineage progression during mouse brain development. The first of these studies, published by Wong and colleagues (2007), performed an *mRNA* microarray on whole brain tissue from surviving P16 *Nfia*$^{-/-}$ and control mice. Among the 356 mis-regulated genes, those relevant to the oligodendrocyte lineage were particularly affected. Compared to control mice, oligodendrocyte precursor genes were upregulated, while genes typically associated with mature oligodendrocyte were downregulated. These data suggested that NFIA might function to promote terminal oligodendrocyte differentiation in the mouse brain (Wong et al., 2007).

The majority of oligodendrocytes are derived from pre-existing oligodendrocyte precursor cells scattered throughout the brain parenchyma (Menn et al., 2006; Kriegstein and Alvarez-Buylla, 2009). Some oligodendrocytes however, are also generated by NSCs from the SVZ of the lateral ventricles where they migrate to the corpus callosum (Menn et al., 2006). In a 2015 study, deletion of NFIX from cultured SVZ neural stem cells, led to increased generation of oligodendrocyte precursor cells, whereas forced overexpression inhibited their production. This data demonstrated that the generation of SVZ-derived oligodendrocytes is inhibited by NFIX (Zhou et al., 2015).

This data from Zhou and colleagues (2015), closely match the findings from Chapter 5 of my thesis. Unlike adult stem cells of the SVZ, AH-NSCs do not generate oligodendrocytes under physiological conditions. AH-NSCs do however, exhibit tri-potentency that is revealed under certain conditions (Sun et al., 2015). Using a retroviral delivery system into the dentate gyrus Braun and colleagues (2015) demonstrated that the expression of genes such as *Sox10* or *Olig2* could force AH-NSCs to generate oligodendrocytes (Braun et al., 2015; Sun et al., 2015). However, the factors inhibiting the tri-potentiality of AH-NSCs are still very poorly defined. I found in Chapter 5 of my thesis that deletion of *Nfix* using either a *nestin-creER^{T2}* or *dcx-creER^{T2}* transgene resulted in elevated oligodendrocyte production in the adult mouse hippocampus. These data suggest that, like in the postnatal SVZ, NFIX functions to inhibit oligodendrocyte production within the hippocampal niche, and might therefore be a key factor that suppresses the *in vivo* tri-potentiality of AH-NSCs.

6.3.4 NFIX promotes astrocyte differentiation during development

Finally, one role of NFIX/NFIs that has been consistently observed, both *in vitro*, and *in vivo* in various regions of the brain is their capacity to promote astrocytic differentiation. The massive delay seen in GFAP expression was among the first phenotypes observed in *Nfi$^{-/-}$* mice (das Neves et al., 1999), and is seen in the forebrain (das Neves et al., 1999; Steele-Perkins et al., 2005; Campbell et al., 2008), cerebellum (Piper et al., 2011) and spinal cord (Kang et al., 2012) of *Nfi$^{-/-}$* mice embryonically. NFIs can directly activate the expression of astrocyte specific genes such as *Gfap* (Cebolla and Vallejo, 2006; Gopalan et al., 2006; Namihira et al., 2009; Singh et al., 2011), *B-fabp* (Bisgrove et al., 2000), *Sparcl1* (Wilczynska et al., 2009), *Apcdd1*, *Mmd2*, *Zcchc24* (Kang et al., 2012) and *a_1-Antichymotrypsin* (Gopalan et al., 2006). In the adult hippocampus I found that deletion of NFIX from AH-NSCs did not lead to any change in the number of S100B^{+ve} astrocytes (Chapter 5). From this data alone however, it is not possible to conclude that astrocyte production occurs completely normally in the absence of NFIX in the adult hippocampus. One caveat is that

S100ß itself is not a completely specific marker for astrocytes (Young et al., 2010). For example, other aspects of glial differentiation may be impaired, as is seen in the spinal cord of *Nfix*$^{-/-}$ mice, where the number/specification of astrocytes is unaffected but the terminal differentiation of these cells is impaired (*Horne* et al., manuscript in preparation). Alternately, I may not have observed an astrocyte phenotype in the adult hippocampus because AH-NSCs rarely generate these cells (Bonaguidi et al., 2011). A better experiment to determine the role of NFIX in astrocyte development in the adult hippocampus might be to overexpress NFIX in AH-NSCs using an *in vivo* retrovirus delivery system. The overexpression of NFIX may then increase astrocyte development as it does upon overexpression during the development of the dorsal telencephalon (Heng et al., 2014).

6.3.5 Does NFIX/NFIs govern neural stem cell fate changes through modulating chromatin accessibility?

The complex and substantial role that NFIX/NFIs have in regulating the differentiation of neurons, oligodendrocytes and astrocytes from neural progenitor cells across development and in the adult hippocampus, demonstrate that these proteins are key determinants of cellular fate in the nervous system. How do NFIX/NFIs fulfil such a varied role in fate determination? Two scenarios are possible. Firstly, in line with their well-known role as transcription factors, NFIX/NFIs promote these different cellular fates by directly activating/repressing the expression of genes associated with these fates. Depending on the cellular context, the binding profile of NFIX/NFIs changes in accordance to which cell type needs to be produced. For instance, during the early development of the dorsal telencephalon, NFIX/NFIs bind to the promoter of *Insc* (Chapter 3) and other genes associated with early neuronal development to promote IPC production (Chapter 3) (Piper et al., 2010; Heng et al., 2014; Piper et al., 2014). Later during the development of the dorsal telencephalon, NFIX/NFIs may then bind *Gfap* and other genes associated with astrocyte development (Piper et al., 2011), and later again, genes associated with oligodendrocyte development (Zhou et al., 2015). These changes in the genome wide chromatin binding profile of NFIs would be likely mediated by the dimerization of NFIs different co-factors. An unbiased approach such as mass spectrometry could be used to identify these NFI co-factors.

The direct activation/repression of cell-type specific gene expression is unlikely to completely account for how NFIs govern neural stem cell fate. Neurons, astrocytes and oligodendrocytes are vastly different cells. For NFIX/NFIs to promote these different cellular fates only through the direct regulation of gene expression, they would likely need to directly activate/repress the

expression of many genes specific to each lineage. Interestingly, different neural cell types have vastly different chromatin architecture. This leads to the intriguing possibility that NFIX/NFIs may control cell fate through regulating chromatin accessibility. Indeed, there is substantial existing and emerging evidence that NFIs may also regulate cell fate through this means, either through nucleosome remodelling, or indirectly, via interactions with epigenetic modifiers [reviewed in (Fane et al., 2017)].

Some of the earliest evidence that the NFI protein family could act in a transcriptionally independent manner was that NFIs can bind to NFI half-sites and serve as initiation factors during DNA replication (Santoro et al., 1988). Early structural analysis also hinted that NFIs could regulate chromatin structure as they contained a trans-activation domain that interacted with histones H1 and H3 (Dusserre and Mermod, 1992; Alevizopoulos et al., 1995) and were able to alter the interaction of reconstituted nucleosomal cores with DNA *in vitro* (Alevizopoulos et al., 1995). *In vivo* evidence also revealed that NFIs are able to alter native chromatin structure at yeast origins of replication (Li, 1999) and other promoter regions through direct interaction with histone proteins.

NFIs have also been shown to affect chromatin remodelling in an indirect manner through regulating and interacting with epigenetic modifiers. For instance, NFIB has been shown to directly repress the epigenetic modifier EZH2 during development of the dorsal telencephalon to promote neuronal differentiation (Piper et al., 2014). Furthermore, NFIs have also been shown to interact with histone deacetylases, such as BAF (Liu et al., 2001; Zhao et al., 2005) and other transcriptional activators such as BRG1 (Hebbar and Archer, 2003).

The most prominent study implicating NFIs as chromatin regulators found that NFIB was a key driver of chromatin accessibility in the metastasis of lung cancer. This study revealed that, compared to primary tumours, metastatic tumors had vastly increased chromatin accessibility. Bioinformatic analyses revealed that the NFI consensus site was strongly enriched in these differential regions of chromatin accessibility. These regions of increased chromatin accessibility depended on NFIB expression. Moreover, the samples with the most accessible chromatin were often correlated with amplification of the *Nfib* locus (Denny et al., 2016).

Collectively, these data suggest that in addition to governing neural stem cell fate by directly regulating the transcription of cell-type specific genes, NFIX/NFIs may also achieve this in part, through regulating chromatin architecture. To validate this hypothesis within neural stem cells, a

range of experimental approaches could be considered. For example, data-mining of Assay for Transposase-Accessible Chromatin sequencing (ATAC-seq) datasets from neural progenitors undergoing neuronal, astrocyte or oligodendrocyte differentiation might reveal whether NFI-binding sites are enriched in accessible regions of the genome specific to each cell state. Subsequent loss- and gain-of-function experiments followed by ATAC-seq could then be used to determine whether the availability of these chromatin sites were dependent upon NFI expression. Another key experiment would be to determine whether NFIs increase chromatin accessibility by interacting with other epigenetic modifying proteins. NFIs have only a limited number of known interacting proteins (Kang et al., 2012), and an unbiased approach, such as mass spectrometry, could be used to identify whether NFIs bind to epigenetic regulator proteins.

6.4 NFIX function in adult hippocampal precursors

Chapter 5 of this thesis demonstrated that NFIX was a central factor controlling the differentiation of adult hippocampal neuroblasts into mature dentate granule neurons. The impaired production of dentate granule neurons from adult hippocampal precursor cells is linked to psychiatric disorders such as depression (Goncalves et al., 2016). The capacity of adult hippocampal precursors to generate cell types other than neurons is thus a less frequently studied process in the literature. Among the most tantalising findings from Chapter 5 of my thesis, was that *Nfix*-deletion from adult hippocampal progenitors biased some cells towards an oligodendrocyte fate. I review these data suggesting that *Nfix* acts as a molecular barrier to oligodendrocyte production in the hippocampus in the context of recent studies exploring similar molecular blocks. I close by briefly discussing the possibilities of programming adult hippocampal precursors to generate oligodendrocytes for the treatment of disorders that feature demyelination of the hippocampus/temporal lobe.

6.4.1 Molecular blocks of adult hippocampal precursor potency

Unlike stem cells in the adult SVZ that generate oligodendrocytes destined for the corpus callosum (Menn et al., 2006), AH-NSCs do not generate significant numbers of oligodendrocytes under physiological conditions (Bonaguidi et al., 2011). Primary cultures of AH-NSCs also show limited capacity to generate oligodendrocytes, suggesting that barriers preventing the generation of oligodendrocytes from AH-NSCs are likely to be cell-intrinsic (Suh et al., 2007; Rolando et al., 2016). Recently, AH-NSCs were shown to be able to undergo a directed differentiation process to generate oligodendrocytes upon the forced expression of *Olig2*, *Sox10* or *Ascl1* using retroviruses (Braun et al., 2015). Two studies followed this, where the removal of molecular blocks, either *neurofibromin 1* (Sun et al., 2015) or *Drosha* (Rolando et al., 2016) were able to bias adult hippocampal precursors towards oligodendrocyte generation. The data in Chapter 5 adds *Nfix* to the short list of genes that function to inhibit oligodendrocyte formation within this population of progenitors.

The three previous studies that have demonstrated the latent potential of adult-hippocampal neural progenitors to generate oligodendrocytes did not determine the precise cell-type within the hippocampus that was giving rise to these cells. Braun and collleagues (2015) used retroviruses that target both dividing AH-NSCs and dividing IPs. Sun and colleagues (2015) used a *glast-creER*^{T2} line, and Rolando and colleagues (2016) a *Hes5-creER*^{T2} line, which, while only recombining in AH-NSCs, does not preclude the possibility that later cells in the lineage were responsible for the

generation of oligodendrocytes. Since AH-NSCs form the base of the lineage tree in the adult hippocampus, the most reasonable assumption from these studies at the time, was that the cells that converted to an oligodendrocyte fate were AH-NSCs.

Similar to these studies, I used a *cre*-recomnbinase line (*nestin-creER^{T2}*) that efficiently deletes *LoxP*-flanked genetic sequences from AH-NSCs (Imayoshi et al., 2006). Upon deleting *Nfix* using this *nestin-creER^{T2}* line, there was an approximate 5-fold increase in oligodendrocyte generation. Remarkably, I also saw evidence of a bias towards an oligodendrocyte fate following deletion of *Nfix* using a *dcx-creER^{T2}* line (Cheng et al., 2011). RNA-seq of tdtomato^{+ve} cells 7 dpi revealed an increase in the *mRNA* levels of oligodendrocyte precursor genes in *Nfix*$^{iDcx\text{-}TD}$ mice relative to controls. There are a number of reasons that suggest this data reflect real changes in neuroblast cell biology rather than an experimental artefact. Firstly, I found that the *dcx-creER^{T2}* line was highly specific. The vast majority of tdtomato^{+ve} cells were DCX^{+ve} at 7 dpi, while less than 2% of tdtomato^{+ve} cells were Olig2^{+ve}. Secondly, the types of mis-regulated genes in the RNA-seq experiment are consistent with the *de novo* generation of oligodendrocytes. For example, only pan-oligo markers or oligodendrocyte precursor genes were upregulated upon *Nfix* deletion (e.g *Olig1*, *Olig2*, *Cspg4*), whereas mature markers of oligodendrocytes were unchanged (e.g *Mbp*, *Mog*). The widespread cell death of DCX^{+ve} cells upon *Nfix* deletion would likely mean that we only detect these changes at a transcriptional level, and not as an increase in the number of tdtomato^{+ve} cells that colocalise with oligodendrocyte markers. Consistent with this, was no substantial increase in the number of Olig2^{+ve}; tdtomato^{+ve} cells in *Nfix*$^{iDCX\text{-}TD}$ mice compared to controls. Therefore these data support a model where *Nfix* deletion from neuroblasts leads to a failure of these cells to execute a program of neuronal differentiation, concomitant with a de-repression of oligodendrocyte precursor gene expression. The cellular death of *Nfix* deficient neuroblasts obfuscates our capacity to determine whether the de-repression of oligodendrocyte precursor gene expression from these cells would be sufficient to convert them into a mature oligodendrocyte state over the long-term. However, these data suggest that if these cells were to survive that this trajectory is possible.

There are two key experiments that can be performed to strengthen my data that adult hippocampal neuroblasts have the potential to generate oligodendrocytes. The first of these experiments would be to perform single-cell RNA-seq on *Nfix*-deficient and control neuroblasts to identify single-cells that are 'in-between' a neuronal and oligodendrocyte fate. This would allow us unequivocally determine that the increase in oligodendrocyte precursor gene expression is coming from single-cells that also express neuronal genes, rather than a contaminating bias in our 'bulk' RNA-seq

experiment. In support of this, a previous single-cell sequencing experiment using a transgenic *Dcx*::dsRed mouse line, detected a sub-population of neuroblasts that expressed oligodendrocyte genes, suggesting that even wild type neuroblasts express some oligodendrocyte markers at an *mRNA* level (Gao et al., 2016). Secondly, it would be of great interest to delete more potent inhibitors of oligodendrocyte fate using the *dcx-creERT2* line, such as *neurofibromin 1* (Sun et al., 2015) and repeat this single-cell sequencing experiment. Because *neurofibromin 1* is not required for neuroblast survival, the deletion of *neurofibromin 1* from neuroblasts would also allow us to determine whether the de-repression of oligodendrocyte precursor genes from within neuroblasts is sufficient to convert this population into mature oligodendrocytes, without the obfuscation caused by cellular death.

6.4.2 Clinical relevance of oligodendrocyte production in the adult hippocampus

The suggestion that AH-NSCs (Braun et al., 2015; Sun et al., 2015; Rolando et al., 2016) (Chapter 5) have the capacity to generate oligodendrocytes is an exciting development. The myelination of the hippocampus is often affected in disorders such as multiple sclerosis, Alzheimer's disease, bipolar disorder and in traumatic brain injury (Chambers and Perrone-Bizzozero, 2004; Meier et al., 2004; Noble, 2004; Geurts et al., 2007). Moreover, the hippocampus has been reported to lack a significant remyelination response to injury relative to other brain regions (Deverman and Patterson, 2012; Braun et al., 2015). In theory, cellular transplantation therapies of oligodendrocyte precursor cells could be developed to treat the demyelination of the hippocampus in disorders such as multiple sclerosis, but these would be inevitably expensive and invasive treatments that run the risk of rejection or tumorigenesis (Walker et al., 2016a). An alternative to cellular transplantations is to harness endogenous neural stem cells/progenitors to generate oligodendrocytes. Indeed, Braun and colleagues (2015) have already demonstrated this in mice, where reprogramming of adult hippocampal precursor cells using retroviruses generated oligodendrocytes and enhanced remyelination after injury. Future studies aimed at identifying small molecules that activate or inhibit specific transcriptional pathways to increase oligodendrocyte differentiation without using of viruses will be important (Braun et al., 2015). The development of small molecules to target these transcriptional pathways would be difficult due to off-target effects and limited drug bioavailability but these issues could be overcome (Walker et al., 2016a). The identification of *Nfix* as a molecule that blocks the potential for adult hippocampal progenitors to generate oligodendrocytes is a step towards the development of these treatments

6.5 Conclusion

A complete understanding of the molecular pathways controlling neural stem cell biology is central to treating neurodevelopmental disorders, degenerative conditions of the nervous system and improving cognitive function. This thesis has revealed that the transcription factor NFIX is a crucial regulator of neural stem cell biology.

During the development of the dorsal telencephalon, NFIX acts to promote the asymmetric division of radial glial progenitors and the production of IPCs (Chapter 3). Without NFIX, the stem cell pool in mice expands and neurogenesis is prolonged. This leads to more neurons and macrocephaly. While this work has deepened our general understanding of brain development, it will also inform future studies that model human disorders caused by *NFIX* mutations, using such techniques such as cerebral organoid culture.

This thesis has also contributed a new method that may assist persons working in the field of adult hippocampal neurogenesis. In Chapter 4, a morphology independent approach to quantifying AH-NSCs was described. This technique is accurate, fast and allows for the quantification of both radially- and horizontally-oriented AH-NSCs. If broadly adopted, this approach may help to provide a more holistic account of changes to AH-NSC populations after experimental manipulation.

Finally, using this newly developed method, and others, this thesis also described the function of NFIX within neural progenitors in the adult hippocampus (Chapter 5). This work revealed that NFIX is an essential factor for promoting neuroblast differentiation and survival, and added *Nfix* to the growing list of genes that function to restrict the potential of AH-NSCs to generate oligodendrocytes.

Collectively, this thesis has substantially increased our understanding of the transcriptional control of neural stem cells in the developing brain and in the adult hippocampus.

Chapter 7 References

Akers KG, Martinez-Canabal A, Restivo L, Yiu AP, De Cristofaro A, Hsiang HL, Wheeler AL, Guskjolen A, Niibori Y, Shoji H, Ohira K, Richards BA, Miyakawa T, Josselyn SA, Frankland PW. 2014. Hippocampal neurogenesis regulates forgetting during adulthood and infancy. Science 344:598-602.

Alevizopoulos A, Dusserre Y, Tsai-Pflugfelder M, von der Weid T, Wahli W, Mermod N. 1995. A proline-rich TGF-beta-responsive transcriptional activator interacts with histone H3. Genes Dev 9:3051-3066.

Altman J, Bayer SA. 1990. Prolonged sojourn of developing pyramidal cells in the intermediate zone of the hippocampus and their settling in the stratum pyramidale. J Comp Neurol 301:343-364.

Anders S, Pyl PT, Huber W. 2015. HTSeq--a Python framework to work with high-throughput sequencing data. Bioinformatics 31:166-169.

Andersen J, Urban N, Achimastou A, Ito A, Simic M, Ullom K, Martynoga B, Lebel M, Goritz C, Frisen J, Nakafuku M, Guillemot F. 2014. A transcriptional mechanism integrating inputs from extracellular signals to activate hippocampal stem cells. Neuron 83:1085-1097.

Andreu Z, Khan MA, Gonzalez-Gomez P, Negueruela S, Hortiguela R, San Emeterio J, Ferron SR, Martinez G, Vidal A, Farinas I, Lie DC, Mira H. 2015. The cyclin-dependent kinase inhibitor p27 kip1 regulates radial stem cell quiescence and neurogenesis in the adult hippocampus. Stem Cells 33:219-229.

Anthony TE, Klein C, Fishell G, Heintz N. 2004. Radial glia serve as neuronal progenitors in all regions of the central nervous system. Neuron 41:881-890.

Arai Y, Pulvers JN, Haffner C, Schilling B, Nusslein I, Calegari F, Huttner WB. 2011. Neural stem and progenitor cells shorten S-phase on commitment to neuron production. Nat Commun 2:154.

Asami M, Pilz GA, Ninkovic J, Godinho L, Schroeder T, Huttner WB, Gotz M. 2011. The role of Pax6 in regulating the orientation and mode of cell division of progenitors in the mouse cerebral cortex. Development 138:5067-5078.

Ayrault O, Zhao H, Zindy F, Qu C, Sherr CJ, Roussel MF. 2010. Atoh1 inhibits neuronal differentiation and collaborates with Gli1 to generate medulloblastoma-initiating cells. Cancer Res 70:5618-5627.

Bader PL, Faizi M, Kim LH, Owen SF, Tadross MR, Alfa RW, Bett GC, Tsien RW, Rasmusson RL, Shamloo M. 2011. Mouse model of Timothy syndrome recapitulates triad of autistic traits. Proc Natl Acad Sci U S A 108:15432-15437.

Barbieri G, De Angelis L, Feo S, Cossu G, Giallongo A. 1990. Differential expression of muscle-specific enolase in embryonic and fetal myogenic cells during mouse development. Differentiation 45:179-184.

Barry G, Piper M, Lindwall C, Moldrich R, Mason S, Little E, Sarkar A, Tole S, Gronostajski RM, Richards LJ. 2008. Specific glial populations regulate hippocampal morphogenesis. J Neurosci 28:12328-12340.

Basak O, Taylor V. 2007. Identification of self-replicating multipotent progenitors in the embryonic nervous system by high Notch activity and Hes5 expression. Eur J Neurosci 25:1006-1022.

Baynash AG, Hosoda K, Giaid A, Richardson JA, Emoto N, Hammer RE, Yanagisawa M. 1994. Interaction of endothelin-3 with endothelin-B receptor is essential for development of epidermal melanocytes and enteric neurons. Cell 79:1277-1285.

Bergmann O, Spalding KL, Frisen J. 2015. Adult Neurogenesis in Humans. Cold Spring Harb Perspect Biol 7:a018994.

Betancourt J, Katzman S, Chen B. 2014. Nuclear factor one B regulates neural stem cell differentiation and axonal projection of corticofugal neurons. J Comp Neurol 522:6-35.

Biressi S, Molinaro M, Cossu G. 2007a. Cellular heterogeneity during vertebrate skeletal muscle development. Dev Biol 308:281-293.

Biressi S, Tagliafico E, Lamorte G, Monteverde S, Tenedini E, Roncaglia E, Ferrari S, Ferrari S, Cusella-De Angelis MG, Tajbakhsh S, Cossu G. 2007b. Intrinsic phenotypic diversity of embryonic and fetal myoblasts is revealed by genome-wide gene expression analysis on purified cells. Dev Biol 304:633-651.

Bisgrove DA, Monckton EA, Packer M, Godbout R. 2000. Regulation of brain fatty acid-binding protein expression by differential phosphorylation of nuclear factor I in malignant glioma cell lines. J Biol Chem 275:30668-30676.

Bonaguidi MA, Wheeler MA, Shapiro JS, Stadel RP, Sun GJ, Ming GL, Song H. 2011. In vivo clonal analysis reveals self-renewing and multipotent adult neural stem cell characteristics. Cell 145:1142-1155.

Braun SM, Pilz GA, Machado RA, Moss J, Becher B, Toni N, Jessberger S. 2015. Programming Hippocampal Neural Stem/Progenitor Cells into Oligodendrocytes Enhances Remyelination in the Adult Brain after Injury. Cell Rep 11:1679-1685.

Calabria E, Ciciliot S, Moretti I, Garcia M, Picard A, Dyar KA, Pallafacchina G, Tothova J, Schiaffino S, Murgia M. 2009. NFAT isoforms control activity-dependent muscle fiber type specification. Proc Natl Acad Sci U S A 106:13335-13340.

Cameron HA, McKay RD. 2001. Adult neurogenesis produces a large pool of new granule cells in the dentate gyrus. J Comp Neurol 435:406-417.

Campbell CE, Piper M, Plachez C, Yeh YT, Baizer JS, Osinski JM, Litwack ED, Richards LJ, Gronostajski RM. 2008. The transcription factor Nfix is essential for normal brain development. BMC Dev Biol 8:52.

Casper KB, McCarthy KD. 2006. GFAP-positive progenitor cells produce neurons and oligodendrocytes throughout the CNS. Mol Cell Neurosci 31:676-684.

Castro DS, Martynoga B, Parras C, Ramesh V, Pacary E, Johnston C, Drechsel D, Lebel-Potter M, Garcia LG, Hunt C, Dolle D, Bithell A, Ettwiller L, Buckley N, Guillemot F. 2011. A novel function of the proneural factor Ascl1 in progenitor proliferation identified by genome-wide characterization of its targets. Genes Dev 25:930-945.

Cebolla B, Vallejo M. 2006. Nuclear factor-I regulates glial fibrillary acidic protein gene expression in astrocytes differentiated from cortical precursor cells. J Neurochem 97:1057-1070.

Chambers JS, Perrone-Bizzozero NI. 2004. Altered myelination of the hippocampal formation in subjects with schizophrenia and bipolar disorder. Neurochem Res 29:2293-2302.

Chang CY, Pasolli HA, Giannopoulou EG, Guasch G, Gronostajski RM, Elemento O, Fuchs E. 2013. NFIB is a governor of epithelial-melanocyte stem cell behaviour in a shared niche. Nature 495:98-102.

Chaudhry AZ, Lyons GE, Gronostajski RM. 1997. Expression patterns of the four nuclear factor I genes during mouse embryogenesis indicate a potential role in development. Dev Dyn 208:313-325.

Chen KS, Harris L, Lim JW, Harvey TJ, Piper M, Gronostajski RM, Richards LJ, Bunt J. 2017. Differential neuronal and glial expression of Nuclear factor I proteins in the cerebral cortex of adult mice. J Comp Neurol.

Cheng X, Li Y, Huang Y, Feng X, Feng G, Xiong ZQ. 2011. Pulse labeling and long-term tracing of newborn neurons in the adult subgranular zone. Cell Res 21:338-349.

Chenn A, Walsh CA. 2002. Regulation of cerebral cortical size by control of cell cycle exit in neural precursors. Science 297:365-369.

Cheung TH, Rando TA. 2013. Molecular regulation of stem cell quiescence. Nat Rev Mol Cell Biol 14:329-340.

Cimadevilla JM, Wesierska M, Fenton AA, Bures J. 2001. Inactivating one hippocampus impairs avoidance of a stable room-defined place during dissociation of arena cues from room cues by rotation of the arena. Proc Natl Acad Sci U S A 98:3531-3536.

Cole TJ, Blendy JA, Monaghan AP, Krieglstein K, Schmid W, Aguzzi A, Fantuzzi G, Hummler E, Unsicker K, Schutz G. 1995. Targeted disruption of the glucocorticoid receptor gene blocks adrenergic chromaffin cell development and severely retards lung maturation. Genes Dev 9:1608-1621.

Collins CA, Olsen I, Zammit PS, Heslop L, Petrie A, Partridge TA, Morgan JE. 2005. Stem cell function, self-renewal, and behavioral heterogeneity of cells from the adult muscle satellite cell niche. Cell 122:289-301.

Costa RH, Kalinichenko VV, Lim L. 2001. Transcription factors in mouse lung development and function. Am J Physiol Lung Cell Mol Physiol 280:L823-838.

Cugola FR, Fernandes IR, Russo FB, Freitas BC, Dias JL, Guimaraes KP, Benazzato C, Almeida N, Pignatari GC, Romero S, Polonio CM, Cunha I, Freitas CL, Brandao WN, Rossato C, Andrade DG, Faria Dde P, Garcez AT, Buchpigel CA, Braconi CT, Mendes E, Sall AA, Zanotto PM, Peron JP, Muotri AR, Beltrao-Braga PC. 2016. The Brazilian Zika virus strain causes birth defects in experimental models. Nature 534:267-271.

Cuylen S, Blaukopf C, Politi AZ, Muller-Reichert T, Neumann B, Poser I, Ellenberg J, Hyman AA, Gerlich DW. 2016. Ki-67 acts as a biological surfactant to disperse mitotic chromosomes. Nature 535:308-312.

Dahmane N, Ruiz i Altaba A. 1999. Sonic hedgehog regulates the growth and patterning of the cerebellum. Development 126:3089-3100.

Dang J, Tiwari SK, Lichinchi G, Qin Y, Patil VS, Eroshkin AM, Rana TM. 2016. Zika Virus Depletes Neural Progenitors in Human Cerebral Organoids through Activation of the Innate Immune Receptor TLR3. Cell Stem Cell 19:258-265.

das Neves L, Duchala CS, Tolentino-Silva F, Haxhiu MA, Colmenares C, Macklin WB, Campbell CE, Butz KG, Gronostajski RM. 1999. Disruption of the murine nuclear factor I-A gene (Nfia) results in perinatal lethality, hydrocephalus, and agenesis of the corpus callosum. Proc Natl Acad Sci U S A 96:11946-11951.

Deciphering Developmental Disorders S. 2017. Prevalence and architecture of de novo mutations in developmental disorders. Nature 542:433-438.

Deng W, Aimone JB, Gage FH. 2010. New neurons and new memories: how does adult hippocampal neurogenesis affect learning and memory? Nat Rev Neurosci 11:339-350.

Denny SK, Yang D, Chuang CH, Brady JJ, Lim JS, Gruner BM, Chiou SH, Schep AN, Baral J, Hamard C, Antoine M, Wislez M, Kong CS, Connolly AJ, Park KS, Sage J, Greenleaf WJ, Winslow MM. 2016. Nfib Promotes Metastasis through a Widespread Increase in Chromatin Accessibility. Cell 166:328-342.

Deverman BE, Patterson PH. 2012. Exogenous leukemia inhibitory factor stimulates oligodendrocyte progenitor cell proliferation and enhances hippocampal remyelination. J Neurosci 32:2100-2109.

Ding B, Wang W, Selvakumar T, Xi HS, Zhu H, Chow CW, Horton JD, Gronostajski RM, Kilpatrick DL. 2013. Temporal regulation of nuclear factor one occupancy by calcineurin/NFAT governs a voltage-sensitive developmental switch in late maturing neurons. J Neurosci 33:2860-2872.

Dooley AL, Winslow MM, Chiang DY, Banerji S, Stransky N, Dayton TL, Snyder EL, Senna S, Whittaker CA, Bronson RT, Crowley D, Barretina J, Garraway L, Meyerson M, Jacks T. 2011. Nuclear factor I/B is an oncogene in small cell lung cancer. Genes Dev 25:1470-1475.

Dranovsky A, Picchini AM, Moadel T, Sisti AC, Yamada A, Kimura S, Leonardo ED, Hen R. 2011. Experience dictates stem cell fate in the adult hippocampus. Neuron 70:908-923.

Driller K, Pagenstecher A, Uhl M, Omran H, Berlis A, Grunder A, Sippel AE. 2007. Nuclear factor I X deficiency causes brain malformation and severe skeletal defects. Mol Cell Biol 27:3855-3867.

Dusserre Y, Mermod N. 1992. Purified cofactors and histone H1 mediate transcriptional regulation by CTF/NF-I. Mol Cell Biol 12:5228-5237.

Englund C, Fink A, Lau C, Pham D, Daza RA, Bulfone A, Kowalczyk T, Hevner RF. 2005. Pax6, Tbr2, and Tbr1 are expressed sequentially by radial glia, intermediate progenitor cells, and postmitotic neurons in developing neocortex. J Neurosci 25:247-251.

Ernst A, Frisen J. 2015. Adult neurogenesis in humans- common and unique traits in mammals. PLoS Biol 13:e1002045.

Fane M, Harris L, Smith AG, Piper M. 2017. Nuclear factor one transcription factors as epigenetic regulators in cancer. Int J Cancer.

Farkas LM, Haffner C, Giger T, Khaitovich P, Nowick K, Birchmeier C, Paabo S, Huttner WB. 2008. Insulinoma-associated 1 has a panneurogenic role and promotes the generation and expansion of basal progenitors in the developing mouse neocortex. Neuron 60:40-55.

Ferrari S, Molinari S, Melchionna R, Cusella-De Angelis MG, Battini R, De Angelis L, Kelly R, Cossu G. 1997. Absence of MEF2 binding to the A/T-rich element in the muscle creatine kinase (MCK) enhancer correlates with lack of early expression of the MCK gene in embryonic mammalian muscle. Cell Growth Differ 8:23-34.

Fraser J, Essebier A, Gronostajski RM, Boden M, Wainwright BJ, Harvey TJ, Piper M. 2016. Cell-type-specific expression of NFIX in the developing and adult cerebellum. Brain Struct Funct.

Gao Y, Wang F, Eisinger BE, Kelnhofer LE, Jobe EM, Zhao X. 2016. Integrative Single-Cell Transcriptomics Reveals Molecular Networks Defining Neuronal Maturation During Postnatal Neurogenesis. Cereb Cortex.

Gao Z, Ure K, Ding P, Nashaat M, Yuan L, Ma J, Hammer RE, Hsieh J. 2011. The master negative regulator REST/NRSF controls adult neurogenesis by restraining the neurogenic program in quiescent stem cells. J Neurosci 31:9772-9786.

Genovesi LA, Ng CG, Davis MJ, Remke M, Taylor MD, Adams DJ, Rust AG, Ward JM, Ban KH, Jenkins NA, Copeland NG, Wainwright BJ. 2013. Sleeping Beauty mutagenesis in a mouse medulloblastoma model defines networks that discriminate between human molecular subgroups. Proc Natl Acad Sci U S A 110:E4325-4334.

Geurts JJ, Bo L, Roosendaal SD, Hazes T, Daniels R, Barkhof F, Witter MP, Huitinga I, van der Valk P. 2007. Extensive hippocampal demyelination in multiple sclerosis. J Neuropathol Exp Neurol 66:819-827.

Glasgow SM, Laug D, Brawley VS, Zhang Z, Corder A, Yin Z, Wong ST, Li XN, Foster AE, Ahmed N, Deneen B. 2013. The miR-223/nuclear factor I-A axis regulates glial precursor proliferation and tumorigenesis in the CNS. J Neurosci 33:13560-13568.

Goecks J, Nekrutenko A, Taylor J, Galaxy T. 2010. Galaxy: a comprehensive approach for supporting accessible, reproducible, and transparent computational research in the life sciences. Genome Biol 11:R86.

Goncalves JT, Schafer ST, Gage FH. 2016. Adult Neurogenesis in the Hippocampus: From Stem Cells to Behavior. Cell 167:897-914.

Gopalan SM, Wilczynska KM, Konik BS, Bryan L, Kordula T. 2006. Nuclear factor-1-X regulates astrocyte-specific expression of the alpha1-antichymotrypsin and glial fibrillary acidic protein genes. J Biol Chem 281:13126-13133.

Gotz M, Huttner WB. 2005. The cell biology of neurogenesis. Nat Rev Mol Cell Biol 6:777-788.

Gotz M, Stoykova A, Gruss P. 1998. Pax6 controls radial glia differentiation in the cerebral cortex. Neuron 21:1031-1044.

Gronostajski RM. 2000. Roles of the NFI/CTF gene family in transcription and development. Gene 249:31-45.

Grunder A, Ebel TT, Mallo M, Schwarzkopf G, Shimizu T, Sippel AE, Schrewe H. 2002. Nuclear factor I-B (Nfib) deficient mice have severe lung hypoplasia. Mech Dev 112:69-77.

Guillemot F, Hassan BA. 2016. Beyond proneural: emerging functions and regulations of proneural proteins. Curr Opin Neurobiol 42:93-101.

Gulbins E, Palmada M, Reichel M, Luth A, Bohmer C, Amato D, Muller CP, Tischbirek CH, Groemer TW, Tabatabai G, Becker KA, Tripal P, Staedtler S, Ackermann TF, van Brederode J, Alzheimer C, Weller M, Lang UE, Kleuser B, Grassme H, Kornhuber J. 2013. Acid sphingomyelinase-ceramide system mediates effects of antidepressant drugs. Nat Med 19:934-938.

Gurrieri F, Cavaliere ML, Wischmeijer A, Mammi C, Neri G, Pisanti MA, Rodella G, Lagana C, Priolo M. 2015. NFIX mutations affecting the DNA-binding domain cause a peculiar overgrowth syndrome (Malan syndrome): a new patients series. Eur J Med Genet 58:488-491.

Hagihara H, Toyama K, Yamasaki N, Miyakawa T. 2009. Dissection of hippocampal dentate gyrus from adult mouse. J Vis Exp.

Harris L, Dixon C, Cato K, Heng YH, Kurniawan ND, Ullmann JF, Janke AL, Gronostajski RM, Richards LJ, Burne TH, Piper M. 2013. Heterozygosity for nuclear factor one x affects hippocampal-dependent behaviour in mice. PLoS One 8:e65478.

Harris L, Genovesi LA, Gronostajski RM, Wainwright BJ, Piper M. 2015. Nuclear factor one transcription factors: Divergent functions in developmental versus adult stem cell populations. Dev Dyn 244:227-238.

Harris L, Zalucki O, Gobius I, McDonald H, Osinki J, Harvey TJ, Essebier A, Vidovic D, Gladwyn-Ng I, Burne TH, Heng JI, Richards LJ, Gronostajski RM, Piper M. 2016a. Transcriptional regulation of intermediate progenitor cell generation during hippocampal development. Development 143:4620-4630.

Harris L, Zalucki O, Piper M, Heng JI. 2016b. Insights into the Biology and Therapeutic Applications of Neural Stem Cells. Stem Cells Int 2016:9745315.

Haubensak W, Attardo A, Denk W, Huttner WB. 2004. Neurons arise in the basal neuroepithelium of the early mammalian telencephalon: a major site of neurogenesis. Proc Natl Acad Sci U S A 101:3196-3201.

Haydar TF, Ang E, Jr., Rakic P. 2003. Mitotic spindle rotation and mode of cell division in the developing telencephalon. Proc Natl Acad Sci U S A 100:2890-2895.

Hebbar PB, Archer TK. 2003. Nuclear factor 1 is required for both hormone-dependent chromatin remodeling and transcriptional activation of the mouse mammary tumor virus promoter. Mol Cell Biol 23:887-898.

Heng YH, McLeay RC, Harvey TJ, Smith AG, Barry G, Cato K, Plachez C, Little E, Mason S, Dixon C, Gronostajski RM, Bailey TL, Richards LJ, Piper M. 2014. NFIX regulates neural progenitor cell differentiation during hippocampal morphogenesis. Cereb Cortex 24:261-279.

Hodge RD, Kowalczyk TD, Wolf SA, Encinas JM, Rippey C, Enikolopov G, Kempermann G, Hevner RF. 2008. Intermediate progenitors in adult hippocampal neurogenesis: Tbr2 expression and coordinate regulation of neuronal output. J Neurosci 28:3707-3717.

Hodge RD, Nelson BR, Kahoud RJ, Yang R, Mussar KE, Reiner SL, Hevner RF. 2012. Tbr2 is essential for hippocampal lineage progression from neural stem cells to intermediate progenitors and neurons. J Neurosci 32:6275-6287.

Holmfeldt P, Pardieck J, Saulsberry AC, Nandakumar SK, Finkelstein D, Gray JT, Persons DA, McKinney-Freeman S. 2013. Nfix is a novel regulator of murine hematopoietic stem and progenitor cell survival. Blood 122:2987-2996.

Hsu YC, Osinski J, Campbell CE, Litwack ED, Wang D, Liu S, Bachurski CJ, Gronostajski RM. 2011. Mesenchymal nuclear factor I B regulates cell proliferation and epithelial differentiation during lung maturation. Dev Biol 354:242-252.

Huang da W, Sherman BT, Lempicki RA. 2009a. Bioinformatics enrichment tools: paths toward the comprehensive functional analysis of large gene lists. Nucleic Acids Res 37:1-13.

Huang da W, Sherman BT, Lempicki RA. 2009b. Systematic and integrative analysis of large gene lists using DAVID bioinformatics resources. Nat Protoc 4:44-57.

Hussaini SM, Jun H, Cho CH, Kim HJ, Kim WR, Jang MH. 2013. Heat-induced antigen retrieval: an effective method to detect and identify progenitor cell types during adult hippocampal neurogenesis. J Vis Exp.

Huttner WB, Kosodo Y. 2005. Symmetric versus asymmetric cell division during neurogenesis in the developing vertebrate central nervous system. Curr Opin Cell Biol 17:648-657.

Imayoshi I, Ohtsuka T, Metzger D, Chambon P, Kageyama R. 2006. Temporal regulation of Cre recombinase activity in neural stem cells. Genesis 44:233-238.

Insolera R, Bazzi H, Shao W, Anderson KV, Shi SH. 2014. Cortical neurogenesis in the absence of centrioles. Nat Neurosci 17:1528-1535.

Jhaveri DJ, Mackay EW, Hamlin AS, Marathe SV, Nandam LS, Vaidya VA, Bartlett PF. 2010. Norepinephrine directly activates adult hippocampal precursors via beta3-adrenergic receptors. J Neurosci 30:2795-2806.

Jhaveri DJ, O'Keeffe I, Robinson GJ, Zhao QY, Zhang ZH, Nink V, Narayanan RK, Osborne GW, Wray NR, Bartlett PF. 2015. Purification of neural precursor cells reveals the presence of distinct, stimulus-specific subpopulations of quiescent precursors in the adult mouse hippocampus. J Neurosci 35:8132-8144.

Johansson EM, Kannius-Janson M, Gritli-Linde A, Bjursell G, Nilsson J. 2005. Nuclear factor 1-C2 is regulated by prolactin and shows a distinct expression pattern in the mouse mammary epithelial cells during development. Mol Endocrinol 19:992-1003.

Kaidanovich-Beilin O, Lipina T, Vukobradovic I, Roder J, Woodgett JR. 2011. Assessment of social interaction behaviors. J Vis Exp.

Kalebic N, Taverna E, Tavano S, Wong FK, Suchold D, Winkler S, Huttner WB, Sarov M. 2016. CRISPR/Cas9-induced disruption of gene expression in mouse embryonic brain and single neural stem cells in vivo. EMBO Rep 17:338-348.

Kandasamy M, Lehner B, Kraus S, Sander PR, Marschallinger J, Rivera FJ, Trumbach D, Ueberham U, Reitsamer HA, Strauss O, Bogdahn U, Couillard-Despres S, Aigner L. 2014. TGF-beta signalling in the adult neurogenic niche promotes stem cell quiescence as well as generation of new neurons. J Cell Mol Med 18:1444-1459.

Kang P, Lee HK, Glasgow SM, Finley M, Donti T, Gaber ZB, Graham BH, Foster AE, Novitch BG, Gronostajski RM, Deneen B. 2012. Sox9 and NFIA coordinate a transcriptional regulatory cascade during the initiation of gliogenesis. Neuron 74:79-94.

Kannius-Janson M, Johansson EM, Bjursell G, Nilsson J. 2002. Nuclear factor 1-C2 contributes to the tissue-specific activation of a milk protein gene in the differentiating mammary gland. J Biol Chem 277:17589-17596.

Karalay O, Doberauer K, Vadodaria KC, Knobloch M, Berti L, Miquelajauregui A, Schwark M, Jagasia R, Taketo MM, Tarabykin V, Lie DC, Jessberger S. 2011. Prospero-related homeobox 1 gene (Prox1) is regulated by canonical Wnt signaling and has a stage-specific role in adult hippocampal neurogenesis. Proc Natl Acad Sci U S A 108:5807-5812.

Karam SD, Burrows RC, Logan C, Koblar S, Pasquale EB, Bothwell M. 2000. Eph receptors and ephrins in the developing chick cerebellum: relationship to sagittal patterning and granule cell migration. J Neurosci 20:6488-6500.

Kato K. 1990. Novel GABAA receptor alpha subunit is expressed only in cerebellar granule cells. J Mol Biol 214:619-624.

Katoh M, Katoh M. 2003. Identification and characterization of human Inscuteable gene in silico. Int J Mol Med 11:111-116.

Kempermann G, Kuhn HG, Gage FH. 1997. More hippocampal neurons in adult mice living in an enriched environment. Nature 386:493-495.

Kilpatrick DL, Wang W, Gronostajski R, Litwack ED. 2012. Nuclear factor I and cerebellar granule neuron development: an intrinsic-extrinsic interplay. Cerebellum 11:41-49.

Kim EJ, Ables JL, Dickel LK, Eisch AJ, Johnson JE. 2011. Ascl1 (Mash1) defines cells with long-term neurogenic potential in subgranular and subventricular zones in adult mouse brain. PLoS One 6:e18472.

Klaassens M, Morrogh D, Rosser EM, Jaffer F, Vreeburg M, Bok LA, Segboer T, van Belzen M, Quinlivan RM, Kumar A, Hurst JA, Scott RH. 2015. Malan syndrome: Sotos-like overgrowth with de novo NFIX sequence variants and deletions in six new patients and a review of the literature. Eur J Hum Genet 23:610-615.

Knoblich JA. 2008. Mechanisms of asymmetric stem cell division. Cell 132:583-597.

Konno D, Shioi G, Shitamukai A, Mori A, Kiyonari H, Miyata T, Matsuzaki F. 2008. Neuroepithelial progenitors undergo LGN-dependent planar divisions to maintain self-renewability during mammalian neurogenesis. Nat Cell Biol 10:93-101.

Kriegstein A, Alvarez-Buylla A. 2009. The glial nature of embryonic and adult neural stem cells. Annu Rev Neurosci 32:149-184.

Kruse U, Qian F, Sippel AE. 1991. Identification of a fourth nuclear factor I gene in chicken by cDNA cloning: NFI-X. Nucleic Acids Res 19:6641.

Kurotaki N, Imaizumi K, Harada N, Masuno M, Kondoh T, Nagai T, Ohashi H, Naritomi K, Tsukahara M, Makita Y, Sugimoto T, Sonoda T, Hasegawa T, Chinen Y, Tomita Ha HA, Kinoshita A, Mizuguchi T, Yoshiura Ki K, Ohta T, Kishino T, Fukushima Y, Niikawa N, Matsumoto N. 2002. Haploinsufficiency of NSD1 causes Sotos syndrome. Nat Genet 30:365-366.

Lagace DC, Whitman MC, Noonan MA, Ables JL, DeCarolis NA, Arguello AA, Donovan MH, Fischer SJ, Farnbauch LA, Beech RD, DiLeone RJ, Greer CA, Mandyam CD, Eisch AJ. 2007. Dynamic contribution of nestin-expressing stem cells to adult neurogenesis. J Neurosci 27:12623-12629.

Laguesse S, Creppe C, Nedialkova DD, Prevot PP, Borgs L, Huysseune S, Franco B, Duysens G, Krusy N, Lee G, Thelen N, Thiry M, Close P, Chariot A, Malgrange B, Leidel SA, Godin JD, Nguyen L. 2015. A Dynamic Unfolded Protein Response Contributes to the Control of Cortical Neurogenesis. Dev Cell 35:553-567.

Lajoie M, Hsu YC, Gronostajski RM, Bailey TL. 2014. An overlapping set of genes is regulated by both NFIB and the glucocorticoid receptor during lung maturation. BMC Genomics 15:231.

Lancaster MA, Renner M, Martin CA, Wenzel D, Bicknell LS, Hurles ME, Homfray T, Penninger JM, Jackson AP, Knoblich JA. 2013. Cerebral organoids model human brain development and microcephaly. Nature 501:373-379.

Lane C, Milne E, Freeth M. 2017. Characteristics of Autism Spectrum Disorder in Sotos Syndrome. J Autism Dev Disord 47:135-143.

Lastowska M, Al-Afghani H, Al-Balool HH, Sheth H, Mercer E, Coxhead JM, Redfern CP, Peters H, Burt AD, Santibanez-Koref M, Bacon CM, Chesler L, Rust AG, Adams DJ, Williamson D, Clifford SC, Jackson MS. 2013. Identification of a neuronal transcription factor network involved in medulloblastoma development. Acta Neuropathol Commun 1:35.

Lee DS, Choung HW, Kim HJ, Gronostajski RM, Yang YI, Ryoo HM, Lee ZH, Kim HH, Cho ES, Park JC. 2014. NFI-C regulates osteoblast differentiation via control of Osterix expression. Stem Cells.

Lee DS, Yoon WJ, Cho ES, Kim HJ, Gronostajski RM, Cho MI, Park JC. 2011. Crosstalk between nuclear factor I-C and transforming growth factor-beta1 signaling regulates odontoblast differentiation and homeostasis. PLoS One 6:e29160.

Leinenga G, Gotz J. 2015. Scanning ultrasound removes amyloid-beta and restores memory in an Alzheimer's disease mouse model. Sci Transl Med 7:278ra233.

Lewis PM, Gritli-Linde A, Smeyne R, Kottmann A, McMahon AP. 2004. Sonic hedgehog signaling is required for expansion of granule neuron precursors and patterning of the mouse cerebellum. Dev Biol 270:393-410.

Li G, Fang L, Fernandez G, Pleasure SJ. 2013. The ventral hippocampus is the embryonic origin for adult neural stem cells in the dentate gyrus. Neuron 78:658-672.

Li R. 1999. Stimulation of DNA replication in Saccharomyces cerevisiae by a glutamine- and proline-rich transcriptional activation domain. J Biol Chem 274:30310-30314.

Liu R, Liu H, Chen X, Kirby M, Brown PO, Zhao K. 2001. Regulation of CSF1 promoter by the SWI/SNF-like BAF complex. Cell 106:309-318.

Lopez F, Belloc F, Lacombe F, Dumain P, Reiffers J, Bernard P, Boisseau MR. 1991. Modalities of synthesis of Ki67 antigen during the stimulation of lymphocytes. Cytometry 12:42-49.

Love MI, Huber W, Anders S. 2014. Moderated estimation of fold change and dispersion for RNA-seq data with DESeq2. Genome Biol 15:550.

Lu W, Quintero-Rivera F, Fan Y, Alkuraya FS, Donovan DJ, Xi Q, Turbe-Doan A, Li QG, Campbell CG, Shanske AL, Sherr EH, Ahmad A, Peters R, Rilliet B, Parvex P, Bassuk AG, Harris DJ, Ferguson H, Kelly C, Walsh CA, Gronostajski RM,

Devriendt K, Higgins A, Ligon AH, Quade BJ, Morton CC, Gusella JF, Maas RL. 2007. NFIA haploinsufficiency is associated with a CNS malformation syndrome and urinary tract defects. PLoS Genet 3:e80.

Lugert S, Basak O, Knuckles P, Haussler U, Fabel K, Gotz M, Haas CA, Kempermann G, Taylor V, Giachino C. 2010. Quiescent and active hippocampal neural stem cells with distinct morphologies respond selectively to physiological and pathological stimuli and aging. Cell Stem Cell 6:445-456.

Lugert S, Vogt M, Tchorz JS, Muller M, Giachino C, Taylor V. 2012. Homeostatic neurogenesis in the adult hippocampus does not involve amplification of Ascl1(high) intermediate progenitors. Nat Commun 3:670.

Madisen L, Zwingman TA, Sunkin SM, Oh SW, Zariwala HA, Gu H, Ng LL, Palmiter RD, Hawrylycz MJ, Jones AR, Lein ES, Zeng H. 2010. A robust and high-throughput Cre reporting and characterization system for the whole mouse brain. Nat Neurosci 13:133-140.

Maekawa M, Takashima N, Arai Y, Nomura T, Inokuchi K, Yuasa S, Osumi N. 2005. Pax6 is required for production and maintenance of progenitor cells in postnatal hippocampal neurogenesis. Genes Cells 10:1001-1014.

Magnusson JP, Goritz C, Tatarishvili J, Dias DO, Smith EM, Lindvall O, Kokaia Z, Frisen J. 2014. A latent neurogenic program in astrocytes regulated by Notch signaling in the mouse. Science 346:237-241.

Malan V, Rajan D, Thomas S, Shaw AC, Louis Dit Picard H, Layet V, Till M, van Haeringen A, Mortier G, Nampoothiri S, Puseljic S, Legeai-Mallet L, Carter NP, Vekemans M, Munnich A, Hennekam RC, Colleaux L, Cormier-Daire V. 2010. Distinct effects of allelic NFIX mutations on nonsense-mediated mRNA decay engender either a Sotos-like or a Marshall-Smith syndrome. Am J Hum Genet 87:189-198.

Mariani J, Coppola G, Zhang P, Abyzov A, Provini L, Tomasini L, Amenduni M, Szekely A, Palejev D, Wilson M, Gerstein M, Grigorenko EL, Chawarska K, Pelphrey KA, Howe JR, Vaccarino FM. 2015. FOXG1-Dependent Dysregulation of GABA/Glutamate Neuron Differentiation in Autism Spectrum Disorders. Cell 162:375-390.

Marino S, Vooijs M, van Der Gulden H, Jonkers J, Berns A. 2000. Induction of medulloblastomas in p53-null mutant mice by somatic inactivation of Rb in the external granular layer cells of the cerebellum. Genes Dev 14:994-1004.

Marshall RE, Graham CB, Scott CR, Smith DW. 1971. Syndrome of accelerated skeletal maturation and relative failure to thrive: a newly recognized clinical growth disorder. J Pediatr 78:95-101.

Martinez F, Marin-Reina P, Sanchis-Calvo A, Perez-Aytes A, Oltra S, Rosello M, Mayo S, Monfort S, Pantoja J, Orellana C. 2015. Novel mutations of NFIX gene causing Marshall-Smith syndrome or Sotos-like syndrome: one gene, two phenotypes. Pediatr Res 78:533-539.

Martinez S, Andreu A, Mecklenburg N, Echevarria D. 2013. Cellular and molecular basis of cerebellar development. Front Neuroanat 7:18.

Martynoga B, Mateo JL, Zhou B, Andersen J, Achimastou A, Urban N, van den Berg D, Georgopoulou D, Hadjur S, Wittbrodt J, Ettwiller L, Piper M, Gronostajski RM, Guillemot F. 2013. Epigenomic enhancer annotation reveals a key role for NFIX in neural stem cell quiescence. Genes Dev 27:1769-1786.

Martynoga B, Morrison H, Price DJ, Mason JO. 2005. Foxg1 is required for specification of ventral telencephalon and region-specific regulation of dorsal telencephalic precursor proliferation and apoptosis. Dev Biol 283:113-127.

Mateo JL, van den Berg DL, Haeussler M, Drechsel D, Gaber ZB, Castro DS, Robson P, Crawford GE, Flicek P, Ettwiller L, Wittbrodt J, Guillemot F, Martynoga B. 2015. Characterization of the neural stem cell gene regulatory network identifies OLIG2 as a multifunctional regulator of self-renewal. Genome Res 25:41-56.

Matsuzaki F, Shitamukai A. 2015. Cell Division Modes and Cleavage Planes of Neural Progenitors during Mammalian Cortical Development. Cold Spring Harb Perspect Biol 7:a015719.

McCloy RA, Rogers S, Caldon CE, Lorca T, Castro A, Burgess A. 2014. Partial inhibition of Cdk1 in G 2 phase overrides the SAC and decouples mitotic events. Cell Cycle 13:1400-1412.

Meier S, Brauer AU, Heimrich B, Nitsch R, Savaskan NE. 2004. Myelination in the hippocampus during development and following lesion. Cell Mol Life Sci 61:1082-1094.

Menn B, Garcia-Verdugo JM, Yaschine C, Gonzalez-Perez O, Rowitch D, Alvarez-Buylla A. 2006. Origin of oligodendrocytes in the subventricular zone of the adult brain. J Neurosci 26:7907-7918.

Messina G, Biressi S, Monteverde S, Magli A, Cassano M, Perani L, Roncaglia E, Tagliafico E, Starnes L, Campbell CE, Grossi M, Goldhamer DJ, Gronostajski RM, Cossu G. 2010. Nfix regulates fetal-specific transcription in developing skeletal muscle. Cell 140:554-566.

Miller BR, Hen R. 2015. The current state of the neurogenic theory of depression and anxiety. Curr Opin Neurobiol 30:51-58.

Ming GL, Song H. 2011. Adult neurogenesis in the mammalian brain: significant answers and significant questions. Neuron 70:687-702.

Mira H, Andreu Z, Suh H, Lie DC, Jessberger S, Consiglio A, San Emeterio J, Hortiguela R, Marques-Torrejon MA, Nakashima K, Colak D, Gotz M, Farinas I, Gage FH. 2010. Signaling through BMPR-IA regulates quiescence and long-term activity of neural stem cells in the adult hippocampus. Cell Stem Cell 7:78-89.

Mizutani K, Yoon K, Dang L, Tokunaga A, Gaiano N. 2007. Differential Notch signalling distinguishes neural stem cells from intermediate progenitors. Nature 449:351-355.

Mori T, Buffo A, Gotz M. 2005. The novel roles of glial cells revisited: the contribution of radial glia and astrocytes to neurogenesis. Curr Top Dev Biol 69:67-99.

Moss J, Gebara E, Bushong EA, Sanchez-Pascual I, O'Laoi R, El M'Ghari I, Kocher-Braissant J, Ellisman MH, Toni N. 2016. Fine processes of Nestin-GFP-positive radial glia-like stem cells in the adult dentate gyrus ensheathe local synapses and vasculature. Proc Natl Acad Sci U S A 113:E2536-2545.

Murtagh J, Martin F, Gronostajski RM. 2003. The Nuclear Factor I (NFI) gene family in mammary gland development and function. J Mammary Gland Biol Neoplasia 8:241-254.

Nagata K, Guggenheimer RA, Enomoto T, Lichy JH, Hurwitz J. 1982. Adenovirus DNA replication in vitro: identification of a host factor that stimulates synthesis of the preterminal protein-dCMP complex. Proc Natl Acad Sci U S A 79:6438-6442.

Nakamura KC, Kameda H, Koshimizu Y, Yanagawa Y, Kaneko T. 2008. Production and histological application of affinity-purified antibodies to heat-denatured green fluorescent protein. J Histochem Cytochem 56:647-657.

Namihira M, Kohyama J, Semi K, Sanosaka T, Deneen B, Taga T, Nakashima K. 2009. Committed neuronal precursors confer astrocytic potential on residual neural precursor cells. Dev Cell 16:245-255.

Nato G, Caramello A, Trova S, Avataneo V, Rolando C, Taylor V, Buffo A, Peretto P, Luzzati F. 2015. Striatal astrocytes produce neuroblasts in an excitotoxic model of Huntington's disease. Development 142:840-845.

Nicola Z, Fabel K, Kempermann G. 2015. Development of the adult neurogenic niche in the hippocampus of mice. Front Neuroanat 9:53.

Nilsson J, Bjursell G, Kannius-Janson M. 2006. Nuclear Jak2 and transcription factor NF1-C2: a novel mechanism of prolactin signaling in mammary epithelial cells. Mol Cell Biol 26:5663-5674.

Noble M. 2004. The possible role of myelin destruction as a precipitating event in Alzheimer's disease. Neurobiol Aging 25:25-31.

Noctor SC, Martinez-Cerdeno V, Ivic L, Kriegstein AR. 2004. Cortical neurons arise in symmetric and asymmetric division zones and migrate through specific phases. Nat Neurosci 7:136-144.

Oliver TG, Read TA, Kessler JD, Mehmeti A, Wells JF, Huynh TT, Lin SM, Wechsler-Reya RJ. 2005. Loss of patched and disruption of granule cell development in a pre-neoplastic stage of medulloblastoma. Development 132:2425-2439.

Paik JH, Ding Z, Narurkar R, Ramkissoon S, Muller F, Kamoun WS, Chae SS, Zheng H, Ying H, Mahoney J, Hiller D, Jiang S, Protopopov A, Wong WH, Chin L, Ligon KL, DePinho RA. 2009. FoxOs cooperatively regulate diverse pathways governing neural stem cell homeostasis. Cell Stem Cell 5:540-553.

Park JC, Herr Y, Kim HJ, Gronostajski RM, Cho MI. 2007. Nfic gene disruption inhibits differentiation of odontoblasts responsible for root formation and results in formation of short and abnormal roots in mice. J Periodontol 78:1795-1802.

Pasca AM, Sloan SA, Clarke LE, Tian Y, Makinson CD, Huber N, Kim CH, Park JY, O'Rourke NA, Nguyen KD, Smith SJ, Huguenard JR, Geschwind DH, Barres BA, Pasca SP. 2015. Functional cortical neurons and astrocytes from human pluripotent stem cells in 3D culture. Nat Methods 12:671-678.

Pereira JD, Sansom SN, Smith J, Dobenecker MW, Tarakhovsky A, Livesey FJ. 2010. Ezh2, the histone methyltransferase of PRC2, regulates the balance between self-renewal and differentiation in the cerebral cortex. Proc Natl Acad Sci U S A 107:15957-15962.

Petros TJ, Bultje RS, Ross ME, Fishell G, Anderson SA. 2015. Apical versus Basal Neurogenesis Directs Cortical Interneuron Subclass Fate. Cell Rep 13:1090-1095.

Picelli S, Bjorklund AK, Faridani OR, Sagasser S, Winberg G, Sandberg R. 2013. Smart-seq2 for sensitive full-length transcriptome profiling in single cells. Nat Methods 10:1096-1098.

Pierfelice T, Alberi L, Gaiano N. 2011. Notch in the vertebrate nervous system: an old dog with new tricks. Neuron 69:840-855.

Piper M, Barry G, Harvey TJ, McLeay R, Smith AG, Harris L, Mason S, Stringer BW, Day BW, Wray NR, Gronostajski RM, Bailey TL, Boyd AW, Richards LJ. 2014. NFIB-mediated repression of the epigenetic factor Ezh2 regulates cortical development. J Neurosci 34:2921-2930.

Piper M, Barry G, Hawkins J, Mason S, Lindwall C, Little E, Sarkar A, Smith AG, Moldrich RX, Boyle GM, Tole S, Gronostajski RM, Bailey TL, Richards LJ. 2010. NFIA controls

telencephalic progenitor cell differentiation through repression of the Notch effector Hes1. J Neurosci 30:9127-9139.

Piper M, Harris L, Barry G, Heng YH, Plachez C, Gronostajski RM, Richards LJ. 2011. Nuclear factor one X regulates the development of multiple cellular populations in the postnatal cerebellum. J Comp Neurol 519:3532-3548.

Pistocchi A, Gaudenzi G, Foglia E, Monteverde S, Moreno-Fortuny A, Pianca A, Cossu G, Cotelli F, Messina G. 2013. Conserved and divergent functions of Nfix in skeletal muscle development during vertebrate evolution. Development 140:1528-1536.

Plachez C, Cato K, McLeay RC, Heng YH, Bailey TL, Gronostasjki RM, Richards LJ, Puche AC, Piper M. 2012. Expression of nuclear factor one A and -B in the olfactory bulb. J Comp Neurol 520:3135-3149.

Plachez C, Lindwall C, Sunn N, Piper M, Moldrich RX, Campbell CE, Osinski JM, Gronostajski RM, Richards LJ. 2008. Nuclear factor I gene expression in the developing forebrain. J Comp Neurol 508:385-401.

Plasari G, Calabrese A, Dusserre Y, Gronostajski RM, McNair A, Michalik L, Mermod N. 2009. Nuclear factor I-C links platelet-derived growth factor and transforming growth factor beta1 signaling to skin wound healing progression. Mol Cell Biol 29:6006-6017.

Plasari G, Edelmann S, Hogger F, Dusserre Y, Mermod N, Calabrese A. 2010. Nuclear factor I-C regulates TGF-{beta}-dependent hair follicle cycling. J Biol Chem 285:34115-34125.

Platt RJ, Chen S, Zhou Y, Yim MJ, Swiech L, Kempton HR, Dahlman JE, Parnas O, Eisenhaure TM, Jovanovic M, Graham DB, Jhunjhunwala S, Heidenreich M, Xavier RJ, Langer R, Anderson DG, Hacohen N, Regev A, Feng G, Sharp PA, Zhang F. 2014. CRISPR-Cas9 knockin mice for genome editing and cancer modeling. Cell 159:440-455.

Postiglione MP, Juschke C, Xie Y, Haas GA, Charalambous C, Knoblich JA. 2011. Mouse inscuteable induces apical-basal spindle orientation to facilitate intermediate progenitor generation in the developing neocortex. Neuron 72:269-284.

Priolo M, Grosso E, Mammi C, Labate C, Naretto VG, Vacalebre C, Caridi P, Lagana C. 2012. A peculiar mutation in the DNA-binding/dimerization domain of NFIX causes Sotos-like overgrowth syndrome: a new case. Gene 511:103-105.

Rando C, Hillson S, Antoine D. 2014. Changes in mandibular dimensions during the mediaeval to post-mediaeval transition in London: a possible response to decreased masticatory load. Arch Oral Biol 59:73-81.

Raymond CS, Soriano P. 2007. High-efficiency FLP and PhiC31 site-specific recombination in mammalian cells. PLoS One 2:e162.

Relaix F, Rocancourt D, Mansouri A, Buckingham M. 2005. A Pax3/Pax7-dependent population of skeletal muscle progenitor cells. Nature 435:948-953.

Renault VM, Rafalski VA, Morgan AA, Salih DA, Brett JO, Webb AE, Villeda SA, Thekkat PU, Guillerey C, Denko NC, Palmer TD, Butte AJ, Brunet A. 2009. FoxO3 regulates neural stem cell homeostasis. Cell Stem Cell 5:527-539.

Rietze RL, Valcanis H, Brooker GF, Thomas T, Voss AK, Bartlett PF. 2001. Purification of a pluripotent neural stem cell from the adult mouse brain. Nature 412:736-739.

Rolando C, Erni A, Grison A, Beattie R, Engler A, Gokhale PJ, Milo M, Wegleiter T, Jessberger S, Taylor V. 2016. Multipotency of Adult Hippocampal NSCs In Vivo Is Restricted by Drosha/NFIB. Cell Stem Cell 19:653-662.

Rossi G, Antonini S, Bonfanti C, Monteverde S, Vezzali C, Tajbakhsh S, Cossu G, Messina G. 2016. Nfix Regulates Temporal Progression of Muscle Regeneration through Modulation of Myostatin Expression. Cell Rep 14:2238-2249.

Rupp RA, Kruse U, Multhaup G, Gobel U, Beyreuther K, Sippel AE. 1990. Chicken NFI/TGGCA proteins are encoded by at least three independent genes: NFI-A, NFI-B and NFI-C with homologues in mammalian genomes. Nucleic Acids Res 18:2607-2616.

Saffary R, Xie Z. 2011. FMRP regulates the transition from radial glial cells to intermediate progenitor cells during neocortical development. J Neurosci 31:1427-1439.

Sahay A, Scobie KN, Hill AS, O'Carroll CM, Kheirbek MA, Burghardt NS, Fenton AA, Dranovsky A, Hen R. 2011. Increasing adult hippocampal neurogenesis is sufficient to improve pattern separation. Nature 472:466-470.

Sanada K, Tsai LH. 2005. G protein betagamma subunits and AGS3 control spindle orientation and asymmetric cell fate of cerebral cortical progenitors. Cell 122:119-131.

Santoro C, Mermod N, Andrews PC, Tjian R. 1988. A family of human CCAAT-box-binding proteins active in transcription and DNA replication: cloning and expression of multiple cDNAs. Nature 334:218-224.

Sauvageot CM, Stiles CD. 2002. Molecular mechanisms controlling cortical gliogenesis. Curr Opin Neurobiol 12:244-249.

Schaefer M, Shevchenko A, Shevchenko A, Knoblich JA. 2000. A protein complex containing Inscuteable and the Galpha-binding protein Pins orients asymmetric cell divisions in Drosophila. Curr Biol 10:353-362.

Scholzen T, Gerdes J. 2000. The Ki-67 protein: from the known and the unknown. J Cell Physiol 182:311-322.

Schuller U, Heine VM, Mao J, Kho AT, Dillon AK, Han YG, Huillard E, Sun T, Ligon AH, Qian Y, Ma Q, Alvarez-Buylla A, McMahon AP, Rowitch DH, Ligon KL. 2008. Acquisition of granule neuron precursor identity is a critical determinant of progenitor cell competence to form Shh-induced medulloblastoma. Cancer Cell 14:123-134.

Scott CE, Wynn SL, Sesay A, Cruz C, Cheung M, Gomez Gaviro MV, Booth S, Gao B, Cheah KS, Lovell-Badge R, Briscoe J. 2010. SOX9 induces and maintains neural stem cells. Nat Neurosci 13:1181-1189.

Seckl JR. 2004. Prenatal glucocorticoids and long-term programming. Eur J Endocrinol 151 Suppl 3:U49-62.

Seib DR, Corsini NS, Ellwanger K, Plaas C, Mateos A, Pitzer C, Niehrs C, Celikel T, Martin-Villalba A. 2013. Loss of Dickkopf-1 restores neurogenesis in old age and counteracts cognitive decline. Cell Stem Cell 12:204-214.

Seri B, Garcia-Verdugo JM, McEwen BS, Alvarez-Buylla A. 2001. Astrocytes give rise to new neurons in the adult mammalian hippocampus. J Neurosci 21:7153-7160.

Sessa A, Mao CA, Hadjantonakis AK, Klein WH, Broccoli V. 2008. Tbr2 directs conversion of radial glia into basal precursors and guides neuronal amplification by indirect neurogenesis in the developing neocortex. Neuron 60:56-69.

Shaw AC, van Balkom ID, Bauer M, Cole TR, Delrue MA, Van Haeringen A, Holmberg E, Knight SJ, Mortier G, Nampoothiri S, Puseljic S, Zenker M, Cormier-Daire V, Hennekam RC. 2010. Phenotype and natural history in Marshall-Smith syndrome. Am J Med Genet A 152A:2714-2726.

Shin J, Berg DA, Zhu Y, Shin JY, Song J, Bonaguidi MA, Enikolopov G, Nauen DW, Christian KM, Ming GL, Song H. 2015. Single-Cell RNA-Seq with Waterfall Reveals Molecular Cascades underlying Adult Neurogenesis. Cell Stem Cell 17:360-372.

Shitamukai A, Konno D, Matsuzaki F. 2011. Oblique radial glial divisions in the developing mouse neocortex induce self-renewing progenitors outside the germinal zone that resemble primate outer subventricular zone progenitors. J Neurosci 31:3683-3695.

Shu T, Butz KG, Plachez C, Gronostajski RM, Richards LJ. 2003. Abnormal development of forebrain midline glia and commissural projections in Nfia knock-out mice. J Neurosci 23:203-212.

Singh SK, Wilczynska KM, Grzybowski A, Yester J, Osrah B, Bryan L, Wright S, Griswold-Prenner I, Kordula T. 2011. The unique transcriptional activation domain of nuclear factor-I-X3 is critical to specifically induce marker gene expression in astrocytes. J Biol Chem 286:7315-7326.

Sotos JF. 2014. Sotos syndrome 1 and 2. Pediatr Endocrinol Rev 12:2-16.

Spalding KL, Bergmann O, Alkass K, Bernard S, Salehpour M, Huttner HB, Bostrom E, Westerlund I, Vial C, Buchholz BA, Possnert G, Mash DC, Druid H, Frisen J. 2013. Dynamics of hippocampal neurogenesis in adult humans. Cell 153:1219-1227.

Steele-Perkins G, Butz KG, Lyons GE, Zeichner-David M, Kim HJ, Cho MI, Gronostajski RM. 2003. Essential role for NFI-C/CTF transcription-replication factor in tooth root development. Mol Cell Biol 23:1075-1084.

Steele-Perkins G, Plachez C, Butz KG, Yang G, Bachurski CJ, Kinsman SL, Litwack ED, Richards LJ, Gronostajski RM. 2005. The transcription factor gene Nfib is essential for both lung maturation and brain development. Mol Cell Biol 25:685-698.

Steiner B, Klempin F, Wang L, Kott M, Kettenmann H, Kempermann G. 2006. Type-2 cells as link between glial and neuronal lineage in adult hippocampal neurogenesis. Glia 54:805-814.

Stone SS, Teixeira CM, Devito LM, Zaslavsky K, Josselyn SA, Lozano AM, Frankland PW. 2011. Stimulation of entorhinal cortex promotes adult neurogenesis and facilitates spatial memory. J Neurosci 31:13469-13484.

Stuchlik A, Petrasek T, Prokopova I, Holubova K, Hatalova H, Vales K, Kubik S, Dockery C, Wesierska M. 2013. Place avoidance tasks as tools in the behavioral neuroscience of learning and memory. Physiol Res 62 Suppl 1:S1-S19.

Suarez R, Fenlon LR, Marek R, Avitan L, Sah P, Goodhill GJ, Richards LJ. 2014. Balanced interhemispheric cortical activity is required for correct targeting of the corpus callosum. Neuron 82:1289-1298.

Suh H, Consiglio A, Ray J, Sawai T, D'Amour KA, Gage FH. 2007. In vivo fate analysis reveals the multipotent and self-renewal capacities of Sox2+ neural stem cells in the adult hippocampus. Cell Stem Cell 1:515-528.

Sun GJ, Zhou Y, Ito S, Bonaguidi MA, Stein-O'Brien G, Kawasaki NK, Modak N, Zhu Y, Ming GL, Song H. 2015. Latent tri-lineage potential of adult hippocampal neural stem cells revealed by Nf1 inactivation. Nat Neurosci 18:1722-1724.

Sun MY, Yetman MJ, Lee TC, Chen Y, Jankowsky JL. 2014. Specificity and efficiency of reporter expression in adult neural progenitors vary substantially among nestin-CreER(T2) lines. J Comp Neurol 522:1191-1208.

Sun Y, Hu J, Zhou L, Pollard SM, Smith A. 2011. Interplay between FGF2 and BMP controls the self-renewal, dormancy and differentiation of rat neural stem cells. J Cell Sci 124:1867-1877.

Supek F, Bosnjak M, Skunca N, Smuc T. 2011. REVIGO summarizes and visualizes long lists of gene ontology terms. PLoS One 6:e21800.

Taglietti V, Maroli G, Cermenati S, Monteverde S, Ferrante A, Rossi G, Cossu G, Beltrame M, Messina G. 2016. Nfix Induces a Switch in Sox6 Transcriptional Activity to Regulate MyHC-I Expression in Fetal Muscle. Cell Rep 17:2354-2366.

Tajbakhsh S. 2005. Skeletal muscle stem and progenitor cells: reconciling genetics and lineage. Exp Cell Res 306:364-372.

Taniguchi H, Kawauchi D, Nishida K, Murakami F. 2006. Classic cadherins regulate tangential migration of precerebellar neurons in the caudal hindbrain. Development 133:1923-1931.

Timmons JA, Szkop KJ, Gallagher IJ. 2015. Multiple sources of bias confound functional enrichment analysis of global -omics data. Genome Biol 16:186.

Trapnell C, Pachter L, Salzberg SL. 2009. TopHat: discovering splice junctions with RNA-Seq. Bioinformatics 25:1105-1111.

Tumbar T, Guasch G, Greco V, Blanpain C, Lowry WE, Rendl M, Fuchs E. 2004. Defining the epithelial stem cell niche in skin. Science 303:359-363.

Urban N, Guillemot F. 2014. Neurogenesis in the embryonic and adult brain: same regulators, different roles. Front Cell Neurosci 8:396.

Urban N, van den Berg DL, Forget A, Andersen J, Demmers JA, Hunt C, Ayrault O, Guillemot F. 2016. Return to quiescence of mouse neural stem cells by degradation of a proactivation protein. Science 353:292-295.

Valcourt JR, Lemons JM, Haley EM, Kojima M, Demuren OO, Coller HA. 2012. Staying alive: metabolic adaptations to quiescence. Cell Cycle 11:1680-1696.

Vidovic D, Harris L, Harvey TJ, Evelyn Heng YH, Smith AG, Osinski J, Hughes J, Thomas P, Gronostajski RM, Bailey TL, Piper M. 2015. Expansion of the lateral ventricles and ependymal deficits underlie the hydrocephalus evident in mice lacking the transcription factor NFIX. Brain Res 1616:71-87.

Vogt MA, Chourbaji S, Brandwein C, Dormann C, Sprengel R, Gass P. 2008. Suitability of tamoxifen-induced mutagenesis for behavioral phenotyping. Exp Neurol 211:25-33.

von Bohlen und Halbach O. 2011. Immunohistological markers for proliferative events, gliogenesis, and neurogenesis within the adult hippocampus. Cell Tissue Res 345:1-19.

Vukovic J, Borlikova GG, Ruitenberg MJ, Robinson GJ, Sullivan RK, Walker TL, Bartlett PF. 2013. Immature doublecortin-positive hippocampal neurons are important for learning but not for remembering. J Neurosci 33:6603-6613.

Walker T, Huang J, Young K. 2016a. Neural Stem and Progenitor Cells in Nervous System Function and Therapy. Stem Cells Int 2016:1890568.

Walker TL, Overall RW, Vogler S, Sykes AM, Ruhwald S, Lasse D, Ichwan M, Fabel K, Kempermann G. 2016b. Lysophosphatidic Acid Receptor Is a Functional Marker of Adult Hippocampal Precursor Cells. Stem Cell Reports 6:552-565.

Wallace VA. 1999. Purkinje-cell-derived Sonic hedgehog regulates granule neuron precursor cell proliferation in the developing mouse cerebellum. Curr Biol 9:445-448.

Wang W, Crandall JE, Litwack ED, Gronostajski RM, Kilpatrick DL. 2010. Targets of the nuclear factor I regulon involved in early and late development of postmitotic cerebellar granule neurons. J Neurosci Res 88:258-265.

Wang W, Mullikin-Kilpatrick D, Crandall JE, Gronostajski RM, Litwack ED, Kilpatrick DL. 2007. Nuclear factor I coordinates multiple phases of cerebellar granule cell development via regulation of cell adhesion molecules. J Neurosci 27:6115-6127.

Wang W, Stock RE, Gronostajski RM, Wong YW, Schachner M, Kilpatrick DL. 2004. A role for nuclear factor I in the intrinsic control of cerebellar granule neuron gene expression. J Biol Chem 279:53491-53497.

Wang X, Tsai JW, Imai JH, Lian WN, Vallee RB, Shi SH. 2009. Asymmetric centrosome inheritance maintains neural progenitors in the neocortex. Nature 461:947-955.

Weissman IL. 2000. Stem cells: units of development, units of regeneration, and units in evolution. Cell 100:157-168.

Wilczynska KM, Singh SK, Adams B, Bryan L, Rao RR, Valerie K, Wright S, Griswold-Prenner I, Kordula T. 2009. Nuclear factor I isoforms regulate gene expression during the differentiation of human neural progenitors to astrocytes. Stem Cells 27:1173-1181.

Wodarz A, Ramrath A, Kuchinke U, Knust E. 1999. Bazooka provides an apical cue for Inscuteable localization in Drosophila neuroblasts. Nature 402:544-547.

Wojtowicz JM, Kee N. 2006. BrdU assay for neurogenesis in rodents. Nat Protoc 1:1399-1405.

Wong YW, Schulze C, Streichert T, Gronostajski RM, Schachner M, Tilling T. 2007. Gene expression analysis of nuclear factor I-A deficient mice indicates delayed brain maturation. Genome Biol 8:R72.

Wu X, Northcott PA, Dubuc A, Dupuy AJ, Shih DJ, Witt H, Croul S, Bouffet E, Fults DW, Eberhart CG, Garzia L, Van Meter T, Zagzag D, Jabado N, Schwartzentruber J, Majewski J, Scheetz TE, Pfister SM, Korshunov A, Li XN, Scherer SW, Cho YJ, Akagi K, MacDonald TJ, Koster J, McCabe MG, Sarver AL, Collins VP, Weiss WA, Largaespada DA, Collier LS, Taylor MD. 2012. Clonal selection drives genetic divergence of metastatic medulloblastoma. Nature 482:529-533.

Yoneda Y, Saitsu H, Touyama M, Makita Y, Miyamoto A, Hamada K, Kurotaki N, Tomita H, Nishiyama K, Tsurusaki Y, Doi H, Miyake N, Ogata K, Naritomi K, Matsumoto N. 2012. Missense mutations in the DNA-binding/dimerization domain of NFIX cause Sotos-like features. J Hum Genet 57:207-211.

Young KM, Mitsumori T, Pringle N, Grist M, Kessaris N, Richardson WD. 2010. An Fgfr3-iCreER(T2) transgenic mouse line for studies of neural stem cells and astrocytes. Glia 58:943-953.

Yousef H, Morgenthaler A, Schlesinger C, Bugaj L, Conboy IM, Schaffer DV. 2015. Age-Associated Increase in BMP Signaling Inhibits Hippocampal Neurogenesis. Stem Cells 33:1577-1588.

Yu G, Wang LG, He QY. 2015. ChIPseeker: an R/Bioconductor package for ChIP peak annotation, comparison and visualization. Bioinformatics 31:2382-2383.

Yun S, Reynolds RP, Masiulis I, Eisch AJ. 2016. Re-evaluating the link between neuropsychiatric disorders and dysregulated adult neurogenesis. Nat Med 22:1239-1247.

Zappelli F, Willems D, Osada S, Ohno S, Wetsel WC, Molinaro M, Cossu G, Bouche M. 1996. The inhibition of differentiation caused by TGFbeta in fetal myoblasts is dependent upon selective expression of PKCtheta: a possible molecular basis for myoblast diversification during limb histogenesis. Dev Biol 180:156-164.

Zhao LH, Ba XQ, Wang XG, Zhu XJ, Wang L, Zeng XL. 2005. BAF complex is closely related to and interacts with NF1/CTF and RNA polymerase II in gene transcriptional activation. Acta Biochim Biophys Sin (Shanghai) 37:440-446.

Zhou B, Osinski JM, Mateo JL, Martynoga B, Sim FJ, Campbell CE, Guillemot F, Piper M, Gronostajski RM. 2015. Loss of NFIX Transcription Factor Biases Postnatal Neural Stem/Progenitor Cells Toward Oligodendrogenesis. Stem Cells Dev 24:2114-2126.

Zuccaro E, Arlotta P. 2013. The quest for myelin in the adult brain. Nat Cell Biol 15:572-575.